QUARTERLY JOURNAL
OF THE
ROYAL METEOROLOGICAL SOCIETY

Editor: J. S. SAWYER

Vol. 87 JULY 1961 No. 373

CONTENTS

PAGE

D. G. KING-HELE—Symons Memorial Lecture for 1961—Satellites and the earth's outer atmosphere 265

S. K. RUNCORN—Napier Shaw Prize Essay—Climatic change through geological time in the light of the palaeomagnetic evidence for polar wandering and continental drift (Plates VI-VII) 282

S. FRITZ—Satellite cloud pictures of a cyclone over the Atlantic Ocean (Plates VIII-IX) 314

R. A. EBDON—Some notes on the stratospheric winds at Canton Island and Christmas Island 322

E. R. REITER—Project Jet Stream Research Flight No. 30, April 1957 332

W. T. ROACH—Some aircraft observations of fluxes of solar radiation in the atmosphere 346

W. T. ROACH—The absorption of solar radiation by water vapour and carbon dioxide in a cloudless atmosphere 364

F. H. BUSHBY and CLARE J. WHITELAM—A three-parameter model of the atmosphere suitable for numerical integration 374

M. H. FREEMAN—A graphical method of objective forecasting derived by statistical techniques 393

A. J. DYER—Measurements of evaporation and heat transfer in the lower atmosphere by an automatic eddy-correlation technique (Plate X) 401

W. C. MACKLIN—Accretion in mixed clouds (Plate XI) 413

Shorter Contributions—

W. G. GRAHAM and K. M. KING—Short-wave reflection coefficient for a field of maize .. 425

R. M. GOODY—A note on the regular model of an absorption band 428

S. D. SMITH—Design of interference filters for the observation of infra-red emission from atmospheric carbon dioxide by an earth satellite 431

Correspondence—

H. E. LANDSBERG and J. MURRAY MITCHELL Jr; G. S. CALLENDAR—Temperature fluctuations and trends over the earth 435

C. H. B. PRIESTLEY; H. A. PANOFSKY—An alternative derivation of the diabatic wind profile 437

Discussions—

F. K. BALL—A theory of fronts in relation to surface stress (*Q.J.*, **86**, p. 51) 439

J. P. FUNK—Measured radiative flux divergence near the ground at night (*Q.J.*, **86**, p. 382) 440

E. KNIGHTING—Some computations of the variation of vertical velocity with pressure on a synoptic scale (*Q.J.*, **86**, p. 318) 442

Report of the Council for 1960 444

Proceedings at meetings of the Society 457

Reviews—

Monsoons of the world, India Meteorological Dept. (A.G.F.); *The earth's problem climates*, G. T. Trewartha (G.B.T.); *A history of the United States Weather Bureau*, D. R. Whitnah (H.W.L.A.); *Space research (Proceedings of first international space-science symposium, Nice)* (P.A.S.); *Klima-atlas von Nordrhein-Westfalen* (W.H.H.); *Das Klima der Bodennahen Luftschicht*, R. Geiger (W.H.H.) 460

Obituary Notices 464

PUBLISHED AND SOLD BY THE
ROYAL METEOROLOGICAL SOCIETY
49 CROMWELL ROAD, LONDON, S.W.7
PRICE THIRTY SHILLINGS ($4.50)
ANNUAL SUBSCRIPTION £5 - 4 - 0 ($16), POST FREE

ROYAL METEOROLOGICAL SOCIETY

Founded on 3 April 1850, for the advancement of meteorological science. The Society was incorporated by Royal Charter in 1866.

Membership

Membership is open to all persons genuinely interested in meteorology. The annual subscription is as follows :

Fellows	£4-4-0	(Entrance fee, 1 guinea)
Foreign Members ..	£4-4-0	„ „
Students	£1-10-0	
Corporate Members..	£21-0-0	

All Members receive free the regular publications of the Society, including the monthly publication *Weather* (annual subscription to non-members 24s. plus 2s. 6d. postage).

The Descriptive Account of the Society and an application form will be sent on request to the Assistant Secretary.

Quarterly Journal

Editing Committee

J. S. Sawyer — *Editor and Chairman*

A. G. Forsdyke	R. F. Jones	J. S. Marshall	B. J. Mason
R. J. Murgatroyd	F. Pasquill	R. C. Rainey	R. S. Scorer

The primary purpose of the *Quarterly Journal* is to publish results of original research and reports of the Society's scientific meetings. Papers intended for the *Journal* **should be submitted in accordance with standards laid down by the Council in the Society's memorandum** ' Preparation of Papers for the *Quarterly Journal*' which is available on request. Failure to conform with these standards involves the Society's officers and staff in much needless work and the Society in unnecessary expense. **Manuscripts will therefore not be considered for publication unless they conform reasonably closely with the procedure laid down.** The attention of authors is drawn particularly to the requirements in regard to mathematics and diagrams and the Assistant Secretary will be pleased to advise authors on their special problems of illustration before papers are formally submitted. Diagrams should, if possible, be submitted flat, not rolled, and a duplicate rough set for refereeing purposes should be included. Where rulings on a diagram are desirable the closest acceptable spacing is approximately 1 cm and this may be done on **blue-lined** graph paper by thickening the centimeter rulings. Manuscripts may be submitted in duplicate to expedite refereeing, but authors must retain complete copies in their possession.

Price to non-members is £5-4-0 (post free) per annum and £1-10-0 for single issues (postage extra).

PUBLICATIONS

Copies of the publications *Centenary Proceedings of the Royal Meteorological Society*, 1950 (£1. 1s.) and *Proceedings Toronto Meteorological Conference* 1953 (£1. 10s.) are still available.

Reprints of papers recently published in the *Quarterly Journal* are generally available, the prices being as follows (postage extra): 8 pp., 1s. 2d.; 16 pp., 1s. 10d.; 20 pp., 2s. 2d.

Weather Lore. Fourth edition of the late Richard Inwards's unique compilation, revised, augmented and edited for the Society by E. L. Hawke. Published in 1950. 4s. 6d., postage 1s.

Rainfall Atlas of the British Isles. Published in 1926. Price to Members, 15s. post free.

Collected Scientific Papers of William Henry Dines, F.R.S. This memorial volume contains reproductions of nearly sixty papers and other original communications by W. H. Dines. 15s., postage 1s.

Cloud study : a pictorial guide. By F. H. Ludlam and R. S. Scorer. 75 photographs. Published in 1957 under the auspices of the Society by John Murray. 12s. 6d. (11s. to Members), postage 1s.

Cloud photographs. A new series of 24 postcards reproduced from the unique Clarke and Cave Collection. Complete set, 7s. 6d., postage 6d.

The Society's Offices

Assistant Secretary — Col. J. H. Willink, C.B.E.

49 Cromwell Road, London, S.W.7.

(*Telephone :* KENsington 0730)

The offices and library of the Society are open daily (Monday to Friday) from 10 a.m. to 5 p.m. All enquiries and correspondence concerning the Society and its publications should be addressed to the Assistant Secretary.

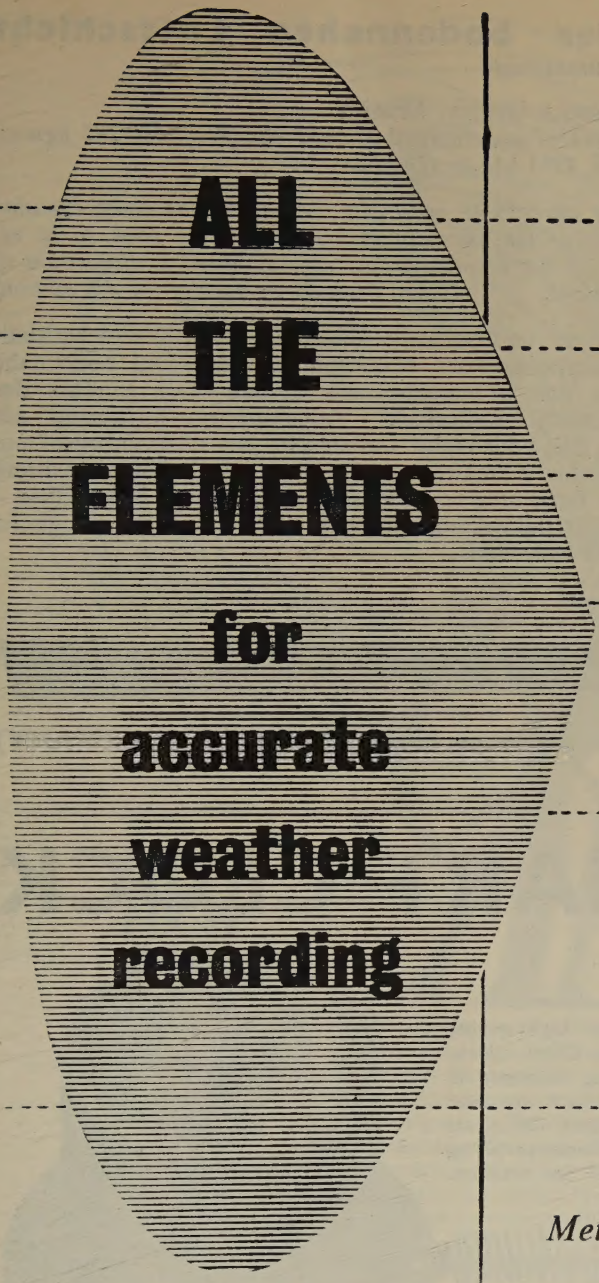

Thermometers

Hygrometers

Barometers

Rain Gauges

Sunshine Recorders

Wind Direction and Velocity Indicators, etc.

Meteorological Instruments by

NEGRETTI & ZAMBRA LTD

Manufacturers of instruments for the indication, recording, controlling of :—
Temperature, pressure, liquid level, volume, specific gravity, humidity, etc.

122, REGENT STREET, LONDON, W.1
'Phone: REGent 3406. 'Grams: Negretti, Piccy, London
Branches : Birmingham, Cardiff, Glasgow, Leeds, Manchester, Nottingham.
Agents or Subsidiaries in most countries.

RUDOLF GEIGER

Das Klima der bodennahen Luftschicht

Ein Lehrbuch der Mikroklimatologie

By Prof. Dr. RUDOLF GEIGER, Munich.
4th, completely revised and enlarged edition. Pp. XII, 648; 281 figures. 1961. Half cloth, DM 54. – – (*German*).

The enormous development since 1950, especially the astonishing comprehension of the practical application of the microclimatology forced the book to be re-written. The enlargement of our knowledge has also admitted a disposition of the subjects clearer than before. (*taken from the preface of the 4th edition*)

Contents : Das Mikroklima und seine Erforschung – Der Wärmehaushalt der Erdoberfläche als Grundlage der Mikroklimatologie – Die bodennahe Luftschicht über ebenem und unbewachesenem Boden – Der Einfluss der Unterlage auf die bodennahe Luftschicht – Zahlenmässige Erfassung der Wärmehaushaltsgrössen – Die bodennahe Luftshcicht bei pflanzenbedecktem Boden – Forstmeteorologische Klimafragen – Einfluss der Geländegestaltung auf das Mikroklima – Die Beziehung von Mensch und Tier zum Mikroklima – Messtechnische Hinweise für mikroklimatologische und mikrometeorologische Untersuchungen – Literaturverzeichnis.

Special prospectus by request.

FRIEDR. VIEWEG & SOHN · BRAUNSCHWEIG (GERMANY)
Post Box 185

HORSTMANN

CHART CLOCK

The robustly constructed movements and high quality jewelled lever escapements of Horstmann Chart Clocks ensure the extremely accurate timekeeping necessary in meteorological equipment. The clocks, which are used extensively by the Air Ministry Meteorological Office, are available in two types – one to drive chart drums revolving once every 24 hours and the other for 7 day rotation.

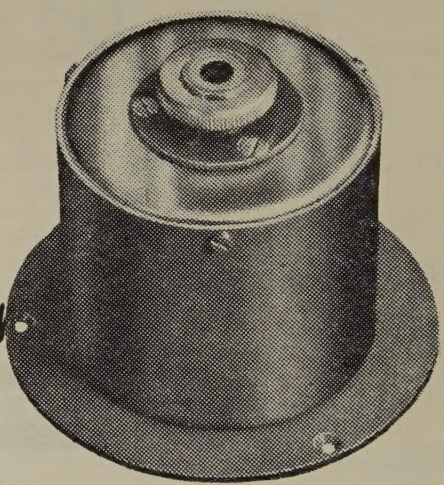

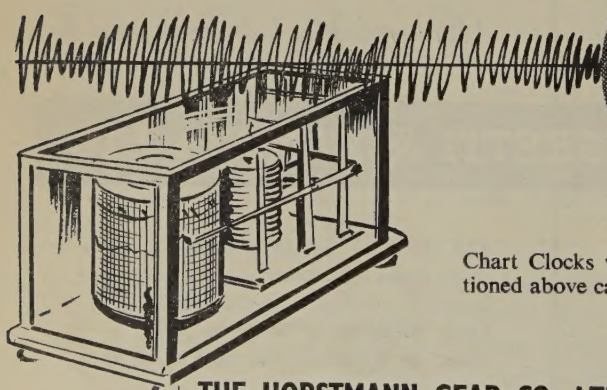

Chart Clocks with speeds other than those mentioned above can also be supplied to special order.

THE HORSTMANN GEAR CO. LTD.
NEWBRIDGE WORKS · BATH · Tel. : Bath 7241

NEWBRIDGE WORKS BATH
REGISTERED TRADE MARK

RED SKY IN THE MORNING

Yesterday's weather lore gives way to today's weather logic – Cossor CR 353 Meteorological Radar meets the need for long range, high-accuracy windfinding and cloud observation equipment. Its ability to track balloon-carried reflectors through local rain, plus reliable working efficiency in all weather conditions, make it suitable for use anywhere in the world.

CR 353 Radar is inexpensive, easily maintained and can be operated with a minimum of staff. Where only the windfinding equipment is required, it can be obtained separately at a lower cost.

CR353

METEOROLOGICAL RADAR

For full details about this advanced meteorological radar system, please write to:-

COSSOR

RADAR AND ELECTRONICS LIMITED

COSSOR RADAR AND ELECTRONICS LIMITED *The Pinnacles, Elizabeth Way, Harlow, Essex.* *Telephone: Harlow 26862*

METEOROLOGICAL INSTRUMENTS

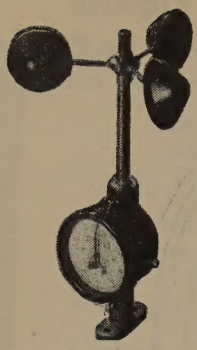

PORTABLE ANEMOMETER
Incorporating synthetic sapphire jewel bearings having a very low frictional torque.
In spite of its high sensitivity it has the large range of 25/5,000 feet per minute.

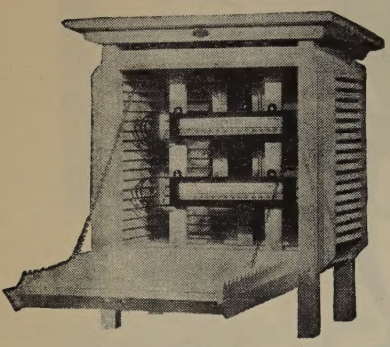

METEOROLOGICAL SCREEN
We supply these in Stevenson and Bilham patterns or to other Meteorological Office specifications complete with thermometers.

HAIR HYGROMETER
Temperature and Humidity at a glance.
The ideal instrument for use in office, store room or factory.
This Hair Hygrometer, which enables the relative humidity to be read accurately and quickly can be fitted with either a Fahrenheit or Centigrade thermometer.

for measuring

- ★ **WIND**
- ★ **PRESSURE**
- ★ **TEMPERATURE**
- ★ **HUMIDITY**
- ★ **PRECIPITATION**
- ★ **EVAPORATION**
- ★ **RAINFALL**
- ★ **SUNSHINE**
- ★ **ETC., ETC.**

Whenever meteorological phenomena have to be recorded, Casella can provide instruments that will give you the most reliable readings. Whether they are well tried standard patterns or specially designed instruments for highly specialised requirements, all embody the high standards of workmanship and finish that have been the Casella manufacturing policy for 150 years. *The new Casella catalogue of meteorological instruments is now ready. Send for your copy.*

CASELLA
LONDON

C. F. CASELLA & CO. LTD.
Dept. (QJM), Regent House,
Britannia Walk, London, N.1
Clerkenwell 8581 (6 lines)

Members Scientific Instrument Manufacturers' Association of Great Britain and the British Scientific Instrument Research Association.

QUARTERLY JOURNAL
OF THE
ROYAL METEOROLOGICAL SOCIETY

Vol. 87 JULY 1961 No. 373

551.507.362.2 : 551.510.3 : 551.510.536

Satellites and the earth's outer atmosphere

By D. G. KING-HELE
Royal Aircraft Establishment, Farnborough

Symons Memorial Lecture, delivered 1 March 1961

1. Introduction

Five years ago very little was known of the atmosphere at heights above 200 km, and the existing theories were conjectural. In the past three years, however, the region has been quite thoroughly explored by satellites and space vehicles. From the evidence they have supplied I shall try to describe the properties of the atmosphere at heights from 200 km (which is near the lower limit for satellites to remain in orbit) up to that very indefinite level where the earth's atmosphere imperceptibly merges into the wider domain of the sun's atmosphere.

Satellites are also adding to our knowledge of the lower atmosphere, through cloud-photographs like those taken by the highly successful Tiros. These weather satellites will probably do more to advance meteorology than will mere knowledge of conditions in the upper atmosphere, and they will also have a greater impact on everyday life : for example, operational weather satellites would have provided warning of the two cyclones which struck East Pakistan in October 1960, and might thereby have saved many of the 18,000 lives lost. But apart from this brief acknowledgment of their importance, I shall not discuss weather satellites here.

My plan is first to look at the atmosphere in general and then to describe, in turn, the successive layers of the outer atmosphere.

2. Past and present models of the atmosphere

From the time of Aristotle till the nineteenth century, the science of meteorology took the whole atmosphere as its province : it bridged the gap between Earth and Heaven. In the Aristotelian terminology, which endured until the seventeenth century, the sphere of Air was sandwiched between the sphere of Earth and the sphere of Fire, while beyond that lay the spheres of the planets and fixed stars. All transient phenomena in the heavens, including comets, meteors and the aurora, as well as what we now call weather, were assigned to the sphere of Air, because the outer spheres were either fixed and eternal or, if not, were at least predictable in their habits. The domain of meteorology was, then, the whole of the corruptible part of the heavens, the sublunary sphere as it was often called. But in the last 150 years meteorology has tended to confine itself to a small fraction of the atmosphere; so the extension I am making in this lecture could be interpreted as a tacit invitation to meteorologists to reclaim some of their former territory.

Before coming to the modern picture of the atmosphere it is salutary to take two glimpses of past views, one from the sixteenth century and one from the eighteenth. In the sixteenth century Aristotle's views still reigned supreme, but the sphere of Air was divided into three regions, as shown in Fig. 1, which is given in Heninger's excellent book Renaissance meteorology (1960). The first and lowest region is warmed by the sun's rays and the earth's heat; the second region is cold, and the watery meteors condense as clouds; the uppermost region is hot because of its contact with the sphere of Fire and also

Figure 1. A sixteenth-century picture of the atmosphere (from G. Reisch, *Margarita Philosophica*, Strasbourg, (1515)).

from the friction of the rotating spheres of Heaven. Although we can no longer accept the friction of the spheres, we do know that the uppermost atmosphere is very hot, largely because it merges into the sun's atmosphere, which may be at a temperature of about 100,000°K near the earth. So we can agree that the outer region is hot from its proximity to the sphere of Fire, though it is only in the last twenty years that this concept has become fashionable again. (For example, Jeans (1925), in developing his theory of the outermost atmosphere, took the temperature as − 53°C).

My second glimpse, from the eighteenth century, is provided by Erasmus Darwin, whose contributions to meteorology are not as well known as they might be, probably because he hid them away among the hundreds of pages of notes to his poem *The Botanic Garden* (1789-91). Darwin also divided the atmosphere into three zones (Fig. 2) : the first was the region where clouds form, up to a height of 4 miles, he estimated; the second extended from here up to the level where density was 1/3,000 of that at sea level, about 35 miles, as we now know; the third and outermost region,

> 'Where lighter gases, circumfused on high,
> Form the vast concave of exterior sky'

was, he believed, composed of hydrogen, then only recently discovered. Although he placed its base far too low, Darwin's outer region corresponds well to what we now call the hydrogen exosphere. This view has finally returned to favour only in the last few years : previously it was thought that all the hydrogen had escaped because of the high temperatures; now it is believed to be continually replenished either from the sun's atmosphere or through the decomposition of terrestrial water vapour by solar ultra-violet light. Each of these old theories thus provides one correct feature which we failed to recognize until recently.

The modern picture of the atmosphere is more complex, and rather controversial : there is little agreement on nomenclature (see Ratcliffe 1960), and even less on theories, so any attempt to draw a diagram of it, as in Fig. 3, is bound to provoke some dissent.

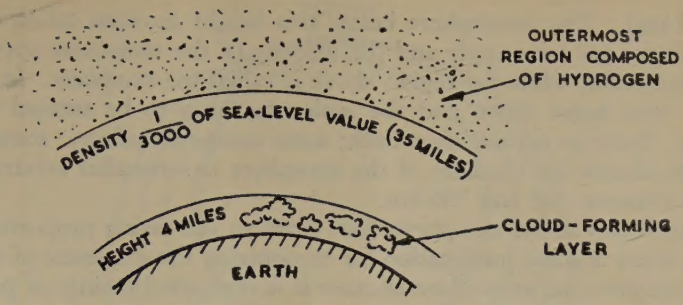

Figure 2. Darwin's picture of the atmosphere (1791) – not to scale.

Fig. 3 should, therefore, be regarded as a visual aid, rather than an authoritative record. The average atmospheric conditions – and a diagram like this can only show average conditions – are perhaps best described in terms of the temperature, which (up to heights of 100 km) does give some indication of the levels at which solar radiation is being absorbed. On climbing from sea level into the troposphere, the temperature falls fairly steadily to about 210°K at a height of roughly 10 km, then remains nearly constant in the stratosphere, up to a height of about 25 km. Above that comes an increase in temperature caused largely by ozone absorbing sunlight, to a maximum of about 280°K at a height of about 50 km. Then the temperature falls again to a minimum of about 180°K at a height of about 80 km. The region from 25 to 80 km is often (but not always) called the mesosphere. Above 80 km the temperature starts increasing, and goes on doing so : it reaches 1,200°K at 200 km and perhaps, 2,000°K at 750 km. The region from 80 km up to about 750 km is generally known as the thermosphere. In this region the electron density reaches two or three peaks, first in the E layer at about 100 km and then in the F region, which in the daytime shows two maxima at heights of about 180 and 350 km. In radio parlance the neighbourhood of the E and F layers is of course the *ionosphere*; but this is rather a misleading word, because the proportion of molecules ionized tends to increase as height is increased above the E and F layers. So meteorologists and aeronomists do well to avoid it wherever possible.

The next major division of the atmosphere is at the height where the mean free path of the molecules begins substantially to exceed the local scale height (equal to the height in which pressure drops by a factor of 2·7; the scale height is about 100 km by day at

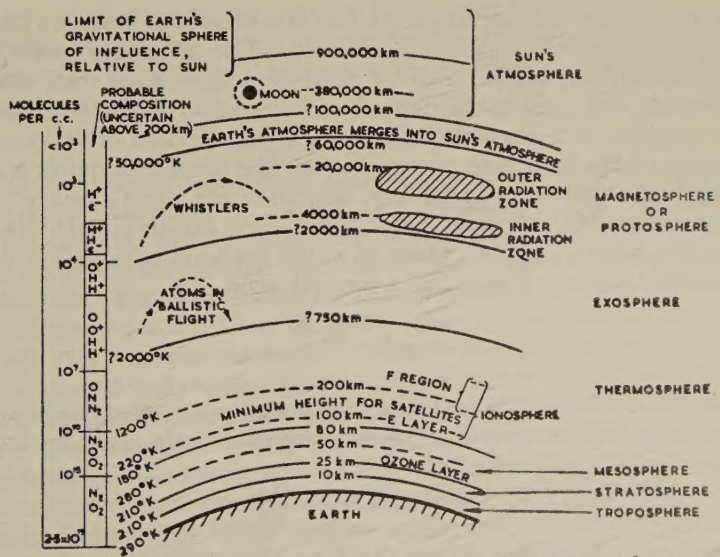

Figure 3. Diagram of the earth's atmosphere – not to scale.

a height of 750 km). The atmosphere below this height is often called the *barosphere*, because the ordinary gas laws apply and the velocity of the molecules approximates to a Maxwellian distribution; while the region above is called the *exosphere*. In the exosphere the normal gas laws break down and the molecules have to be treated like miniature ballistic missiles. Some go up and drop back; some escape to infinity; some go into orbit. The exact height chosen for the base of the exosphere is somewhat arbitrary, but it can probably be set between 500 and 750 km.

As height increases in the exosphere, ions form an increasing proportion of the total population, and there is some justification for recognizing the existence of another region called the *magnetosphere* (or *protosphere* because it is composed mainly of protons), where the earth's magnetism rather than its gravitation becomes the most important force. This region, which begins at a height of perhaps 2,000 km, is the happy hunting ground of ' whistlers ' and the home of the radiation zones. When the sun is quiet the magnetosphere extends out to at least 60,000 km. Beyond that the particles streaming out from the sun are more important than earth-born material, and the atmosphere can be said to have ended. But it is worth remembering that the earth's gravitational sphere of influence, relative to the sun, does extend much further, to 900,000 km.

The composition of the atmosphere up to the height of 200 km which I have arbitrarily taken as the base of the ' outer atmosphere ' is not so very different from that at sea level. More molecules are ionized than at sea level and some oxygen molecules become dissociated; but the average molecular weight of the air has not departed much from its ground-level value of 29 – it is probably between 22 and 25. As height increases from 200 to 500 km, however, oxygen becomes predominant over nitrogen and, since most of it is by then in atomic form, the molecular weight falls to somewhere near 16. Then, at some height above 1,500 km, the oxygen yields pride of place to hydrogen.

In describing the outer atmosphere I shall, like Erasmus Darwin and the medieval meteorologists, make a division into three regions, dealing first and most fully with heights between 200 and 750 km, where the satellites have provided a fairly clear picture; then, cursorily, with what might be called the ' neutral exosphere,' from 750 km to about 2,000 km, and with the outermost regions of charged particles.

3. The atmosphere from 200 to 750 km height, as determined from satellite orbits

3.1 Method

The usual procedure for launching a satellite into orbit is to have two phases of thrust from the motors separated by a period of coasting. The launching rocket, after a steep initial ascent, gradually reduces its angle of climb to a value such that, when the power is cut off, the missile will coast to the desired orbital height. There the final-stage motor accelerates the satellite, in a horizontal direction, to its required orbital speed.

The outcome of the launching process is that the satellite acquires a speed v, say, when travelling horizontally at a distance r, say, from the earth's centre. The satellite will move in a circular orbit if its radial acceleration v^2/r is exactly equal to the gravitational acceleration at this height, $g_0 R^2/r^2$, where g_0 is the sea-level acceleration due to gravity and R is the earth's radius. Hence, for a circular orbit,

$$v^2 = v_c^2 = \frac{g_0 R^2}{r} \quad . \quad . \quad . \quad . \quad (1)$$

If the speed slightly exceeds v_c, the satellite swings out to a greater height at the opposite side of the earth, moving in an ellipse whose semi-major axis a can be found from the energy equation,

$$v^2 = g_0 R^2 \left(\frac{2}{r} - \frac{1}{a}\right) \quad . \quad . \quad . \quad . \quad (2)$$

The point of entry into orbit then becomes the point of minimum height, the *perigee*.

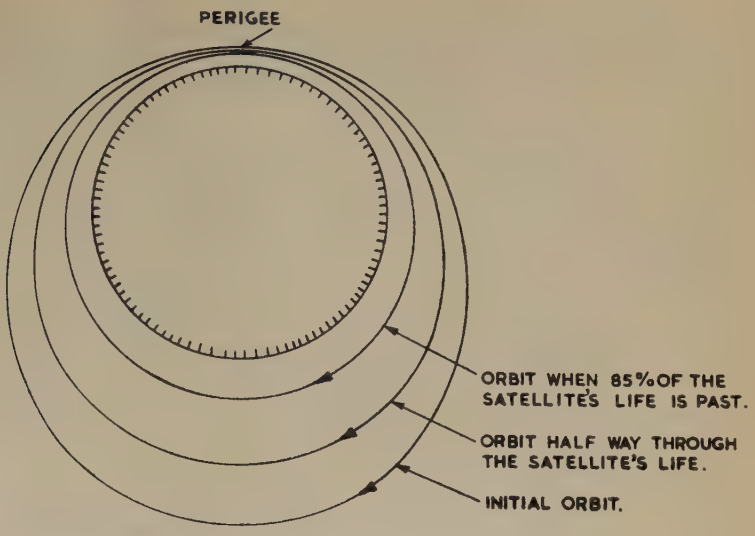

Figure 4. Contraction of satellite orbit under the action of air drag.

Most of the satellites so far launched have had appreciably elliptic orbits, rather than circular ones. Since the air density decreases rapidly as height increases, the drag acting on a satellite in an elliptic orbit rises to a sharp maximum at the perigee point, and is almost negligible except in the neighbourhood of perigee. Thus the effect of air drag is to retard the satellite slightly as it passes perigee, and consequently it does not swing out quite so far on the other side of the earth : the small decrease in v slightly reduces the value of a in Eq. (2).

Under the influence of air drag, an elliptic satellite orbit contracts and becomes more nearly circular, as shown in Fig. 4. The maximum height is steadily reduced but the minimum height, at perigee, is very little altered. By measuring the rate of contraction of the orbit – or the rate of decrease of its orbital period, which is the simplest quantity to measure – the air density at heights near that of perigee can be found if we know the weight and dimensions of the satellite. Since the perigee height remains so nearly constant, each satellite will, during most of its life, sample the atmosphere at almost the same height (within, say, 20 km of its original perigee height), and so provide a continuous ' daily weather record ' at this height, usually for many years.

In calculating the air density, we assume that the air drag D on the satellite acts in a direction opposite to its velocity V relative to the ambient air, and may be expressed in the form usual in aerodynamics.

$$D = \tfrac{1}{2} \rho V^2 S C_D \quad . \quad . \quad . \quad . \quad (3)$$

where ρ is the air density, C_D a drag coefficient, and S the mean cross-sectional area perpendicular to the direction of motion. In evaluating S, we take advantage of the fact that an uncontrolled satellite will, after quite a short time in orbit, rotate about an axis of maximum moment of inertia. It is then in the condition of least energy for a given angular momentum. The direction of the axis of rotation in space will slowly vary and is not usually known exactly. S is therefore taken as the mean of the cross-sectional areas under the two extreme modes of rotation – which, for a long, thin satellite, are tumbling end-over-end and rotating exactly like a propeller. The value of S thus obtained has a standard deviation ranging between 10 per cent, for a slender cylindrical satellite, and zero for a spherical satellite. The appropriate value of C_D for free-molecule flow, with diffuse reflexion and a molecular speed ratio of 6 to 8, is near 2·2 for rotating cylindrical and conical satellites, with a standard deviation of perhaps 5 per cent.

We assume further that at the heights where drag is most important – up to not more than 50 km above perigee height – the air density can be taken as varying exponen-

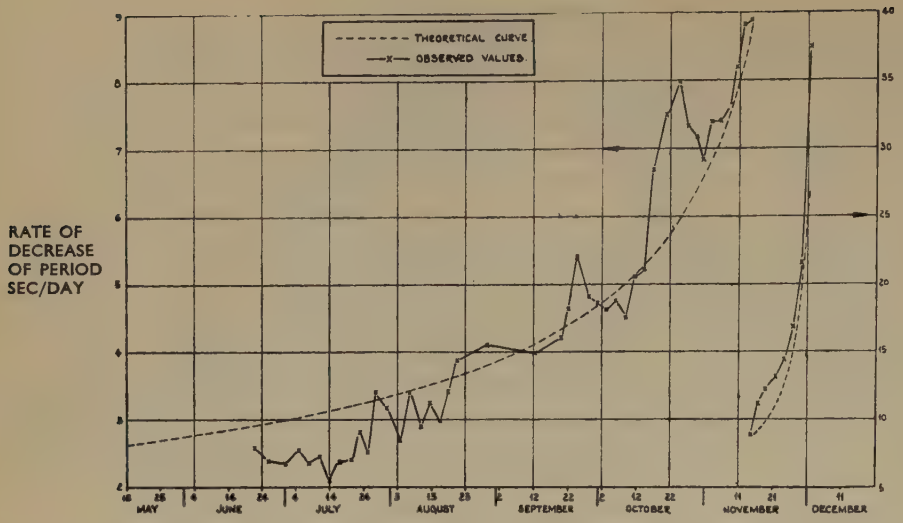

Figure 5. Rate of change of period for Sputnik 3 Rocket (1958).

tially with height y, so that

$$\rho = \rho_p \exp\{-(y - y_p)/H\} \quad . \quad . \quad . \quad . \quad (4)$$

where H is constant. H is nearly equal to what is usually called the atmospheric scale height.

Under these assumptions, the rate of decrease of orbital period, dT/dt, can with the aid of orbital theory (Cook, King-Hele and Walker 1960) be related to the air density at perigee ρ_p. The resulting expression for ρ_p in terms of dT/dt is however not very satisfactory in practice, because it is inversely proportional to $\sqrt{H}$; and at heights of 200-750 km H is subject to errors of 20-30 per cent. This difficulty can be avoided, however : if H^* is the best estimate of H, the air density ρ_A at a height $\frac{1}{2}H^*$ above perigee height proves to be insensitive to errors in H^* (King-Hele 1959). In terms of the semi major axis a and eccentricity e, ρ_A is given by

$$\rho_A = -\frac{0{\cdot}158}{\delta}\frac{dT}{dt}\sqrt{\frac{e}{aH^*}}\left\{1 - 2e + \tfrac{5}{2}e^2 - \frac{H^*}{8ae}\left(1 - 10e + \frac{7H^*}{16ae}\right) + \frac{\epsilon}{e}\sin^2 i \cos 2\omega\right\} \quad . \quad (5)$$

where $\delta = FSC_D/m$, m is the mass of the satellite, and F is a factor (lying between 0·85 and 1·15) which allows for rotation of the atmosphere. The last term takes account of atmospheric oblateness : i is the inclination of the orbit to the equator, ω is the argument of perigee (the angle from the equator to perigee, measured along the orbit), and ϵ is the ellipticity of the atmosphere, which may be taken as 0·00335. If $0{\cdot}02 < e < 0{\cdot}2$, as for most satellites, and H^* does not differ from the true value H by a factor of more than 1·5, the error in Eq. (5) is less than 3 per cent.

3.2 Dependence of upper-air density on solar activity

In Eq. (5) the quantities δ, a, e and H^* vary only slowly with time, and the air density depends primarily on the rate of change of orbital period, dT/dt. If the density were constant from day to day, the period would decrease in a smooth and regular fashion. In practice it does nothing of the sort. Fig. 5 shows the rate of decrease of period for Sputnik 3 rocket (King-Hele and Walker 1959), and the observed values are seen to fluctuate about the theoretical value (i.e., the value obtained if density is constant from day to day), thus implying that the air density departs from its average value by up to about 25 per cent.

Fig. 6 shows the variation of upper-air density during 1958 as revealed by Sputnik 2 and Sputnik 3 rocket, at a height of 200-250 km, with the gap between them bridged by

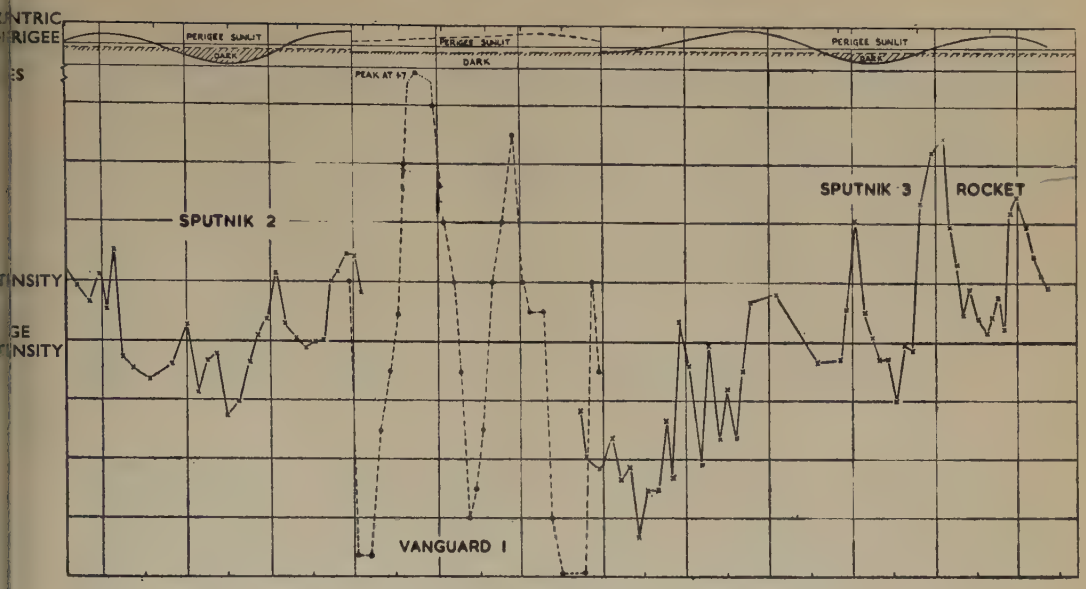

Figure 6. Variation in air density during 1958, as given by Sputnik 2 and Sputnik 3 Rocket (200-250 km height) and Vanguard 1 (650-700 km).

Vanguard 1 (height 650-700 km). The grid lines in this figure are at intervals of 28 days and it is apparent that the maximum values of density occur near the grid lines. This periodicity is particularly well defined towards the end of the year : the peaks in September, October and November are quite massive. The results from Vanguard 1, though applying to different heights and latitudes, fit in well with those from the Sputniks, but have a larger amplitude. We therefore conclude that the density showed a strong tendency to fluctuate once every 28 days during 1958 and that this was a world-wide phenomenon occurring over a great depth of the atmosphere.

The 28-day fluctuation is controlled by the sun, which rotates, relative to the earth, once every 27 or 28 days (the exact value depends on the solar latitude), and gives rise to well-known 27/28-day periodicities in geomagnetic records, cosmic rays and displays of the aurora. These latter effects can be envisaged as due to streams of particles which shoot out from the sun and rotate with it, rather like the spray from a revolving water-sprinkler, and sweep across the earth at intervals of about 27 or 28 days. The periodicity is not infallible or exact, since the source of disturbance on the sun may shift in position or intensity, but a tendency towards a 28-day recurrence is usually detectable. Several

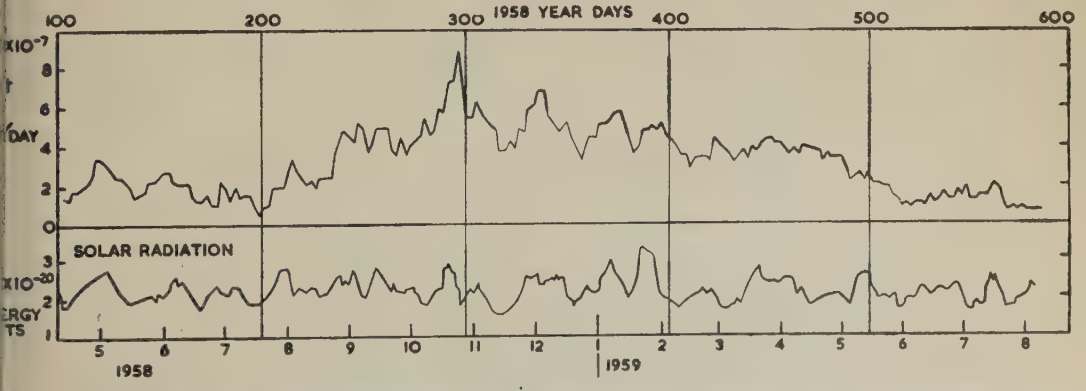

Figure 7. The rate of decrease of period $-\dot{T}$, for Vanguard 1, compared with solar 10·7 cm radiation (after Jacchia, *Smithsonian Ast. Obs. Spec. Rpt.* 29, 1959).

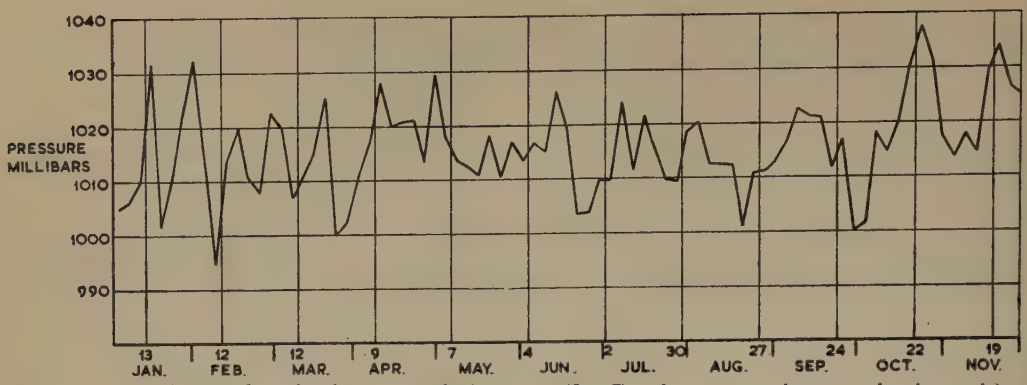

Figure 8. Variation of sea-level pressure during 1958 (for Croydon, averaged over 4-day intervals).

comparisons between solar radiation energy on wavelengths from 3 to 20 cm and the air density as indicated by satellites have confirmed the hypothesis of solar control. Fig. 7 shows on one diagram the rate of decrease of orbital period for Vanguard 1 (which is a measure of the air density) and the solar radiation on a wavelength of 10·7 cm, adapted from results given by Jacchia (1959). The agreement in detail between the two records, though imperfect, is probably as good as can ever be expected in a solar-terrestrial link.

To summarize, the atmosphere at heights between 200 and 750 km can be said to respond vigorously to the changing flux of solar radiation. When the sun is most active, the density and temperature are at their highest.

It is not yet certainly known how the sun exercises its powerful control over the upper atmosphere. At present the most likely mechanism seems to be the heating of the air at heights of about 200 km through the absorption of solar radiation, in the far ultra-violet or X-ray region, though streams of particles from the sun and conduction down from the solar corona may play some part.

Meteorologists may well ask whether there are any traces of this solar control at sea level. One answer to this question is provided by Fig. 8, which gives the sea-level pressure for 1958, with the same 28-day grid as in Fig. 6; the values, for Croydon, are taken from Whitaker's Almanack (1959-60), since these are apparently the only daily values published in list form, and are averaged over four-day intervals. There is no obvious indication of a 28-day periodicity in Fig. 8, though it is of interest that the clearest periodicity in the upper-air densities, in October and November, is almost exactly paralleled by the sea-level pressure; and for both quantities the maximum value during the year is attained on October 23.

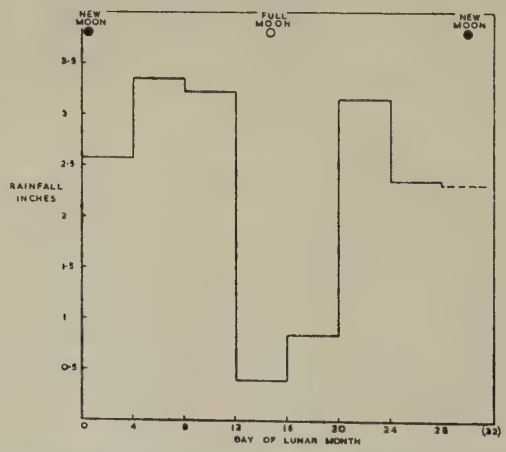

Figure 9. Rainfall during 1807, summed over 4-day intervals in each of 14 lunar months (after Luke Howard, *Climate of London*).

A convenient second answer to the question comes from Luke Howard's famous book *The climate of London* (1818-20). Howard classified his observations in lunar months, and he found that in 1807 the rainfall and pressure showed a striking 29-day periodicity, with high pressure and low rainfall near full moon. Fig. 9 shows the total rainfall during 14 lunar months from December 1806 to January 1808, distributed into seven 4-day intervals in the lunar month. Thus, each block represents the rainfall for 56 days, and the very low values for the days near full moon do undoubtedly demonstrate a 29-day periodicity during 1807.

Alleged periodicities are a recurrent bugbear for meteorologists, and I do not wish to advocate another; but the discovery that the upper atmosphere is under solar control does provide at least a semi-scientific reason for the occasional 28-day (or 29-day) periodicities in weather which have been found in retrospect by Howard and no doubt others; and we may perhaps even be persuaded to look a little more charitably upon the erroneous belief that the moon influences weather. However, the link between upper and lower atmosphere is at best only a tenuous one.

The dependence of upper-air density upon solar activity also implies that, in addition to the day-to-day variations in density, there will be a slower change in the course of a sunspot cycle. The average annual density should be much lower at sunspot minimum than at the maximum (see § 3.5) and the day-to-day variations will also be smaller at the sunspot minimum than those shown in Figs. 5 and 6.

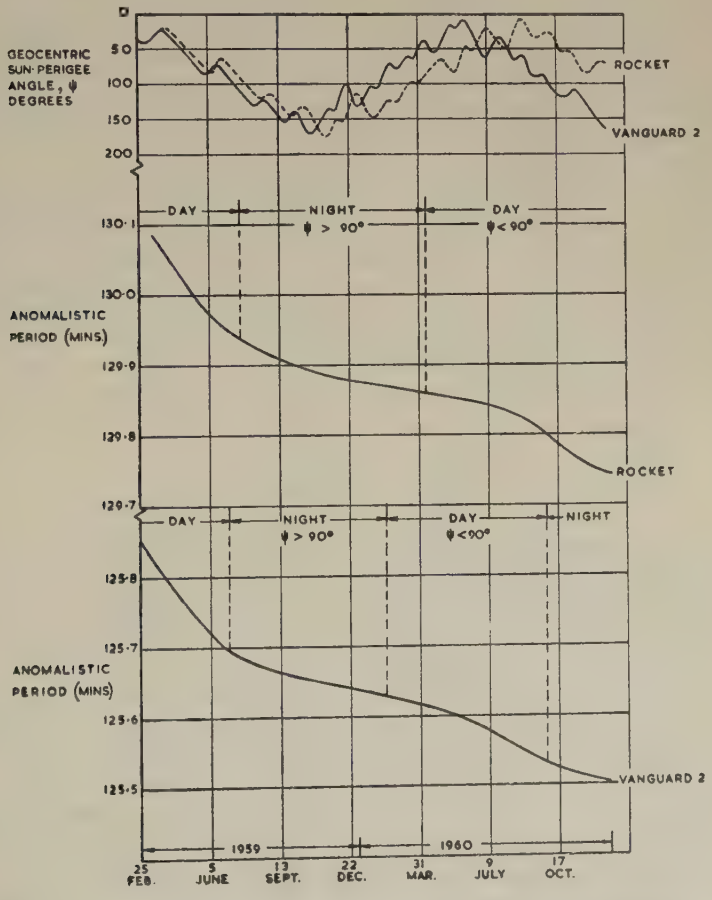

Figure 10. Orbital period and geocentric sun-perigee angle for Vanguard 2 and Rocket.

3.3 Changes in air density between day and night

At a height of 200 km, the difference in density between day and night is quite small, the density being about 10 per cent higher by day. But, as height increases, this day-to-night variation becomes steadily more important, until at heights between 400 and 750 km it is the most important feature of the atmosphere. The effect is displayed very clearly by satellites, because their perigee points move slowly relative to the sun, taking at least two months, and sometimes several years, to go through a complete day-to-night cycle. Since the air density is reflected primarily by the rate of change of orbital period, any differences in density between day and night should reveal themselves by changes in the slope of the period-versus-time curve.

Fig. 10 shows the variation of period with time for Vanguard 2 and its rocket, which have perigee heights of 560 km : the curves clearly have a steeper slope by day than by night, and the maximum day-time slope exceeds the minimum night-time slope by a factor of about 8. The air density therefore varies between day and night by a factor of about 8 at heights near 600 km. The density attains a maximum in the early afternoon, then falls gradually, reaching its lowest ebb just before dawn and rising again during the morning.

Results from many other satellites have unanimously confirmed that the density is much higher near noon than at night. Fig. 11 shows the variation of period with time for seven satellites (King-Hele and Walker 1960); for all, the slope has a maximum by day.

These strong variations in density also imply that the air temperature is much higher by day than by night at heights above 400 km. For, since the rate of decrease of density, $-d\rho/dy$, is inversely proportional to the temperature, high temperatures and high densities tend to go together. At a height of 600 km the maximum daytime temperature is probably about 1,800°K and the minimum night-time temperature about 1,000°K (see § 3.6). The day-to-night changes can be interpreted as due to heating of the upper atmosphere by solar radiation during the day, a hypothesis which seems almost too plausible to be true; but it probably is true, although the details remain obscure.

The variation of density between day and night, which depends on the *position* of the sun, is quite distinct from the first solar effect, the link between air density and solar *activity*. The two effects occur independently : at heights above 400 km the contours of constant density are raised into a permanent hump on the sun-facing hemisphere of the earth, while all the density contours, on both dark and sunlit hemispheres, pulsate up and down in response to solar activity.

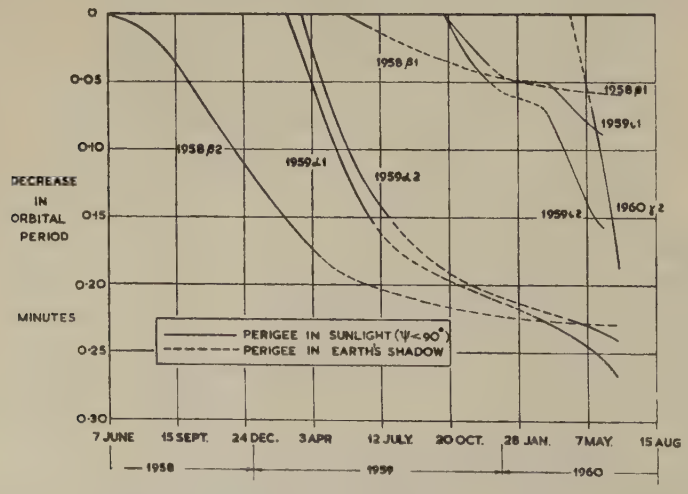

Figure 11. Decrease in orbital period for satellites with perigee heights of 360-700 km.

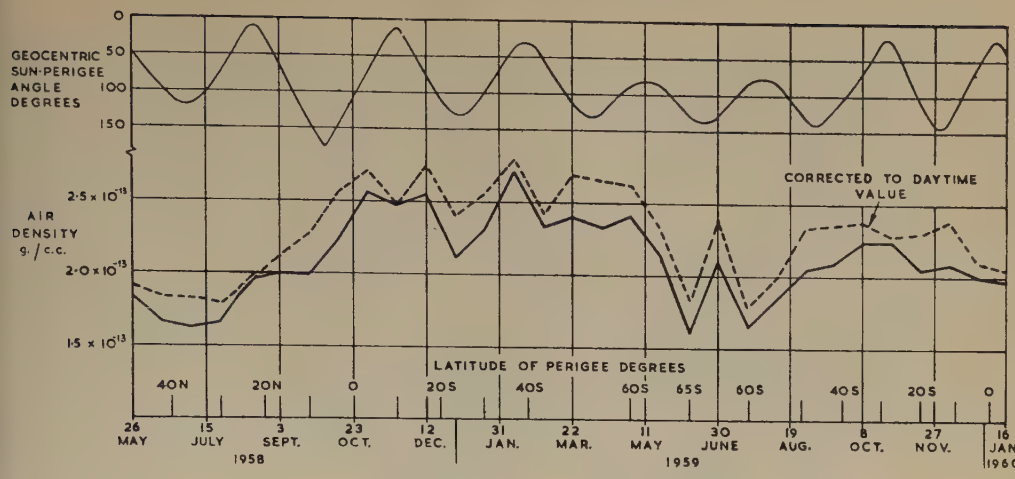

Figure 12. Air density at height of 235 km, as given by Sputnik 3.

3.4 Other variations

Direct measurements of air density by research rockets suggested that there might be wide variations of density with latitude or season, perhaps by a factor as high as 5 at heights of 200-300 km. But the results from satellites have shown that at these heights the density does not depart from its average value by more than 25 per cent and that most of this variation is due to solar effects. Some of the best evidence on this question has come from Sputnik 3, whose perigee point moved slowly from latitude 50°N to 65°S and then back to the equator. Fig. 12 shows air density at a height of 235 km from Sputnik 3 at dates between May 1958 and January 1960. When a correction is made for the day-to-night effects, as shown by the broken line, the density is found to depart from its mean value by a factor which never exceeds 1·25, and much of the variation could be attributed to solar activity.

At heights above 300 km the density, which there depends primarily on the sun's elevation, will appear to vary with latitude and season : for example, it will be low near the poles in winter. But it would be misleading to call such effects ' variation with latitude,' since this would tacitly attribute to terrestrial geometry an effect whose true source is solar.

3.5 Average values of air density

The information from satellite orbits, as well as revealing unexpected variations in air density, which help to elucidate the forces controlling the atmosphere, has provided a detailed picture of the average air density between heights of 200 and 700 km. Fig. 13 shows results from 29 satellites at dates between 1957 and February 1961.

The first point worth noting in Fig. 13 is the excellent agreement between the results from the many different satellites, which are of widely varying shapes and sizes, and operate quite independently of each other. This is especially shown by the large group at heights below 300 km; but even here the scatter is less than it at first seems, because the density at heights of 180-300 km appears to have decreased by about 20 per cent between 1958 and 1960, in consonance with the decrease in solar activity. Most of the points above the curve in Fig. 13 refer to 1957 or 1958; most of those below the curve refer to late 1959 or 1960. It would have been possible to split the curve into two branches, one giving 10 per cent higher density and the other 10 per cent lower density; but this is scarcely practicable without increasing the scale of the diagram.

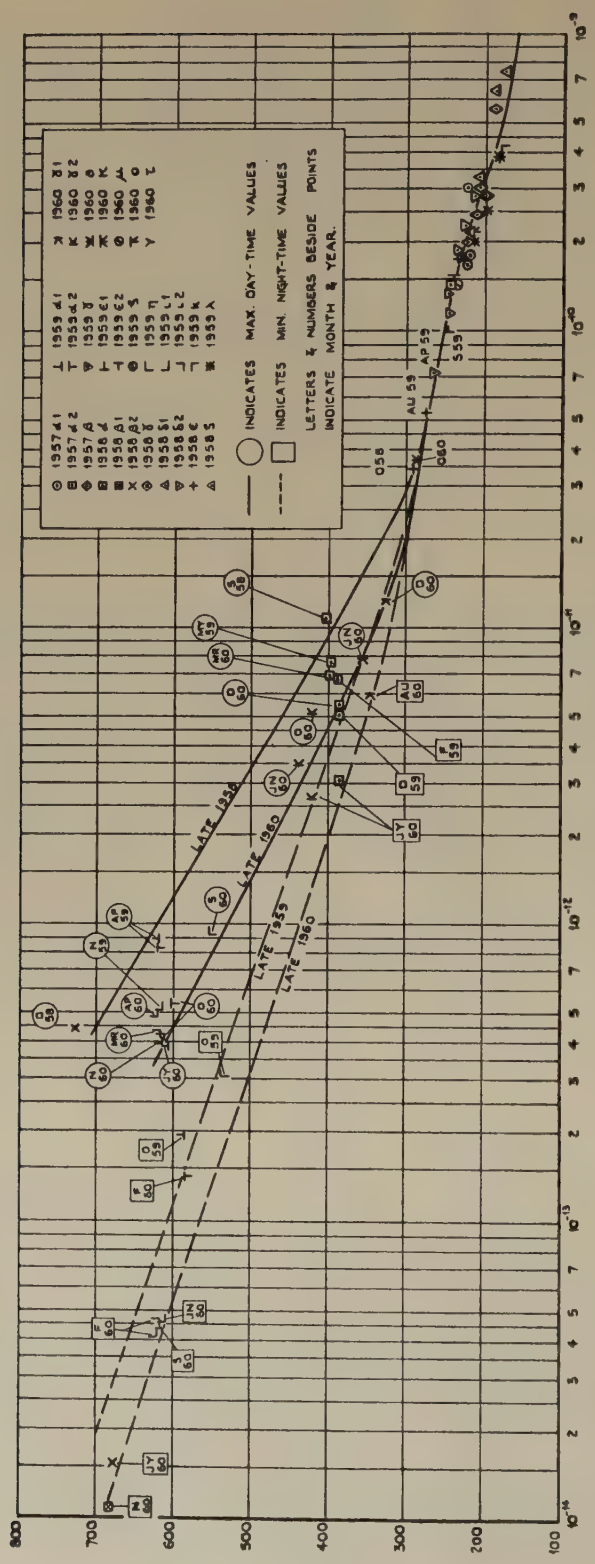

Figure 13. Upper-atmosphere density obtained from the orbits of 29 satellites launched before January 1961.

At heights above 300 km the curve in Fig. 13 is divided into four parts : the two full lines indicate the maximum day-time density at the end of 1958 and of 1960; the two broken lines show the minimum night-time density at the end of 1959 and of 1960. Each of the calculated points is labelled to show its date, and whether it refers to day or night. Once again, the points, although quite independent, fit into a consistent pattern. The group of 7 day-time points at a height near 600 km are particularly good in this respect. The curves indicate that at heights between 400 and 600 km the maximum day-time density decreased by a factor of a little over 2 between late 1958 and late 1960. The minimum night-time density decreased by a factor of slightly less than 2 between late 1959 and late 1960. The maximum day-time density exceeded the minimum night-time value in late 1960 by a factor which increased from about 2·5 at 400 km height to about 8 at 600 km : although the factor seems to have increased slightly between 1958 and 1960, this cannot be regarded as well established, since at these heights the values of density are based on very small changes in orbital period and are liable to errors of perhaps 20 per cent.

3.6 Scale height and temperature

The value of the constant H in Eq. (4) can be found from the slope of the density-versus-height curve, since $H = -\rho\, dy/d\rho$. Because of inaccuracy in measuring the slope, the values are subject to a maximum error of about 20 per cent at heights between 200 and 400 km, and to rather larger errors at greater heights. H is found to have an average value of about 45 km at heights between 200 and 300 km. At greater heights it remains near 50 km by night, but increases steadily by day, the values at 600 km being 100 km in 1958 and 90 km in 1960.

From the equation of state and the hydrostatic equation, the air temperature τ at height y may, if H is in km and $H' = dH/dy$, be expressed (King-Hele 1961) as

$$\tau = \frac{1{\cdot}18\, MHg}{(1 - H')\, g_0}\ ^\circ\mathrm{K}, \qquad (6)$$

where g and g_0 are the acceleration due to gravity at height y and at sea level respectively, and M is the mean molecular weight of the air at height y. Unfortunately M is not known exactly at heights above 200 km; but, taking $M = 25$ at 200 km decreasing to $M = 16$ at 500 km (where atomic oxygen is preponderant) and constant thereafter, the temperatures obtained are, by day, 1,200°K at 200 km rising to about 1,800°K at 600 km, and by night a near-constant value of about 1,000°K. These values are liable to maximum errors of about 25 per cent because of the errors in H and M.

4. The neutral exosphere

When the mean free path of the air molecules exceeds $2H$, the upward-moving neutral molecules rarely suffer further collisions, because by the time they have covered a distance equal to their mean free path, the density has decreased by a factor of 7 and the chance of collision is greatly reduced. The molecules then proceed upwards on ballistic trajectories; most of them are moving at speeds much slower than escape speed, and after a brief excursion aloft they fall back into the thicker atmosphere; but a few escape from the earth altogether, some suffer ionization, and others are deflected into satellite orbits by chance collisions. Under these conditions the familiar results of the kinetic theory of gases become invalid, and it is useful to have a separate name, the *exosphere*, for this region of the atmosphere. The height chosen for the base of the exosphere is rather arbitrary, since it merges imperceptibly into the regions below it, but a height between 500 and 750 km would probably be acceptable to most of the theorists on this subject. Since the results from satellites have already taken us to 750 km, it will be convenient here to regard that as the lower limit of the exosphere.

Observational results on the physical properties of the neutral exosphere are sparse : we enter the realms of theory and conjecture. The theory of the exosphere was developed in some detail by Jeans (1925) and modified by Spitzer (1952); but they assumed both a Maxwellian velocity distribution and the conventional gas laws, assumptions which Öpik and Singer (1959-60) have shown to be invalid. Öpik and Singer note that, in the absence of collisions, the assumption of local thermodynamic equilibrium which underlies the hydrostatic equation is unfounded, and the concept of gas pressure balancing gravitation has no meaning. Also, at great heights the particles tend to stream outwards in a nearly radial direction, and so their velocities, as well as being non-Maxwellian in magnitude, are non-isotropic in direction. Öpik and Singer show how the density of a particular component falls off with height; but since the composition at the base of the exosphere is not known at all precisely, the composition at higher levels remains very uncertain.

At the base of the exosphere, neutral atomic oxygen is the main component; but it loses this leading role at a height of perhaps 1,500 km, according to Singer (1960). At the height of 2,000 km which has been arbitrarily taken here as the upper limit of the neutral exosphere, the neutral atomic oxygen is only a minor constituent, the three main ones probably being atomic oxygen ions, and atomic hydrogen in either neutral form or as protons, though it is possible that helium is also important.

Though the composition of the atmosphere remains dubious in this region, a good indication of its density has been obtained from the contraction of the Echo satellite's orbit, and by deduction from the behaviour of the radiation zones. The number of atoms (or ions) per cm^3 falls from about 5×10^5 at a height of 1,200 km to about 5×10^4 at a height of 1,600 km. The air density, expressed relative to sea-level density, as in Fig. 13, is about 10^{-14} at 1,200 km and 10^{-15} at 1,600 km.

5. The protosphere, or magnetosphere

At heights above about 2,000 km – again the exact figure is dubious – the atmosphere appears to consist mainly of protons and electrons. We have already noticed the growing importance of protons as height increases in the neutral exosphere; but electrons have not been mentioned, because at heights below 2,000 km they form such a trivial proportion of the total mass. The electron density reaches a peak value of about 2×10^6 electrons per cm^3 in the F region at a height of about 300 km, where the total density is about 10^9 molecules per cm^3. So the proportion of molecules ionized is there very small. At heights above 300 km the electrons decrease in density, but do so more slowly than the heavier particles; electrons therefore form a steadily increasing proportion of the total, until at heights above 2,000 km they share the leading place (numerically, not by mass) with protons.

Since charged particles interact upon each other without a direct collision, their effective cross-sections are much greater than those of neutral particles and their mean free paths correspondingly smaller. As height increases, however, their mean free paths also eventually become large, and at heights above 2,000 km it is fair to regard the atmosphere largely as a cloud of charged particles let loose in a vacuum, pervaded by a magnetic field.

At present the general density of electrons in the magnetosphere can best be determined from the behaviour of whistlers, the radio waves which travel from one hemisphere of the earth to the other along lines of magnetic force; and, even before the advent of satellites, the whistlers showed that the atmosphere extended out to a height of at least 30,000 km. The results from whistlers suggest that the electron density decreases from about 3×10^4 per cm^3 at 2,000 km to about 10^3 per cm^3 at 10,000 km height (Allcock 1959). From here outwards there is, by and large, a steady decrease in the number of protons and electrons towards the interplanetary particle-density, which is probably in the neighbourhood of 100 particles per cm^3, though this is very uncertain.

The qualification ' by and large ' in the previous sentence covers a multitude of singularities and exceptions. The outer atmosphere is being bombarded from above by cosmic rays and from below by the debris reflected back after their impact on the lower atmosphere. It is also being bombarded by the streams of charged particles shooting out from the sun, which at times of severe solar disturbance play havoc with the outer reaches of the atmosphere.

Figure 14. The zones of radiation round the earth, as first determined in 1958-9 (after King-Hele 1960).

These extraneous high-energy particles have served to form the two famous radiation zones : the inner zone was discovered by the Explorer 1 satellite early in 1958, and the outer was first charted by Pioneer 3 in December 1958 and Lunik 1 in January 1959 (see Fig. 14). The inner zone, bean-shaped in cross-section, is relatively stable in position and can be said to lie between heights of about 2,500 km and 5,000 km, and geomagnetic latitudes of 30°N and 30°S, if we take 10,000 counts per second on the Geiger tubes of Explorer 1 as the boundary contour (corresponding to an omnidirectional flux of 16,000 particles/sec. through a sphere of 1 sq. cm cross-section). The inner zone has as its most important component protons with energies of order 100 Mev, formed by the decay of neutrons in the cosmic-ray albedo (Van Allen 1960).

The outer zone of radiation is extremely variable in position and intensity, being very sensitive to solar disturbances. When first discovered, its form was as shown in Fig. 14, banana-shaped in cross-section, extending from heights of 12,000 km to 20,000 km and from geomagnetic latitude 50°N to 50°S. It is composed chiefly of electrons with energies in the range 20 to 100 Kev, which are supplied mainly by the efflux of charged particles from the sun. The supply is probably not direct, however. From measurements made by Explorer 6 and Pioneer 5 it seems that the first effect of a solar outburst is to make the outer zone ' dump ' its charged particles into the atmosphere, often producing aurorae; but then in a few days the concentration of electrons builds up to a much higher value than before the outburst, subsequently returning slowly to normal. Much more investigation of this region is needed.

It has lately become apparent, from measurements of micrometeorite impacts on various satellites, that the upper atmosphere is far more dusty than had been thought. At a height of 2,000 km the dust concentration is about 1,000 times that in interplanetary space. Whipple (1961) has suggested that the dust comes largely from material thrown up by meteorite impacts on the moon. Though this dust cloud enveloping the earth is scarcely worth more than a mention here, it may be of some significance to meteorology, as a source of condensation-nuclei.

The outer limit of the atmosphere is uncertain, and in some ways a meaningless concept. If we call the outermost atmosphere the *protosphere*, there is really no limit, because protons abound among the particles streaming out from the sun. But if we call the outermost atmosphere the *magnetosphere*, we can set its limit as that of the earth's magnetic field, which is, on average, at roughly 10 earth radii or 60,000 km when the sun is quiet. But when vigorous particle-streams from the sun impinge on the earth, the outer magnetic field, and consequently the outer limit of the atmosphere, is seriously distorted.

The values of temperature (and even its definition) are uncertain in these outermost regions; but it appears reasonable to expect a gradual transition in temperature between the earth's atmosphere and the solar corona in which it is immersed. If so, the outermost atmosphere must be at a high temperature, perhaps of order 50,000°K (Chapman 1960), and consequently the atmosphere may extend to a greater distance than previously mentioned, perhaps 100,000 km. With such high temperatures, most outward-moving protons would escape; but this loss would be largely balanced in the outermost regions by inflow from the corona, which is probably streaming away from the sun with velocities of up to 500 km/sec (Parker 1960). This outflow, the ' solar wind,' subjects the earth's outer atmosphere to a penetrating bombardment, which might well lead to higher temperatures over the sunlit hemisphere in the protosphere, just as at lower heights (see § 3.3). The solar wind also distorts the earth's magnetic field, which is compressed over the sunlit hemisphere and elongated over the dark hemisphere (Johnson 1960), so that the magnetosphere might be re-named the magneto tear-drop.

6. Conclusions

In conclusion, it is only fair to point out that most previous speculations on the nature of the outer atmosphere have proved to be entirely wrong : the same fate probably awaits my account of the exosphere and protosphere; but at heights between 200 and 750 km the picture given here should be a good approximation to the truth. In all these upper regions of the atmosphere our knowledge is growing fast, and as it grows it also becomes more meteorological, i.e., more concerned with transient phenomena and changes with time and place. We already know roughly the shape of the isobars at heights up to 700 km and how they vary with time – from day to night, and during part of a sunspot cycle.

Our situation to-day brings to mind one of Luke Howard's remarks, ' Like fishes inhabiting the bottom of an ocean, we are insensible to much of what passes over our heads.' For now, at last, we are in process of reversing this dictum, and many meteorologists will no doubt soon be emerging from their seclusion in the lowest levels of the ocean of air to explore the rougher seas above, where many of the waves have a lethal frequency, and the winds blow at 500 km/sec.

References

Allcock, G. M. 1959 ' The electron density distribution in the outer ionosphere derived from whistler data.' *J. Atmos. Terr. Phys.*, **14**, pp. 185-199.

Chapman, S. 1960 ' The thermosphere – the earth's outermost atmosphere,' *Physics of the upper atmosphere*, Academic Press, New York, London, pp. 1-16.

Cook, G. E., King-Hele, D. G. and Walker, D. M. C. 1960 ' The contraction of satellite orbits under the influence of air drag,' Pt. I : ' With spherically symmetrical atmosphere,' *Proc. Roy. Soc. A*, **257**, pp. 224-249. Pt. II : ' With oblate atmosphere ' (to be published).

Darwin, E. 1789-91 *The Botanic Garden*, Johnson, London. Pt. I : ' The economy of vegetation,' especially additional notes I, III, XII, XXV, XXXIII. Quotation : Canto 1, lines 123-4.

Heninger, S. K. 1960 *A handbook of Renaissance meteorology*, Duke Univ. Press, North Carolina, p. 40.

Howard, Luke. 1818-20 *The climate of London* (2nd ed., 3 vols., London, 1833). **1**, pp. 160-166 and **2**, pp. 4-36.

Jacchia, L. G. 1959 'Solar effects on the acceleration of artificial satellites.' Smithsonian Astrophys. Obs. Spec. Rep. No. 29.

Jeans, J. H. 1925 *The dynamical theory of gases*, (4th ed.), Cambridge Univ. Press, pp. 337-348.

Johnson, F. S. 1960 'The gross character of the geomagnetic field in the solar wind,' *J. Geophys. Res.*, **65**, pp. 3,049-3,051.

King-Hele, D. G. 1959 'Density of the atmosphere at heights between 200 and 400 km, from analysis of satellite orbits,' *Nature*, **183**, pp. 1,224-1,227.

1960 *Satellites and scientific research*, Routledge and Kegan Paul, London, p. 149.

1961 'Properties of the atmosphere, revealed by satellite orbits,' *Progress in the Astronautical Sciences I.* North Holland Pub. Co., Amsterdam.

King-Hele, D. G. and Walker, D. M. C. 1959 'Irregularities in density of the upper atmosphere : results from satellites,' *Nature*, **183**, 527-529.

1960 'Atmospheric densities at heights of 180-700 km.' Paper presented at I.A.G.A. Symposium on Aeronomy, Copenhagen.

Öpik, E. J. and Singer, S. F. 1959-60 'Distribution of density in a planetary exosphere,' *Phys. Flu.*, **2**, pp. 653-655 and **3**, pp. 486-488.

Parker, E. N. 1960 'Extension of the solar corona into interplanetary space,' *The exploration of space*, Macmillan, New York, pp. 28-34.

Ratcliffe, J. A. (Ed.) 1960 *Physics of the upper atmosphere*, Academic Press, New York, London.

Singer, S. F. 1960 'Structure of the earth's exosphere,' *J. Geophys. Res.*, **65**, pp. 2,577-2,580.

Spitzer, L. 1952 'The terrestrial atmosphere above 300 km,' *The atmospheres of the earth and planets*, Univ. of Chicago Press (2nd ed.).

Van Allen, J. A. 1960 'The geomagnetically trapped corpuscular radiation,' *The exploration of space*, Macmillan, New York. pp. 35-41.

Whipple, F. L. 1961 'The dust cloud about the earth,' *Nature*, **189**, pp. 127-128.

Whitaker. 1959-60 *Almanack*.

551.583.3 : 550.384.5 : 551.311.3 : 551.41

Climatic change through geological time in the light of the palaeomagnetic evidence for polar wandering and continental drift

By S. K. RUNCORN
Physics Department, King's College, Newcastle-upon-Tyne

Napier Shaw Prize Essay, 1959

SUMMARY

The key to the understanding of the gross changes of climate throughout geological time indicated by the geological record in the various continents depends on finding a physical method of determining latitudes in the geological past. The palaeomagnetic method seems to be the most hopeful, but for this one must assume that the average geomagnetic field is a dipole along the axis of rotation. The palaeomagnetic evidence shows this to be true for late Tertiary times – the poles derived from the mean palaeomagnetic directions of Tertiary rocks cluster about the present geographical pole and are distinctly different from the present position of the magnetic pole. There are strong theoretical grounds for believing that it has been true throughout the earth's history. The theory of the irregular fluctuations in the length of the day indicates that the rotation of the core and mantle are only weakly coupled. The electro-magnetic torque to which this coupling is ascribed is variable because of the short term changes in the geomagnetic field. These fluctuations appear to accumulate with time and so there is always a small differential angular velocity between core and mantle, probably of either sign. Therefore, to an observer fixed on the earth's crust, the earth's magnetic field is axisymmetrical when averaged over periods of the order of the secular variation, i.e., extremely small times geologically speaking.

The palaeomagnetic surveys of the various continents show systematic differences which, it appears, cannot be explained even by assuming that the earth's magnetic field was non-dipolar, though axial, in times earlier than the Tertiary. Continental drift, as well as polar wandering, must therefore be inferred.

There is a prima facie case that the latitudes thus inferred for the various continents from palaeomagnetic observations do agree with the commonly held inferences concerning the past climates of the earth made by geologists from the study of evaporite deposits, red beds, zonation of fossils, and glacial deposits. A new important check has been provided by palaeowind observations. The inference from the palaeomagnetic studies of Europe and North America that these continents were in low latitude between the Devonian and Triassic is consistent with the wind directions inferred from dune sandstones in Britain and the western United States. The consistency of the directions in the western United States over large distances seems to show that the winds were not affected by local geography.

It appears that an explanation of Continental drift involves the hypothesis of convection currents in the earth's mantle which requires that the mantle is fluid when subjected to small stresses existing for many millions of years.

1. INTRODUCTION

Since the discovery last century of the great Permo-Carboniferous glaciations of Australia, India, South America and South Africa close to the present equator, the study of the climatic changes which have occurred in the various continents throughout geological time by the methods of geology and their explanation in terms of geophysical theory present among the greatest challenges of the earth sciences. The explanation of these spectacular climatic changes is either that, owing to causes external to the earth, the climate of the globe has fluctuated to a degree unfamiliar in recent times or that the relative positions of the continents with respect to one another and to the geographical poles have varied.

As it is a plausible suggestion that the Pleistocene Ice Ages were caused by a variation in the solar radiation received by the earth, it is often supposed in geological textbooks that because such oscillations in climate of external origin can be envisaged, there is no barrier to supposing that larger oscillations in the global climate have occurred over geological time and that they present the most straightforward explanation of the great Permo-carboniferous glaciation of India and the three southern continents. But Simpson (1957) argues that extensive sea-level glaciation could not have occurred at lower latitudes than 50°. In this paper the fluctuation of climate within a short geological period (such

as the Pleistocene) will not be discussed, but the explanation for the great climatic changes seen in the geological column in each continent will be sought.

Recently a new light has been thrown upon this problem by the palaeomagnetic data which have been collected in various parts of the world. The interdependence of the subjects of palaeoclimatology and palaeomagnetism depends on the acceptance of the following proposition : that throughout geological time the mean geomagnetic field has been a geocentric dipole oriented along the earth's axis of rotation. The latitude (λ) of the site when the rock series was deposited and magnetized can then be simply calculated from the angle of inclination I of the mean direction of magnetization of the series (corrected if necessary for geological dip), according to the dipole formula :

$$\tan I = 2 \tan \lambda$$

Because of the divergence of the magnetic and geographical poles at the present time, it is necessary to state carefully how the coincidence of the mean geomagnetic axis of the earth and the axis of rotation can be deduced from our present knowledge of the geomagnetic field and the dynamics of the earth's interior.

2. The assumed coincidence of the mean geomagnetic axis with the axis of the earth's rotation

The distribution of the geomagnetic field at the earth's surface is determined by electromagnetic induction arising from convective fluid motions in the core, either a self-excited dynamo exists in the earth's core as suggested by Elsasser (1946a, b; 1947) and Bullard (1949) or the basic electric-current systems result from specific electromotive forces, such as the thermo-electric effects on the core-mantle boundary as suggested by Runcorn (1954). Runcorn (1954) argued that, as the Coriolis force could be shown by dimensional analysis to be a dominant term in the hydrodynamic equations of the earth's core, the geomagnetic field should, on the average, be symmetrical about the axis of rotation.

However, theories of the interaction between the fluid motions in the earth's core and the magnetic field have not yet been developed to make this argument mathematically satisfying. It is, however, possible to show that, even if the geomagnetic field generated in the core has a permanent non-axial component, the relative rotation of the core and mantle will cause it to be averaged out from the point of view of an observer at the earth's surface over times long compared with the period of one relative rotation of the core and mantle, which is some thousands of years (Runcorn 1959a). That the core and mantle have had, over the last few centuries, angular velocities differing by about one part in 10^8 is inferred from (a) the westward drift of the non-axial parts of the geomagnetic field and (b) the astronomical evidence of the irregular changes in the length of the day – these arguments have been summarized by Runcorn (1956c). From the westward drift it is inferred that the earth's core is, at present, rotating about 0·2% more slowly than the mantle because in large-scale magneto-hydrodynamic phenomena it can be assumed that magnetic lines of force remain fixed to moving fluid particles. Vestine (1953) has shown that the velocity of the westward drift has varied over the last 50 years in a way which correlates roughly with the irregular fluctuation in the earth's angular velocity. That this correlation implies that interchange of angular momentum between the core and mantle is continually occurring is indeed the only conclusion that can be admitted once Munk and Revelle (1952) had demonstrated the quantitative inadequacy of atmospheric, tectonic or other surface or external causes as explanations of the irregular variations in the length of the day.

It is evident that in order to establish the coincidence of the mean geomagnetic axis with the axis of the earth's rotation throughout geological time, it is necessary to show that the cause of the present differential velocity of the core and mantle is a fundamental result of the earth's dynamics which can be assumed to have been present through geological time.

The secular variation of the geomagnetic field, assumed to originate in the eddying motions of the electrically conducting fluid core, causes induced currents to flow in the lower part of the earth's mantle, which is moderately conducting (Runcorn 1955a). The electromechanical interaction of fields and current cause a fluctuating torque between the core and mantle which can be shown to be adequate to cause the irregular fluctuations in the length of the day inferred from astronomical observations in the last few centuries (Spencer Jones 1939; 1956).

Spencer Jones (1956) has described the investigations by which it has been found that the angular velocity of the earth's mantle, w, is not uniform. The annual variation will not be discussed here, as only the longer-term variations are relevant to this paper. As these variations are much too large to be explained as changes in the moment of inertia of the earth, the existence of torques which accelerate (and decelerate) the mantle must be postulated. Suppose those due to the moon's and sun's tidal effects are N and N' respectively (decelerating) whilst that due to the earth's core is N^* (taken conventionally to be accelerating). All these torques may vary with time T.

Then
$$-N - N' + N^* = +C\frac{dw}{dT} \quad . \quad . \quad . \quad (1)$$

and also
$$N^* = -C^*\frac{dw^*}{dT} \quad . \quad . \quad . \quad . \quad . \quad (2)$$

where C and C^* are the moments of inertia of the mantle and core respectively and w^* is the angular velocity of the core.

Let the mean angular velocities of the moon, sun, Mercury and Venus about the centre of the earth be n, n', n'' and n''', the masses of the earth, moon and sun be M, m and m' and the present distances of the moon and sun from the earth be c and c' respectively.

Taking moments about the centre of gravity of the earth-moon system we obtain

$$+N = \frac{Mm}{m+M}\frac{d(c^2 n)}{dT} \quad . \quad . \quad . \quad . \quad (3)$$

and Kepler's third law gives

$$n^2 c^3 = G(M+m) \quad . \quad . \quad . \quad . \quad (4)$$

where G is the gravitational constant.

Similarly for the earth-sun system we obtain

$$+N' = \frac{Mm'}{m'+M}\frac{d(c'^2 n')}{dT} \quad . \quad . \quad . \quad . \quad (5)$$

and
$$n'^2 c'^3 = G(M+m') \quad . \quad . \quad . \quad . \quad (6)$$

Then
$$\frac{dn}{dT} = -3nN/P \quad . \quad . \quad . \quad . \quad . \quad (7)$$

and
$$\frac{dn'}{dT} = -3n'N'/P' \quad . \quad . \quad . \quad . \quad (8)$$

where $P = Mm\,c^2\,n/(M+m)$ the orbital angular momentum of the earth-moon system and P' is the orbital angular momentum of the earth-sun system.

Now $(dn/dT - nw^{-1}\,dw/dT)$ is the apparent angular acceleration of the moon about the geo-centre, and $(dn'/dT - nw^{-1}\,dw/dT)$ is that of the sun about the geo-centre.

Jeffreys (1952) has shown that dn'/dT is observationally negligible. Thus if the observed minus the tabular longitudes of the moon, sun, Mercury and Venus, are δL, $\delta L'$, $\delta L''$ and $\delta L'''$ respectively, which are functions of time given by the earth's rotation, then using Eqs. (1) and (7)

$$\delta L/n = \int_0^T \int_0^T [-3\,N/P + (N + N' - N^*)/Cw]\,dT\,.\,dT \quad . \quad . \quad . \quad (9)$$

and

$$\delta L'/n' = \delta L''/n'' = \delta L'''/n''' = \int_0^T \int_0^T [(N + N' - N^*)/Cw]\,dT\,.\,dT \quad . \quad (10)$$

N and N' result from tides in the ocean and atmosphere, and have been assumed to be constant over the course of a few centuries causing a steady rate-of-change in the length of the day. The torque N^* appears to arise from interaction between electric currents in the lower part of the earth's mantle and the geomagnetic field originating in the earth's core, and this coupling will vary with the secular change of the geomagnetic field. This hypothesis is supported by the fact that the irregular fluctuations in the earth's rotation and the secular change of the geomagnetic field have a similar time scale which is not that of any other geophysical phenomenon.

Thus, over times of the order of a few hundred years, we can express Eqs. (9) and (10) as quadratic expressions in T plus a term $B\,(T)$ called the irregular variations in the length of the day.

$$\delta L = a + bT + cT^2 + B\,(T) \quad . \quad . \quad . \quad . \quad . \quad (11)$$

and

$$\delta L' = a' + b'\,T + c'\,T^2 + \frac{n'}{n}\,B\,(T) \quad . \quad . \quad . \quad . \quad (12)$$

and

$$\delta L'' = a'' + b''\,T + \frac{n''}{n'}\,c'\,T^2 + \frac{n''}{n}\,B\,(T) \quad . \quad . \quad . \quad (13)$$

and

$$\delta L''' = a''' + b'''\,T + \frac{n'''}{n'}\,c'\,T^2 + \frac{n'''}{n}\,B\,(T)\,. \quad . \quad . \quad (14)$$

where

$$c = \frac{n}{2}\,[-3N/P + (N + N')/Cw] \quad . \quad . \quad . \quad . \quad (15)$$

$$c' = \frac{n'}{2}\,(N + N')/Cw\,. \quad . \quad . \quad . \quad . \quad . \quad (16)$$

and

$$B\,(T) = (n/Cw) \int_0^T \int_0^T (-N^*)\,dT\,.\,dT$$

Spencer Jones (1939) has shown that Eqs. (11 and 14) are consistent with the observations over the past few centuries. These results, as Murray (1957) has pointed out, can be used to determine the coefficient of the term $q\,T^2$ in the longitude of the moon caused by the real angular acceleration of the moon about the geocentre. He finds a value of this coefficient q equal to $-\,11''\cdot22 \pm 0''\cdot53$ centuries^{-2}.

But Murray further obtains a value of q, derived from fitting the ancient observations in the second century B.C. by parabolic expressions in T, equal to $-\,21'' \pm 3''$ centuries^{-2}, thereby showing that the torque due to the lunar tidal friction has varied over the last 2,000 years. This consequently means that it is incorrect to fit the observations over thousands of years by a parabolic equation in T. It seems reasonable to postulate a linear change in N. Therefore $N = N_0\,(1 - \alpha T)$ where N_0 is the value of the lunar tidal torque at epoch 1900·0.

Now $N = 2q\,P/3n$, where P equals K (= 4·82) times the angular momentum of the earth and $n = 0{\cdot}55''$ sec^{-1}. Thus, over the last few centuries, N has been equal to $+\,(3{\cdot}9 \pm 0{\cdot}2) \times 10^{23}$ dynes cm^{-1}.

By Eq. (10), the coefficient of T^2 in the mean longitude of the sun attributable to the deceleration of the earth's rotation by lunar tidal friction, is found to be $(n'/n)\,(P/Cw)\,(q/3) = 0{\cdot}122\,q$.

The torque N' consists partly of an accelerating torque due to the resonance of the solar atmospheric tides. For the present day Holmberg (1952) has calculated this from the observed atmospheric pressure data and found the torque to be $3{\cdot}7 \times 10^{22}$ dynes cm^{-1} (i.e., $0{\cdot}095\ N_0$), a value which should be correct to within a few per cent. This effect will contribute $0''{\cdot}13$ century^{-2} to the observed coefficient and may presumably be thought to remain of the same order of magnitude over some thousands of years, being determined by the general mass of the atmosphere and the temperature distribution within it, which depends on the solar constant. Holmberg's discussion supposes that the present angular velocity of the earth is the result of the lunar tidal friction having reduced the angular velocity of the earth through its life to a value at which resonance between the length of the solar day and the natural period of oscillation of the atmosphere has produced an accelerating torque to balance the decelerating one. The above discussion shows that the balance cannot be an exact one over the last few thousand years but the coincidence between these periods suggests that the torques have cancelled on the average over much longer times. As Quaternary times have seen many changes of sea level, the present lack of balance between the accelerating and decelerating torques is perhaps not surprising. The lunar tidal torque is much more likely to change as Jeffreys (1952) shows this to be determined largely by shallow seas. The other part of the torque N' is the decelerating torque from the solar oceanic tides, which Jeffreys (1952) estimates to be between 1/5 and 1/3·4 of that due to the lunar tides. Let this part at all times be equal to $+\beta N$. Because of its smallness and its sign, the torque N' may either be omitted or taken into account without greatly affecting the main argument of this paper. Thus $N' = \beta N - 0{\cdot}095\ N_0$.

Consequently, the observed minus tabular longitude of the moon and sun over the last 2,000 years are given by the following expressions (omitting the correction to the longitude and mean motion at epoch as being negligible).

$$\delta L = n \int_0^{-T} \int_0^{-T} [-3\ N_0 (1 - \alpha T)/P + (N_0 (1 + \beta)(1 - \alpha T) - 0{\cdot}095\ N_0)/Cw]\, dT\, dT - \int_0^{-T} \int_0^{-T} (nN^*/Cw)\, dT\, dT$$

$$\delta L' = n' \int_0^{-T} \int_0^{-T} [(N_0 (1 + \beta)(1 - \alpha T) - 0{\cdot}095\ N_0)/Cw]\, dT\, dT - \int_0^{-T} \int_0^{-T} (n'\ N^*/Cw)\, dT\, dT$$

Let the secular acceleration terms obtained from the ancient eclipse data by Fotheringham (1920) be sT^2 and $s'\ T^2$ for the moon and sun respectively.

Then

$$S/(-q) = -(1 + \alpha T/3) + K/3\,[(1 + \beta)(1 + \alpha T/3) - 0{\cdot}095] - \int_0^{-T} \int_0^{-T} (N^*\ K/3\ N_0)\, dT\, dT$$

and

$$s'\, n/(-q)\, n' = K/3\,[(1 + \beta)(1 + \alpha T/3) - 0{\cdot}095] - \int_0^{-T} \int_0^{-T} (N^*\ K/3\ N_0)\, dT\, dT$$

$$(1 + \alpha\ T/3) = 2{\cdot}148 - 0{\cdot}465 = 1{\cdot}683$$

Therefore $$\alpha T = 2{\cdot}049$$

$$\int_0^{-T} \int_0^{-T} (N^*\ K/3\ N_0)\, dT\, dT = 1{\cdot}61\,[(1 + \beta)\, 1{\cdot}683 - 0{\cdot}095] - 2{\cdot}148$$

$$= 2{\cdot}71\,(1 + \beta) - 2{\cdot}301$$

$$= 0{\cdot}409 + 2{\cdot}71\,\beta$$

$$= 0{\cdot}409 \quad \text{if} \quad \beta = 0$$

$$\text{or} \quad 0{\cdot}951 \quad \text{if} \quad \beta = 1/5$$

$$\text{or} \quad 1{\cdot}207 \quad \text{if} \quad \beta = 1/3{\cdot}4$$

Thus it is clear that even allowing for the change in the lunar tidal friction over the last 2,000 years it is still impossible to reconcile the determinations of the secular accelerations of the moon and sun, without assuming that the irregularities of the earth's rotation, due to the coupling between the mantle and core, accumulate.

If Ω is the westward drift of the core with respect to the mantle

$$\Omega = w - w^*$$

Assuming the change takes place gradually over time T

$$[\Omega]_0^{-T} = \int_0^{-T} N^* (1/C + 1/IC_c^*)\, dT$$

$$= \frac{3N_0}{K} \cdot (0{\cdot}409 + 2{\cdot}71\,\beta) \cdot \frac{(I_M + I_c)}{I_M I_c} \cdot T$$

$$= 0{\cdot}326\,(0{\cdot}409 + 2{\cdot}71\,\beta)\ ^\circ/\text{year}$$

$$= 0{\cdot}133\ ^\circ/\text{year if } \beta = 0$$

$$= 0{\cdot}31\ ^\circ/\text{year if } \beta = 1/5$$

$$= 0{\cdot}39\ ^\circ/\text{year if } \beta = 1/3{\cdot}4$$

As the core is at present rotating more slowly than the mantle by about 0·2°/year, it appears likely that 2,000 years ago the core was rotating eastwards relative to the mantle.

The nature of the electromagnetic coupling of the core to the mantle, which gives rise to torque N^*, will now be examined. The lower part of the mantle has appreciable electrical conductivity, but the geomagnetic field originates in the more highly conducting core. From the westward drift of the non-axial parts of the field it is inferred that at the present time the core is rotating westward relative to the mantle. As a result, induced currents will be induced in the mantle even by the steady part of the non-axial field. This will cause the relative angular velocity of the mantle and core to decrease through electromagnetic damping. This part of the torque N^* will be equal to $k\,(w^* - w)$ if the time of free decay of electric currents in the mantle is short compared to the period of variation of the relative velocity of the core and mantle. Another part $\epsilon\,(T)$ will arise from the torques produced by the currents induced in the mantle by the geomagnetic field variation in the core which has an irregular time-scale of the order of decades and centuries. It will be assumed that, over a time long compared to the time of free decay of the field, the mean value of $\epsilon\,(T)$ will be zero.

Let $$Cw + C^* w^* = (C + C^*)\, w_0$$

or $$w^* = [(C + C^*)\, w_0 - Cw]/C^*$$

$$\epsilon\,(T) + k\,(w^* - w) = C\frac{dw}{dT}$$

Putting $w_1 = w - w_0$ and $\tau = CC^*/k\,(C + C^*)$

$$C\frac{dw_1}{dT} = -\frac{Cw_1}{\tau} + \epsilon\,(T)$$

Let the angular displacement of mantle at time T be θ,

then $$C\,\theta\,.\,\ddot{\theta} = -\frac{C}{\tau}\,\theta\,\dot{\theta} + \theta\,\epsilon\,(T).$$

Therefore $$\frac{C}{2}\frac{d^2}{dT^2}(\theta^2) - C\,\dot{\theta}^2 = -\frac{C}{2\tau}\frac{d}{dT}(\theta^2) + \theta\,.\,\epsilon\,(T).$$

On the average, $\theta \cdot \epsilon(T) = 0$ as $\epsilon(T)$ is as likely to be $+ve$ as $-ve$,

therefore
$$\frac{d^2(\bar{\theta})^2}{dT^2} + \frac{1}{\tau}\frac{d}{dT}(\bar{\theta})^2 = 2\dot{\theta}^2 = \frac{E}{C}$$

if
$$\frac{d\bar{\theta}^2}{dT} = x. \quad \text{Then } \frac{dx}{dT} + \frac{1}{\tau} \cdot x = \frac{E}{C}$$

$$x = \frac{\tau E}{C} \text{ as } Ae^{-T/\tau} = 0 \text{ for times much longer than } \tau.$$

Therefore
$$\bar{\theta}^2 = \frac{\tau E}{C} T$$

Thus we have represented the irregular fluctuations in the earth's rotation as a random walk with damping. This seems physically more realistic than the representation by Brouwer (1952) in terms of the simple random walk in which the mean angular displacement of the earth increases as $T^{3/2}$ from which he deduces that the determination of the true secular deceleration of the earth from ancient eclipse data must be subject to serious uncertainty. But Brouwer's analysis does not rest on any physical theory of the irregular fluctuations; it is, in fact, difficult to think of any mechanism which would give rise to a simple random walk in angle unless the earth was being bombarded by particles from random directions in space (meteorites are quantitatively inadequate for this purpose).

We thus conclude that the net acceleration of the earth over the last 2,000 years (after the tidal actions of the moon and sun on the earth have been allowed for) must arise from an interchange of angular momentum between the core and the mantle, which over the last few centuries appears as an irregular fluctuation but has accumulated over the last 2,000 years. It may therefore be reasonably held that this loose coupling of the core and mantle has always been a feature of the earth's internal dymanics and that, in consequence, the relative rotation of the core and mantle has never vanished except momentarily. The proof given above of the coincidence of the magnetic and rotational axes is, in consequence, applicable through geological time.

3. The palaeomagnetic survey of the continents

In the preceding section the relevance of the directions of the geomagnetic field in past geological time to the problem of the earth's ancient climates has been established. It will now be assumed that the directions of the geomagnetic field during various geological periods are coincident with those of the natural remanent magnetization of red sandstones and lavas of the same geological ages, corrected where necessary for geological dip and for secondary magnetization acquired since the formation of the rock.

Cainozoic rocks have been examined in many parts of the world and confirm the theoretical prediction of Section 2. Fig. 1 shows the pole positions* for various rock series plotted on the polar stereographic projection. It will be noticed that there is a marked tendency for the poles for early Tertiary times (Eocene and Oligocene) to be farther from the present pole than those of Miocene, Pliocene and Pleistocene times. Because the length of the Cainozoic is thousands of times greater than the time of free decay of electric currents in the core, the hypothesis of the coincidence of the mean geomagnetic and geographical axes is therefore very strongly supported.

Those palaeomagnetic surveys of the various continents, which are most extensive in terms of coverage of geological time, are as follows :

* The results of Cox (1957) on Eocene flows from Oregon present a difficult problem : the pole position is quite remote from any other Tertiary pole.

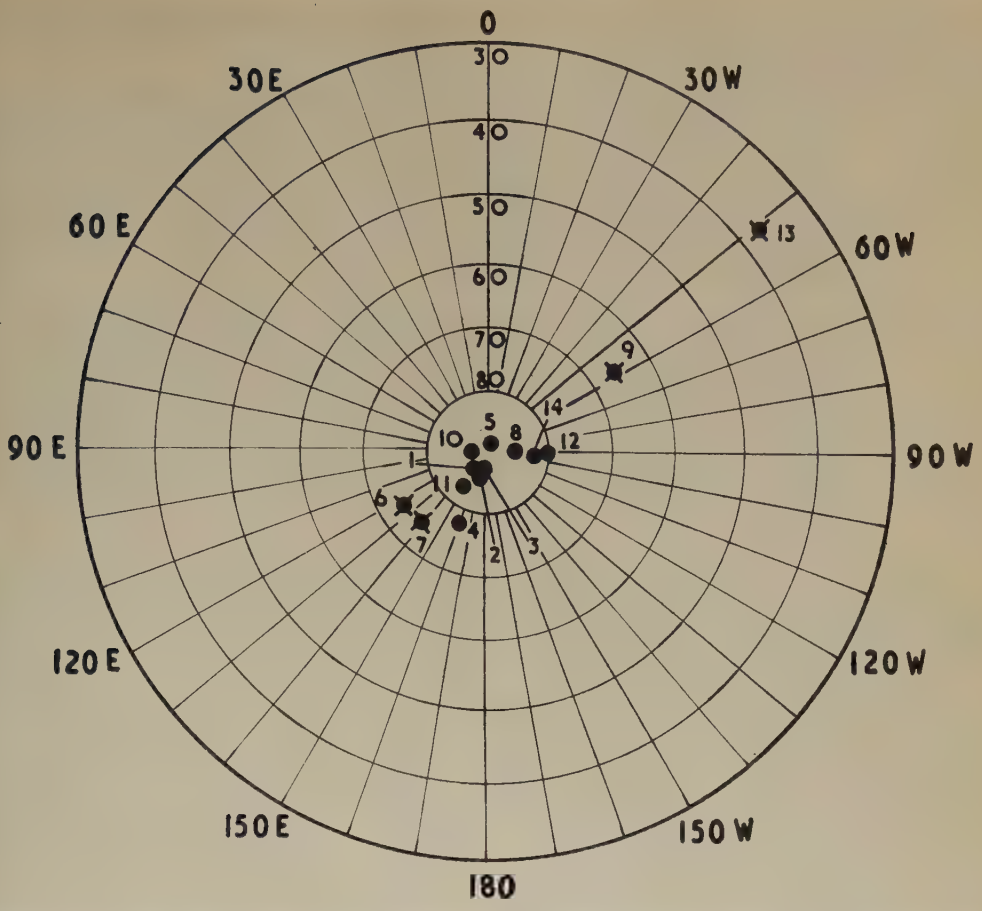

Figure 1. 1 – Recent lavas of Mt. Etna (Chevallier, R. ' L'aimantation des laves de l'Etna,' *Ann. de Phys.*, Paris (10) **4**, p. 5-162, 1925). 2 – Recent lavas of Iceland (Hospers 1955). 3 – Early Pleistocene lavas of Iceland (Hospers 1955). 4 – Plio/Pleistocene lavas of Central France (Roche, A. ' Sur les inversions de l'aimantation remanentes des roches volcaniques dans les monts d'Auvergne,' *C. R. Acad. Sci.*, Paris, **233**, p. 1132-1134, 1951). 5 – Miocene lavas of Iceland (Hospers 1955). 6 – Oligocene intrusives of Central France (Roche, A. ' Sur les caractères magnétiques du system eruptif de Gergovie,' *C. R. Acad. Sci.*, Paris, **230** p. 113-115, 1950). 7 – Eocene lavas of Antrim (Hospers and Charlesworth 1954). 8 – Newer Volcanics of Victoria (Irving and Green 1958). 9 – Older Volcanics of Victoria (Irving and Green 1958). 10 – Columbia River Basalts (Campbell and Runcorn 1956). 11 – Quaternary lavas from Argentina (Creer 1958). 12 – Cenozoic lavas from Antarctica (Turnbull 1959). 13 – Eocene lavas from Oregon (Cox 1957). 14 – Tertiary Duchesne River formation, Utah (Collinson and Runcorn 1960).

(a)	Europe (Great Britain)	Creer, Irving and Runcorn (1954); Creer, Irving and Runcorn (1957).
(b)	North America	Runcorn (1955a), Collinson and Runcorn (1960).
(c)	South America	Creer (1958)
(d)	South Africa	Nairn (1959)
(e)	India	Clegg, Deutsch and Griffiths (1956); Deutsch, Radakrishnamurty and Sahasrabudhe (1958)
(f)	Australia	Irving and Green (1958)
(g)	Antarctica	Turnbull (1959)

Determinations of other workers are in good accord with those in the above mentioned publications and are discussed in them.

There are two methods by which the results of a palaeomagnetic survey of one continent through the geological column may be displayed :

Method (1) by a ' polar-wandering curve ' for that continent, which is a plot on a projection (usually stereographic) of the present globe, of the pole for each geological period of that geocentric dipole which would give a magnetic field in the observed direction at the locality taken. The Equator and lines of latitude corresponding to the pole may be drawn in. However, if continental drift has occurred, the map will only be correct for the continent from which the data were collected;

Method (2) by drawing, on a projection of an imaginary grid of lines of latitude and longitude referred to the earth's axis of rotation, the continent in question for the various geological periods. The angle of inclination determines the latitude, and the orientation of the continent is fixed by the angle of declination D. The direction of the present geographical meridian at the site makes an angle $-D$ with the meridian on the reference projection. The ancient longitude of the continent is indeterminate from the palaeomagnetic data alone.

Blackett, Clegg and Stubbs (1960) have argued that, because both these methods assume that the mean geomagnetic field has been dipolar through geological time, the primary observational data is obscured by assumptions about the entirely distinct problem of the theory of the main geomagnetic field. They, therefore, attempt to present the data for one site (or sites close together in one continent) by plotting the angle ϕ, between the mean palaeomagnetic directions for each geological period and the observed field directions in late Tertiary times (that corresponding to a dipole along the present geographical axis). They show that ϕ increases with geological time, measured from the present, for each continent, a result parallel to that of Creer, Irving and Runcorn (1954; 1957) who show that the pole calculated by method (1) moves gradually along a smooth path over the earth's surface through geological time. Both approaches are therefore equivalent in indicating that the phenomena of rock magnetization are not likely to have been produced by causes of local origin. The quantity ϕ however has no simple relation to any parameter of world-wide significance, so that we hold that either one of the above two methods is more useful as a method of examining rock magnetism data.

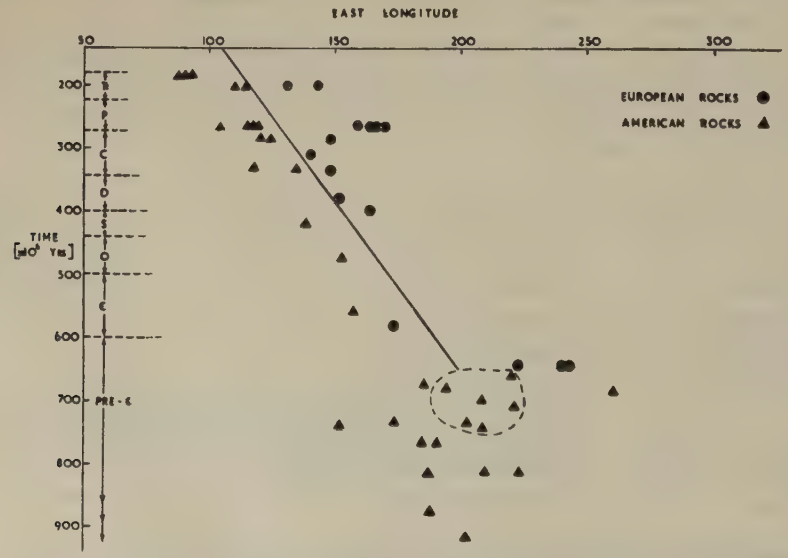

Figure 2. Longitudes of pole-positions derived from American and European rocks.

Creer, Irving and Runcorn (1954) showed that the British results plotted by method (1) are equivalent to a progression of the pole since Pre-Cambrian times at a rate of roughly $\frac{1}{3}^\circ$ per million years around what is at present the northern part of the Pacific Ocean. Runcorn (1956a) shows that this is also true for the polar-wandering curve for North America, although there is a systematic westward displacement of the North American curve relative to that for Europe estimated at 24° by Runcorn (1956b), about 40° by Du Bois *et al.* (1957) and about 30° by Collinson and Runcorn (1960). The systematic nature of the westward displacement is best shown by plotting the longitudes of the poles against time for different geological periods. Fig. 2, based on the pole positions in publications (a) and (b) shows that since the Pre-Cambrian, a straight line can be drawn dividing (with one exception) all the British from all the American results.

Accepting the various assumptions outlined above, large discrepancies between the polar wandering curves for the various continents must be interpreted in terms of continental drift. Irving and Green (1958) have shown that the polar-wandering curve for Australia lies about 180° of longitude away from those of North America and Europe. It is convenient, as is shown by Creer, Irving, Nairn and Runcorn (1958), to represent the palaeomagnetic data from Australia by method (2) : their diagram is shown in Fig. 3 and a similar diagram for South Africa derived from the results of Nairn (1959) is shown in Fig. 4. On the basis of data (c), (d), (e), (f) and (g) a reconstruction of the southern continents for mid-Mesozoic time is attempted in Fig. 5.

It should perhaps be noted that good agreement is obtained for the pole position from contemporaneous deposits from within a single continent. For example, Du Bois *et al.*, (1957) compare the pole positions from Upper Triassic rocks from the east and west of the U.S.A. and find good agreement, the ovals of confidence intersecting.

The discussion in Section 2 established that, averaged over times longer than the time scale of its secular variation, the geomagnetic field is symmetrical about the axis of rotation. The theory of the field is however insufficiently developed to determine whether it has necessarily to be that of a dipole. One might argue that for a given surface field there is minimum energy in the dipole configuration and that this would be the most likely form for the magnetic energy derived from the fluid motions in the core. Or, one could argue that the free decay time of the electric currents which produce a dipole field is longer than that corresponding to higher multipoles, so that the intensity of the dipole field is less likely to decay. These, however, are not conclusive arguments.

Earlier in this section we have shown that the palaeomagnetic evidence is in favour of the dipole hypothesis for Cainozoic time. We can legitimately speculate, however, whether the field in earlier geological periods was an axial multipole, or a combination of an axial dipole and multipole. It is easily seen that polar wandering must still be postulated to explain the palaeomagnetic evidence, but it is not immediately evident that continental drift is then required. Runcorn (1959) attempts to work out the consequences of trying to explain the discrepancies between the polar-wandering curves from the different continents by the axial non-dipole hypothesis alone.

If it is assumed that no continental displacements have occurred, the horizontal component of the mean palaeomagnetic direction at a site defines the meridian of that particular geological period. Thus if there are more than two widely separated sites at which contemporaneous palaeomagnetic directions are available, these meridians should all meet in one point, the ancient pole, within the limits of error. Runcorn (1959b) shows that the data for the Cambrian, Carboniferous, Permian and Triassic from Europe, North America and Australia enables such poles to be determined. It is then possible by plotting the angle of inclination I for a given geological period at each site against the colatitude θ of that site with respect to the pole for that period, to examine how far the geomagnetic field must be assumed to have deviated from that of a dipole. Figs. 6, 7, 8 and 9 show the plots compared with the calculated variation of I against θ for the axial dipole, quadrupole and octupole fields, the potentials of which are represented by zonal harmonics of order $n = 1$, 2 and 3 respectively. It is seen that the actual palaeomagnetic results have to be represented by a curve which varies more rapidly with θ than any of these.

Figure 3. Position of Australia through geological time (stereographic projection centred on ancient pole of rotation).

PPR Pleistocene, recent
E Eocene
J Jurassic
TR Triassic
P1, P2 Permian (two separate determinations)
C Carboniferous
D Devonian
S Silurian
ϵ1, ϵ2 Cambrian (two separate determinations)
Pre ϵ3 Top of Upper Proterozoic
Pre ϵ2 Upper Proterozoic
Pre ϵ1 Lower part of Upper Proterozoic

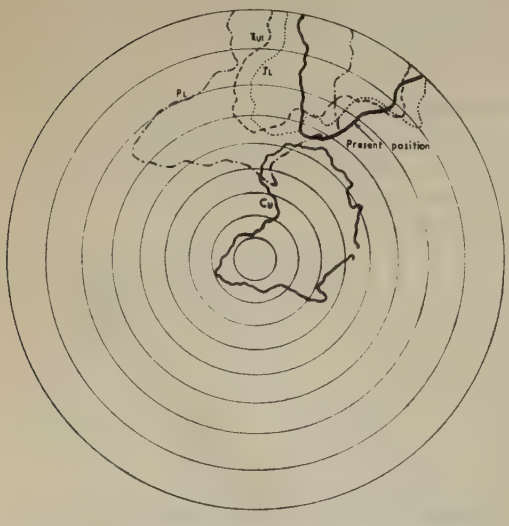

Figure 4. Positions of Africa since late Palaeozoic (stereographic projection centred on ancient pole of rotation).

JL Lower Jurassic
TRU1 Upper Triassic
PL Lower Permian
CU Upper Carboniferous

Figure 5. Attempted reconstruction of the continents of South America, Africa, India, Australia and Antarctica for mid-Mesozoic time (stereographic projection centred on ancient pole of rotation).

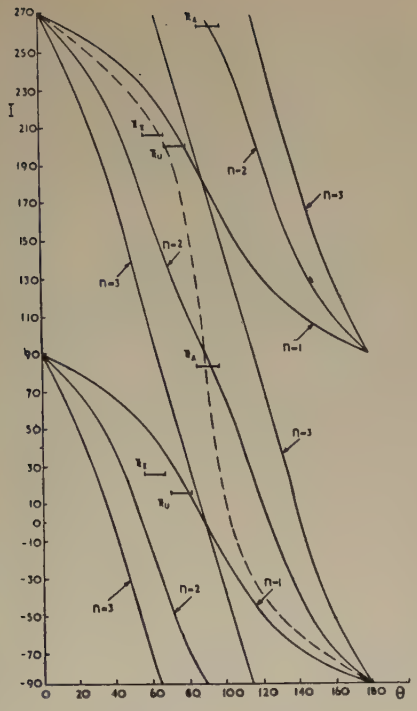

Figure 6. Triassic.

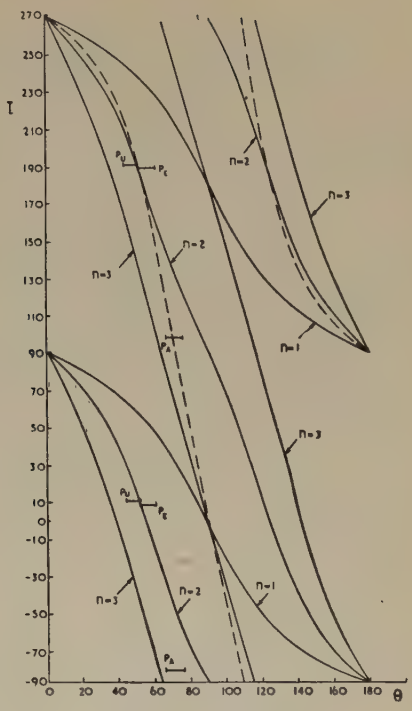

Figure 7. Permian.

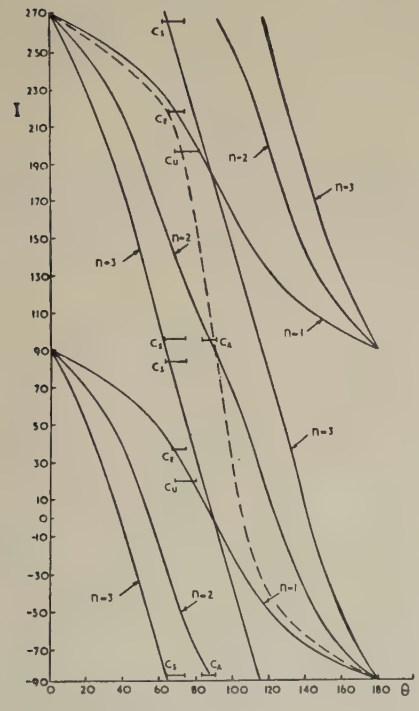

Figure 8. Carboniferous.

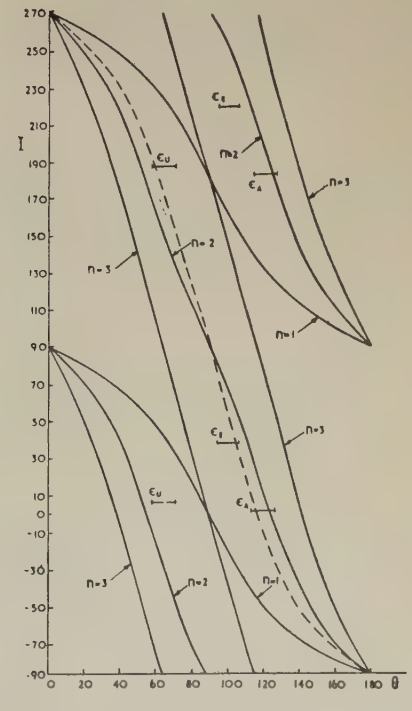

Figure 9. Cambrian.

Figures 6, 7, 8 and 9. Observed variation of angle inclination (I) with colatitude (θ), assuming no continental drift. (Key to suffixes. U – N. America; A – Australia; E – Europe; S – South Africa).

In Figs. 6, 7, 8 and 9 the broken curve is the simplest smooth curve which will satisfy the observations in the three continents of Australia, Europe and North America. The Carboniferous data from South Africa cannot be satisfied (see Fig. 8), but is based only on a small number of samples. If it is assumed that an axial field with non-dipole components existed in the various periods of the Mesozoic and Palaeozoic, it is evident that the field distribution must have been the same in the two hemispheres. Mathematically, this means that the field must have a scalar potential which is either a series of spherical harmonic terms of odd degree only or of even degree only. The former implies that, at the same latitude north and south of the Equator, the angles of inclination are equal but opposite in sign and the angles of declination both equal, whereas in the latter case the angles of inclination are equal and have the same sign while the angles of declination are 180° apart. The broken curves for the Triassic, Carboniferous and Cambrian correspond to even harmonics and in the Permian to odd harmonics.

We conclude, therefore, that if continental drift is to be abandoned in favour of the hypothesis that the mean geomagnetic field has had for long periods in the past higher harmonic components, then the field consisted of even harmonics only in the Cambrian, Carboniferous and Triassic and of odd harmonics in the Permian and in the late Palaeozoic and Mesozoic it had an extraordinarily large variation of I with θ. A small fourth harmonic in the Cambrian and a larger one for the Carboniferous and Triassic have to be assumed in addition to the second harmonic. For the Permian a mixture of first and third harmonics is necessary.

However, the fatal objection to this interpretation of the data for the Carboniferous, Permian and Triassic is that Australia is placed in latitudes less than about 20°. This is, in fact, in contradiction to the palaeoclimatic data which will be reviewed in the next section. There is perhaps no insuperable obstacle to explaining the Cambrian palaeomagnetic results without continental drift by assuming a non-dipole field, but the logical position for doing so is destroyed if it cannot also be done for the later periods. The palaeomagnetic surveys of the other continents will, of course, enable the non-dipole hypothesis to be tested more rigorously.

4. Geological evidence of palaeoclimates

Geologists, in inferring the climates of the remote past, have recognized climatic zones similar to those of the present time. The following four zones may be recognized in the geological column by the following features in the sedimentary deposits :

(a) *Tropical zone* : plants without growth rings, laterites, coral reefs, abundant and varied fauna, red beds*, thick limestones

(b) *Arid zone* (*tropical and mid-latitude deserts*) : dune bedded sandstones, thick evaporite deposits and red beds*

(c) *Temperate zone* : tree-rings, temperate coal-seams without laterites

(d) *Polar zone* : glacial tillites, scratched erratics and striated pavements, paucity of fossils.

Oscillations, or permanent changes, in the earth's climate may alter the latitudinal extent of the zones, perhaps with the disappearance of one or more of them, and distortion of the zones due to local geography may occur, but it seems likely that the rough symmetry of the zones about the earth's axis of rotation and the decrease of temperature with increase of latitude must have persisted throughout geological time. Therefore it should be possible to examine whether the climatic zone inferred in a continent for one geological period is in agreement with the latitude inferred from palaeomagnetic observations from contemporaneous deposits in the same continent.

* Certain geologists hold that red beds are derived from laterite soils indicating an origin in a tropical climate, in contrast to the earlier view that they represent deposition in an arid climate.

We begin by noting that geologists are in agreement that no appreciable change in climatic zoning occurred during Cainozoic times except that the general climate then was warmer than at present (Durham 1952). This is in good agreement with the palaeomagnetic data for the Tertiary discussed in Section 3.

The palaeoclimatic method is too qualitative to test the possibility of small amounts of continental drift and polar wandering having occurred since the early Tertiary, for which Irving and Green (1957) and Hospers and Charlesworth (1954) find evidence from volcanic lavas.

The main inferences from the geological record on the past climate of the different continents are not in dispute and are set down in the various textbooks of historical geology (e.g., Dunbar 1949). There is general agreement in rejecting, for this purpose, isolated occurrences of the various climatic indicators. Thus the Permian Squantum tillite near Boston and numerous other isolated examples of supposed glacial remains, such as are recorded by Coleman (1923), are either thought to be mistaken interpretations or the result of mountain glaciers.

The evidence for the principal glaciations is as follows :

(1) Pre-cambrian

(a) *Canada.* The Huronian (Gowganda) tillite of the southern Canadian shield of lower Proterozoic age. The polar-wandering curve given by Creer, Irving and Runcorn (1957, p. 147) begins in the south-east Pacific in late Pre-Cambrian times (the earliest poles being based on the Beltian and Grand Canyon series). The Huronian glaciation is older than the latter, so extrapolating the polar-wandering curve back in time (which it is reasonable to do, for it is fairly smooth throughout geological time), we see that it is possible that Canada was close to the Pole at this time.

(b) *Australia.* Tillites and varved sediments of the Adelaidian system and outwash gravels of the Nullogine lavas (Upper Proterozoic) (David 1950). The proximity of Australia to the pole at this time on palaeomagnetic evidence is shown in Fig. 3.

(c) *South Africa.* Numees tillite in south-west Africa (late Proterozoic). Gough (1956) gives for the Pilansberg dykes of late Pre-Cambrian age a pole position in Abyssinia; the age of these dykes has recently been determined as 1290 million years (Schreiner 1958), but the age-relation between the tillite and the dykes is not known.

(2) Permo-carboniferous

(a) *Australia.* Kuttung Series (Upper Carboniferous) (David 1950). The palaeomagnetic data show that Australia was close to the pole in Permian and Carboniferous times as shown in Fig. 3.

(b) *South Africa.* Dwyka tillite, Union of South Africa and Rhodesia (Upper Carboniferous) (Du Toit 1939).

South Africa was near the pole in Carboniferous times as shown in Fig. 4.

(c) *South America.* (Jenks 1956). Tubarão series of Brazil.

(d) *India.* Talchir tillite (Krishnan 1956). No palaeomagnetic data are yet available for South America and India for these geological periods, but Jurassic reconstructions of the southern hemisphere land mass suggest that the four continents had previously been close together (Fig. 5), and therefore in high latitude in the late Palaeozoic.

The evidence for the principal regions of warm climates is as follows :

(a) Lower Palaeozoic era

(1) *Europe and North America* (Dunbar 1949)

(*i*) *Cambrian.* Limestones and dolomites are extensive in the deposits of this period in Quebec, Newfoundland, NW. Scotland and N. Greenland.

(*ii*) *Ordovician.* Coral reefs with the same species occur in New Mexico, Wyoming, Alaska, Manitoba, N. Greenland and arctic Canada. Limestones also occur extensively.

(*iii*) *Middle Silurian.* Identical species in coral reefs occur in southern U.S.A., New York, Hudson Bay and N. Greenland. Limestones and dolomites also occur extensively. Invertebrates (cephalopods) are widely distributed in Europe and throughout N. America. There are also striking similarities between brachipods found in Britain and Scandinavia and eastern N. America in the lower and middle Silurian.

(*iv*) *Late Silurian.* Extensive deposits of salt and gypsum show that desert conditions existed in eastern North America.

Fig. 10 shows the positions of the two continents with respect to the equators, 60°N, 20°N and 20°S lines of latitude for Cambrian, Ordovician and Silurian times drawn on a polar stereographic projection of the northern hemispheres with America moved 24° eastwards in longitude. It is evident that the distribution of fossils and other indicators, which is puzzling if referred to the present globe, is close to the equators at these times, given by the palaeomagnetic data.

(2) *Australia* (David 1950)

Extensive occurrence of thick limestones. Spjeldnaes (1961) concludes that the Ordovician faunas of Southern Australia, especially the cephalopods, were tropical. Fig. 3 shows that the palaeomagnetic data place Australia in low latitudes at this time.

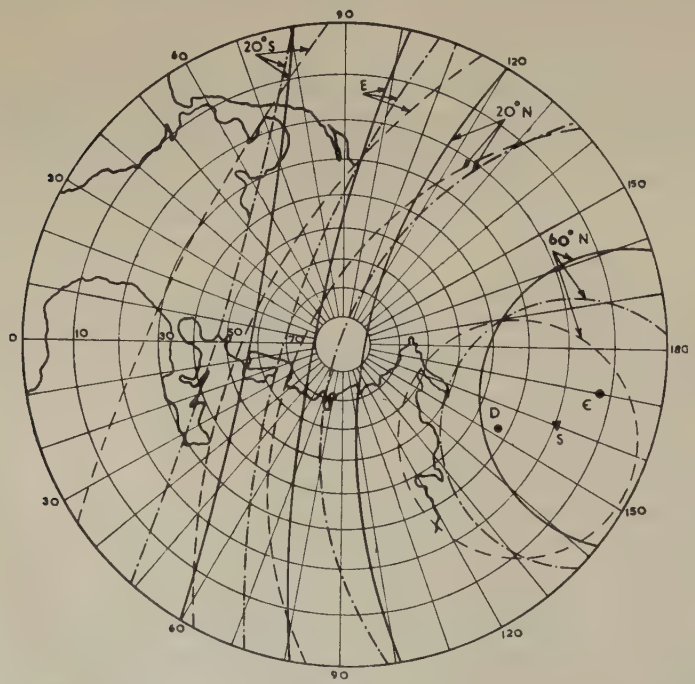

Figure 10. Stereographic projection of present Northern Hemisphere showing pole positions 20°N., 20°S., latitude lines and Equator for the Cambrian, Silurian and Devonian; Europe and N. America being 24° closer than at present.

(b) Upper Palaeozoic era

(1) *Europe and North America* (Dunbar 1949)

(*i*) *Devonian.* Extensive coral reefs and plants of the same genera and species in southern U.S.A., Hudson Bay region and Europe; red beds in the Catskill region and in E. Greenland; and the Old Red Sandstone in Europe indicate by their abundance of fossils a warm humid climate.

(*ii*) *Carboniferous.* Coal deposits, large insects, coral reefs in Spitzbergen, trees with succulent foliage, large fusulinids in Spitzbergen indicate a hot climate, probably subtropical or nearly tropical.

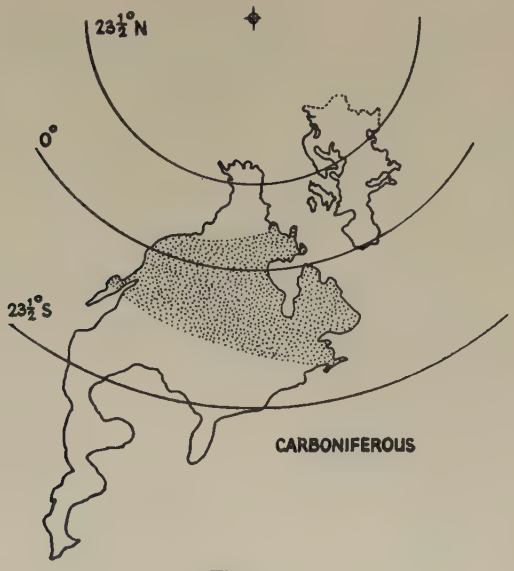

Figure 11.

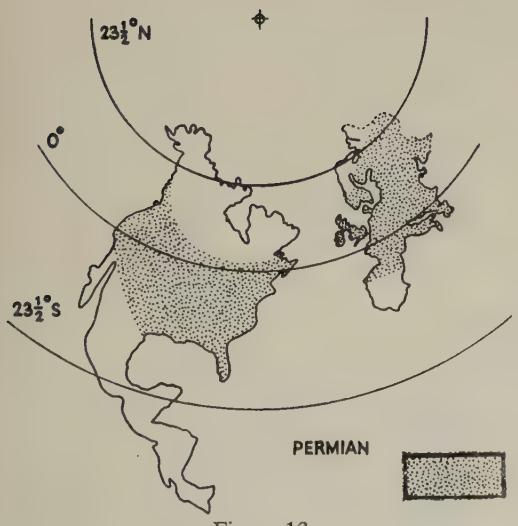

Figure 12.

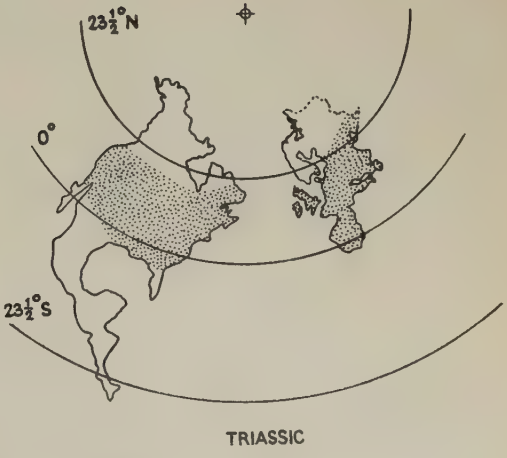

Figure 13.

Salt Deposits

Figures 11, 12 and 13. Latitude of Europe and North America in Carboniferous, Permian, and Triassic times derived from palaeomagnetic results.

(*iii*) *Permian.* Dune sands and widespread salt and gypsum deposits occur in central and western U.S.A. and in central Europe; in the Ural Mountains area great salt deposits were formed. Dune sandstones and red beds are common in central and western Europe.

Figs. 11 and 12 show the positions of the two continents relative to the Carboniferous and Permian equators, 20°N and 20°S lines of latitude, drawn on polar stereographic projections of the northern hemispheres relative to the poles at that time. The areas of salt deposits given by Lötze (1957) are shown.

(c) Mesozoic era

(1) *Europe and North America*

(*i*) *Triassic period.* Widespread aridity is indicated by red beds and evaporites in both continents. In addition there are thick limestones in the Alps.

Fig. 13 shows the positions of the two continents relative to the Triassic equators, 60°N, 20°N and 20°S lines of latitude, drawn on a polar stereographic projection of the Northern Hemisphere with America moved 24° eastwards in longitude.

It will be seen that from the Devonian to the Triassic, the palaeomagnetic evidence places Europe and North America much closer to the equator than they are at the present day. There appears here to be accord with the palaeoclimatic evidence.

Inferences drawn from the palaeontological evidence concerning the position of the axis of rotation in remote geological times depend on studying those species whose tolerance to environment restricted them to a comparatively narrow range of latitude. Stehli (1957) has studied the occurrence of Permian brachipods and fusilinids in outcrops over the world. He assumes that those groups which do not show a random distribution are warm-water types distributed about the then Equator. His data (Runcorn 1958 and Stehli 1958) fit the distribution of the continents inferred for the Permian by palaeomagnetic data better than they fit the present distribution, except for the serious anomaly that the palaeontological data imply a low latitude for North China and Manchuria, a conclusion also supported by the extensive dune-bedded sandstones and evaporite deposits of the Triassic in the same region. This difficulty can be resolved if the northward movement of India implies a similar movement of Asia in the last 200 million years.

There is thus a prima facie case that the range of latitudes inferred from palaeoclimatic considerations for each continent fit those deduced from the rock-magnetism work in each continent, as, indeed, Irving (1956) and Blackett (1961) have maintained. The small but systematic difference between the polar-wandering curves for Europe and North America and the large difference between these and those for other continents, e.g., India and Australia, must therefore be interpreted as continental drift. It is, however, necessary to say that the assumptions made in palaeoclimatic reasoning are all based on very imperfect knowledge of how the various key sedimentary deposits were laid down.

5. Palaeowind directions

1. Introduction

The lack of definition in the stratigraphic and palaeontological methods of determining the latitudes of places in past geological periods lends significance to any physical measurement which can be made on rocks, other than the magnetic ones, which will depend on the latitude of rocks at the time of their formation, such as temperature of the water in which the sediment was deposited and wind directions. O^{18} measurements suggest that the former may eventually be possible throughout geological time, but at present the measurements have not been pushed back far enough in geological time to be helpful in these studies. The determination of the ancient wind directions in the various continents is therefore of importance.

At the present day between latitudes of about 20°N and 20°S, except in the monsoon belt in India, trade winds blow with more or less constancy depending on the topography. Over the oceans the trade winds are remarkably constant (Crowe 1951), but in continental areas we have much less information and it appears that the wind pattern is somewhat less consistent.

In the hydrodynamics of the atmosphere, as in the earth's core, the Coriolis force plays a decisive role because of the large-length scales. The present general atmospheric circulation consisting of an equatorial easterly trade-wind zone, a mid-latitude westerly zone and a polar zone, arises from the deflection by the Coriolis force of the air flowing in to the equatorial region to take the place of rising air heated by the sun. The heat-flow balance of the atmosphere, the temperature difference between the equatorial and polar regions and the angular velocity of the earth may have changed during the geological time, but conservation of angular momentum implies that a trade-wind zone would always have existed, though its range in latitude may have varied. Of course, if polar wandering and continental drift have occurred, the parts of the land area lying within the trade-wind zone and their orientation to it will be different from that of the present day.

There are various ways in which ancient wind directions may be inferred with reasonable certainty from the geological record. Swineford (1949) has examined the variation of the thickness of the Pearlette volcanic ash of Pleistocene age, which is scattered from west-central Texas to south-eastern South Dakota and from western Kansas to south-central Iowa, and shows that a SW wind similar to that prevailing at the present day in the Great Plains was responsible for the ash distribution. Raasch (1958) has determined the lee and windward shores of the Cambrian strata of a palaeo-island in Wisconsin from the evidence of shore features and detrital trains and concluded that the wind blew from a few degrees east of north at this time. Opportunities in which such arguments can be utilized are necessarily few and the wind directions determined are likely to be inadequately averaged over space and time. These difficulties are overcome, to a considerable degree, in measurements on fossilized sand seas, i.e., aeolian sandstones.

Bagnold (1941) states that, in deserts in which the supply of sand is limited, barchan (or crescemtic) dunes are formed by steady winds of constant direction. The convex windward slope is a gentle one from which sand is being continually blown by saltation. Deposition occurs on the steep lee-side slopes, over which the sand slumps, resting at its angle of repose, which is about 33°. In plan, the lee-side slopes are crescents with the points downwind. The barchan is only the simplest form, and where there is more sand transverse dunes are formed. These consist of a sinuous line of steep lee slopes, parts of which resemble barchans. An air photograph is shown in Fig. 14, Pl. VI.

Successive layers of sand deposited on these lee slopes slightly differ in packing or in size distribution or vary in colour. Thus if a vertical cut is made through a sand dune traces of these ' bedding planes ' may be observed, as McKee (1957) showed.

Similar sand seas to these have become fossilized in the past and are preserved in the geological record as aeolian sandstones, thus, the Coconino sandstone of the Grand Canyon was proved to have this origin by McKee (1933). In these sandstones traces of the bedding surfaces on the lee slope remain and can be observed in exposures. By measuring the azimuth of the line of greatest slope of the exposed parts of these bedding planes and taking an average, the mean direction of movement of the sand dunes and hence the wind direction can be found. The scatter of the azimuths will depend on the curvature of the lee slopes of the dunes and on the variation of the wind direction.

Other types of dunes are, however, more common in modern deserts, as emphasized by Bagnold (1958). In the absence of vegetation, and in the presence of normal winds from one direction and occasional storm winds from a somewhat different direction, the longitudinal dune is commonly found. The dunes lie along the direction of the normal wind and can be up to 60 mi long; the slip face has a general direction along the normal wind but is wavy. When vegetation is present, great masses of sand (dra'a) with overlying chains of barchans broadside to the ridge are commonly found. Yet in all the aeolian sandstones with prominent cross-stratification, it is found that barchan-like structures

are found and no case of longitudinal dunes or dra'a fossilized as a geological deposit has been found. Possibly the reason is that only steady winds are able to create a dune sea of sufficient depth for the process of consolidation and cementation to set in, and barchans and transverse dunes are the product of steady winds.

The process by which a sea of dunes gets preserved is not well understood, but, as in other sedimentary deposits, the land falls relative to sea level and subsequent deposits form, perhaps marine or lacustrine beds. The sand will become cemented by silica or carbonate-bearing solutions permeating through it perhaps long after its initial deposition. Cycles of wind erosion will occur and the dunes may be planed down to a nearly flat surface on which later dunes will accumulate. Such presumed erosion surfaces are shown in Fig. 15, Pl. VI by the well marked horizontal lines. In Fig. 17, Pl. VII it can be seen that one dune has built up on the back slope of another.

In an exposure of aeolian sandstone it is rare to see a large part of a single dune. Usually the vertical face of rock reveals sections through a number of dunes each at different angles to the lee slope. The traces of the parallel-bedding planes from one dune is known as a set of cross-strata. Examples of these are shown in Fig. 15, Pl. VI and Figs. 16, 17 and 18, Plate VII.

The following criteria should all be satisfied in a sandstone before aeolian deposition is inferred (Pettijohn 1957; Twenhofel 1932, 1950).

(a) Presence of highly inclined cross-bedding up to the angle of rest of dry sand (33°) occurring in very large-scale units some of which exceed 50 ft in height (see, for example, (Fig. 18), Pl. VII. Similar cross-stratified structures can be produced by marine and fluviatile deposition in the presence of strong currents, but the structures are usually smaller in scale than dunes and their cross-strata have more variable angles of dip.

(b) Absence of micaceous material : owing to winnowing by the wind, these fissile minerals break on impact with the sand grains and are blown away.

(c) Absence of marine fossils : this indicates continental environment of deposition.

(d) High coefficient of sorting and roundness due to the sand's mode of transport; very small grains of sand will be transported much farther and very large grains much less far and so in any dune, grains of one size will predominate : frequent impacts will round off grains.

2. *Technique of field measurements*

It is quickly noticed, at an outcrop of aeolian sandstone that, in any one set of cross-strata, the azimuth of the line of greatest dip is the same for every stratum, as each set represents one part of a single dune. A reading is therefore taken on a well-exposed surface of any cross-stratum in one set. Only those cross-strata which have a dip greater than, say, 20°, are used, thus excluding the lower parts of the cross-strata where the azimuth may be affected by the irregularities of the surface on which the dune was formed. Determinations on other sets are made in a similar way, so that about 30 readings at any one locality are obtained, the readings being then taken randomly from different parts of the lee-side slopes of different dunes. If the beds have been tilted since deposition, then a correction for this must be applied. This is done by correcting the pole of the plane of cross-bedding for the strike and dip of the geological tilt; these quantities having been determined by measurements on sediments lying conformably above or below the aeolian sandstones, which have bedding likely to be nearly horizontal on deposition.

Figure 14. Typical sand sea with barchan and transverse dunes taken from the air over Southern Utah.

Figure 15. Wingate sandstone (Triassic age) in Colorado River Valley East of Moab, Utah.

Figure 16. Navajo sandstone (Jurassic) on Mount Carmel Highway, Zion National Park, Utah.

Figure 17. Close-up of Chequerboard Mesa, Navajo sandstone (Jurassic), Zion National Park, Utah.

Figure 18. Weber sandstone (Pennsylvanian), Brush Creek Gorge, Utah.

3. *Statistical methods*

The determination of the azimuths of the lines of greatest dip on N cross-strata from one locality enables a median or a vector mean to be calculated, which will be an estimate at that locality of the mean dominant wind direction. Were the dunes exactly similar in shape with their axes parallel the frequency distribution function $P(\theta)$ of azimuths θ obtained randomly from different parts of a number of dunes would be a function of the shape of the dune, but this is unlikely to be constant. Consequently it is postulated that the observations can be satisfactorily described by the circular normal distribution $P(\theta) = \exp(K \cos \theta)/2\pi I_0(K)$ where θ is measured from the mean and the normalizing function $I_0(K)$ is the modified Bessel function of the first kind of zero order. The precision K is a parameter of the scatter of the directions and can be estimated from the value of the length R of the vector sum of the N directions, each of which is represented by a unit vector. Reiche (1938) used the value of R/N, which he called the consistency ratio (now usually called the vector strength) as an empirical measure of dispersion in his analysis of the cross-lamination of the Coconino sandstone. For closely clustered directions, the above equation approaches the normal distribution with a standard deviation in degrees equal to $57\sqrt{1/K}$. For the widely scattered directions met with in this study this is not quite adequate, but suitable tables have been computed for estimating K from R/N (Court 1952; Gumbel, Greenwood and Durand 1953).

The circular normal distribution and the assumption that the vector mean is the best estimate of the true direction bear the same relationship as do the Gaussian distribution and the arithmetic mean of a sample of a variable linear quantity is the most probable value, as is shown in the following analysis.

If a sample of N observations $\theta_1, \theta_2 \ldots . \theta_N$ are taken, the likelihood function L is given by $L = f(\theta_1 - \theta) \cdot f(\theta_2 - \theta) \ldots . f(\theta_N - \theta)$ when f is the frequency distribution function and θ is the true direction taken for the moment to be a variable. After taking logarithms and applying the principle of maximum likelihood, i.e., that the most likely value of θ is that for which the joint probability of obtaining that particular sample is maximized we get $\sum_N f'(\theta_N - \theta_m)/f(\theta_N - \theta_m) = 0$, but $\sum_N \sin(\theta_N - \theta_m) = 0$ if θ_m is the vector mean of the sample.

Since these two identities are equal for arbitrary values of θ_N we have

$$\frac{f'(\theta_N - \theta_m)}{f(\theta_N - \theta_m)} = \sin(\theta_N - \theta_m)$$

and integrating $$f(\theta_N - \theta_m) = C \exp(K \cos \theta)$$

and normalizing $$f(\theta_N - \theta_m) = \frac{\exp(K \cos \theta)}{2\pi I_0(K)}$$

Therefore $$L = (2\pi)^{-N} I_0^{-N}(K) \exp\left[K \sum_N \cos(\theta_N - \theta_m)\right]$$

To estimate K we put $dL/dK = 0$, then $I_0'(K)/I_0(K) = \sum_N \cos(\theta_N - \theta_m)/N = R/N$.

The parameter K may be therefore estimated from a sample for which R/N has been determined by the equation

$$I_1(K) - (R/N) I_0(K) = 0 \text{ where } I_1(K) = I_0'(K)$$

4. *Directions of dip of the cross-strata of aeolian sandstones in Europe and N. America*

Table 1 collects together in a uniform way all available measurements of the azimuths of the lines of greatest dip in various aeolian sandstones. The number of readings N, the value of K derived from the length of the vector R and the value of the standard deviation of the mean are given. Histograms of all the observations from each of the formations are given separately in Figs. 19 to 31.

TABLE 1. DATA ON DIRECTIONS OF TRANSPORT IN AEOLIAN SANDSTONES

Fig. No.	Geological Age		Mean direction	N	K	σ
		WESTERN U.S.A.				
19	Tertiary	Chuska Sandstone (Wright)	N 19° E	176	1·28	3·8°
20	Upper Jurassic	Entrada Sandstone (Harshbarger)	N 171° E	87	1·56	4·9°
21	Upper Jurassic	Cow Springs Sandstone (Harshbarger)	N 201° E	170	1·05	4·3°
22	Lower Jurassic	Navajo Sandstone (Harshbarger)	N 152° E	75	1·57	5·8°
23	Lower Jurassic	Navajo Sandstone (upper) (Kiersh)	N 210° E	121	1·03	5·1°
24	Lower Jurassic	Navajo Sandstone (middle) (Kiersh)	N 126° E	107	1·36	4·8°
25	Permian	Coconino Sandstone (Reiche)	N 180° E	135	2·5	3·1°
26	Permo-Pennsylvanian	Tensleep Sandstone (Opdyke and Runcorn)	N 200° E	239	2·01	2·6°
27	Permo-Pennsylvanian	Weber Sandstone (Opdyke and Runcorn)	N 216° E	161	2·75	2·5°
28	Permo-Pennsylvanian	Casper Sandstone (Opdyke and Runcorn)	N 207° E	87	2·03	4·5°
29	Pennsylvanian	Casper Sandstone (Knight)	N 214° E	812	1·00	2·0°
		GREAT BRITAIN				
30	Lower Triassic	Bunter Sandstone Midlands (Shotton)	N 251° E	387	1·55	2·3°
31	Permian	Dumfries Sandstone Dumfries (Shotton)	N 249° E	132	1·98	3·5°

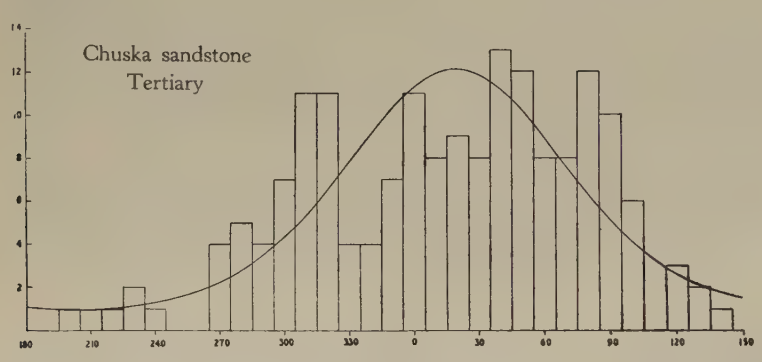

Figure 19.

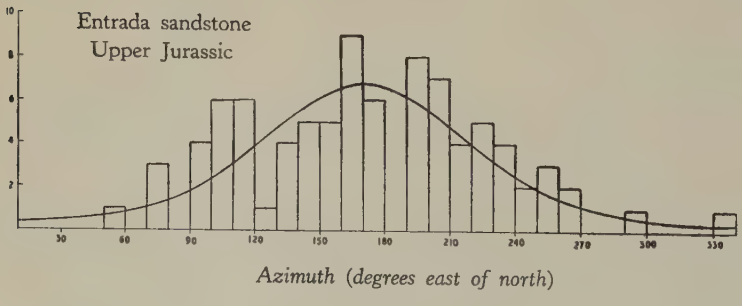

Figure 20.

Figures 19 and 20. Histograms showing distribution of directions of dip of cross-strata of aeolian sandstones listed in Table 1 (numbering as in Table 1).

Circular normal distributions are fitted to each histogram.

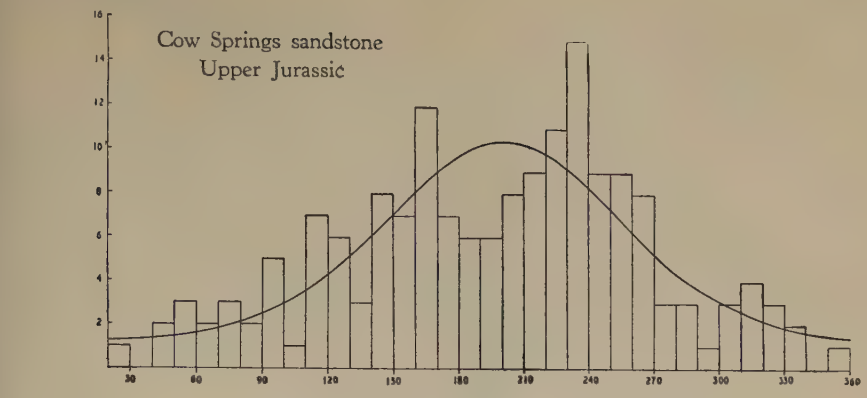

Figure 21.

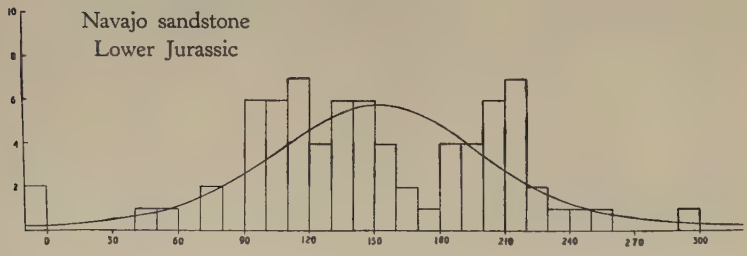

Figure 22.

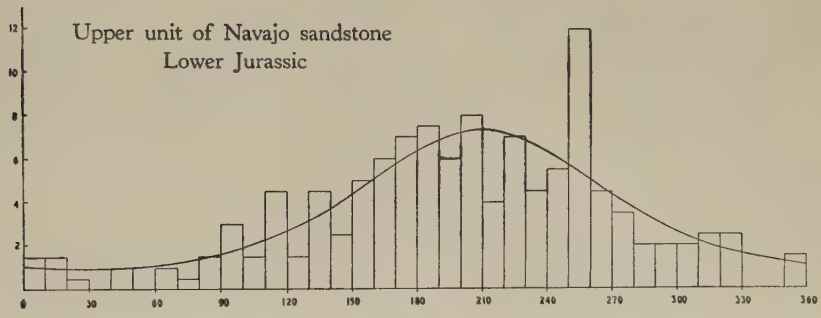

Figure 23.

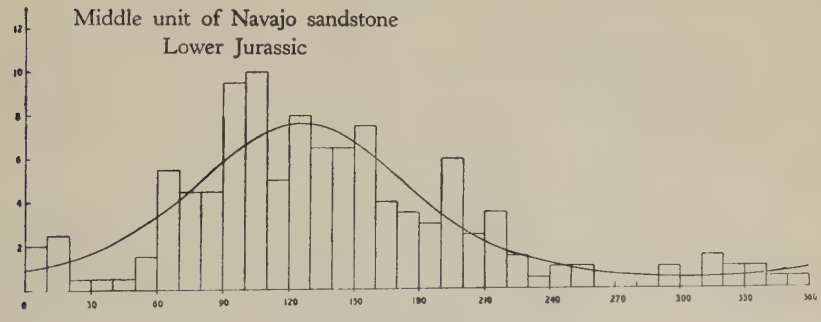

Figure 24.

Figures 21 to 24. Histograms showing distribution of directions of dip of cross-strata of aeolian sandstones listed in Table 1 (numbering as in Table 1).

Circular normal distributions are fitted to each histogram.

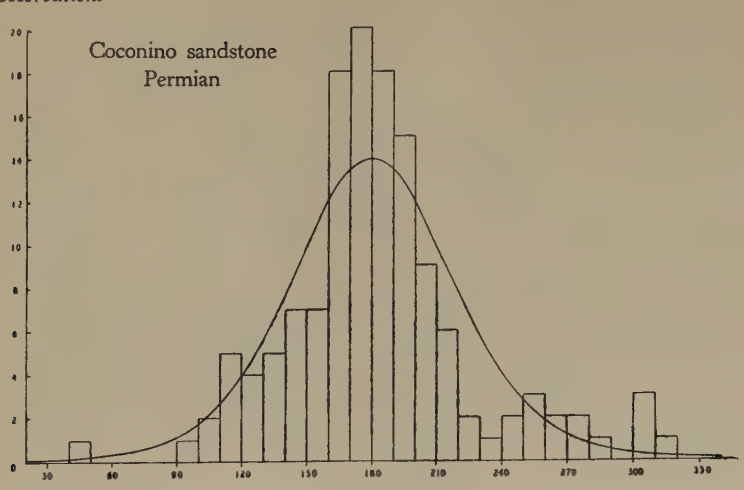

Figure 25.

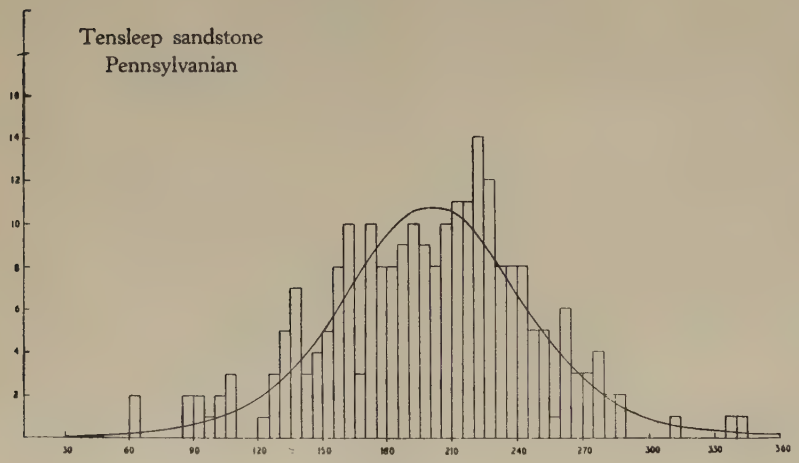

Figure 26.

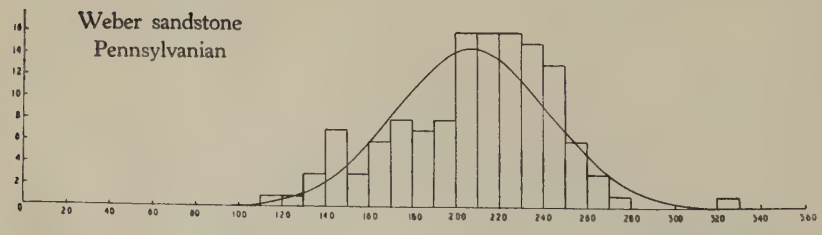

Figure 27.

Figures 25 to 27. Histograms showing distribution of directions of dip of cross-strata of aeolian sandstones listed in Table 1 (numbering as in Table 1).

Circular normal distributions are fitted to each histogram.

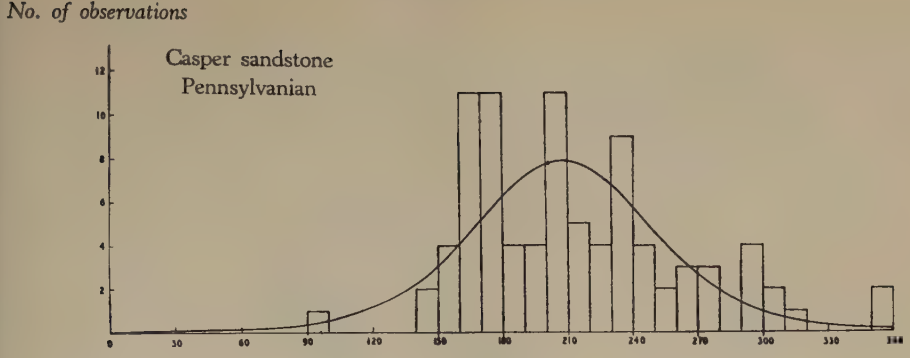

Figure 28.

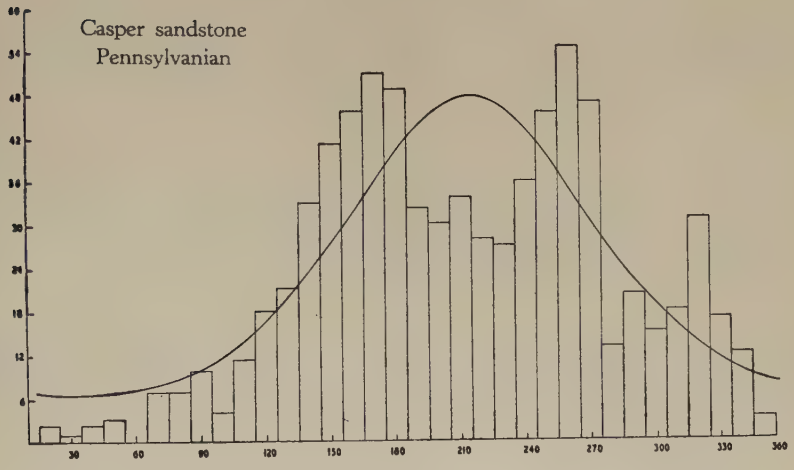

Figure 29.

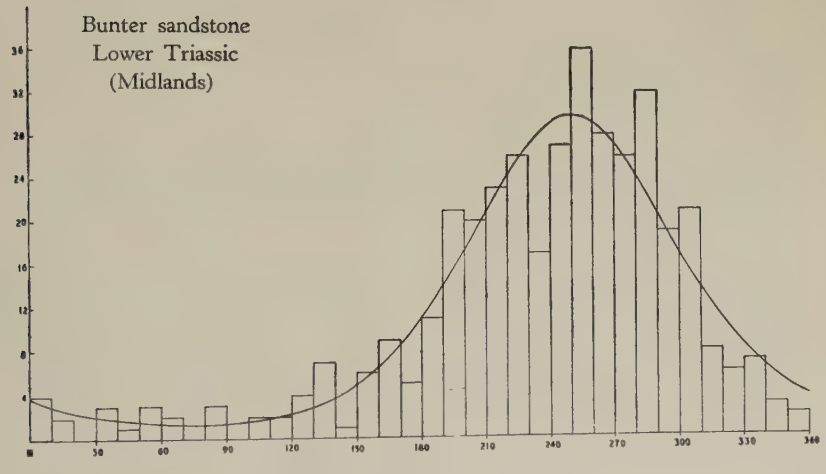

Figure 30.

Figures 28 to 30. Histograms showing distribution of directions of dip of cross-strata of aeolian sandstones listed in Table 1 (numbering as in Table 1).

Circular normal distributions are fitted to each histogram.

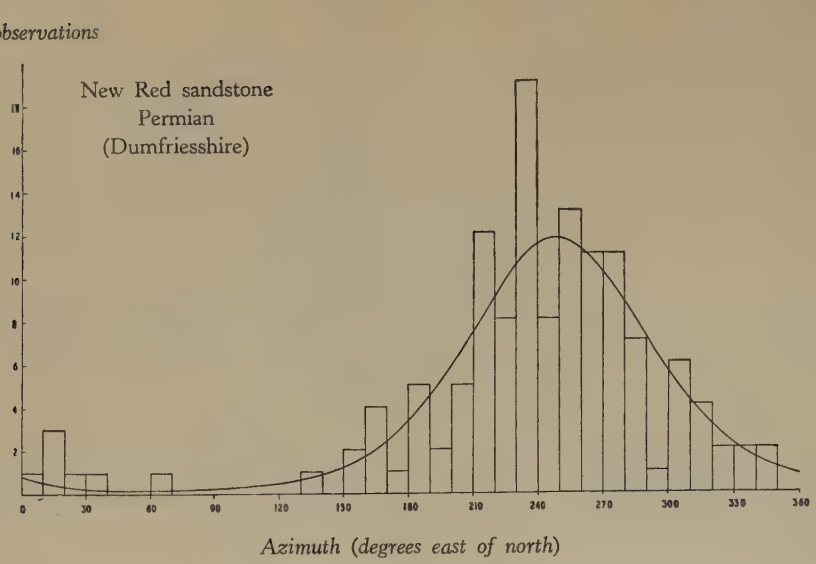

Figure 31.

Figure 31. Histogram showing distribution of directions of dip of cross-strata of aeolian sandstones listed in Table 1 (numbering as in Table 1).

Circular normal distributions are fitted to each histogram.

From the values of K and the vector mean calculated from each of the sets of observations of each of the aeolian sandstones in the western U.S.A. and Great Britain the theoretical frequency distribution formation has been plotted on Figs. 19-31, using the tables given by Grumbel, Greenwood and Durand (1953). The fit is seen to be good in each case (a Gaussian curve would only be adequate for $K > 3$ or 4).

The striking result is at once seen that for western U.S.A. between the late Palaeozoic and the Jurassic, the wind is predominately northerly. The data on the Jurassic by Harschbarger (1949) and Kiersch (1950) are based on comparatively restricted areas so that the variability of the mean directions should perhaps not yet be given too much attention. Poole (1957) briefly reports much more extensive studies on the Navajo sandstone of Jurassic age as well as the Wingate sandstone of Triassic age which show consistent northerly winds. The studies by Reiche (1938) and Opdyke and Runcorn (1956; 1960) on the late Palaeozoic aeolian sandstones in a large number of separate localities show a very consistent north-easterly wind, the mean directions at the various sites being shown in Fig. 32. There is only one anomalous group (of westerly directions) found by Reiche (1938), near Holbrook, Arizona, but the area is so restricted that it does not invalidate the conclusion that the palaeowind pattern in western U.S.A., shows such a consistency over space and time, that it must be explained by a hypothesis of world-wide implications. One must suppose that the long time represented by any series of sedimentary rocks smooths out very effectively deviations of wind direction due to local geography.

That the Tertiary aeolian sandstones of Arizona give a palaeowind similar to that observed in mid-latitudes today (Wright 1956) is further proof that studies of aeolian sandstones give a reliable palaeowind direction.

In Great Britain, various parts of the New Red Sandstones series are thought to be of aeolian origin. Dakyns, Tiddeman and Goodchild (1879) concluded this in the Penrith sandstones around Appleby, Cumberland, and deduced that the wind depositing them was from the east. Shotton (1937; 1956) studied the Bunter sandstone of the Midlands and of Dumfriesshire concluding that it was aeolian and demonstrating an easterly wind. D. J. C. Laming (Ph.D. thesis, London) and myself made determinations independently

Figure 32. Mean directions of the palaeowind at various outcrops of the Tensleep, Casper and Weber formations (with Reiche's data on the Coconino sandstone for comparison).

on the Dawlish sands near Exeter and found almost exactly the same mean direction, N 340°E. A. E. M. Nairn and myself independently made determinations on small outcrops of the Permian sands at Lossiemouth and found directions N 235°E and N 258°E. We therefore conclude that, apart from some variations, possibly due to lack of extensive outcrops, the New Red Sandstone gives an easterly wind. The consistency over space and time of the palaeowind determinations from western U.S.A. suggests that the palaeowind directions inferred for Great Britain should similarly be interpreted as planetary winds.

Palaeomagnetic observations give the ancient meridian and the latitude of the site and using the data from U.S.A. by Collinson and Runcorn (1960) and from Europe, we can relate these ancient wind directions to the ancient geographical coordinates. This is done in Table 2 and shows that these palaeowinds find a satisfactory explanation as the easterly wind belt of that time.

TABLE 2. Comparison of palaeowind direction (corrected to palaeomagnetic meridian) with palaeomagnetic latitude

Palaeodesert	Palaeowind direction	Latitude
Western U.S.A. (late Palaeozoic)	S 53°E	11°N
Great Britain (New Red)	S 37°E	13°N

No further palaeowind determinations have been made as yet, apart from a study by Almeida (1953) of the Botucatú sandstone of Jurassic age of South America.

6. *Geophysical explanation of polar wandering and continental drift*

We have seen that palaeomagnetic evidence, and that from climates, suggest that the poles of rotation of the earth and the land masses have gradually changed their relative positions through geological time. We must therefore consider the mechanism by which polar wandering and continental drift could have been brought about. Although the latter involves more degrees of freedom than the former, their explanation requires both that the earth is able to flow if subjected to steady stresses maintained over millions of years and that there are motions of the order of a few centimetres per year at depth within the mantle. Gold (1955) and Runcorn (1955b; 1957) have shown that for polar wandering to occur it must be supposed that the axis of figure of the earth is displaced from the axis of rotation by an infinitesimal amount and that the resulting stresses due to the centrifugal forces cause the earth to flow so that the equatorial bulge returns to a plane perpendicular to the new axis of rotation. The time constant of this process appears to be between a few hundred-thousand years and a few million years. The physical cause which displaces the two axes in the first place is a matter for conjecture. Tectonic disturbances in the crust or movements in the mantle are possibilities. In particular, mountain building and convection currents in the mantle have been shown to be quantitatively sufficient. It should perhaps be emphasized that no change in the direction of the axis of rotation in space, i.e., no change in the angular momentum of the earth, is involved in these processes.

To explain continental drift we start from the commonplace observation that the present distribution of the continents over the globe has two striking features. First, they are grouped largely into one hemisphere, opposite to the Pacific Ocean, and secondly, the areas antipodal to all but 6 per cent of the land masses are ocean. A mathematical description of these features was given by Prey (1922), who expressed the height of the land above sea level by a series of spherical harmonics (counting the depth of the ocean bottom negative). He showed that those harmonics of degree $n = 1$, $n = 3$, $n = 4$ and $n = 5$ are much larger than the others. Now the odd harmonics are characterized by having opposite sign at antipodal points. Thus Prey's mathematical result simply appears to confirm the above observation. Vening Meinesz (1960) has interpreted this as implying that thermal convection described by harmonics of corresponding degree is occurring in the earth's mantle. It would then be reasonable to suppose that the lighter sialic material of the continents would be drawn towards those parts of the earth's surface where the convection currents were falling and that, in consequence, the present distribution of the continents is not fortuitous. That it is the result of such a fundamental process within the earth's interior has been used as an argument against continental drift; however, we shall show that it is in fact a possible key to the theoretical understanding of how the drift has occurred.

Vening Meinesz (1952), Jeffreys (1952) and Chandrasekhar (1953) have discussed the onset of thermal convection in a sphere or spherical shell, ignoring the effects of rotation which seems permissible for motions in a highly viscous fluid such as the mantle. These results are of considerable interest because Chandrasekhar shows that if one supposed the present mantle to be a viscous fluid, and the core inviscid, a relation exists between the radius of the core, expressed as a fraction of the earth's radius, and the degree of the spherical harmonics of the convection pattern which appears at marginal stability. In particular, with a core of the present size, the degrees $n = 3$, 4 and 5 are first excited.

Other geophysicists, however, have felt that the most striking feature of the present distribution of the continents, which must be explained by theories of the earth's evolution, is the predominance of the harmonic $n = 1$ (i.e. the concentration of the continents in the non-Pacific hemisphere). Hills (1947) suggested that this was the result of thermal convection, but hitherto the fatal objection to this theory has been that in the presence of a core of the present size, a convection pattern corresponding to the harmonic $n = 1$ would *not* be excited at marginal stability (Jeffreys 1952). As the gross concentration of the continents in one hemisphere must be assumed to have happened at a very early stage in the history of the earth, acceptance of the results of convection theory involves postulating that the core was very much smaller some 10^9 years ago than it is today.

The conflict between these two opposed trends of thought concerning the distribution of the continents may be resolved by accepting continental drift and by adopting the idea of a core growing continuously through the earth's history. The latter possibility was suggested by Urey (1952) in his theory of the development of the earth by accretion. He was concerned with the problem of how a molten core could separate from a primeval earth of ' cold origin,' i.e., a mixture of iron and silicate bodies, supposedly similar to meteorites. Urey showed that the presence of volatile elements in the earth's crust appears to preclude the earth ever having been at a high enough temperature for complete melting. Urey found some difficulty in explaining the separation of the core if the earth was solid and proposed that the iron had melted in the mantle and moved along the boundaries of the silicate crystals by capillarity.

In geophysical discussion the sharp line drawn between the liquid nature of the core and the solid character of the mantle, appropriate for the discussion of the response of the core and mantle to seismic waves (of periods of a few seconds) and to tidal and nutation stresses (of periods of between a month and a year), has been carried over into more general discussion of the earth's properties. However, liquids like water will transmit shear waves of sufficiently high frequency or of a period less than a time characteristic of the fluid.

Supposing, therefore, that convection of the order of 1 cm year^{-1} may occur in the mantle, it is of interest to describe the evolution of the earth. During the process of accretion, the heat generated at the surface by impact is radiated quickly out into space; thus when the process of accretion is complete, the temperature gradient inside the earth will be the adiabatic gradient due to pressure, supposing at the moment that appreciable radioactive heating only occurs over a longer time than the time taken for accretion. If the heat due to radioactivity is greater than that conducted away along the adiabatic gradient and there is no threshold of stress, convection will occur. In the initial stages, with a small core, the convection system will be that of spherical harmonic of degree 1. The process of convection itself will, of course, assist in the separation of the dense iron to the centre, and would assist in the accumulation of the lighter silicates, of which the crust is composed, to the surface. This continental material would be expected to be concentrated in one block near the descending convection current. This situation would persist until the radius of the core became about one-third of that of the earth (see Chandrasekhar 1953), when a convection pattern of degree $n = 2$ would become that which would set in at marginal stability. This would begin the dispersion of the continents.

Conclusions

It is concluded that the main changes in the climates of the continents receive an adequate explanation in terms of the theories of polar wandering and continental drift. The palaeomagnetic survey of the continents now in progress is providing definite evidence of the former positions of the continents relative to each other and to the pole. How closely the reconstructions will agree with those of Wegener and Du Toit, it is too early to judge; but in general, their ideas have proved to be correct. In particular, the late Palaeozoic wind directions of Great Britain and western U.S.A. become intelligible in the light of the palaeomagnetic data.

These conclusions do not, of course, provide an explanation of the oscillations of climate witnessed in the four Ice Ages of Pleistocene times and the presumed similar retreats and advances in the Permo-Carboniferous Ice Age. Further determinations of the pole position in Pleistocene times may, however, be an important test of the theory of Ewing and Donn (1956), who suggest that the period of Ice Ages began when the pole moved into the Arctic Ocean; at present the palaeomagnetic data seem to exclude this possibility, as is seen in Fig. 1.

In this paper we have not gone into the details of the geological evidence of palaeoclimates; much of it is controversial and we wished to take only those data generally accepted. It does, however, appear that the completed palaeomagnetic survey of the continents, and the detailed reconstructions of the land masses for successive geological periods which will follow, will stimulate a study into the details of palaeoclimatology. It would, for example, be interesting to attempt the determination of the changes in the extent of the trade-wind belt with geological time, although to accomplish this a method for inferring wind directions from geological deposits of greater applicability than observations on aeolian sandstones must be discovered. One might expect that among other factors, a steady change in the angular velocity of the earth through geological time would affect the latitudinal extent of the trade-wind belt and might therefore be determined indirectly by such measurements. As the change in the earth's angular velocity is, of course, a most important piece of information in the study of the evolution of the earth-moon system, it seems excusable to speculate as to the way in which this change might have left its mark in the geological record.

Acknowledgments

It is a pleasure to record the help of Mr. G. Turnbull, Dr. J. H. Parry and Dr. L. Molyneux in the preparation of this paper.

References

Almeida, F. F. M. de 1953 *Botucatu, a Triassic desert of South America*, Inter. Geol. Congress, Comptes Rendus, Algiers (1952) Section VII, pp. 9-24.

Bagnold, R. A. 1941 *The physics of blown sand and desert dunes*, Methuen, London.

1958 Contribution to Geophysical discussion, *Observatory*, **78**, pp. 65-68.

Blackett, P. M. S. 1961 To be published.

Blackett, P. M. S., Clegg, J. A. and Stubbs, P. 1960 'An analysis of rock magnetic data,' *Proc. Roy. Soc., A*, **256**, pp. 291-322.

Brouwer, D. 1952 'A study of the changes in the rate of rotation of the earth,' *Astron. J.*, **57**, pp. 125-146.

Bullard, E. C. 1949 'The magnetic field within the earth,' *Proc. Roy. Soc. A*, **197**, p. 433.

Campbell, C. D. and Runcorn, S. K. 1956 'Magnetization of the Columbia River basalts in Washington and Northern Oregon,' *J. Geophys. Res.*, **61**, pp. 449-458.

Chandrasekhar, S. 1953 'The onset of convection by thermal instability in spherical shells,' *Phil. Mag.*, **44**, p. 233 and p. 1,129.

Clegg, J. A., Deutsch, E. R. and Griffiths, D. H. 1956 'Rock magnetism in India,' *Phil. Mag.*, **1**, pp. 419-431.

Coleman, A. P. 1923 *Ice ages : recent and ancient*, Macmillan, New York.

Collinson, D. W. and Runcorn, S. K. 1960 'Polar wandering and continental drift : evidence from palaeomagnetic observations in the United States,' *Bull. Geol. Soc. Amer.*, **71**, pp. 915-958.

Court, A. 1952 'New statistical techniques in geophysics,' *Advances in Geophysics*, **1**, pp. 45-48, (Ed. H. E. Landsberg); Academic Press, New York.

Cox, A. 1957 'Remanent magnetization of Lower to Middle Eocene basalt flows from Oregon,' *Nature*, **179**, pp. 685-686.

Creer, K. M. 1958 'Preliminary palaeomagnetic measurements from South America,' *Ann. Geophys.*, **14**, pp. 373-390.

Creer, K. M., Irving, E., Nairn, A. E. M. and Runcorn, S. K. 1958 'Palaeomagnetic results from different continents and their relation to the problem of continental drift,' *Ibid.*, **14**, pp. 492-501.

Creer, K. M., Irving, R. and Runcorn, S. K. 1954 'The direction of the geomagnetic field in remote epochs in Great Britain,' *J. Geomag. Geoelec.*, **6**, pp. 163-168.

1957 'Palaeomagnetic investigations in Great Britain, VI : Geophysical interpretation of palaeomagnetic directions from Great Britain,' *Phil. Trans. Roy. Soc. A.*, **250**, pp. 144-156.

Crowe, P. H. 1951 'Wind and weather in the equatorial zone,' *Transactions Inst. Brit. Geographers*, **17**.

Dakyns, J. R., Tiddeman, R. H. and Goodchild, J. G. 1879 'The geology of the country between Appleby, Ullswater and Haweswater,' *Mem. Geol. Survey*, new series, H.M.S.O., London.

David, T. W. E. 1950 *The geology of the Commonwealth of Australia*, 2 vols., Arnold and Co., London.

Deutsch, E. R., Radakrishnamurty, C. and Sahasrabudge, P. W. 1958 'On the remanent magnetism of some lavas in the Deccan traps,' *Phil. Mag.*, **3**, pp. 170-184.

Dunbar, C. O. 1949 *Historical geology*, John Wiley & Sons, New York.

Durham, J. W. 1952 'Early Tertiary marine fauna and continental drift,' *Amer. Jour. Sci.*, **250**, pp. 321-343.

Du Bois, P. M. 1957 'Comparison of palaeomagnetic results for selected rocks of Great Britain and North America,' *Adv. in Phys.*, **6**, pp. 177-186.

Du Bois, P. M., Irving, E., Opdyke, N. D., Runcorn, S. K. and Banks, M. R. 1957 *Nature*, **180**, pp. 1,186-1,187.

Du Toit, A. L. 1939 *Geology of S. Africa*, Oliver and Boyd, Edinburgh.

Elsasser, W. M. 1946a 'Induction effects in terrestrial magnetism, 1, Theory,' *Phys. Rev.*, **69**, pp. 106-116.

1946b 'Induction effects in terrestrial magnetism, 2, The secular variation,' *Ibid.*, **70**, pp. 202-212.

1947 'Induction effects in terrestrial magnetism, 3, Electric modes,' *Ibid.*, **72**, pp. 821-833.

Ewing, M. and Donn, W. L. 1956 'A theory of Ice Ages,' *Science*, **123**, pp. 1,061-1,066.

Fotheringham, J. K. 1920 'A solution of ancient eclipses of the sun,' *M.N.R.A.S.*, **80**, pp. 578-581, **81**, pp. 104-126.

Gold, T. 1955 'Instability of the earth's axis of rotation,' *Nature*, **175**, p. 526.

Gough, D. I. 1956 'A study of the palaeomagnetism of the Pilansberg dykes,' *M.N.R.A.S. Geophys. Suppl.*, **7**, pp. 196-213.

Gumbel, E. J., Greenwood, J. A. and Durand, D. 1953 'The circular normal distribution : theory and tables,' *J. Amer. Statistical Assoc.*, **48**, pp. 131-152.

Harshbarger, J. W. 1949 'Petrology and stratigraphy of Upper Jurassic rocks of Central Navajo Reservation, Arizona,' Ph.D. thesis, University of Arizona.

Hills, G. F. S. 1947 *The formation of the continents by convection*, Arnold, London.

Holmberg, E. R. R. 1952 'A suggested explanation of the present value of the velocity of rotation of the earth,' *M.N.R.A.S., Geophys. Suppl.*, **6**, pp. 325-330.

Hospers, J. 1955 'Rock magnetism and polar wandering,' *J. Geol.*, **63**, pp. 59-74.

Hospers, J. and Charlesworth, H. A. K. 1954 'The natural permanent magnetization of the lower basalts of N. Ireland,' *M.N.R.A.S., Geophys. Suppl.*, 7, pp. 32-43.

Irving, E. 1956 'Palaeomagnetic and palaeoclimatological aspects of polar wandering,' *Geofis. pur. appl.*, **33**, pp. 23-41.

Irving, E. and Green, R. 1957 'The palaeomagnetism of the Kainozoic Basalts of Victoria,' *M.N.R.A.S. Geophys. Suppl.*, **7**, pp. 347-359.

1958 'Polar wandering relative to Australia,' *Geophys. J.*, **1**, pp. 64-72.

Jeffreys, H. 1952 *The Earth – its origin, history and physical constitution*, Cambridge Univ. Press.

Jenks, W. F. 1956 Handbook of South American geology, *G.S.A. Memoir*, 65.

Kiersch, G. A. 1950 'Small scale structures and other features of the Navajo sandstone, northern part of the San Rafael Swell, Utah,' *Bull. Amer. Assoc. Petrol. Geol.*, **34**, pp. 293-942.

Knight, S. H. 1929 'The Fountain and Casper formations of the Laramie Basin,' a study in genesis of sediments, *Univ. Wyoming, Publ. in Geol. Sci.*, **1**, pp. 1-82.

Krishnan, M. S. 1956 *Geology of India and Burma*, Higginbothams, Madras.

Lötze, F. 1957 *Steinsalz und Kalisalze*, 2nd ed., Borntraeger, Berlin.

McKee, E. D. 1933 *The Coconino sandstone – its history and origin*, Carnegie Institution of Washington publication.

1957 'Primary structures in some recent sediments,' *Bull. Amer. Assoc. Petrol. Geol.*, **41**, pp. 1,704-1,747.

Munk, W. H. and Revelle, R. 1952 'On the geophysical interpretation of irregularities in the rotation of the earth,' *M.N.R.A.S., Geophys. Suppl.*, **6**, pp. 331-343.

Murray, C. A. 1957 'The secular acceleration of the moon, and the lunar tidal couple,' *M.N.R.A.S.*, **117**, pp. 478-482.

Nairn, A. E. M. 1959 'Palaeomagnetic survey of the Karroo system : progress report,' *Overseas geology and mineral resources*, **7**.

Opdyke, N. D. and Runcorn, S. K. 1956 Palaeoclimates and palaeomagnetism, *Proc. Intern. Geol. Congress*, Mexico City.

1960 'Wind direction in the western United States in the late palaeozoic,' *Bull. Geol. Soc. Amer.*, **71**, pp. 959-972.

Pettijohn, F. J. 1957 *Sedimentary Rocks*, Harper & Bros., New York.

Poole, P. G. 1957 'Palaeowind directions in late palaeozoic and early mesozoic time on the Colorado plateau as determined by cross-strata, abstract,' *Geol. Soc. Am. Bull.*, **68**, p. 1,870.

Prey, A. 1922 'Darstellung der Hohen und Tiefenverhaltnisse der Erde,' *Abh. Ges. der Wissenschaften Math. Phys. Klasse* (Gottingen) **11**, 1.

Raasch, G. O. 1958 'Baraboo Monadnock and palaeowind directions,' *J. Alberta Society of Petroleum Geologists*, **6**, pp. 183-187.

Reiche, P. 1938 'An analysis of cross laminations in the Coconino sandstone,' *J. Geol.*, **46**, pp. 905-932.

Runcorn, S. K. 1954 'The earth's core,' *Trans. Amer. Geophys. Un.*, **35**, p. 49.

1955a 'The electrical conductivity of the earth's mantle,' *Trans. Amer. Geophys. Un.*, **36**, pp. 191-198.

1955b 'Rock magnetism geophysical aspects,' *Phil. Mag.*, **4**, pp. 244-291.

1956a 'Palaeomagnetic survey in Arizona and Utah,' : Preliminary results, *Bull. Geol. Soc. Amer.*, **7**, pp. 301-316.

1956b 'Palaeomagnetic comparisons between Europe and North America,' *Proc. Geol. Ass.*, Canada, **8**, pp. 77-85.

1956c 'The magnetism of the Earth's body,' *Handbuch der Physik*, **47**, pp. 498-533.

1958 'On the Permian climatic zonation and palaeomagnetism,' *Amer. J. Sci.*, **256**, pp. 235-238.

1959a 'On the theory of the geomagnetic secular variation,' *Ann. Geophys.*, **15**, pp. 87-92.

1959b 'On the hypothesis that the mean geomagnetic field for parts of geological time has been that of a geocentric axial multipole,' *J. Atmos. Terr. Phys.*, **14**, pp. 167-174.

Schreiner, G. D. L. 1958 'Age of a Pilansberg dyke of palaeomagnetic significance,' *Nature*, **181**, pp. 1,330-1,331.

Simpson, G. C. 1957 'Further studies in world climate,' *Quart. J. R. Met. Soc.*, **83**, pp. 459-485.

Spjeldnaes, N. 1960 'Ordovician climatic zones,' *Norsk. Geol. Tids.*, **41**, pp. 45-77.

Spencer Jones, H. 1939 'The rotation of the earth and the secular accelerations of the Sun, Moon and Planets,' *M.N.R.A.S., Geophys. Suppl.*, **99**, pp. 541-558.

1956 'The rotation of the earth,' *Handbuch der Physik*,, **47**, p. 1.

Stehli, F. G. 1957 'Possible Permian climatic zonation and its implications,' *Amer. J. Sci.*, **255**, 607-618.

1958 'Reply to Professor Runcorn on the Permian climatic zonation and palaeomagnetism,' *Ibid.*, **255**, pp. 239-240.

Shotton, F. W. 1937 'The Lower Bunter Sandstones of North Worcestershire and East Shropshire,' *Geol. Mag.*, **74**, pp. 534-553.

1956 'Some aspects of the new Red Desert in Britain,' *Liverpool and Manchester Geol. J.*, **1**, pp. 450-466.

Swineford, A. 1949 'Source area of Great Plains Pleistocene volcanic ash,' *J. Geo.*, **57**, pp. 307-3.

Turnbull, G. 1959 'Some palaeomagnetic measurements from Antarctica,' *J. Arctic Inst. N. Amer.*, **12**, No. 3, pp. 151-157.

Twenhofel, W. H. 1932 *Treatise on sedimentation*, (2nd ed.), Bailliere, Tindall-Cox, London.

1950 *Principles of sedimentation*, (2nd ed.), McGraw-Hill, New York.

Urey, H. C. 1952 *The planets : their origin and development*, Yale Univ. Press, New Haven.

Vening Meinesz, F. A. 1952 'Convection currents in the earth and the origin of the continents,' *Kon. Ned. Akad. Weten*, **55**, pp. 527-553.

1960 'Continental and ocean-floor topography; mantle-convection currents,' *Kon. Ned. Acad. Weten*, B, **63**, pp. 410-421.

Vestine, E. H. 1953 'On variations of the geomagnetic field, fluid motions, and the rate of the earth's rotation,' *J. Geophys. Res.*, **58**, pp. 127-145.

Wright, H. E., Jr. 1956 'Origin of the Chuska sandstone, Arizona and New Mexico. A structural and petrographic study of a Tertiary Aeolian sediment,' *Bull. Geol. Soc. Amer.*, **67**, pp. 413-454.

551.507.362.2 : 551.515.12 : 551.576 : 77

Satellite cloud pictures of a cyclone over the Atlantic Ocean

By S. FRITZ

Meteorological Satellite Laboratory, U.S. Weather Bureau, Washington

(Manuscript received 26 January 1961; communicated by J. S. Sawyer)

Summary

A composite of Tiros 1 pictures describing the cloud system in a mature cyclone, centred in the Atlantic Ocean to the west of Ireland, is described. Comparison of the pictures with conventional meteorological data shows that a stratiform cloud surrounding the storm was identical in position with a warm moist tongue of air flowing around the storm. In the centre of the storm where the clouds were more broken, giving the appearance of cumuliform clouds, a large mass of cold, dry air extended from the surface up to the tropopause above 400 mb. A few areas of steady precipitation were present in the stratiform cloud regions while more scattered showers existed in the central cumuliform region. An area of relatively high winds circled the storm, in conformity with the expectations from the thermal wind relation when cold air and warm air layers reside side by side. A brief comparison is made between the vertical motion computations based on conventional data and the cloud areas.

1. Introduction

The meteorological satellite, Tiros 1 (Sternberg *et al.*) launched on 1 April 1960 has photographed many interesting patterns of clouds (Staff, Met. Sat. Lab. 1961; Fritz and Wexler 1960; Wexler and Fritz 1960; Fritz 1960; Bristor and Ruzecki 1960; Winston 1960). The satellite did this with the aid of two television cameras; one, a wide-angle camera, photographed an area of approximately 800 × 800 mi when the camera axis was pointed straight down, and the second, narrow-angle, camera then covered an area of about 80 × 80 mi. Under these circumstances the wide-angle camera resolution was about 2 mi, whilst in the narrow-angle pictures the resolution was about ½ mi.

During the second day of its existence, on 2 April 1960, Tiros 1 sped over the North Atlantic Ocean; and at about 1110 GMT, it began taking a series of snapshots spaced at 30 sec intervals. These photographs included the cloud system associated with an old, well-developed cyclonic vortex centred about 400 mi west of Ireland. About 100 min later, during the next orbital pass, Tiros again photographed the same storm. From these photographs, two composites have been prepared which clearly show the pattern of the clouds associated with the cyclone. Fig. 1 (a), (Plate VIII) contains the composite made from several frames taken during the first orbit, and Fig. 1 (b) is a composite made from frames in the next orbit.

2. Description of Tiros cloud pictures

(a) *Wide-angle pictures*

To facilitate discussion and to orient the pictures geographically, the major features of the clouds in Fig. 1, (Plate VIII) have been sketched on a polar-stereographic map* in Fig. 2, (Plate VIII). Fig. 1 (a) best describes the clouds which occupied the western, northern and eastern parts of the cloud system, while Fig. 1 (b) shows the western, southern, and eastern portions best. We see that the clouds in the pictures of Fig. 1 extended from a point in the Atlantic Ocean, over 1,000 mi west of the European Coast, eastward into the European continent, covering much of the intervening Atlantic Ocean and the countries bordering the Atlantic.

* A separate study showed that the major cloud features were located within about 60 mi of their exact locations.

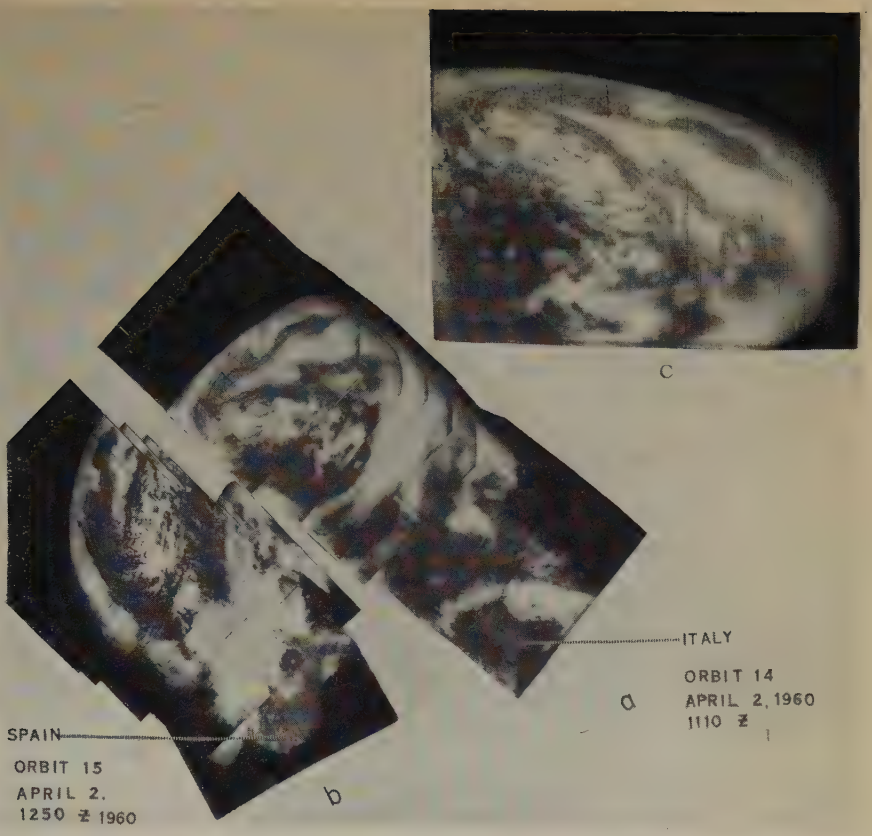

Figure 1. (a) Composite of frames photographed at about 1110 GMT, 2 April 1960, showing stratiform cloud surrounding cumuliform cloud in an Atlantic Ocean vortex. Italy appears just below an extensive bright area in the picture; this bright area is the snow-covered Alps. (b) Composite of frames photographed at about 1250 GMT, 2 April 1960, showing the same Atlantic Ocean storm, 100 min later. The eastern part of Spain is nearly cloudless. (c) Single frame showing continuous stratiform cloud.

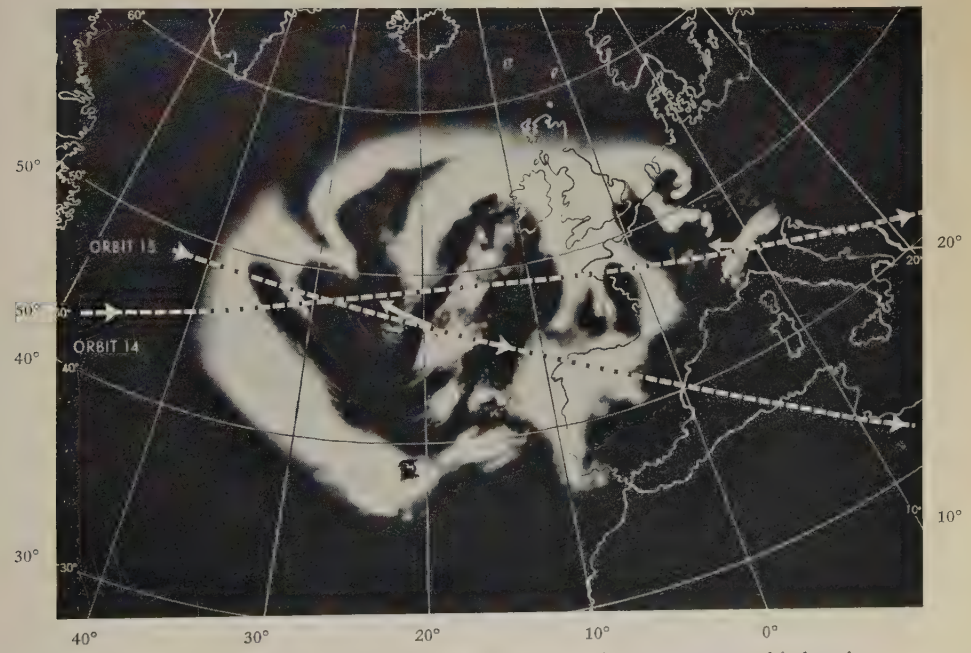

Figure 2. A sketch of the picture in Fig. 1 arranged in proper geographic location.

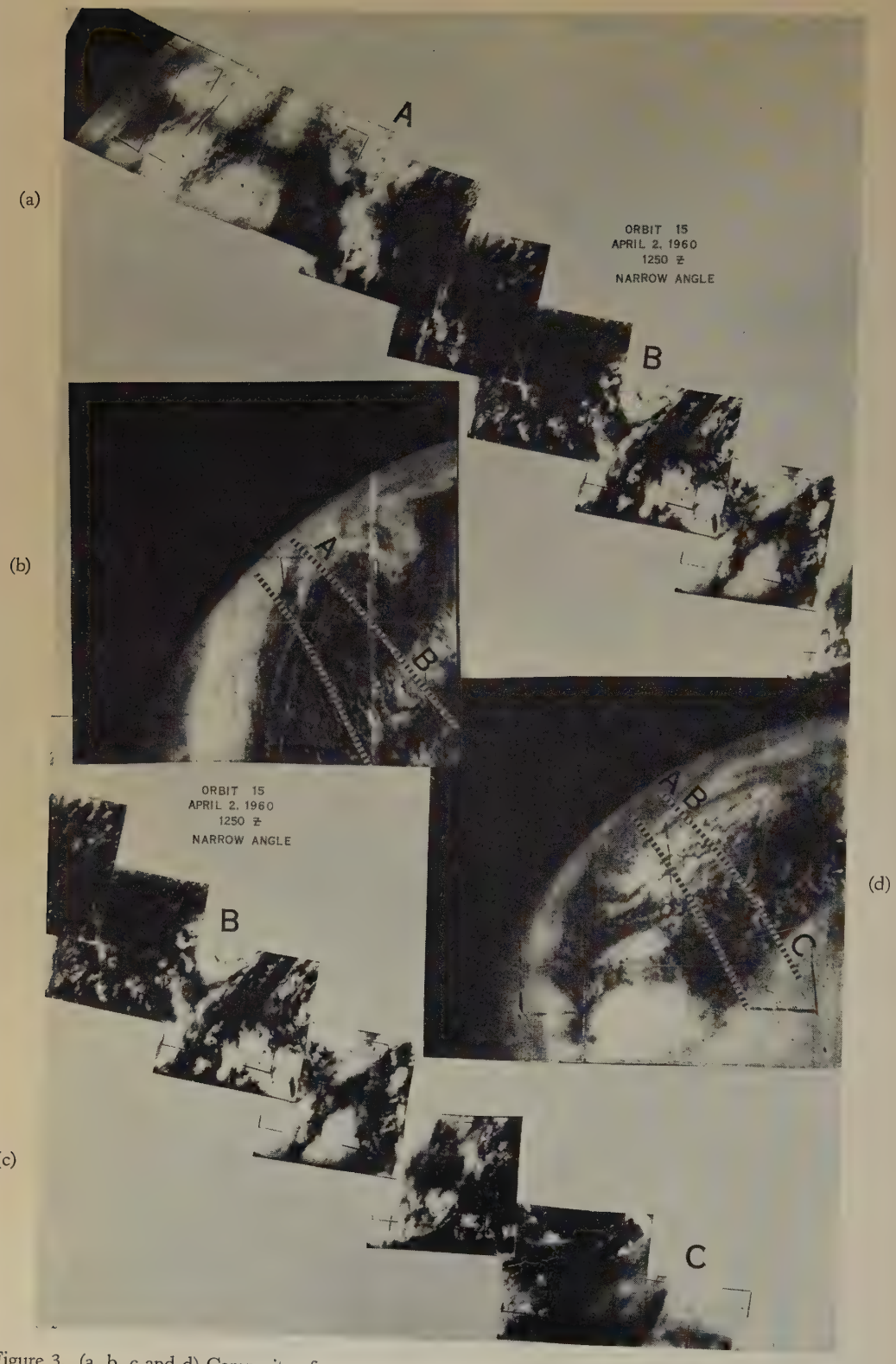

Figure 3. (a, b, c and d) Composite of narrow-angle camera pictures across centre of cloud system shown in Fig. 1 (b), with associated wide-angle pictures (see text).

One of the main features of the cloud pictures is the broad band of stratiform cloud which, in Figs. 1 (a), 1 (b) and 2, terminates in the arrowhead-like cloud near the centre of the vortex. The figures show that the stratiform cloud is a quasi-circular band of cloud. Starting with the protuberance in the wall of the cloud, near 50°N 30°W, the cloud sweeps southward in a band about 300 mi wide, joining with a widespread cloud mass over western Spain (eastern Spain is nearly cloud-free). The cloud over Spain may, in part, be enhanced by orographic effects, but it extends also to the south-southwest into the Atlantic Ocean just west of Gibraltar, suggesting the existence of a weak frontal system there.

The main stratiform cloud continues over Spain into France, but contains some fairly large holes over the Bay of Biscay region (Figs. 1 (a) and 2). The stratiform cloud continues to circle the storm area passing over England and Ireland, and then, moving out over the Atlantic Ocean near latitude 55°, it divides into two parts. One part goes into the arrowhead cloud near the centre of the vortex, and the other part completes the circuit by joining the protuberance just to the west of the 'arrowhead'; the continuity of the cloud around the northern side of the vortex can be better seen in an individual frame (shown in Fig. 1 (c)). In addition, Fig. 1 (c) suggests that the cloud may have had a fairly sharp boundary in its northern section.

In the pictures, this quasi-circular stratiform cloud encircles a swirling galaxy-like mass of more broken, cumuliform clouds which lies near the centre of the cloud system. In addition, we note that very narrow cloud streets seem to originate in the wall of the stratiform cloud, most prominently near the west-wall protuberance. These cloud streets, several hundred miles in length, circle south of the 'arrowhead' cloud and sweep into the cumuliform, central cloud mass.

It is interesting to note the similarity of several cloud features in Figs. 1 (a) and 1 (b) in view of the fact that 100 min had elapsed between the two sets of pictures. The arrowhead and the protruding cloud in the inner west wall of the stratiform cloud persist essentially unchanged. The very narrow cloud streets which seem to issue from the inner west-wall protuberance and to sweep south of the arrowhead into the cumuliform mass in the centre are clearly evident in both Figs. 1 (a) and 1 (b). Certainly the form of the cloud system had hardly changed at all in this 100 min interval.

(*b*) *Narrow-angle pictures*

During the second pass when the pictures in Fig. 1 (b) were observed, the narrow-angle camera also photographed a swath across the centre of the cloud system, and a composite of these narrow-angle pictures is shown in Fig. 3, Plate IX, together with associated wide-angle pictures. Actually the composite in Fig. 3 stretches farther to the west than the pictures in Fig. 1 (b) because there is evidence that the narrow-angle camera started photographing the Earth somewhat earlier than did the wide-angle camera.

Fig. 3 (a) shows the narrow-angle pictures taken in the western half of the cyclonic pattern of Fig. 1 (b). The approximate boundaries of the narrow-angle pictures swath is shown in the wide-angle picture, Fig. 3 (b), by the broken lines. In Fig. 3 (c) the narrow-angle pictures for the eastern half of the cyclone cloud pattern is shown. Fig. 3 (d) shows the swath which contains the composite of Fig. 3 (c). The letters A, B and C are given to indicate the corresponding positions in the wide-angle and narrow-angle pictures. Position A is the place where the cloud 'streets' emerge from the stratiform cloud; position B is the end of the arrow-head cloud; and position C is near the inner edge of the stratiform cloud on the eastern side of the cyclonic cloud pattern. In Fig. 3, the rather uniform stratiform clouds on both the western and eastern sides of the cloud pattern can be seen to have almost no small-scale detail, but they do contain relatively large patches of dark area denoting thinner clouds or actual holes*. The cumuliform cloud

* The narrow-angle pictures contain a defect which makes the stratiform clouds appear less uniform than they really are. In Fig. 3 the apparent thinning of the cloud occurs in a narrow band across the whole composite, and is especially noticeable in the stratiform cloud. Note, for example, the darker areas along the satellite path in the upper left-hand frames of Fig. 3 (a). These darker areas which are oriented along the length of the pictures in Fig. 3 are spurious.

seems to be made up of small elements, especially in the cloud streets; but, near the tip of the arrow head cloud (position B) and in the 'galaxy-like' cloud (between B and C), the elements are fairly large and bright, sometimes over 40 mi in length. They were, doubtless, the cloud elements associated with the scattered shower activity reported in the surface observations.

3. The meteorological situation

The cloud system of Figs. 1, 2 and 3 is, of course, the result of physical processes in the atmosphere. To relate these processes to the cloud pictures we need to examine the meteorological state of the atmosphere at the time of the pictures. To facilitate the discussion, the meteorological charts which are presented here contain an outline of the stratiform cloud area taken from Fig. 2. The surface and 500 mb analyses were prepared by the National Weather Analysis Center, independent of the cloud pictures.

(*a*) *Surface data*

At the time Tiros took the pictures of Fig. 1, a large, mature cyclone was centred about 400 mi west of Ireland. The sea-level pressure chart for 1200 GMT, 2 April, 1960 (Fig. 4) shows the cyclone with its central pressure of about 974 mb. The cyclone was characterized by practically circular isobars and strong pressure gradients, which were associated with reported surface winds of up to 50 kt. A weak front, which has been entered on the map along the west coast of Europe, sweeps southward and westward across the Azores.

The cloud amount and cloud forms, observed from the earth's surface, are also shown in Fig. 4, and we note that near the frontal zone a band of overcast sky was present, in which low and middle cloud (as seen from the surface) predominated. Cirrus cloud forms were also reported over parts of Spain and France. Surrounded by the overcast band, an area of broken clouds predominated in the surface reports over the ocean although scattered clouds were also reported there. The low clouds in this non-overcast area were mainly cumulus clouds in various states of development, and stratocumulus types. Altocumulus and cirrus clouds were also reported. Along the inland edge of the overcast band, cirriform clouds predominated.

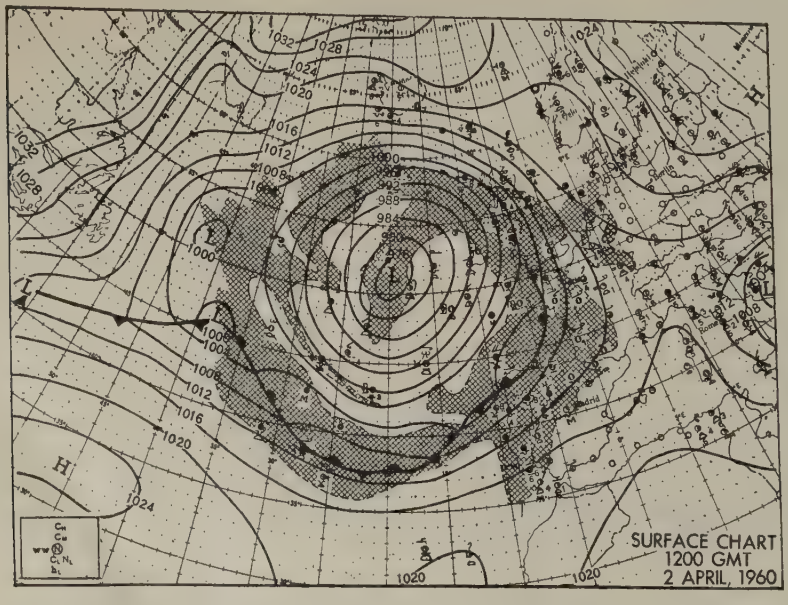

Figure 4. Sea-level chart for 1200 GMT, 2 April 1960, showing mature cyclone with outline of stratiform cloud area from Fig. 2 superimposed. Surface cloud observations are also shown.

Precipitation occurred in a few reports. More steady rain was reported in the overcast band near the frontal zone, over and near Spain and the British Isles, and over some adjacent ocean areas; a few showers were also noted in the central overcast region over the ocean.

Although the surface cloud reports were not sufficient, even in this rather dense shipping zone, to outline the cloud areas completely, similarity between the surface reports (Fig. 4) and the Tiros picture (Figs. 1 and 2) is apparent.

(*b*) *Upper-air data*

The cyclone in Fig. 4 was quite symmetrical with height. The ' low ' centre on the 500 mb chart (Fig. 5), at a height of about 16,800 ft, was located nearly above the surface low-pressure centre.

Fig. 5 contains an analysis of the temperature field; and the dew-point temperatures are also plotted near each reporting radiosonde station. If we denote the centre of the cyclone by the position of the lowest height on the 500 mb chart, then we note that a cold, dry mass of air resided close to, but somewhat to the southeast of, the centre; the exact positions cannot, of course, be given with the data available. Moreover a warm, moist mass of air circles the centre from the Azores, across Spain and England and into the Atlantic.

A region of relatively strong winds, with up to 60 kt reported, encircles the southern and eastern sides of the 500 mb vortex. This weak jet stream lies in or near the inside edge of the semi-circular zone of warm moist air, and therefore near the inner edge of the cloud system in Fig. 1.

The flow of the moist air around the cyclone is seen even more clearly on the 300°K isentropic chart (Fig. 6). On this chart, both the relative humidity and water-vapour mixing ratio are given; and isolines of pressure and of mixing ratio have been analysed. This isentropic chart reaches a pressure of less than 400 mb in its centre, indicating the deep cold air which had already been noted on the 500 mb chart (Fig. 5). Moreover, the moist air (high-mixing ratio) flows with the winds around the vortex, and especially

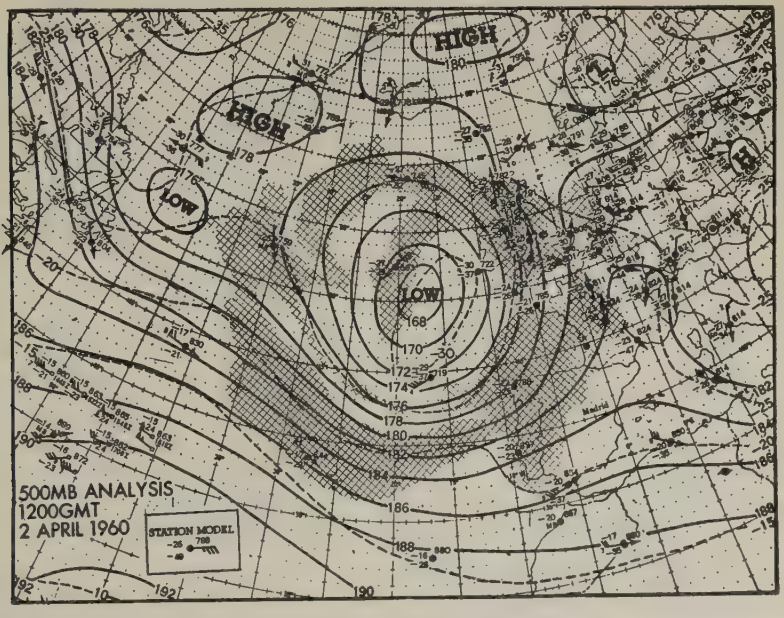

Figure 5. 500 mb chart for 1200 GMT, 2 April 1960. Solid lines are 200 ft contours, dashed lines are isotherms. Dew-point temperatures are shown at lower left of each station circle.

on the eastern side of the centre the air flows up the isentropic surface. The presence of condensation obscures the real significance of this chart, but the existence of overcast clouds and precipitation in this region (Figs. 2 and 4) attests to the reality of the ascent in this case.

In order to note the vertical extent of the cold, dry air in the vortex centre, and of the warm, moist air around the periphery of the vortex, several cross-sections have been prepared. One of these cross-sections, along the line marked A-A in Fig. 6, is shown in Fig. 7. Here the cold air is shown to reach from the earth's surface to the tropopause near 300 mb. Relative humidity is also shown in Fig. 7, since this moisture quantity is readily discussed in relation to clouds. It is clear that except for the levels near the ocean surface, the air above ship station *K* is much drier than the air over ship station *J* up to the 400 mb level. To the south of ship *K*, over the Azores, the air has about the same relative humidity as that at station *K*; small differences do appear but may not be reliable in view of the inaccuracies in humidity measurement.

Commercial air-plane cloud reports (K.L.M. and Alitalia) indicated that near latitude 56°N in this cross-section (Fig. 7), a stratiform cloud top was located at a height of 10,000 to 12,000 ft. This information is shown in the cross-section. The latitude where the cross-section crosses the inner edges of the stratiform cloud as seen by Tiros (Fig. 2) have also been included in Fig. 7.

Finally, since the cloud formation is generally associated with vertical motion in the atmosphere, the vertical motion chart for the 600 mb pressure level deduced by the Joint Numerical Weather Prediction Unit (U.S.W.B.) is shown in Fig. 8. The vertical motion is shown to be slightly downward in the north centre of the cloud pattern. In the overcast cloud region the vertical motion often changes sign, denoting alternations between upward and downward motion.

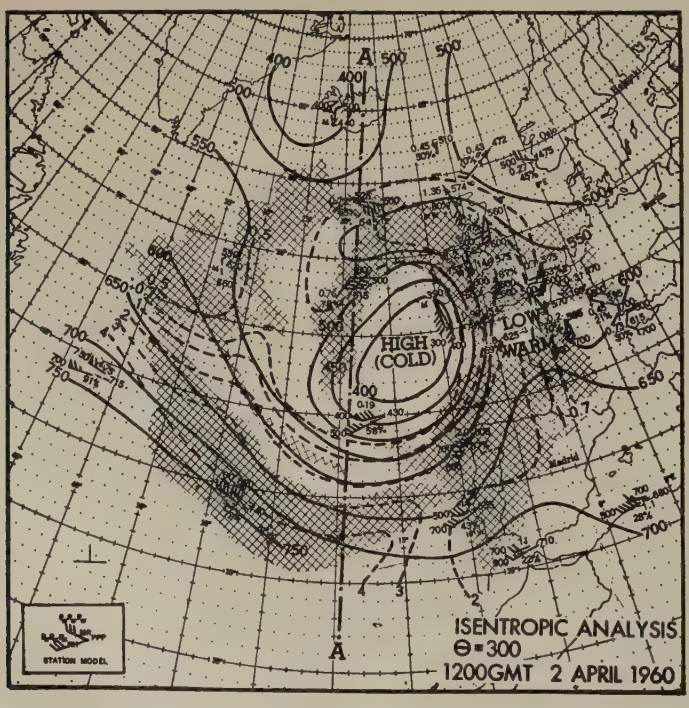

Figure 6. Isentropic chart ($\theta = 300°K$), 1200 GMT, 2 April 1960, showing deep core of cold air with warm moist air flowing around it. Solid lines are isobars on the isentropic surface; dashed lines are lines of constant water vapour (mixing ratio). Line AA shows the region of the cross-section in Fig. 7. The winds are shown at two pressure levels near the level of the isentropic chart. High and low refers to the elevation of the isentropic surface.

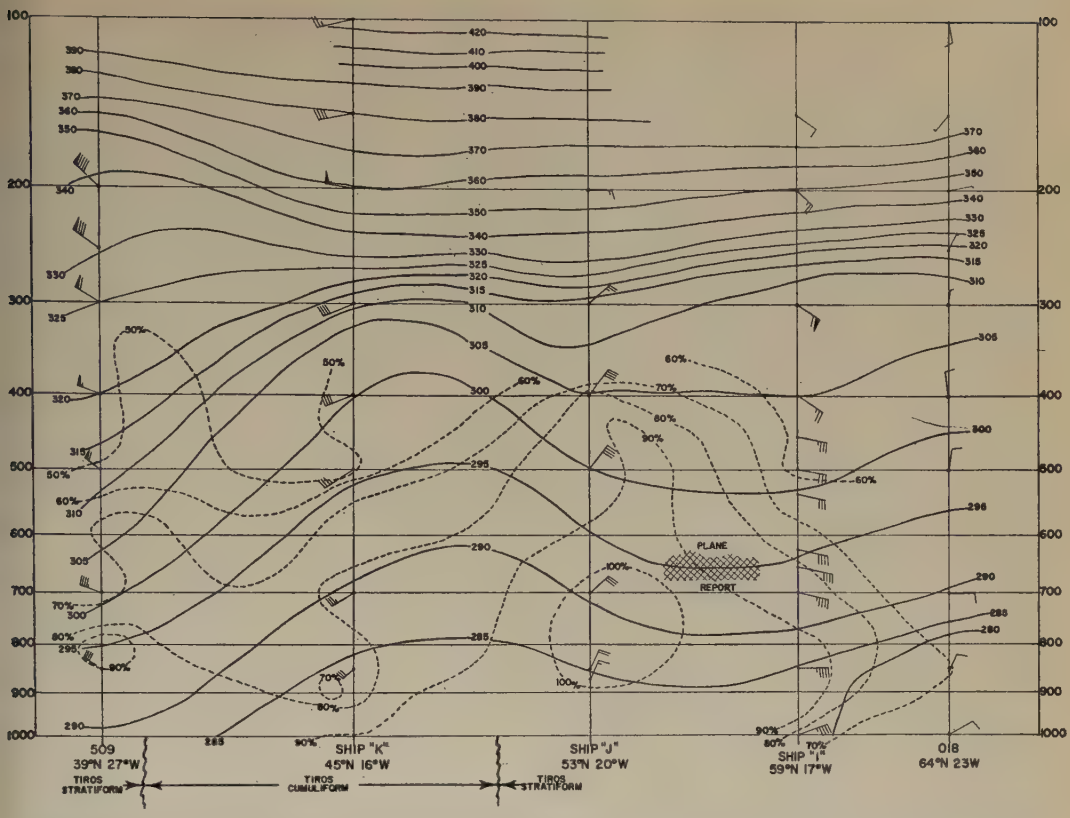

Figure 7. North-south cross-section through the atmosphere along the line AA of Fig. 6, 1200 GMT, 2 April 1960. Solid lines are lines of constant potential temperature; dashed lines are lines of constant relative humidity. The inner boundaries of the stratiform cloud (from Fig. 2) are shown below the diagram.

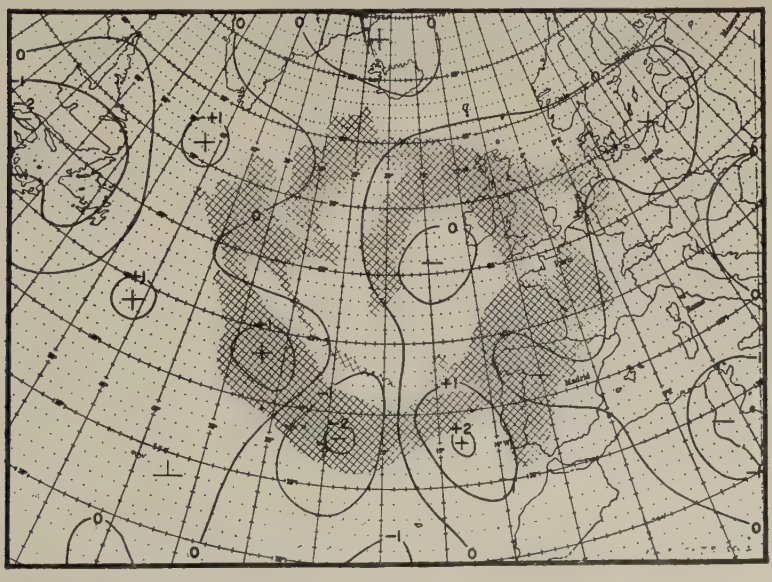

Figure 8. Vertical motion chart for 600 mb at 1200 GMT, 2 April 1960, computed by JNWP Unit. Units are cm sec^{-1}. + denotes upward motion; — denotes downward motion.

4. Comparison of Tiros cloud pictures with meteorological data

From the description of the pictures (Figs. 1-3) and of the meteorological situation (Figs. 4-8) it is easy to see the association between the two sets of data. First the clouds as observed from the surface (Fig. 4) agree, as they must, with the Tiros pictures; the small discrepancies which occur near the edges of the cloud picture patterns may be due to slight mislocations of the cloud elements in Fig. 2, or to the fact that the surface observer does actually see past the edge of the overcast. Although it would not be possible from the surface-cloud observations alone to delineate the details of the cloud field, the areas of overcast as observed from the surface appear in the uniform, stratiform cloud areas of pictures (Figs. 2 and 4). Moreover, the area in the centre of the cloud vortex, where the non-overcast cumuliform clouds appear in the pictures, is also the broken to scattered cloud area in the surface observations. Judging by the surface reports, the cumuliform area contained also some altocumulus and cirrus clouds. Some showers occurred in this region which were doubtless associated with the brighter cloud masses in Fig. 1. The relatively cloudless area which parallels the stratiform cloud and separates it from the cumuliform cloud, is more difficult to find in the surface reports. It should be noted that the array of clouds in Fig. 1 bears a marked similarity to the clouds in the Atlantic cyclone studied by Ludlam and Miller (1959).

Now looking at the gross features, it is quite apparent that the stratiform cloud which covers the European coast and then spirals into the arrowhead cloud of Figs. 1 and 2 is a manifestation of the warm moist ' tongue ' of air which circles the 500 mb vortex (Fig. 5) and appears as an ascending moist tongue in the 300°K isentropic chart (Fig. 6).

Furthermore, the broken cloud area in the middle of the cloud vortex coincides very well with the deep, cold, dry mass of air. Judging by the continuous cloud in the west side of the vortex, this cold mass of air has been cut off from its cold air source further to the west and is now completely encircled by warm moist air. The variation in brightness and size of the cumuliform elements in Fig. 1 (b) suggests that the clouds had greater vertical extent to the east of the arrowhead cloud than to the west of it. Thus the pictures suggest that the air was more stable in the northerly flow to the west of the arrowhead cloud, and more unstable in the southerly flow near the cyclone centre. Ludlam and Miller (1959) found similar distribution of the height of the cloud tops.

The stratiform cloud doubtless slopes downward from the arrowhead towards the north. This can be ascertained from the cross-section in Fig. 7. At ship station *J*, judging by the high relative humidities, the cloud top was about 23,000 ft high (near the 400 mb level). At ship station *I*, the relative humidities are much lower at that level suggesting a lower cloud level and the airplane reports support the cloud existence at 12,000 ft.

An area of relatively strong winds (about 60 kt) is present along the inner edge of the stratiform cloud near the 500 mb level. This is to be expected since the wind will increase with height in the region between the warm and cold air according to the thermal wind relation. Thus strong winds are bound to appear in this region.

Moreover, it is interesting to note that the cloud streets of Figs. 1 and 2 lie closely parallel to the contour lines of the 500 mb chart (Fig. 5); but since the ' streets ' join the central cloud mass which is near the lowest 500 mb height, the streets apparently cross the contours as they approach the centre. Since the wind direction was constant with height (Fig. 7) these streets serve as good wind-direction indicators and also suggest (Fig. 1) a convergence into the ' galaxy-like ' cloud mass, which is itself near the centre of low pressure. These cloud streets could not of course be discovered from the surface observations alone.

Finally, a word should be said about the vertical motion chart (Fig. 8). The slight downward motion in the centre of the cloud vortex would agree with the fact that the stratiform cloud did not appear there, although the bright broken cloud may have been associated with clouds existing or built up to high levels. It would also suggest that most of the central cumuliform cloud was below 600 mb (about 13,000 ft). This was perhaps

truer near the cloud streets near station *K* and in the dim clouds west of the arrowhead than in the central cloud mass itself.

In the stratiform cloud-area, the computed upward motion also agrees with the cloud's existence. However, the strong downward motions near 37°N, 25°W seem questionable; although one cannot prove that upward motion was occurring *at that instant*, the presence of the cloud casts doubt on the existence of strong downward motion in the area in the recent past. Had the motion actually been upward, where downward motion had been computed in the stratiform cloud region of Fig. 8, the initial conditions which were used in the numerical computation model would have been different; and the forecast resulting from the real conditions might have been different. Thus the cloud pictures may eventually serve as a valuable additional observation to aid in the determination of the actual state of the three-dimensional motion in the atmosphere, as well as of the moisture and temperature structure.

5. Conclusions

The stratiform clouds observed by Tiros in Fig. 1 were clearly associated with a warm, moist tongue of air which encircled the vortex in the Atlantic Ocean at 1200 GMT, 2 April 1960. In the centre of the vortex a cold, relatively dry mass resided, apparently cut off from its main cold-air source. This cold air was associated with the non-overcast, galaxy-like cloud area which was surrounded by the stratiform cloud. This region between the cold and warm air is also the region of maximum jet-like winds, and is therefore to be expected near the inner edge of the stratiform cloud. Finally, cloud streets, which cannot be seen from surface observations, serve to outline the wind flow, in the mature storm in which the wind direction does not change much with height.

Finally, a great deal of additional detail is evident in the photographs. The pattern in the form of a nearly closed circle over the European coast near North Germany (Figs. 1 (a) and 2) is an interesting example. Is this the counterpart of a meso-scale eddy in the atmosphere ? Was the shape of the arrowhead cloud in Fig. 1 (a) produced by meso-scale eddies ? Looking southward along the ' arrow,' in Figs. 1 (a) and 2, the appearance of the cloud suggests the possibility that a small cyclonic eddy existed on the eastern side near latitude 50°N, and an anticyclonic eddy on the western side of the arrowhead.

It will of course be interesting to examine other cloud patterns which appear like that of Fig. 1 to see if similar meteorological conditions are associated with them and to see if generalizations can be formulated.

Acknowledgment

This work has been supported by the National Aeronautics and Space Administration.

References

Bristor, C. L. and Ruzecki, M. A. 1960 ' Tiros I photographs of the Midwest storm of April 1, 1960,' *Mon. Wea. Rev.*, **88**, p. 315.

Fritz, S. 1960 ' Cyclone prints from satellite, Tiros I,' *Interavia*, **15**, p. 1,384.

Fritz, S. and Wexler, H. 1960 ' Cloud pictures from satellite, Tiros I,' *Mon. Wea. Rev.*, **88**, p. 79.

Ludlam, F. H. and Miller, L. I. 1959 ' Research on the properties of cloud systems.' Imperial College Sci. and Tech., London, *Tech. (Final) Rep.* No. AF-61 (514)-1,292.

Staff, Meteorological Satellite Laboratory, (U.S. Weather Bureau) 1961 ' Some meteorological results from Tiros I,' in ' Report on Tiros I,' *Nat. Aeronaut. and Space Admin.* (to be published).

Sternberg, S. *et. al.* 1960 ' Roundup of Tiros I,' *Astronautics*, **5**, p. 32.

Wexler, H. and Fritz, S. 1960 ' Tiros reveals cloud formations,' *Science*, **131**, p. 1,708.

Winston, J. S. 1960 ' Satellite pictures of a cut-off cyclone in the Eastern Pacific,' *Mon. Wea. Rev.*, **88**, p. 295.

551.557.2 (265) : 551.557.3

Some notes on the stratospheric winds at Canton Island and Christmas Island

By R. A. EBDON
Meteorological Office, Bracknell

(Manuscript received 25 October 1960)

Summary

Stratospheric wind data for Canton and Christmas Islands show a fluctuation with a period of about 24 to 28 months in the zonal component. Christmas Island data also show that the fluctuation exists from below 60 mb to 10 mb (the highest level for which data are available) and that the amplitude of the fluctuation increases with height. The change in wind direction from W to E, or vice versa, is evident first at the higher levels and appears to work gradually downwards; at 60 mb the reversal of wind direction is evident about six months after that at 25 mb, and about twelve months after that at 10 mb.

Attempts to connect events in the equatorial stratosphere with events in the equatorial troposphere were not successful.

1. Introduction

In an earlier note (Ebdon 1960) an account was given of the contrasting flow patterns at 50 mb over tropical and sub-tropical areas in January 1957 and January 1958. It was shown that whereas the mean vector wind was close to E'ly in January 1957 over large areas near the equator it was close to W'ly over the same area in January 1958, and that the winds on individual days were persistently E'ly in January 1957 and persistently W'ly in January 1958.

Because of this contrast in flow patterns it was decided to examine the monthly mean winds at 50 mb for stations near the equator covering as long a period as possible. Prior to the commencement of the International Geophysical Year, radiosonde or radar-wind reporting stations near the equator were very few, but 50 mb wind data are available for Canton Island (02° 46'S; 171° 43'W) from late 1953 onwards and for Christmas Island (02° 00'N; 157° 23'W) from October 1956 to August 1959. The data used for Christmas Island were monthly mean values (based on all ascents) held in the Climatological Research Branch of the Meteorological Office. For Canton Island, daily values (using only the 00 to 03 GMT ascent) were used, as published in the U.S.A. *Daily Series Synoptic Weather Maps*, Pt. II, or the New Zealand *Daily Weather Bulletin*. The number of ascents reaching 50 mb was very good both for the westerly and easterly regimes. At Canton Island in only one month, January 1955, were there fewer than 10 observations and for this month winds at 65,000 ft were used. At Christmas Island there were several months with fewer than 10 observations towards the end of the period.

2. Discussion

Curves showing the monthly mean values of zonal and meridional wind components at 30, 40, 50, 60 and 80 mb for Christmas Island are shown in Fig. 1 (a-e) and at 50 mb for Canton Island in Fig. 2. (The approximate heights in feet, corresponding to some of the pressure levels, are shown in Fig. 9). It will be noted from Fig. 1 that the zonal wind component shows similar fluctuations at the 60, 50, 40 and 30 mb levels. The amplitude of the fluctuation increases over this range of height and may not have reached its maximum at 30 mb – the highest level at which data were considered adequate for this form of presentation. (At 30 mb there were more than 10 observations in each month, except in June 1958 (9 observations), February 1959 (6 observations) and November, December 1958, January 1959 (1 observation per month); at 25 mb the data were more sparse). At 80 mb the flow pattern is probably affected by the proximity of the equatorial tropopause and from the curve of monthly means for this level in Fig. 1, the fluctuation

is not detectable, but that it does exist at 80 mb can be shown by 12-monthly running means. The curve showing the zonal wind component for 50 mb at Canton Island (Fig. 2) also displays similar fluctuations during the period for which data were available. It will be seen from the curves that there is a ' periodicity ' of about 24 to 28 months. It will

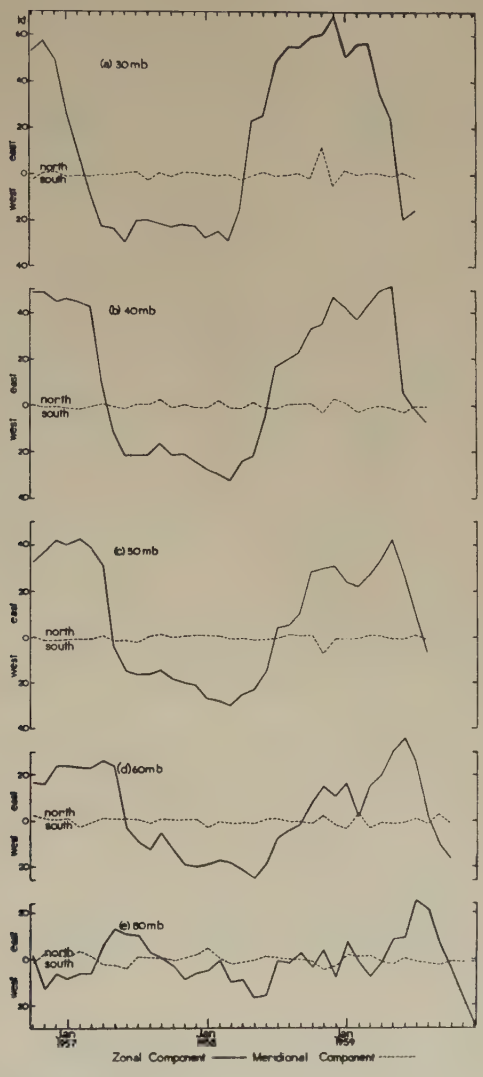

Figure 1. Monthly mean values of zonal and meridional wind components at Christmas Island.

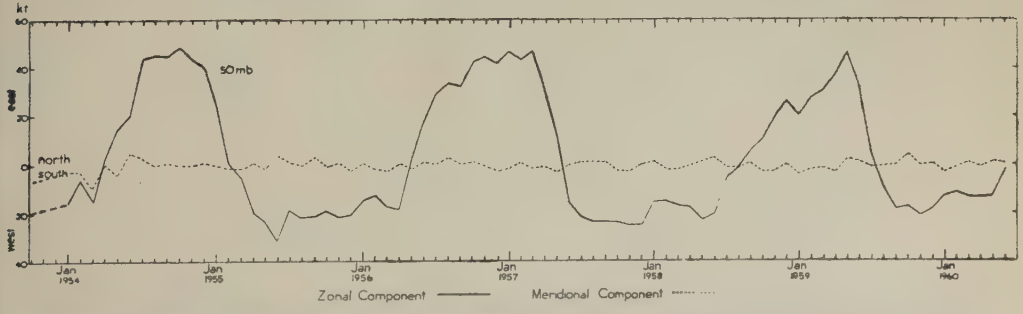

Figure 2. Monthly mean values of zonal and meridional wind components at 50 mb at Canton Island.

be also noted (Figs. 1 and 2) that the meridional wind components at the stratospheric levels considered were usually very small; in fact, the wind is nearly always either almost due E'ly or almost due W'ly, except during the months when the change-over from one regime to another occurs. Table 1 gives the number of occasions during selected months when the wind direction at 50 mb was within certain 30-degree ranges; it shows that in a month when easterly winds prevailed there could be one or two days when the wind was W'ly – and vice versa. It was noted that such reversals of wind direction were generally short-lived, lasting for not more than a day or two, or even for only a few hours. The frequencies for August and September 1958 are also given to illustrate the behaviour of the wind during a period when the change-over from easterly to westerly winds occurs.

TABLE 1. NUMBER OF OCCASIONS WITH 50 mb WIND WITHIN 30 DEGREE DIRECTION RANGES DURING SELECTED MONTHS AT CANTON ISLAND

Date	Direction range											
	346 — 015	016 — 045	046 — 075	076 — 105	106 — 135	136 — 165	166 — 195	196 — 225	226 — 255	256 — 285	286 — 315	316 — 345
1954 Sept.			2	21	1							
1956 June			7	13	4					1	1	
1955 Sept.									3	15	10	
1957 July				2				1	2	20	5	
1958 Aug.		2	3	3	3	1	2	2	5	4	3	2
1958 Sept.	2	2	4	7	3	4	1	1			1	2

An important feature of the stratospheric winds both at Canton Island and Christmas Island is that, for some months, year-to-year variations can be considerable. In fact, the curves suggest that once a predominantly easterly or westerly flow is established it is likely to persist for some 10-13 months. Work now in progress, which will form the subject of another paper, has shown that the fluctuation exists at Nairobi (01° 18'S; 36° 45'E) at the 80 and 60 mb levels, at Singapore (01° 20'N; 103° 53'E) at 60,000 ft (about 65 mb) and Recife (08°S; 35° 53'W) at the 50 mb level and, to a lesser extent at the 60 mb level at Aden (12° 49'N; 45° 02'E) and Khartoum (15° 36'N; 32° 33'E).

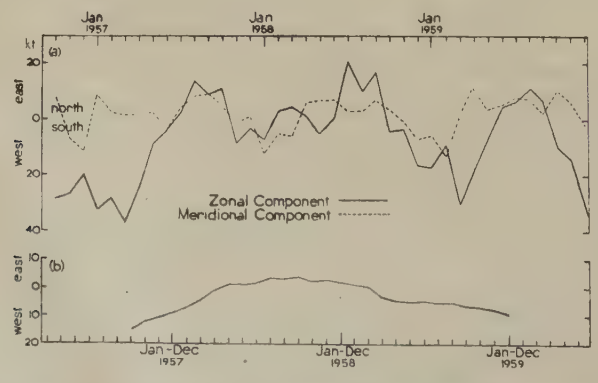

Figure 3. (a) Monthly mean values of zonal and meridional wind components at 200 mb at Christmas Island; (b) 12-monthly running means of 200 mb zonal wind components at Christmas Island.

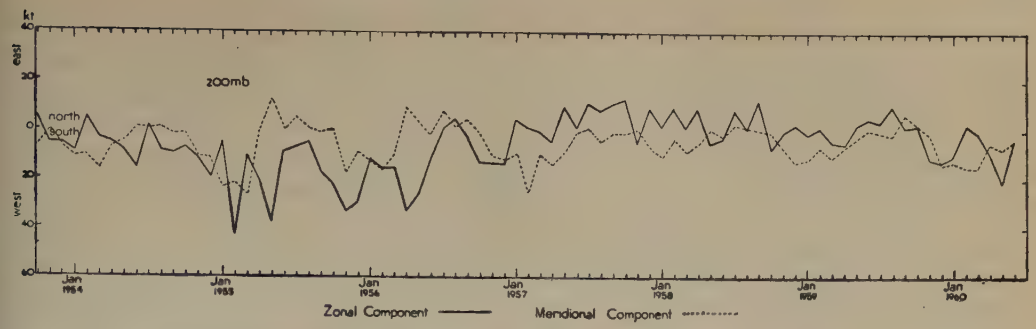

Figure 4. Monthly mean values of zonal and meridional wind components at 200 mb at Canton Island.

To see whether a similar phenomenon occurred in the troposphere, the winds at the 100, 200, 300 and 500 mb levels for Christmas Island and at the 200 mb level for Canton Island were examined, but a parallel fluctuation was not found. Fig. 3 (a) shows the monthly mean values of the zonal and meridional wind component at 200 mb for Christmas Island. It will be noted that, in this case, there is a definite annual variation in the zonal component and the meridional component is appreciably stronger than at 50 mb. In order to remove the annual variation, twelve-monthly running means of the 200 mb zonal wind component were plotted. The resulting curve (Fig. 3 (b) might suggest an oscillation in antiphase with that at 50 mb (Fig. 1 (c)), but the period available for analysis is too short for any useful comparison, and the monthly mean zonal wind components at Canton Island for 200 mb (Fig. 4) and 50 mb (Fig. 2), which cover a more adequate period, do not seem to confirm such an antiphase relationship.

In order to investigate the apparently close agreement between the fluctuation in 50 mb winds at Canton Island and Christmas Island with the suggested 2-3 year periodicity of the Southern Oscillation (Berlage 1957a), the surface pressures were examined.

Twelve-monthly running means of surface pressure were plotted for Christmas Island and it was found that all the values were within the range 1008·4 to 1009·0 mb; as with the curve of the 200 mb zonal wind component for this station, there was a suggestion of a periodicity of about 2 years, but, in view of the short period for which data were available and the weakness of pressure gradients near the equator, no importance can be attributed to this result. From the monthly mean surface pressures for Apia, Samoa Islands (13° 48′S; 171° 46′W) given in the Monthly Meteorological Summary of Apia Observatory, the six-monthly running means of surface pressure anomalies during 1954-1959 were plotted (Fig. 5). It will be seen that during these six years there is no evidence of a 2-3 yr periodicity in the surface pressure anomalies. In fact, for much of 1954, 1955 and 1956 the anomalies were generally positive (during these three years, according to a curve published by Berlage (1957b), the surface pressure anomalies at Djakarta, Java, were negative), whereas in 1957, 1958 and 1959 the anomalies at Apia were negative. This suggests there is no relation between surface pressures and winds at 50 mb although from Figs. 4 and 5 it will be seen that the predominantly westerly winds at 200 mb at Canton Island coincide with the mainly positive surface pressure anomalies at Apia. With a mainly easterly wind direction at 200 mb at Canton, the surface pressure anomalies at Apia are more usually negative.

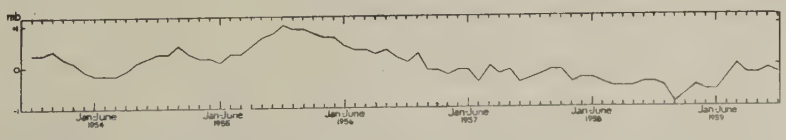

Figure 5. 6-monthly running means of surface pressure anomalies at Apia.

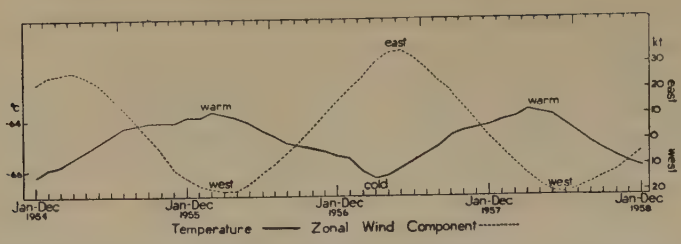

Figure 6. 12-monthly running means of 50 mb temperature and zonal wind component at Canton Island.

To see if there was any corresponding periodicity in precipitation, the rainfall data for Canton Island (1951 to 1959) and Christmas Island (1956 to 1959) were examined, but no connexion was found between rainfall amounts and the 24 to 28 month fluctuation in the stratospheric winds.

Tropopause data for Christmas Island were examined to see if the easterly and westerly regimes in the stratosphere were associated with any changes in tropopause height or temperature, but owing to the large day-to-day variations in the level (pressure) of the tropopause, and the not infrequent occurrence of more than one tropopause (determined by the widely accepted W.M.O. definitions), it was difficult to make good use of the data. However, from the results obtained there was no obvious connexion between the reversal of the 50 mb flow pattern and changes in the pressure (or temperature) at the tropopause.

An examination was also made of the monthly mean temperatures at 50 and 60 mb for Christmas Island for the period during which radiosonde ascents were made at the station. This showed that, for any given month, a westerly regime was accompanied by higher temperatures than an easterly regime. A similar comparison at 50 mb for Canton Island (1954 to 1959) supported this finding to the extent that the lowest monthly mean temperature for any individual month was usually associated with an easterly wind flow, and the highest mean monthly temperature with a westerly flow, but there were exceptions to this in May, July and August. The 50 mb monthly mean temperature at Canton Island in months when the mean zonal wind component was easterly was — 65·5°C and in months when it was westerly the monthly mean temperature was — 64·0°C. A 2 to 3-yr periodicity in the monthly mean 50 mb temperatures at Canton Island was hardly discernible, but the 12-monthly running means (Fig. 6) over the years 1954 to 1958, show clearly a fluctuation with a period of about 24 to 28 months. To facilitate comparison a curve is given in Fig. 6 showing the 12-monthly running means of zonal wind component at 50 mb; it will be noted that there is a slight lag between the E–W fluctuations in the zonal wind components and the fluctuations in the temperatures.

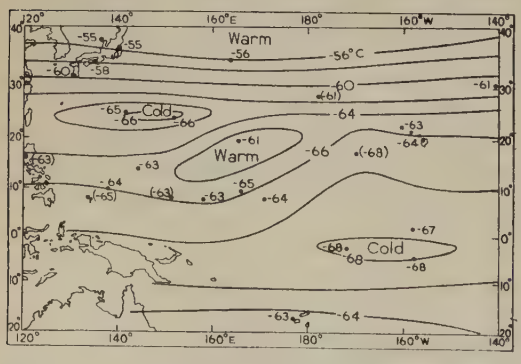

Figure 7. Average 50 mb temperatures for January 1957 in °C. (Monthly means based on less than 10 observations are shown in brackets).

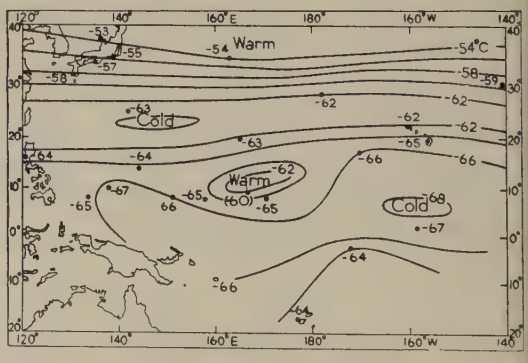

Figure 8. Average 50 mb temperatures for January 1958 in °C. (Monthly means based on less than 10 observations are shown in brackets).

In a study of the atmospheric circulation in equatorial regions, Palmer (1954a) attaches considerable importance to ' thermal winds,' and it can hardly be doubted that temperature gradients may have an important bearing on the flow patterns. For this reason, Figs. 7 and 8 were prepared. They show the monthly mean isotherms at 50 mb over the Central Pacific for January 1957 and January 1958. It will be seen that, although the patterns are generally similar on both charts, there are some differences in the detail. For example, Yap (09° 31′N, 138° 08′E), Ponape (06° 58′N, 158° 13′E) and Wake Island (19° 17′N; 166° 39′E) show a temperature in 1958 some 2°C lower than in 1957, whereas at Canton Island and Iwojima (24° 47′N; 141° 20′E) January 1958 was warmer by 4°C and 2°C respectively. In January 1957 (Fig. 7), the cold pool lies near, and rather south of Christmas Island and Canton Island, whereas in January 1958 (Fig. 8) it is farther away and to the north of Christmas Island, thus resulting in a reversal of the temperature gradient. When considering these temperature data it is important to bear in mind, especially in view of the general weakness of temperature gradients in equatorial regions, the possible sources of error, e.g., the use of different types of radiosonde, the occasional use of only a small number of observations for computing monthly means, the relatively small number of upper-air stations in the area and errors in the temperature and pressure elements of the radiosonde. In conjunction with the preparation of Figs. 7 and 8, vertical cross-sections were drawn, showing temperatures and zonal wind components through the Central Pacific from 30°N to 30°S, for ' representative ' days in the easterly/westerly regimes, i.e., for 15 January 1957 (Fig. 9) and 15 January 1958 (Fig. 10). (It should be noted that these are not true meridional cross-sections as the stations used cover a range of over 40 degrees of longitude). The temperature structure appeared to be very similar on

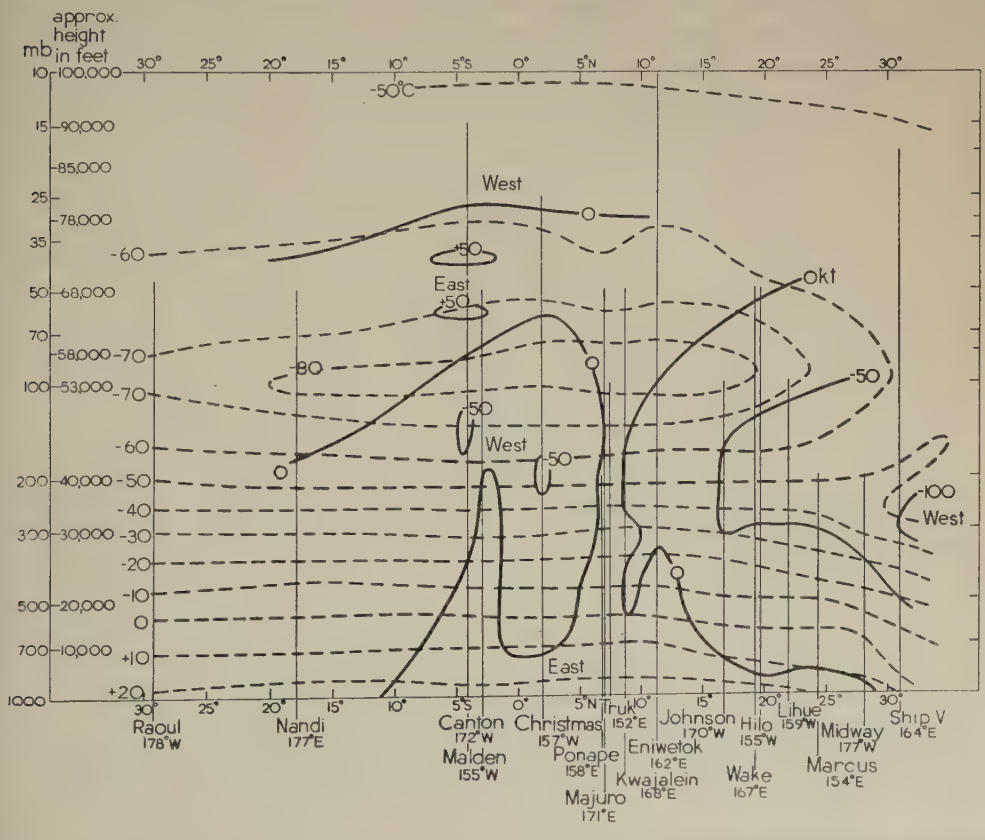

Figure 9. Meridional vertical cross-section at 0300 GMT 15 January 1957, showing zonal wind components in knots (easterly winds positive) as continuous lines and isotherms in °C as dashed lines.

both occasions but more reporting stations with data at levels additional to the standard ones may have produced differences in the detail. The cross-sections of zonal wind component were very different near the equator in both the troposphere and the stratosphere. On 15 January 1957, between 5°N and 5°S, the zonal wind component was mainly westerly from 700 mb to 70 mb, easterly above 70 mb and westerly above 30 mb (no wind reported above 15 mb). On 15 January 1958, over the same area, although winds were generally easterly to above 90 mb there is an indication of a narrow column of westerlies near the equator. Above the general easterlies there were westerlies to about 25 mb with easterlies above (no wind reported above 20 mb). This cross-section for 15 January 1958 (Fig. 10) bears a marked similarity to that for 30 January 1954, published by Palmer (1954b).

Owing to lack of long-period data at levels above 50 mb it was not possible to study the general behaviour of the winds in the higher equatorial stratosphere in relation to those at the lower stratospheric levels. Using Christmas Island data for January to July 1957, Viezee (1958) presents vertical profiles of the zonal wind component which show a gradual lowering of the base of the stratospheric westerlies from January to July in that year. In amplification of the period considered by Viezee, the vertical profiles of the mean monthly zonal wind components above 200 mb at Christmas Island were constructed for each month during which ascents were made and those for alternate months from November 1956 to November 1959 are shown in Fig. 11 (a-j). The values plotted are based on monthly mean winds using 10 obervations or more. It is mentioned earlier that it might be inferred from Fig. 1 that the magnitude of the fluctuation of the zonal wind component at Christmas Island is probably not at its maximum value at 30 mb. From Fig. 11 (a-j), it is evident (in spite of there being some months with no observations above 30 mb) that during the short period for which data are available, the winds at 25 mb display approximately the same regular fluctuation (about 26 months) as those in the lower stratosphere.

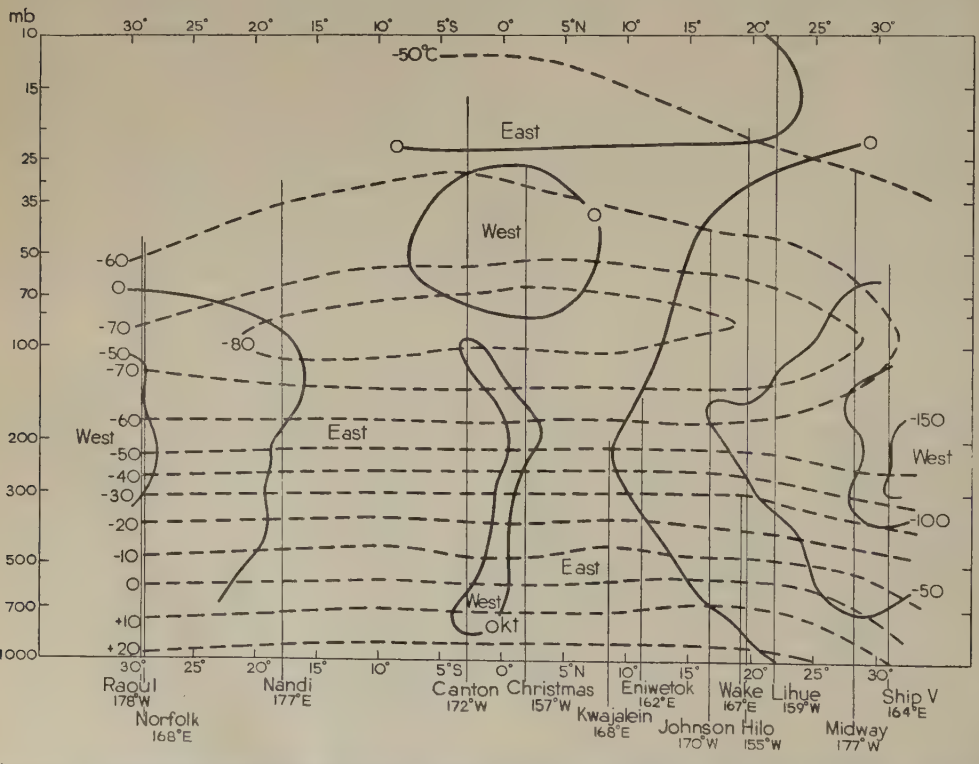

Figure 10. Meridional vertical cross-section at 0001 GMT 15 January 1958, showing zonal wind components in knots (easterly winds positive) as continuous lines and isotherms in °C as dashed lines.

This is true also of the winds at 20 mb, but in this case there are many more months with no observations at that level. At both the 25 and 20 mb levels the magnitude of the fluctuation of the monthly mean zonal wind component is approximately 90 kt (from easterly 60 kt to westerly 30 kt) compared with maxima of 61 kt (from easterly 36 kt to westerly 25 kt at 60 mb) and 73 kt (from easterly 43 kt to westerly 30 kt at 50 mb).

Wind observations above 20 mb at Christmas Island are very few but, in an attempt to determine the highest level at which this change of wind regime takes place, the 10 mb data were examined. Table 2 contains the zonal wind component of the maximum wind at 10 mb together with the number of observations which reached that level during each month. It will be seen that, despite the lack of data, there is strong evidence to suggest that the fluctuation also occurs at 10 mb with values of the zonal wind component varying between easterly 74 kt and westerly 61 kt. Teweles, Rothenberg and Finger (1960), draw attention to this fluctuation in a recent study of circulation patterns at the 10 mb level. It is apparent from Fig. 11 (a-j) that an easterly or westerly wind first appears in the high stratosphere and gradually extends downwards through the stratosphere. This effect has already been illustrated by Graystone (1959) who used 10-day means of the zonal components of the stratospheric winds at Christmas Island. Table 3 shows the months during which the mean zonal wind component at levels above 60 mb at Christmas Island changed from easterly to westerly or vice versa. (The two bracketed entries are based on maximum winds reported and do not refer to the monthly mean value). It will be seen from Table 3 that when the change in wind direction takes place at 25 mb it is about six months later before the corresponding change occurs at 60 mb. The one occasion when it was possible to detect the change at 10 mb suggests that it takes almost a year before the change in wind direction at 10 mb reaches 60 mb. Fig. 11 and Table 3 show that the base of the stratospheric westerlies fell from 21 mb in November 1956 to 76 mb in September 1957 (and to 90 mb in October 1957). From November 1957 to January 1958, the mean monthly winds were westerly at all levels from 200 mb to above 25 mb.

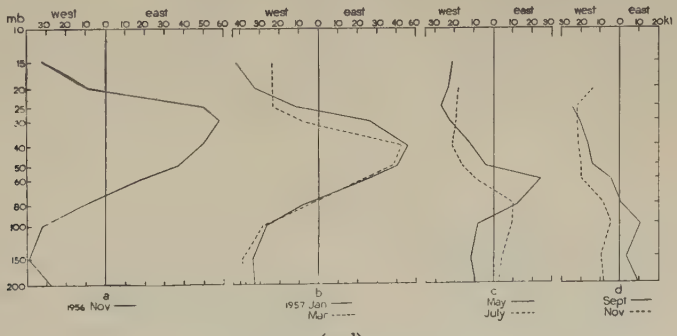

(a-d)

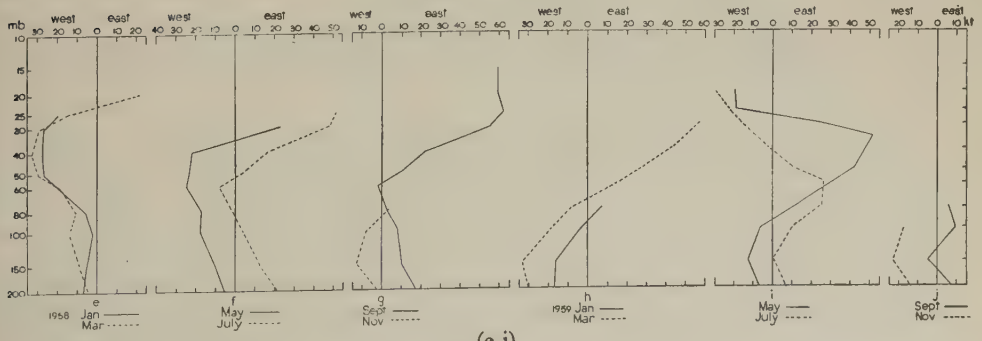

(e-j)

Figure 11. Vertical profiles of the mean monthly zonal wind component (kt) above 200 mb at Christmas Island.

In March 1958 (Fig. 11 (f)), easterlies appeared with their base at 23 mb (the base was at 22 mb in February 1958 and probably near 10 mb in October to November 1957) and these easterlies gradually descended to reach 94 mb in January 1959 (Fig. 11 (h)). In May 1959 (Fig. 11 (i)), the westerlies again appeared at 27 mb (almost certainly some months earlier at higher levels) and by July their base had fallen to 40 mb (and to 58 mb in August).

TABLE 2. Zonal wind component (kt) of the maximum wind at 10 mb at Christmas Island

	Jan.	Feb.	Mar.	Apr.	May	June	July	Aug.	Sept.	Oct.	Nov.	Dec.
1956											− 39 (5)	− 61 (8)
1957	− 27 (1)		− 37 (6)	− 26 (4)	− 44 (20)	− 29 (4)				− 28 (1)	+ 33 (1)	
1958		+ 63 (7)			+ 57 (1)			+ 74 (4)	+ 70 (4)			
1959					− 27 (1)	− 35 (2)	− 41 (3)					

East – positive; West – negative ( ) No. of observations.

TABLE 3. Months during which the mean zonal wind component at Christmas Island changed sign

Level	From East to West	From West to East	From East to West
10 mb		(Oct. 1957) – (Nov. 1957)	
20 mb	Oct. 1956 – Nov. 1956	(Dec. 1957) – (Jan. 1958)	
25 mb	Dec. 1956 – Jan. 1957	Mar. 1958 – Apr. 1958	Apr. 1959 – May 1959
30 mb	Feb. 1957 – Mar. 1957	Apr. 1958 – May 1958	May 1959 – June 1959
40 mb	Apr. 1957 – May 1957	June 1958 – July 1958	June 1959 – July 1959
50 mb	Apr. 1957 – May 1957	June 1958 – July 1958	July 1959 – Aug. 1959
60 mb	May 1957 – June 1957	Sept. 1958 – Oct. 1958	Aug. 1959 – Sept. 1959

( ) denotes maximum wind reported and not monthly mean value.

3. Conclusions

Available data indicate a fluctuation with period 24 to 28 months in the stratospheric winds over Canton Island and Christmas Island, but in view of the shortness of the period studied (less than seven years) it would be unwise to draw any firm conclusions regarding the probable persistence or vertical extent of this periodicity, although Christmas Island data indicate that during the period October 1956 to July 1959 the phenomenon was evident above 20 mb, and that the change in wind direction from easterly to westerly, or vice versa, takes about six months to descend from 25 to 60 mb and about twelve months to descend from 10 to 60 mb.

From such studies as have been possible with the data available there was no detectable connexion between events in the equatorial stratosphere and the equatorial troposphere – apart from the slight suggestion of a fluctuation with a period of a little over 2 years in the 200 mb monthly mean zonal wind component at Christmas Island (Fig. 3 (b)). Whilst it may well be possible to associate changes in the equatorial stratospheric wind regimes with changes in horizontal or vertical temperature gradients and with vertical motion, the reporting network prior to the International Geophysical Year was unfortunately not close enough to facilitate this, and in any case it is questionable whether the accuracy of the radiosonde would allow it. However, an analysis of the higher level data from the increased number of reporting stations during the I.G.Y. may help to increase our knowledge of the stratospheric circulation in both the Central Pacific and other tropical

areas, especially Africa. (Radiosonde ascents commenced at Gan, Maldive Islands (00° 41′S; 73° 10′E) in October 1959 and these data should prove extremely interesting when a period long enough to analyse is available). Meanwhile, until more accurate and homogeneous and more plentiful upper-air data, reaching the higher levels become available, many problems regarding meteorological phenomena in the equatorial regions may remain unanswered.

Words written by Sir Gilbert Walker in 1923, during his early work on the Southern Oscillation, seem equally appropriate now – ' the only hope at present is that of ascertaining the facts and of arranging them in such a way that interpretation shall be possible.' These notes do not explain the reasons for the behaviour of the equatorial stratospheric winds, but it is hoped that they go a little way towards ascertaining and arranging the facts.

Acknowledgments

This paper is published by permission of the Director-General of the Meteorological Office. I should like to express my appreciation to Mr. R. G. Veryard for his very helpful advice during the preparation of this work.

References

Berlage, H. P.	1957a	Koninklijk Ned. Met. Inst. Mededelingen en Verhandelingen, **69**, p. 123.
	1957b	*Ibid.*, **69**, p. 65.
Ebdon, R. A.	1960	*Quart. J. R. Met. Soc.*, **86**, p. 540.
Graystone, P.	1959	*Met. Mag.*, **88**, p. 117.
Palmer, C. E.	1954a	*Weather*, **9**, p. 341.
	1954b	*Ibid.*, **9**, p. 343.
Teweles, S., Rothenberg, L. and Finger, F. G.	1960	*Monthly Weather Review*, **88**, p. 148.
Viezee, W.	1958	*A.F.C.R.C.*, TB-58-270, University of California, p. 60.
Walker, Sir G. T.	1923	*India Met. Mem.*, **24**, p. 75.

551.507.352 : 551.557.5

Project Jet Stream Research Flight No. 30, April 1957

By E. R. REITER

Meteorology and Geophysics Institute, Innsbruck University, Austria

(Manuscript received 19 July 1960; communicated by G. A. Corby)

Summary

An analysis is made of Project Jet Stream Research Flight No. 30, conducted on 8 April 1957. This flight made several traverses through a pronounced jet stream over the New England States. The fields of wind speed, potential temperature, vorticity and divergence are presented in vertical cross-sections. Special reference is made to the differences between geostrophic and actual vertical wind shear in the vicinity of the jet core.

1. Introduction

In several recent publications, the author has described methods for evaluating and analysing data, which have been gained from detailed aircraft measurements (Reiter 1960a; 1960b). It has been pointed out that small-scale perturbations in the fields of wind and temperature, comprising only 3 points of measurement or less, will have to be considered as ' instrumental errors,' even though they may at times be larger than the lower limit of the accuracy of the instruments, which has been listed by Endlich and Rados (1959). These fluctuations have been disregarded in the analysis of the data, although in some instances they might have been indicative of some real micro-structure of the jet stream.

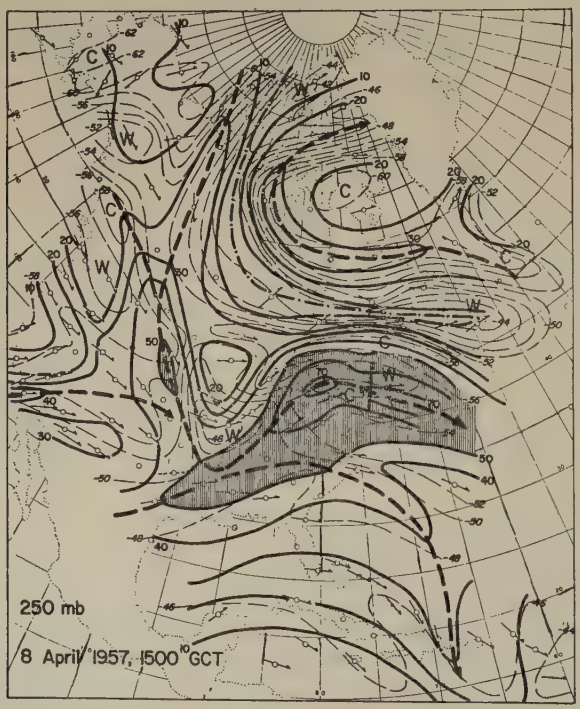

Figure 1. 250 mb isotachs (heavy solid lines, upright figures give m sec^{-1}) and isotherms (thin dashed lines, slant figures give °C) of 8 April 1957, 1500 GCT. Shaded area indicates wind speeds in excess of 50 m sec^{-1}. The route of flight No. 30 is marked by a heavy dotted line. Jet axes are drawn in heavy dashed lines, a shear line is represented by a heavy dash-dotted line.

With a point of measurement approximately every 30 sec, and with a true airspeed of about 450 kt, the scale of horizontal variations of the wind speed is known to 20 km. Fluctuations in this field, which have at least this horizontal extent, will be called the meso-structure of the jet stream. A second process of smoothing is now adopted which eliminates these structural details, and we arrive at the basic field of flow upon which the meso-structure appears to be superimposed as perturbations.

This avenue of approach has been followed successfully in the evaluation of several project jet stream flights. The results have been published in the two papers cited above. The present investigation dealing with flight No. 30, flown on 8 April 1957, takes advantage of the same methods of evaluation and analysis. Special reference will be made to problems arising from the non-verticality of the flight cross-section, and from considerations which relate the thermal wind with the actual vertical wind shear.

2. The synoptic situation

Fig. 1 gives the 250 mb chart of 8 April 1957, 1500 GMT. The flight path, which is marked by a heavily dotted line, runs between New York and Quebec, cutting through the rear end of a jet maximum with peak speeds exceeding 70 m sec^{-1}. A shear line with predominant sinking motion (to be deduced from the high stratospheric temperatures and the cloudless surface weather) overlies central and eastern Canada.

The jet stream through which flight No. 30 has been made, appears to be of the ' polar front ' type, i.e., it is associated with a well-defined baroclinic zone which extends from the earth's surface to the tropopause. On the ground it appears as a pronounced front (Fig. 2). Precipitation areas are indicative of ascending motion in the rear right quadrant of the jet maximum, whose centre is to be sought off the New England coast.

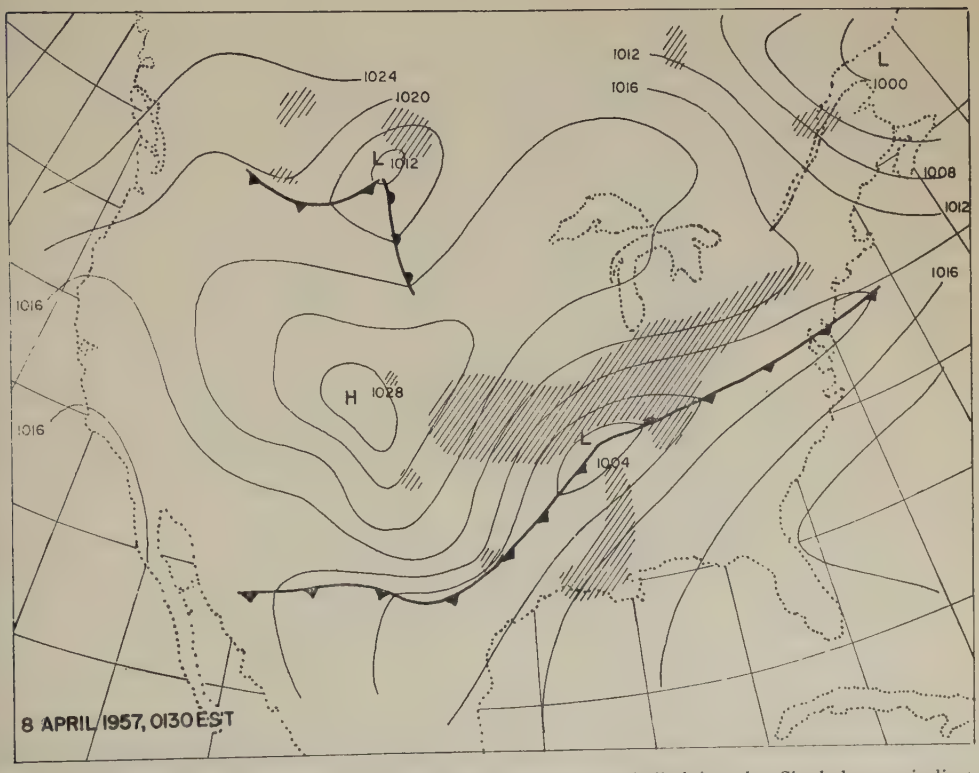

Figure 2. Surface chart, 8 April 1957, 0130 EST. Isobars are labelled in mb. Shaded areas indicate precipitation.

Considering the vorticity advection in an anticyclonically curved jet stream, this quadrant favours high-level divergence and subsequent upward motions. A small secondary wind maximum north of Lake Erie should not be trusted too much. It is mainly based upon the wind report at Flint (637) with 69 m sec^{-1} (134 kt). Allowing for possible irregularities in the wind sounding (Reiter 1958), this value might be slightly too high.

The merging of several ' jet fingers ' into one jet stream is revealed in Fig. 1. Structural details of this kind have also been noted in other examples of analysis. It might be noted as a specific point of interest, that the jet maximum over the eastern declivities of the Rocky Mountains overlies the centre of a high pressure area, in which the lower troposphere is more or less barotropic. Since such jet streams, in which the baroclinic zone is confined to the upper troposphere, are usually classified as ' subtropical jet streams,' the present weather situation contains the paradox of the subtropical jet occurring north of the polar-front jet. This demonstrates that the nomenclature of jet streams leaves something to be desired. Furthermore, the existence of a transition mechanism between the two types of jet streams suggests itself, which has been commented on in an earlier paper (Reiter 1960a).

3. The aircraft measurements

Fig. 3 shows an analysis of the basic field of motion (kt) in which the meso-structure of wind speed has been eliminated. Quantitatively, the speeds are in good agreement with the values given in Fig. 1. The fact that measurements have not been made simultaneously is not considered to have a serious effect upon the basic field thus obtained. It takes the aircraft 40 to 50 min approx. to complete one flight leg. The total flight cross-section of Fig. 3 took $3\frac{1}{2}$ hr. Since the analysis rests mainly upon successive legs, the maximum time difference involved in the estimate of vertical gradients is only $1\frac{1}{2}$ hr. During the

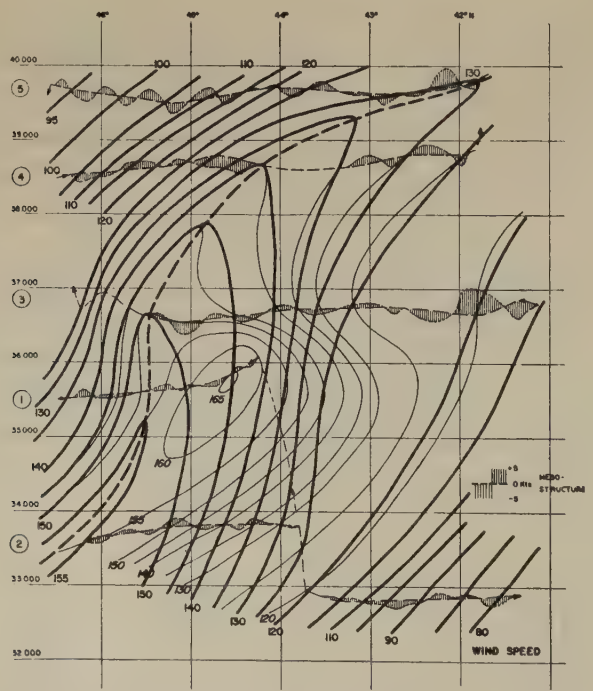

Figure 3. Isotachs (kt) of the double-smoothed wind field, flight No. 30; heavy lines : excluding level 1, thin lines : including level 1 into the analysis. The heavy dashed line gives the position of the jet axis. The flight legs (thin dashed lines) are numbered on the left margin of the diagram. Shaded areas indicate the meso-structure of the wind field. Its amplitudes have to be read off with respect to the flight route as base line. A scale is given on the lower right-hand side of the diagram.

12 hr following map time of Fig. 1, the jet stream in the vicinity of the flight cross-section changed only little. Its core remained near Albany, New York, with the speeds decreasing by about 15 kt. A quasi-synoptic interpretation of the flight data seems, therefore, justified for this flight.

The analysis of Fig. 3 is designed to point out fallacies which might arise when the position of the flight legs are not considered carefully in constructing the vertical cross-section. The aircraft, B–47E, took off from Portsmouth Air Force Base, New Hampshire, at 1724 GMT 8 April 1957. After reaching an operational altitude of about 35,800 ft, the airplane headed toward Quebec. Flight leg No. 1 (the leg numbers are given by digits in circles on the left margin of Fig. 3) ran slightly to the east of the rest of the cross-section, as much as 60 naut. mi at 44°N. At 46°N this leg meets with the vertical plane, in which the rest of the flight has been conducted.

If an analysis of the wind-speed data, irrespective of the position of the flight legs is attempted, a pronounced wind maximum is found between 44°N and 45°N on leg No. 1. There is no maximum counterpart at other flight levels in this particular geographic latitude, and the result is the peculiar-shaped jet stream, represented by the light solid lines in Fig. 3. This distribution of wind speed must be regarded as highly doubtful, since it rests upon one flight-level only. Apparently a horizontal departure of a flight leg from the vertical cross-section plane of only 60 naut. mi can create quite an unrealistic picture of the atmospheric flow pattern.

The heavy solid lines in Fig. 3 are isotachs which have been constructed *without* the use of level No. 1. They give a rather smooth appearance of the flow inside the jet-stream core, and may be considered with greater confidence as being representative of the basic field of wind speeds.

A comparison between speed values recorded along leg No. 1, and the heavy isotachs reveals quite strong horizontal accelerations. Between 43·5°N and 44·5°N they have an order of magnitude of about 20 kt in 60 naut. mi or $9{\cdot}26 \times 10^{-5}$ sec^{-1}. This value needs to be considered when calculating the field of divergence. North of 44·5°N the acceleration will be of similar magnitude. Because the horizontal distance between leg No. 1 and the vertical cross-section approaches zero, an estimate of accelerations from flight data appears to be of questionable value in this region.

An analysis of potential temperatures is shown in Fig. 4. These have been calculated from pressure altitude and vortex thermometer readings with the aid of Bellamy's pastagram (Bellamy 1945). No corrections have been applied to these temperatures.

In this analysis no significant change could be detected through a consideration of the eastward displacement of leg No. 1. This stands in agreement with the isotherm pattern of Fig. 1 (dashed lines), which does not indicate any appreciable change of temperature along the streamlines in the immediate vicinity of the flight. Thus, Fig. 4 can be accepted as representative of the basic field of temperature.

The details of this field, especially the stable layers, which appear to be sandwiched between near-adiabatic layers, and their connexion with meso-structure of the wind field and clear-air turbulence will be commented on later. At the moment we shall compare Figs. 3 and 4. It is evident that the thermal-wind equation in the vicinity of the jet-stream core does not hold qualitatively in several regions of this cross-section (Cunningham 1956).

By and large, the increase of wind speed with height is met by a corresponding baroclinicity in the right-hand lower portion of the cross-section. The rather well-pronounced decrease of wind speed with height, which should be expected from the potential isotherm pattern at about 36,000 ft and 44·5°N is not evident from the *heavy* isotachs of Fig. 3. It does, however, appear in the *thin* isotachs of this layer which make use of flight leg No. 1 farther east. Unfortunately, we do not have any information from aircraft measurements as to the distribution of vertical wind shear in the region of leg No. 1. The shears indicated by the thin isotachs are to a great extent enforced by the data from the other flight-levels. A superficial inspection of Fig. 3 would indicate, however, that the thermal-wind requirements of Fig. 4 are met farther downstream from the speed cross-section given by the heavy isotachs.

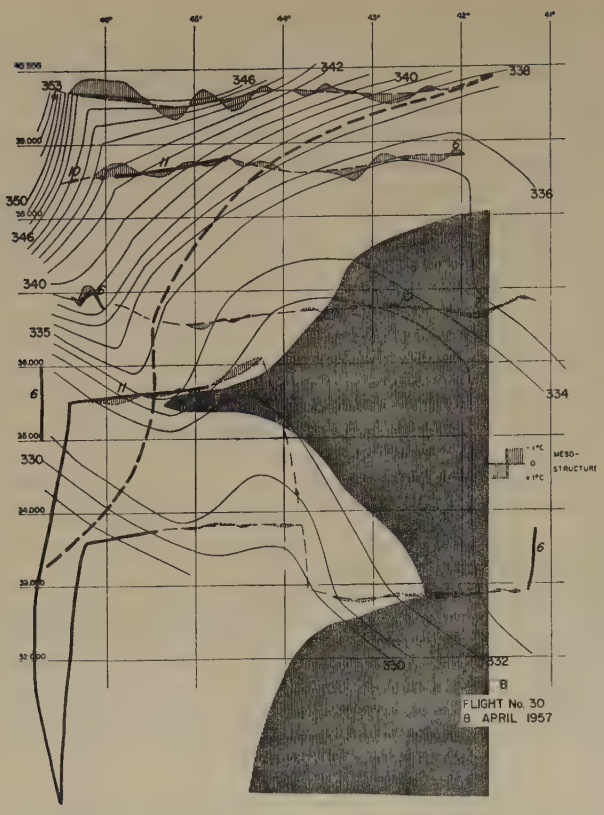

Figure 4. Potential temperatures, flight No. 30 (thin solid lines) in °K. Flight legs and jet axis as in Fig. 3. The meso-structure of temperature is entered along the flight legs in a fashion similar to the previous figure. The large shaded area stands for clouds. The heavy solid lines along the flight legs indicate zones of clear-air-turbulence as measured by the VGH instrument; slant figures give maximum gust velocities (fps) within these zones.

This must follow, if one adopts Raethjen's principle of adaptation (Raethjen 1959) whereby the wind field seeks to orient itself after the existing pressure field, without accomplishing an immediate adjustment. The existence of such a mechanism of adaptation becomes evident from *ageostrophic* components of flow. The thermal wind which can be calculated from Fig. 4, yields geostrophic wind shears. The discrepancies between thermal wind and actual wind shear of Fig. 3 have to be attributed to the presence of ageostrophic motions. These in turn tend to accelerate or decelerate the basic flow, enforcing an adaptation of the wind field to the pressure and temperature fields farther downstream, which, in themselves, are not stationary either, but undergo gradual changes (Newton 1959).

(*a*) *The thermal-wind equation and ageostrophic flow*

Whilst these speculations have to be merely qualitative in the absence of a complete flight cross-section downstream of Fig. 3, certain quantitative deductions can be made about the magnitude of the ageostrophic u-component.

Using Poisson's equation and the assumption that $\Theta\, p^{\kappa}/\Theta_0\, p_0^{\kappa} \cong 1$, we obtain the geostrophic wind shear from the thermal wind equation as

$$\frac{\Delta u_g}{\Delta z} = \frac{u_g - u_{g_0}}{\Delta z} = -\frac{g}{f\,\Theta}\,\frac{\partial \Theta}{\partial y} \quad . \quad . \quad . \quad . \quad (1)$$

where $\kappa = (c_p - c_v)/c_p$ is Poisson's constant and $\overline{\Theta}$ is the mean potential temperature of the layer under consideration.

The difference between actual vertical wind shear, which can be determined from Fig. 3, and the geostrophic shear of Eq. (1) yields the ageostrophic component of motion, which will be denoted by an asterisk :

$$\frac{\Delta u}{\Delta z} - \frac{\Delta u_g}{\Delta z} = \frac{\Delta u^*}{\Delta z} \quad . \quad . \quad . \quad . \quad . \quad (2)$$

or

$$u^* = \int_{z_0}^{z} \left(\frac{\partial u}{\partial z} - \frac{\partial u_g}{\partial z} \right) dz + A \quad . \quad . \quad . \quad . \quad (3)$$

A is a constant of integration, which gives the value of u^* at the level z_0.

Part of the ageostrophic component u^* may be due to gradient flow along *curved* trajectories; the contribution of curvature could not be evaluated from the flight data, however.

Fig. 5 contains an analysis of Δu_g, the geostrophic component of shear normal to the cross-section, per 500 ft height. This shear distribution has been calculated by means of Eq. (1) from the potential temperature pattern of Fig. 4. The actual wind shear $\partial V/\partial z$ is shown in Fig. 6. Shear values have been computed over 10 kt intervals in places where the isotachs in Fig. 3 are crowded. From this chart it is evident, that above the jet axis the vertical wind shear changes almost discontinuously. A ' peaked ' vertical wind profile, as has been advocated as a model for the smoothing of rawin data (Reiter 1958), can be justified at least for the present jet stream.

To be correct, one would have to take $\partial u/\partial z$ instead of $\partial V/\partial z$ in the evaluation of Eq. (3). As can be seen from Fig. 7, which contains an analysis of wind direction, the error involved in this approximation does not exceed 4 per cent. (The cosine of

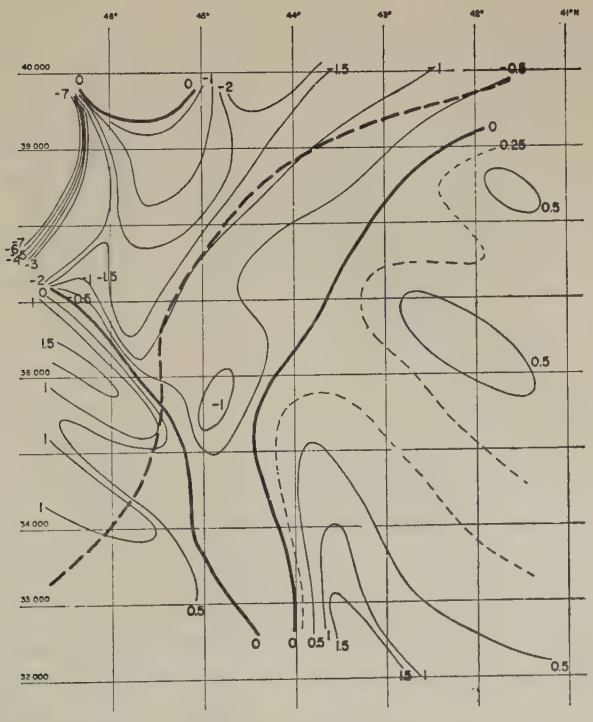

Figure 5. Geostrophic wind shear Δu_g (m sec^{-1}) in 500 ft vertical intervals. Jet axis as in Fig. 3. Zero shear is marked by heavy lines.

14° arises from a wind direction of 256°, which constitutes the extreme deviation from due-west winds in this cross-section). Since the measurements of the wind vector and its analysis are probably in error by that amount, a computation of the u-component has not been undertaken.

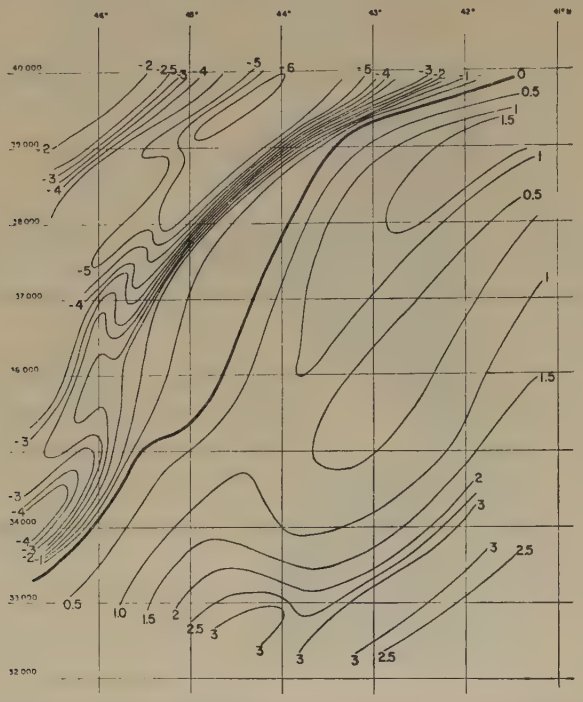

Figure 6. Actual vertical shear ΔV (m sec^{-1}) in 500 ft vertical intervals. Zero shear is marked by heavy line.

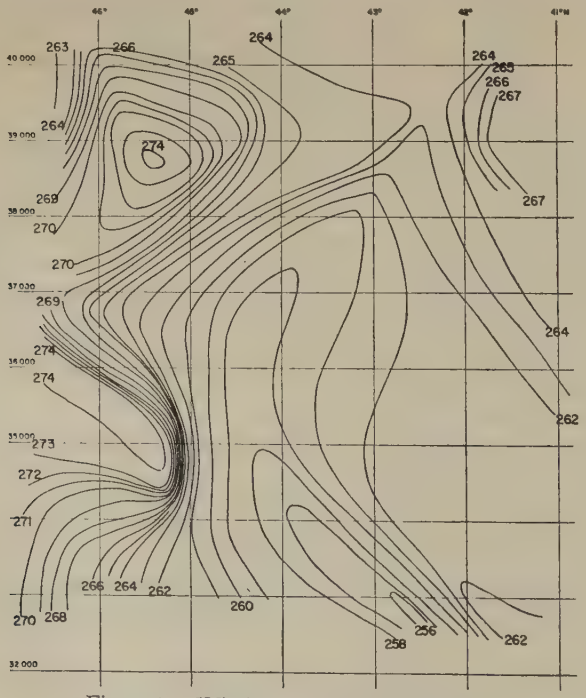

Figure 7. Wind directions, flight No. 30.

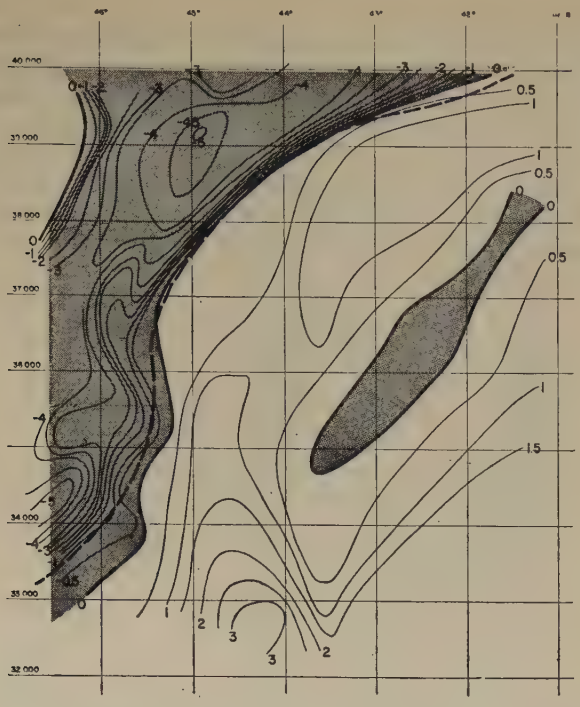

Figure 8. Difference between actual and geostrophic vertical wind shear (m sec $^{-1}$) in 500 ft vertical intervals. Areas with negative values of this difference are shaded.

The difference Δu^* between ΔV and Δu_g computed in terms of 500 ft deep layers has been analysed in Fig. 8. Certainly, the detailed features of this chart will have to be accepted with some reservation in view of the subjectivity in the interpretation of the data. The gross features, however, lead to some interesting conclusions.

In order to obtain the ageostrophic component u^* at a particular level, we have to know the constant A of integration in Eq. (3). Any assumption which we might make about this constant would be arbitrary. The absolute magnitude of u^*, therefore, must remain unexplored. We might, of course, help ourselves by comparing the geostrophic with the actual flow on the 250 mb chart, but these macroscale data cannot readily be compared with the more detailed flight data; therefore this possibility had to be abandoned.

Nevertheless, the increase or decrease of u^* with height can be estimated clearly from Fig. 8. There is a striking agreement between the line of $\Delta u^* = 0$ (heavy solid line) and the axis of the jet core (heavy dashed line). This indicates, that the *ageostrophic component u^* shows a maximum in the jet core.* In the present situation the winds in the jet axis of the flight cross-section are super-geostrophic ($u^* > 0$). Part of this ageostrophic component will have to be attributed to the fact, that the trajectory curvature is slightly anticyclonic in this region (cf. Fig. 1). Although the speeds are already super-geostrophic inside the jet core, there is still further acceleration taking place downstream from the cross-section, as can be seen from the speed values along leg No. 1.

As will be demonstrated later from an evaluation of the ' normal component,' convergence seems to be concentrated within the baroclinic zone in the vicinity of the jet axis. The geostrophic divergence of a zonal current is zero, therefore the divergence of the wind field has to be attributed to ageostrophic components only : $D = \nabla \cdot \mathbf{V}^*$. Thus, the maximum of ageostrophic flow inside the jet core corroborates the distribution of horizontal divergence.

The strong decrease of Δu^* above the jet axis leads to the conclusion that winds become sub-gradient or even sub-geostrophic in the stratosphere on the left-hand side of the jet stream. This agrees well with the findings of Endlich and McLean (1960), who observed on the average of straight jet streams sub-gradient flow above and to the left of the core. Their values were computed by comparing flight data with contour analyses of upper-air charts, while the present investigation rests on flight data only.

A further interesting detail is presented by the 'island' of negative Δu^* – values well to the anticyclonic side of the jet stream in Fig. 8. It is produced by a minimum in vertical wind shear and it lies inside a rather deep adiabatic layer.

(b) *The field of vorticity*

The absolute vorticity may be written as :

$$Q = V/r - \frac{\partial V}{\partial n} + f \quad . \quad . \quad . \quad . \quad (4)$$

V being the total wind speed, r the radius of streamline curvature and n the direction normal to the streamlines, positive towards the left of the motion.

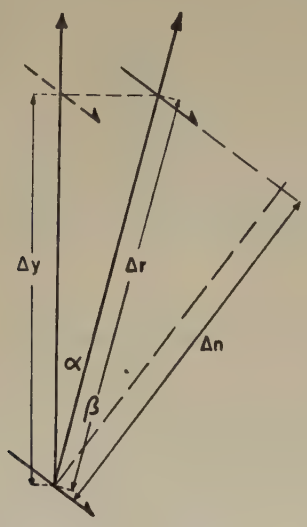

Figure 9. Calculation of $\Delta V/\Delta n$ from $\Delta V/\Delta y$ (for explanation see text).

The expression $-\partial V/\partial y$ can readily be calculated from Fig. 3. In order to obtain $-\partial V/\partial n$ we shall have to consider the deviation angle α of the flight track from the meridian, on to which the aircraft measurements have been projected, and the angle β between flight track and normal n to the wind direction (Fig. 9). From trigonometric considerations we obtain (Reiter 1960b) :

$$\frac{\Delta V}{\Delta n} = (\cos \alpha/\cos \beta)\frac{\Delta V}{\Delta y} \quad . \quad . \quad . \quad . \quad (5)$$

For flight No. 30, α is approximately 19 degrees.

If Eq. (5) is expressed percentage-wise we obtain

$$\Delta V/\Delta n = (\Delta V/\Delta y)\left(1 + \frac{p}{100}\right) \quad . \quad . \quad . \quad (6)$$

where $1 + p/100 = \cos \alpha/\cos \beta$ or $p = 100\,(\cos \alpha/\cos \beta) - 100$, the per cent increase or decrease which has to be applied to the measured values of $\Delta V/\Delta y$ in order to obtain $\Delta V/\Delta n$.

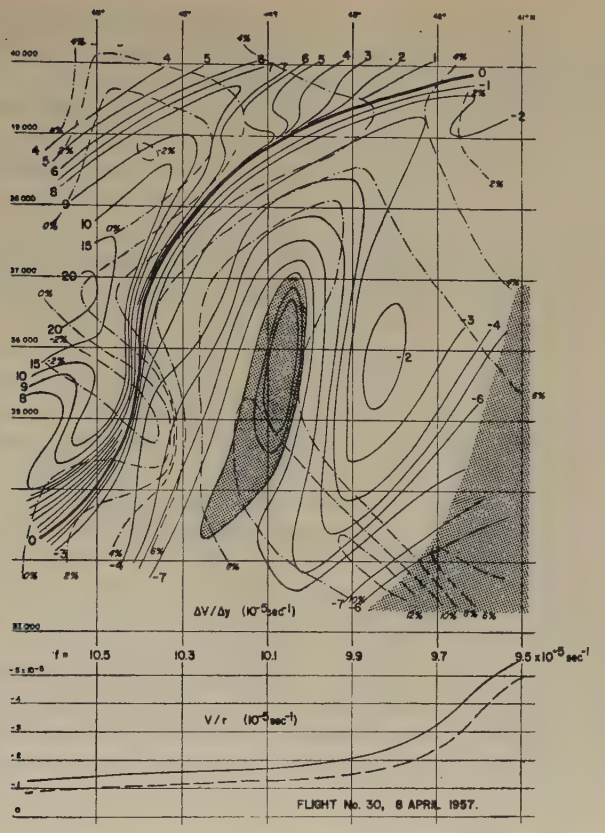

Figure 10. Upper part of diagram : $\Delta V/\Delta y$ in units 10^{-5} sec^{-1} (thin solid lines, upright figures). Dash-dotted lines and slant figures give per cent correction of $\Delta V/\Delta y$ in order to obtain $\Delta V/\Delta n$. Shaded areas indicate values of absolute vorticity $Q < 0$. Lower part of diagram contains values of Coriolis parameter f (heavy numbers) and of V/r at the 250 mb level (solid line) and the 200 mb level (dashed line) in units 10^{-5} sec^{-1}.

Fig. 10 shows an analysis of $\Delta V/\Delta y$ (full lines). Iso-lines of p (in per cent) have been entered with dashed-dotted lines.

The computation of the stream-line curvature term in Eq. (4) has been made from the 250 and 200 mb charts (the latter is not reproduced in this report). The values in units 10^{-5} sec^{-1} are entered in the lower part of Fig. 10.

Assuming that between the 250 and 200 mb levels, a linear interpolation of the curvature term is permissible, and considering the Coriolis parameter (numerical values are given in the lower part of Fig. 10, units 10^{-5} sec^{-1}), it appears that in the shaded areas Q attains values < 0.

The zone of dynamic instability about 100 naut. mi to the south of the jet axis is rather narrow, and its reality might be argued about, because the minimum values of negative absolute vorticity are to be found in between two flight levels. The isotach pattern of Fig. 3 could be forced in such a way that negative values of Q become negligibly small.

From Fig. 1 it may be concluded, however, that the anticyclonic shear increases downstream from the flight-cross section. It is, therefore, reasonable to assume that a zone of dynamic instability does exist along the jet maximum over the east coast of the United States. Furthermore a jet stream in the same position on 4 April 1957 (flight No. 29) showed a well-established wide region with $Q < 0$ (Reiter 1960b). Evidence of dynamically unstable zones in the jet stream region directs attention to the question of how these findings can be brought into agreement with the theorems of conservation of absolute and potential vorticity. The latter also needs consideration because negative potential vorticity ($- Q_z \cdot \Delta\Theta/\Delta p$) occurs where $Q_z < 0$.

From both flights No. 29 and No. 30 it appears that dynamic instability favours the regions near which potential temperatures show an upward ' hump.' However, this statement will have to be checked by further case studies.

It has been shown from Fig. 8 that the geostrophic unbalance of vertical shear attains maximum values near these humps, mostly on their cyclonic sides, that is, the actual wind field has not yet adjusted itself to the conditions prescribed by the geostrophic vertical wind shear. The same conclusions could be drawn from the analyses of Flight No. 29, although they have not been calculated explicitly there. It deserves further investigation, whether the ageostrophic component of motion may have some bearing upon the establishment of dynamically unstable zones.

(c) *The field of divergence*

Fig. 11 contains an analysis of the ' normal component ' of the wind speed, defined as the component of motion normal to the wind direction which has been measured at the point of maximum wind speed.

It has been seen from Fig. 3 that the maximum values of wind speed have been eliminated from the analysis, because they occurred along leg No. 1. Therefore the normal component analysed in Fig. 11 does not give true values of the flow across the jet-stream core. The zero-isopleth of this component does not coincide with the jet axis, for this reason. Nevertheless, certain conclusions may be drawn from this analysis.

The cross-section of flight No. 30 is located to the rear of a jet maximum. One would, therefore, expect the streamlines to cross the jet axis towards the low-pressure side. This is qualitatively the case in Fig. 11, which leads to the conclusion that the presence of ageostrophic components in the entrance region of the jet maximum, counter-balances, to a certain degree, the effect created by the elimination of leg No. 1.

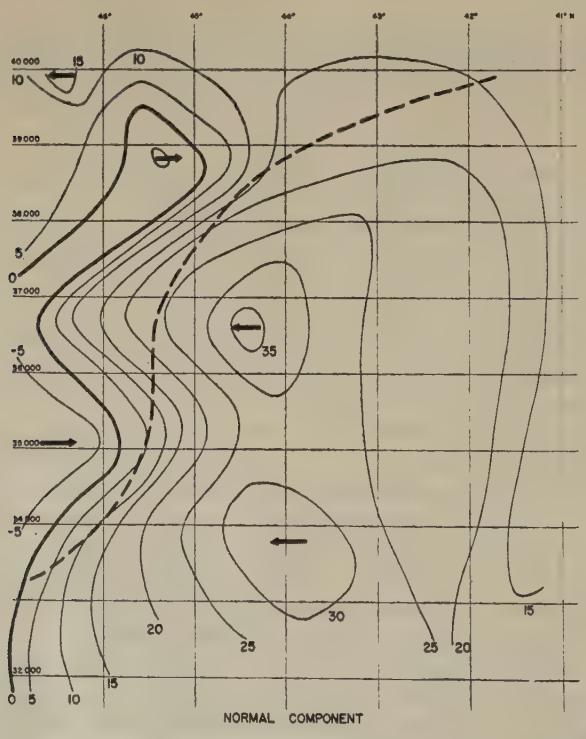

Figure 11. Normal component (kt), flight No. 30. Positive sign denotes winds blowing from the anticyclonic towards the cyclonic side of the jet axis. Jet axis as in Figure 3.

Although Fig. 11 does not give the true component of flow normal to the jet axis, the horizontal gradients of speed, which can be calculated from this analysis, closely resemble the values of $\Delta v/\Delta y$. The distribution of this quantity in units 10^{-5} sec^{-1} is shown in Fig. 12. The fact that $\Delta v/\Delta r$ has been reduced into $\Delta v/\Delta y$ bears no significance.

The two-dimensional horizontal divergence

$$D = \partial v/\partial y + \partial u/\partial x \quad . \quad . \quad . \quad . \quad (7)$$

into which the term shown in Fig. 12 enters, is rather difficult to estimate. From the 250 mb chart shown in Fig. 1 it appears that the value $\Delta u/\Delta x$ increases from the north towards the south of the flight cross-section. At 200 mb $\Delta u/\Delta x$ seems to attain rather small values, therefore it may be neglected at this level. From Fig. 3 we have seen that in the centre part of the cross-section $\Delta u/\Delta x$ may be as much as $+ 9{\cdot}26 \times 10^{-5}$ sec^{-1}. This would mean that the horizontal divergence on the anticyclonic side of the jet stream would be of the order of magnitude of 10 to 14 $\times 10^{-5}$ sec^{-1}, while the convergence on the cyclonic side, indicated in Fig. 11 by the negative sign of $\Delta v/\Delta y$, is reduced in magnitude. Nevertheless, an area of pronounced horizontal convergence remains where the stable baroclinic zone extends in the stratosphere just above the jet core. Other areas of convergence seem to be located to the left of the hump in the potential-isotherm pattern. The hump itself coincides well with the zero-line of Fig. 12, which divides areas with positive and negative $\Delta v/\Delta y$.

Strong divergence is found inside the adiabatic and cloud-filled layer on the right-hand side of the flight cross-section, similar to what became evident from flight No. 29.

The gross distribution of divergence and convergence agrees well with what one might expect from the vorticity-advection pattern in the rear of a jet maximum. Some smaller details, however, as for instance the divergence area in the upper-left corner of the cross-section, which coincides with another hump in the isentropic surface, do not follow this simple model.

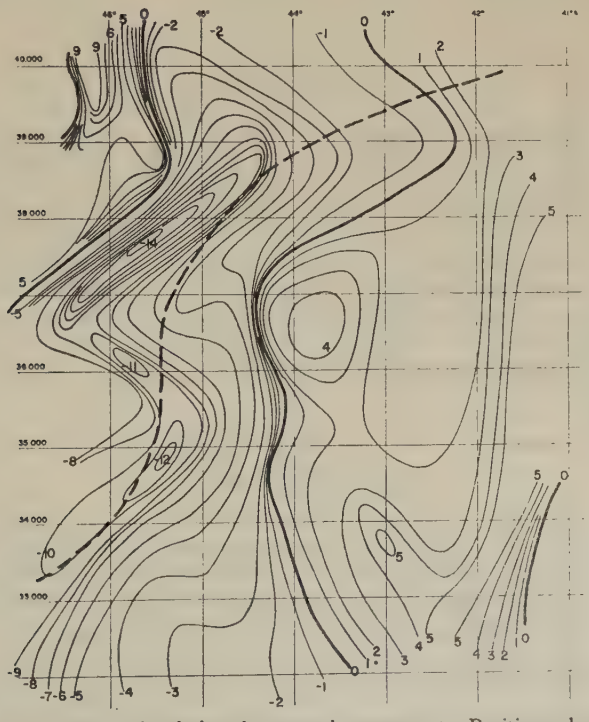

Figure 12. $\Delta v/\Delta y$ in units 10^{-5} sec^{-1}, v being the normal component. Positive values stand for divergence. Zero lines are drawn heavily. Jet axis as in Fig. 3.

Comparing Fig. 12 with Fig. 8, it becomes evident that the axis of maximum convergence follows the line of maximum ageostrophic component of flow (which coincides closely with the jet axis) rather well. There appears to be a slight trend, however, for the largest values of convergence to occur slightly to the cyclonic side of the jet. The divergence pattern on the anticyclonic side of the jet stream shows no significant correlation with the pattern of $\Delta u^*/\Delta z$.

A direct estimate of vertical motion has not been attempted, although a method using aircraft pitch and true airspeed as indicators of up- and down-draughts, has been advanced by Kuettner and McLean (cf. Endlich and Rados 1959). From the cloud distribution (given in Fig. 4 by hatching) one may conclude that upward motions prevail on the anticyclonic side of the jet, and to the right of the ' hump ' in the isentropic surfaces. The pattern of the normal component (Fig. 11) corroborates this conclusion. The cloud sheet ends abruptly near the jet axis.

(*d*) *Meso-structural details of the wind and temperature field and clear-air turbulence*

Figs. 3 and 4 contain the meso-structure of the wind and temperature fields respectively (shaded areas), entered as perturbations whose magnitudes may be read off with respect to the flight route as a base line. Furthermore, in Fig. 4 clear-air turbulence as recorded by the VGH instrument is entered in heavy solid lines along the flight legs. The slant numbers in this diagram stand for maximum gust velocities (fps) recorded within the respective turbulent zone.

Areas of turbulence encountered during *level* flight coincide well with stable baroclinic zones. This agrees with earlier findings (Reiter 1960a, b, c).

While no significant correlation seems to exist between the sign and wave lengths of the temperature and speed perturbations, the largest amplitudes of the latter occur inside the stable and baroclinic zones mentioned.

4. Conclusions

The structure of the atmosphere in the vicinity of jet streams is far more detailed than any cross-sections constructed from radiosonde data would reveal. Analyses of aircraft data, when exercised carefully, may bring to light some of this fine structure. Especially, the troposphere in the vicinity of the jet-stream core shows a succession of stable and close-to-adiabatic layers on top of each other. The thermal-wind relationship is not fulfilled in the jet-stream region, owing to the presence of strong ageostrophic components of motion. Large deviations between actual and geostrophic wind shear seem to be present in an area to the south of the jet axis, where the isentropic surfaces show an upward hump, and above the tropopause to the left of the jet axis, inside a very stable baroclinic zone.

Acknowledgments

The research reported in this paper has been sponsored by the Department of Traffic of the German Federal Republic, Project ' Route Planning ' (Streckenplanung) of the German Lufthansa. The author wishes to thank Messrs. Roy M. Endlich, Dr. Ralph Shapiro and George S. McLean Jr., Geophysics Research Directorate, Air Force Cambridge Research Center, for making available the most excellent flight data of Project Jet Stream (Staff members 1959). To Prof. Dr. H. Flohn, Offenbach, and to Dr. H.-J. Tanck, Hamburg, acknowledgment is given for help in organizing this research project. Mrs. Gabriella Reiter assisted in the preparation of the raw data.

References

Bellamy, J. C.	1945	*J. Met.*, **2**, pp. 1-79.
Cunningham, N. W.	1956	'A study of thermal wind in the vicinity of a jet stream,' *Sci. Rep.*, **8**, Contract A.F. 19 (604)-559.
Endlich, R. M. and McLean, G. S.	1960	*J. Met.*, **17**, p. 135.
Endlich, R. M. and Rados, R. M.	1959	*Geophys. Res. Pap.*, No. 64.
Newton, C. W.	1959	*J. Met.*, **16**, p. 638.
Raethjen, P.	1959	*Proc. Internat. Sci. Congress*, 'Jet stream and mountain wave,' Torino, p. 25.
Reiter, E. R.	1958	*J. Met.*, **15**, p. 27.
	1960a	*Beitr. z. Phys. d. Atmos.*, (in press).
	1960b	*J. Met.*, **18**, p. 9.
	1960c	*Berichte d. Deutsch. Wetterd.*, No. 61.
Staff members	1959	'Flight data pertaining to jet streams,' Jet No. 30, 8 Apr. 1957. Project Jet Stream, and Data Reduction Laboratory, Univ. of Dayton, Ohio.

551.507.352 : 551.521.14 : 551.521.3

Some aircraft observations of fluxes of solar radiation in the atmosphere

By W. T. ROACH
Meteorological Research Flight, Farnborough

(Manuscript received 1 September 1960; in revised form 15 December 1960)

SUMMARY

An account is given of some recent observations of solar-radiation fluxes from aircraft of the Meteorological Research Flight. This account consists of two parts :

(1) High-level measurements of the albedo of the earth and atmosphere from a Canberra aircraft over southern England in 1958 and 1959, and over the Sahara Desert and Equatorial East Africa in June 1958 and January 1960.

(2) Observations from a Hastings aircraft of the absorption and reflection of total and visible solar radiation from a cloud-free atmosphere over the English Channel.

From (1), frequency distributions of observations within given albedo ranges have been extracted and correlation of albedo with the observed cloud cover attempted. The mean of albedo observations over southern England was 0·5 in 1958 and 0·3 in 1959; over the Sahara Desert about 0·3 and over Equatorial Africa about 0·2.

The Hastings flights show that instantaneous heating rates in excess of 5°C/day at some level below 10,000 ft occur quite frequently. When allowance is made for heating due to absorption by the near infra-red bands of water vapour and carbon dioxide (1-2°C/day) it is found that the residual absorption does not depart significantly from greyness except in a few cases when the absorption appears to be concentrated in the near infra-red.

For the lowest levels, the absorption coefficient due to haze for total radiation is estimated to average about 20 per cent and for visible radiation about 5 per cent of the attenuation coefficient. Back-scattered radiation accounts for about 5 per cent of the total attenuation.

1. INTRODUCTION

(*a*) *High-level observations*

The Meteorological Research Flight Canberra aircraft is equipped with solarimeters which measure the upward and downward fluxes of solar radiation in the wavelength band 0·3-3 μ.

The solarimeters were installed to obtain measurements of the total albedo of the earth and atmosphere from above the tropopause over southern England for the International Geophysical Year programme. Fluxes of solar radiation at this height will differ little from their extra-terrestrial values and the resultant albedos should approximate to the local planetary value such as would be observed from a similarly equipped artificial satellite.

Albedo observations over southern England have thus been accumulated during 1958 and 1959 whenever it was convenient to combine them with other programmes. Continuity was broken by aircraft unserviceability and also during the mid-winter period when the sun was too low to obtain useable readings. Albedo observations were also made during the Canberra detachment to Africa in June 1958 and January 1960. Full details will appear with the reports on these detachments, but a summary of results is included in this paper.

(*b*) *Observations in a cloudless atmosphere*

The Hastings aircraft is equipped with upward and downward facing solarimeters and photometers. The photometers are sensitive to visible wavelengths only (0·43-0·7 μ) and used in conjunction with the solarimeters (0·3-3 μ) provide a rough discrimination between visible and near infra-red fluxes of solar radiation.

From measurements of upward and downward fluxes of visible and total solar radiation as a function of height, it is possible to estimate :

(i) the direct solar heating of the atmosphere from measurements of flux divergence;

(ii) the contribution to this heating in visible wavelengths;

(iii) the visible and total albedo of the atmosphere and of the sea surface below.

These flights were made during the period April to October 1959 and are a logical continuation of a programme for the measurement of the albedo of cloud and land surfaces and the absorption of cloud (using solarimeters only) carried out by Robinson (1958).

2. Experimental

(*a*) *Instrumental*

The radiation instruments consist of two Moll-Gorczynski solarimeters (Type G.18) employing Moll Thermopiles and two photometers employing Weston selenium cells (Model S123). The sensitivity of the solarimeters is constant over the pass band (0·3-3 μ), but the sensitivity of the photometers is variable within a pass band of 0·30-0·75 μ. This band is reduced to pass radiation in the range 0·43-0·70 μ by the interposition of a filter designed to give a resultant sensitivity curve approximating to that of the human eye for photopic vision so that the output is calibrated directly in photometric units.

The outputs from the solarimeters on the Canberra aircraft were connected across millivoltmeters (by Sifam Electrical Instrument Co.) and their readings photographically recorded. This rather crude method had to be adopted owing to space restrictions.

The output from the radiometers on the Hastings aircraft were recorded on a 6-channel Cambridge potentiometer recorder which operated satisfactorily throughout the programme. The mounting of the radiation instruments has been described by Robinson (1958).

(*b*) *Flight procedure*

Observations from the Canberra aircraft were made whenever the aircraft was in straight and level flight above the tropopause over southern England. In equatorial regions it was not possible to reach the tropopause, but all albedo observations were made between 30,000 and 50,000 ft.

Flights with the Hastings aircraft were made near mid-day over the English Channel because the upward fluxes of radiation over sea are small and steadier than over land : the aircraft can fly as low as the pilot deems safe (about 100 ft) and is not subject to the statutory limit of 2,000 ft operative over land. The procedure was to fly parallel to the Sussex coast (heading east or west) about 15 miles out to sea at several levels between 100 and 20,000 ft. Each level was flown for 2-3 min with the aircraft turning on to reciprocal bearing between levels. Given levels were repeated as a check on the reproducibility of conditions. Air temperatures and frost points were observed at all levels and a watch was kept for the appearance of any cloud likely to invalidate the observations. The heights of any haze layers were also noted.

Two flights on a similar plan were made with the Canberra aircraft to extend observations of clear-air absorption and albedo to 40,000 ft, but owing to the cruder nature of the recording installation, no useful results were obtained.

(*c*) *Calibrations*

Absolute calibrations of all radiation instruments at Kew Observatory were supplemented by comparisons of relative sensitivities on the ground at Meteorological Research Flight. Most of the instruments exhibited a marked azimuthal dependence of sensitivity in direct sunlight which increased with solar zenith angle ($\pm$ 5 per cent at 30° to nearly

± 10 per cent at 60°). In flight, errors are also introduced by variations in aircraft attitude, so that allowance was made for both azimuth and attitude effects by flying consecutive legs on reciprocal headings and correcting for the differences observed. A simple cosine correction was applied for the small change of solar zenith angle during the flight (about 1 hr).

Further calibration of the solarimeters used in the Canberra aircraft in conjunction with millivoltmeters was necessary since the latter possessed an internal resistance comparable to the solarimeter thermopiles (10 ohms) and thus only recorded about half the total potential developed across the circuit.

(d) *Pressure and temperature dependence of sensitivities*

Laboratory tests were made to study effects of temperature and pressure changes on sensitivity.

(i) *Pressure*: No appreciable effects of pressure change within the range 120-1,000 mb were observed on the sensitivity of either photometers or solarimeters. Bener (1951) found no effect on solarimeter sensitivity in the range 840-1,190 mb.

(ii) *Temperature*: The effect of temperature produced changes of less than 1 per cent in photometer sensitivities (in agreement with maker's specification), but increases of up to 5 per cent in solarimeter sensitivity occurred for a decrease from 20°C to − 40°C. This is less than the figure of − 0·2 per cent per °C measured by Bener (1951). For purposes of reduction, a temperature coefficient of − 0·1 per cent per °C was used and the temperature of the solarimeter element assumed to be that indicated by the flat plate thermometer installed on the skin of the aircraft.

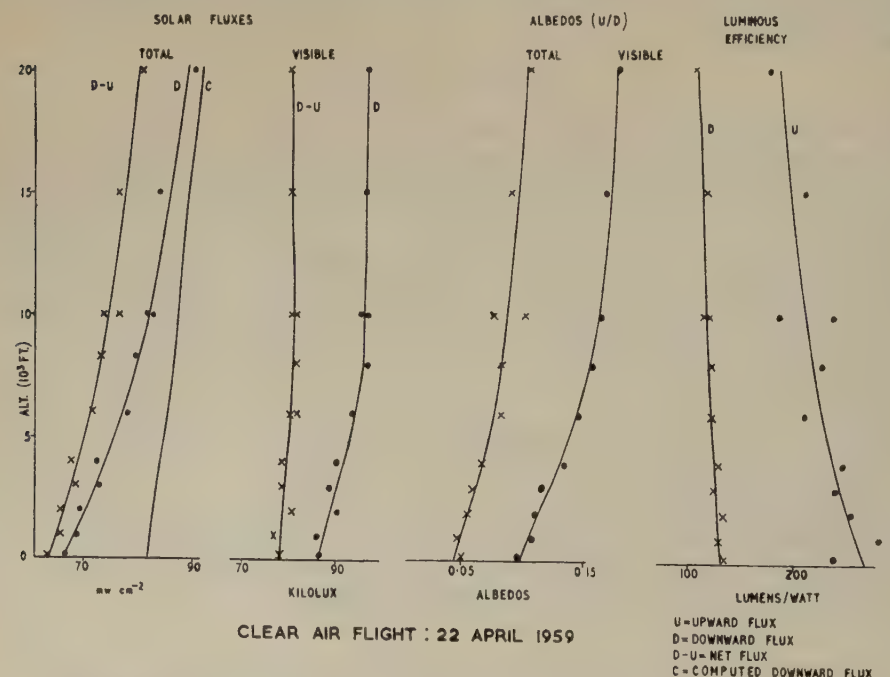

Figure 1. An example of a typical flight. The points are observations corrected for changing solar altitude and temperature coefficient of solarimeter. The curves of best fit are drawn by eye. The albedos are the direct ratios of upward and downward fluxes; the intersection of the albedo curves with the zero height ordinates have been taken as the total and visual albedos of the sea surface. Luminous efficiency is expressed in conventional units (1 kilolux = 0·1 lumen cm^{-2}).

3. Theory

(a) *Symbols*

The elementary theory of the deduction of albedo and absorption of an atmospheric layer is given below. The symbols used are :

D – Downward flux of solar radiation
U – upward flux of solar radiation
} mw cm^{-2} for total radiation, kilolux for visible radiation

r – observed albedo of atmospheric layer

R – Rayleigh albedo of atmospheric layer

r_s – albedo of sea surface

a – fractional absorption of atmospheric layer

Z – height (ft)

p – pressure (mb)

ψ – solar zenith angle

γ_d – dry adiabatic lapse rate

H – heating rate (°C/day), with subscripts

$_T$ – total

$_V$ – visible

$_C$ – computed

$_R$ – residual (total – computed)

$_T$ – subscript denotes any of the above quantities referred to total solar radiation (0·3-3 μ)

$_V$ – subscript denotes visible radiation only (0·43-0·70 μ).

(b) *The absorption and albedo of an atmospheric layer*

Consider a slab of atmosphere lying between the levels Z_0 (p_0) and Z_1 (p_1) ($p_0 > p_1$). The flux of radiation leaving either surface consists of radiation reflected (back-scattered) from the slab, plus radiation transmitted from the other side of the slab. This can be stated :

$$U_1 = r_1 D_1 + (1 - r_0 - a_0) U_0 \quad . \quad . \quad . \quad (1)$$

$$D_0 = r_0 U_0 + (1 - r_1 - a_1) D_1 \quad . \quad . \quad . \quad (2)$$

In general, $a_0 \neq a_1$, and $r_0 \neq r_1$, since the reflectivity and absorptivity of a slab depend upon the directional distribution of the incident radiation and the amount and distribution of absorbing and scattering centres within the slab. For optically thin slabs, the effect of distribution of matter within the slab becomes negligible so that a_0 and r_0 will differ from a_1 and r_1 only if the incident radiation fluxes have a different distribution as they will have in the atmosphere : a horizontal slab being illuminated by diffuse radiation from below and mainly by the direct solar beam from above. However, we are able to make use of two simplifications :

(1) The downward fluxes (D_0, D_1) are in general much larger (10-30 times) than the upward fluxes (U_0, U_1) consisting largely of radiation reflected from the sea.

(2) The slab of atmosphere on which measurements were made can be considered optically thin, so that a_0, a_1, r_0, r_1 will be rather small compared to unity. Hence the terms in Eqs. (1) and (2) may be classified into three orders of size : the largest, or zero order terms which are D_0 and D_1; the first-order terms which are U_0, U_1, $r_1 D_1$, $a_1 D_1$; and the second-order terms which are $a_0 U_0$, $r_0 U_0$. Neglecting the second-order terms we obtain

$$r_1 = (U_1 - U_0)/D_1 \quad . \quad . \quad . \quad . \quad . \quad (3)$$

$$a_1 = -\Delta E/D_1 \quad . \quad . \quad . \quad . \quad . \quad (4)$$

where

$$\Delta E = (D_0 - D_1) + (U_1 - U_0) \quad . \quad . \quad . \quad (5)$$

$$= \text{flux divergence in the slab.}$$

All terms in a_0 and r_0 have disappeared, which indicates, as would be expected, that practically all radiation absorbed and scattered within the slab originates from the downward fluxes of radiation and that the main terms in Eqs. (1) and (2) are very insensitive to the values of a_0 and r_0 (which in any case are not likely to be very different from a_1 and r_1, except for very large solar zenith angles – say $> 80°$).

Hence the values of a and r entered in Table 1 are derived from Eqs. (3), (4) and (5). The mean heating rate of the slab is obtained via the hydrostatic equation :

$$H = \frac{dT}{dt} = -\gamma_d \frac{\Delta E}{\Delta p} \quad . \quad . \quad . \quad . \quad (6)$$

where

$$\Delta p = (p_0 - p_1).$$

All heating rates are expressed in °C/day, in accordance with usual practice, although they are in fact instantaneous values measured near the solar culmination. For instance, a reported heating rate of 3°C/day near mid-day would suggest a temperature rise during the day of about 1°C, assuming all other factors constant other than solar zenith angle.

(c) *Absorption and albedo in visible wavelengths*

In order to estimate the solar heating of the atmosphere in visible wavelengths (H_V) the observations (expressed in photometric units) must be converted to energy units. The conversion factor is known as the luminous efficiency K, and is defined by

$$[K]_{\lambda_2}^{\lambda_1} = \int_{\lambda_2}^{\lambda_1} K_\lambda I_\lambda \, d\lambda \Big/ \int_{\lambda_2}^{\lambda_1} I_\lambda \, d\lambda \quad . \quad . \quad . \quad (7)$$

(from *Smithsonian Tables*, 6th Ed., p. 449).

K_λ = Monochromatic luminous efficiency of radiation at wavelength λ

I_λ = Monochromatic intensity (or flux) of radiation.

It is usual to take the limits λ_1 and λ_2 at 0 and ∞, but in this case, the signal from the photometers only gives information about radiation falling between 0·43 and 0·70 μ. Taking these wavelengths as λ_1 and λ_2 in Eq. (7), and using the wavelength sensitivity calibration given by Blackwell (1953), we obtain

$$[K]_{0.70\,\mu}^{0.43\,\mu} = 254 \text{ lumens/watt}$$

for extraterrestrial radiation (Allen 1958). This figure is not likely to be appreciably different in the lower troposphere since there is little selective absorption in this region, and it has been used to estimate the energy flux of radiation and thus the heating of the atmosphere by absorption of visible radiation.

(d) *Errors of observation*

(i) *Error in absolute calibration* : A rough check was kept on this by using the sun as a standard source by comparing its computed downward flux with the observed flux well above the haze layer. The probable error in flux measurements is estimated to be between ± 5 and ± 10 per cent for both solarimeters and photometers. For readings obtained from the Canberra aircraft, this error is likely to be at least ± 10 per cent.

(ii) *Dependence of sensitivity on altitude*: This will have a negligible effect on total flux measurements, but becomes important in the estimation of flux divergence. A sensitivity change of $-0{\cdot}1$ per cent per °C of the solarimeters not accounted for would result in an over-estimation of heating rate of the order 0·3°C/day for typical lapse rates in the lower troposphere. The error due to this is estimated to be not greater than $\pm 0{\cdot}5$°C/day.

(iii) *Observational scatter*: In deriving heating rates, smooth curves have been drawn through the observations of flux as a function of height (see Fig. 1) and the error in ΔE for any layer is estimated to be $\pm 0{\cdot}5$ mw cm^{-2} below 10,000 ft increasing to ± 2 mw cm^{-2} at the highest levels flown. This corresponds to an error of about $\pm 50/\Delta p$ to $\pm 200/\Delta p$ °C/day (Δp is in mb). Obviously the thicker the layer, the more accurate the observations of mean heating rate through the layer.

(iv) *Changing conditions*: Flights normally lasted one hour and checks were made near the beginning and end of the flight at given levels, and changes observed were generally of the order of 1-3 per cent of the total flux. The main contribution of this error was to observational scatter. Taking all errors into consideration, the error in total heating rate is estimated to be slightly less than ± 1°C/day for a layer 100 mb thick, dropping to about $\pm 0{\cdot}5$°C/day for the 0-10,000 ft layer. The corresponding error in the estimation of heating rates due to visible radiation are about half these values owing to the smaller energies involved.

The error in albedo observations is dependent mainly on the accuracy to which relative sensitivities of upward and downward facing instruments are known. It is estimated to be $\pm 0{\cdot}01$ for both total and visible radiation fluxes. For observations from the Canberra aircraft, the error of individual albedo measurements is estimated to be greater than $\pm 0{\cdot}02$ and they exceed $\pm 0{\cdot}05$ for large solar zenith angles.

4. Results

(*a*) *Canberra flights*

The results of the Canberra flights over southern England are summarized in Fig. 2 and the results of the overseas detachments in Fig. 3.

(i) *Southern England results*: These are limited in usefulness by the small sampling time which amounted to about 15 hr each year. 1958 is very different in character to 1959: the former was an unsettled year, while the latter was dry and sunny.

Individual values of albedo observed range from 0·05 over sea and 0·15 over land on a clear day to 0·85 over a troposphere filled with cloud.

An attempt has been made to correlate albedo with cloud amounts extracted from the observer's flight notes. For southern England, the cloud has been divided into two sections: (i) Cu., St., Sc., and (ii) Ci., As., Ac. Occasions when clouds from both categories were present were ignored, and reports on (ii) have only been included when it was reasonably certain that no underlying cloud was present.

The spread of observations is due mainly to the dependence of albedo on cloud thickness as well as cloud cover. The observations lie within fairly well-defined envelopes (dotted lines in Fig. 2) and will be of climatological interest.

(ii) *Overseas results*: There was much less cloud than over southern England – particularly over the Sahara desert (El Adem-Khartoum run), and all observed cloud was reported as Cu., Sc., or Ac., and has been lumped together for the correlation of cloud cover with albedo. This correlation was assisted on the January 1960 detachment by photographs taken by a 35 mm camera installed in the tail-cone of the Canberra aircraft with its optical axis tilted towards the ground at an angle of about 10°.

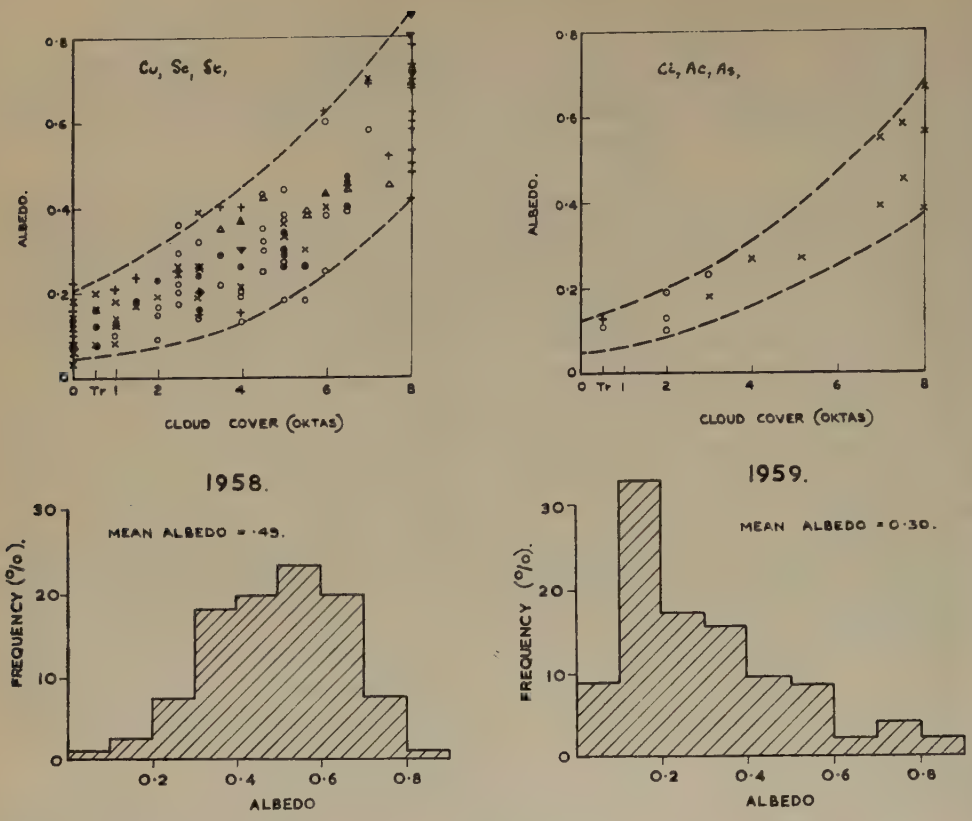

Figure 2. Summary of albedo measurements from the Meteorological Research Flight Canberra aircraft over southern England. The different symbols represent different observers. It has been assumed that reports of a trace (Tr) of cloud represents a cover of half an okta. A cloud amount reported as n to $(n + x)$ oktas has been entered as $(n + x/2)$ oktas.

Over high ground (e.g., Kenya) most of the cloud reported as Cu. or Sc. was in fact in medium levels. One feature of interest was the occasional reports of extremely thin (100-300 ft thick) stratocumulus in apparently stable and at times almost unbroken layers, generally over the desert. Since the albedo of the desert is already high – about 0·3, though albedos in the range 0·18-0·40 were reported – the effect of even a complete cloud cover was to raise the albedo by less than 0·1.

It was practically never possible to climb above the cirrus that frequently covered the equatorial skies, although the aircraft was often in cirrus. For this reason the planetary albedos of the Khartoum-Nairobi and Aden-Nairobi strips are probably at least 50 per cent higher than the mean values of 0·22 and 0·31 observed. Values of albedo reported in cirrus cloud reached 0·75-0·8 (probably anvil cirrus) but were generally in the range 0·3 to 0·5. It was noted that the ground ceased to be visible for albedos of about 0·4 which implies an albedo for cirrus which is opaque from above of 0·2-0·3.

There was generally no cirrus above the desert, and so the mean value of 0·32 (El Adem-Khartoum run) is probably close to the planetary value. The mean albedo of 0·31 for the Aden-Nairobi run in June is greater than the value of 0·22 for the Khartoum-Nairobi run in January, owing mainly to greater cloud amounts in June when the equatorial rain belt is further north.

(*b*) *Hastings flights*

The main features of the results are shown in Table 1 and Figs. 4-6. Relevant synoptic information is displayed in Table 2. Also included for comparison are the heating

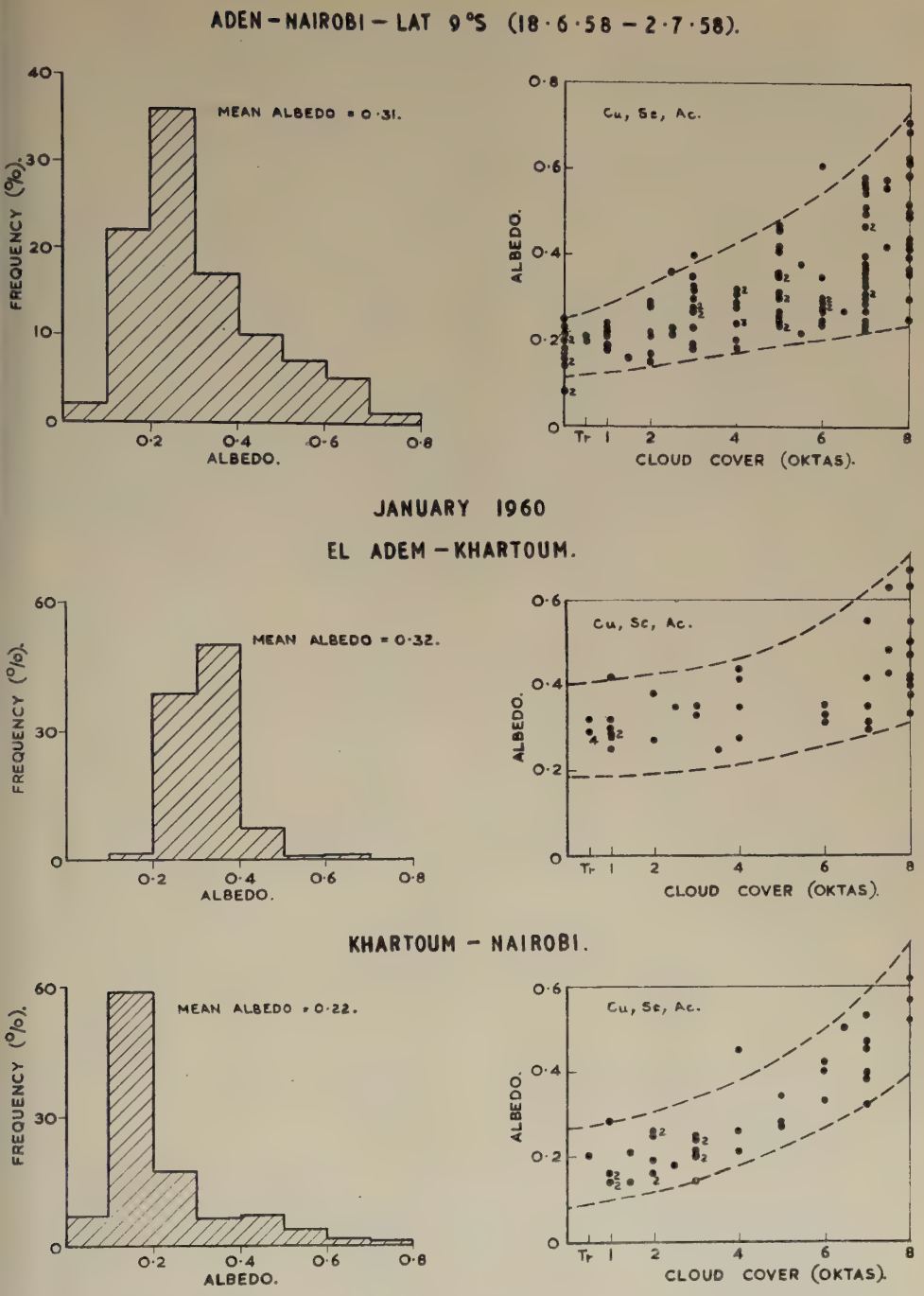

Figure 3. Summary of albedo measurements from the Meteorological Research Flight Canberra aircraft on overseas detachments.

rates due to the absorption of near infra-red solar radiation by bands of water vapour and carbon dioxide computed from laboratory data compiled by Howard, Burch and Williams (1955); the method of computation is described in a companion paper. The heating rate due to this absorption will hereafter be referred to as H_C.

TABLE 1. SUMMARY OF OBSERVED MEAN VALUES FOR THE LAYER 0-10,000 FT

	Date	21 April	22 April	17 June	19 June	6 July	15 Sept.	24 Sept.	30 Sept.	5 Oct.	Mean
	ψ°	39	41	38	32	33	60	55	55	56	46
Heating Rates (°C/day)	H_T	4·5	2·7	2·6	2·9	2·2	3·2	1·7	2·5	3·3	2·8
	H_C	1·4	1·3	1·6	1·5	1·4	1·2	1·0	1·2	1·4	1·3
	H_V	1·1	0·3	0·2	—	0·3	1·0	0·1	0·3	0·4	0·5
	H_R	3·1	1·4	1·1	1·4	0·9	2·0	0·6	1·3	1·9	1·5
Fractional Absorptions	a_T	0·23	0·14	0·12	0·13	0·11	0·26	0·13	0·18	0·23	0·17
	a_C	0·07	0·07	0·07	0·07	0·07	0·10	0·08	0·09	0·10	0·08
	a_V	0·11	0·03	0·02	—	0·03	0·13	<0·01	0·03	0·05	0·05
	a_R	0·16	0·07	0·05	0·06	0·04	0·16	0·05	0·09	0·13	0·09
Albedos	r_T	0·09	0·06	(<0·01)	0·05	0·02	0·07	0·05	(0·02)	0·05	0·05
	r_V	0·12	0·09	0·04	—	0·03	0·11	0·07	0·04	0·05	0·07
	R_T	0·02	0·02	0·02	0·02	0·02	0·02	0·02	0·02	0·02	0·02
	R_V	0·02	0·02	0·02	0·02	0·02	0·04	0·03	0·03	0·03	0·03

Doubtful values are enclosed in brackets

(i) *Heating rates*: Referring first to Table 1 which summarizes the observations for the 0-10,000 ft layer taken as a whole, the total solar heating, H_T, is observed to average about twice H_C. On individual occasions this factor varies between 1·3 and 3, and at individual levels from slightly less than unity to about 5 (Fig. 4). The solar heating in the visible region, H_V, is generally small, especially above 10,000 ft, but exceeds 1°C/day in very hazy conditions (e.g., 21 April, 15 September, 5 October).

In Fig. 5, an attempt has been made to correlate H_R with H_V. The line labelled 'grey absorption' represents the ratio H_R would have to H_V if the fractional absorption was a constant throughout the spectrum. Since 39 per cent of the total solar radiation lies in the visible region (0·43-0·70 μ), it follows that $H_V = 0{\cdot}39\ H_R$ for grey absorption. The dotted lines represent an estimate of the confidence limits within which points do not depart significantly from the grey absorption case. Most of the points lie within these limits but there are a few in which infra-red absorption appears to predominate.

(ii) *Albedos*: The principal comparison which can be made with theoretical work is that of Kano (1958). The comparison cannot be exact since Kano's computations were restricted to illumination of a total Rayleigh atmosphere by a parallel beam of extra-terrestrial radiation whereas the observations were only of that part of the atmosphere below 10,000 ft i.e., 700-1,000 mb – about one-third of the total atmosphere. Furthermore, the top of the layer is illuminated by diffuse radiation from the rest of the atmosphere

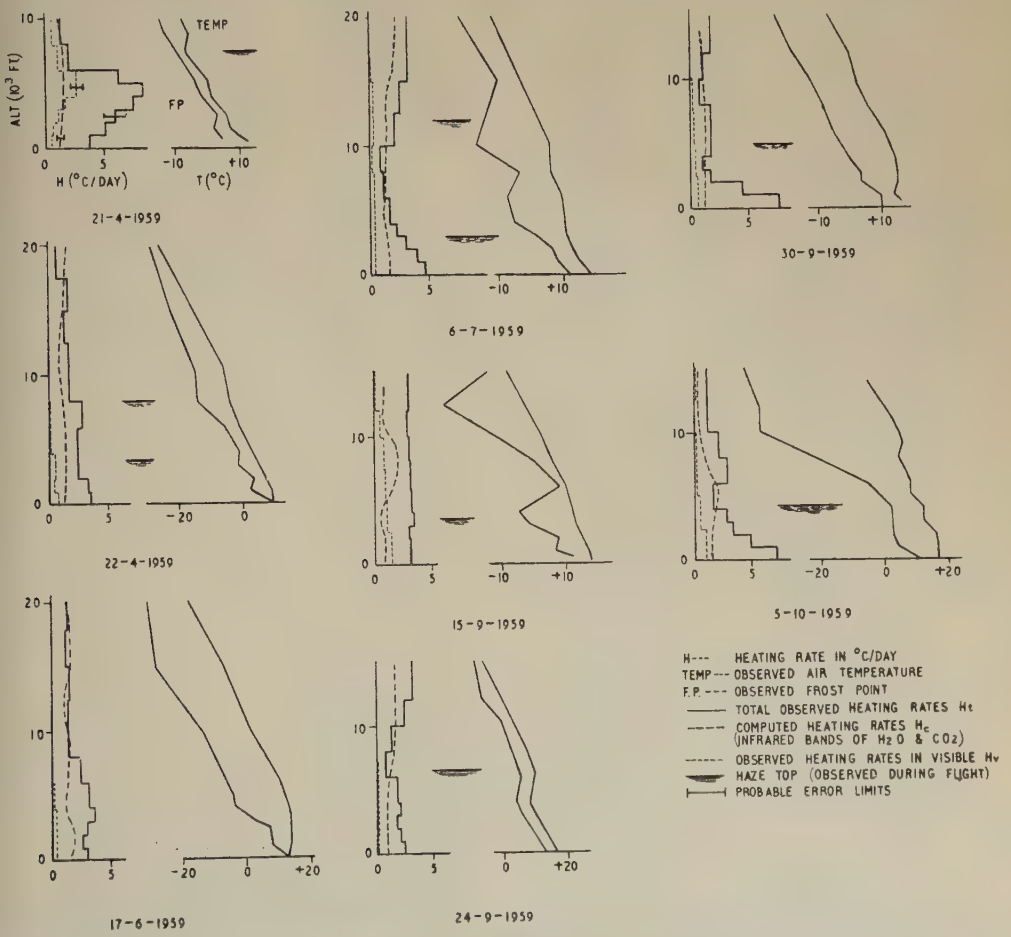

Figure 4. The observed heating rates in slabs of atmosphere between flight levels. The values of H_C are plotted as a smooth curve for clarity.

as well as by the direct solar beam, and this must produce some error. However, since the total flux of this diffuse radiation is unlikely to exceed 10 per cent of the direct solar flux except for very large solar zenith angles ($> 80°$) – the solar zenith angle during the flights was never greater than 60° – the error incurred by scaling Kano's results (see Table 1) to the 300 mb thickness of atmosphere under observation should be negligible. This simple scaling procedure is only valid for an atmosphere of small optical thickness. An optical depth of 0·1 may be considered small.

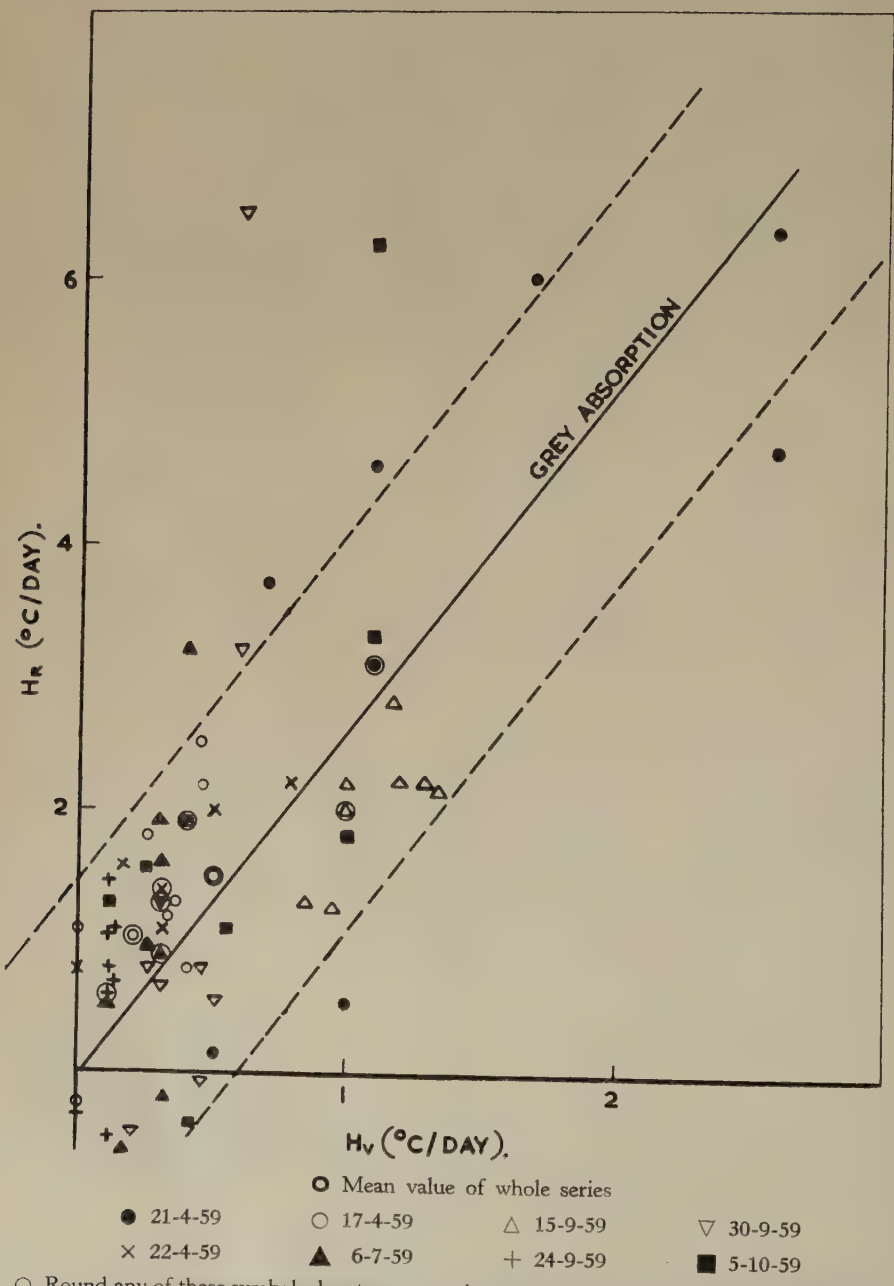

Figure 5. Observations of the heating rate, H_R, not accounted for by H_C ($H_R = H_T - H_C$) plotted against simultaneous observations of H_V.

The observed albedos average 2-3 times the albedos obtained from Kano's paper n the way described. In most cases there is a rapid increase in albedo in the first few housand feet after which the rate of increase drops to about that of the Rayleigh value. The observed ratio of visible to total albedo (r_V/r_T) is about 1·5 – similar to the ratio of he Rayleigh values.

Some of the observed curves of total albedo appear anomalous (e.g., 17 June – this light has been included because no experimental reason for its rejection could be found).

(iii) *Individual Flights*: *21 April.* This was a very hazy day; values of H_T reached 3°C/day and H_V approached 3°C/day near 5,000 ft – about 2,000 ft below the observed haze top. The observed albedos were also very high. The similarity in the profile shapes of H_T and H_V are more marked in this flight than in any subsequent flight.

The winds (Table 2) were N to NNE above 3,000 ft, so that the air above this level passed over the London area a few hours previously. The inference that the heavy absorption between 3,000 ft and the haze top is largely due to London pollution is therefore strong. Visibility at the surface decreased during the day as, presumably, the pollution settled out of the main layer.

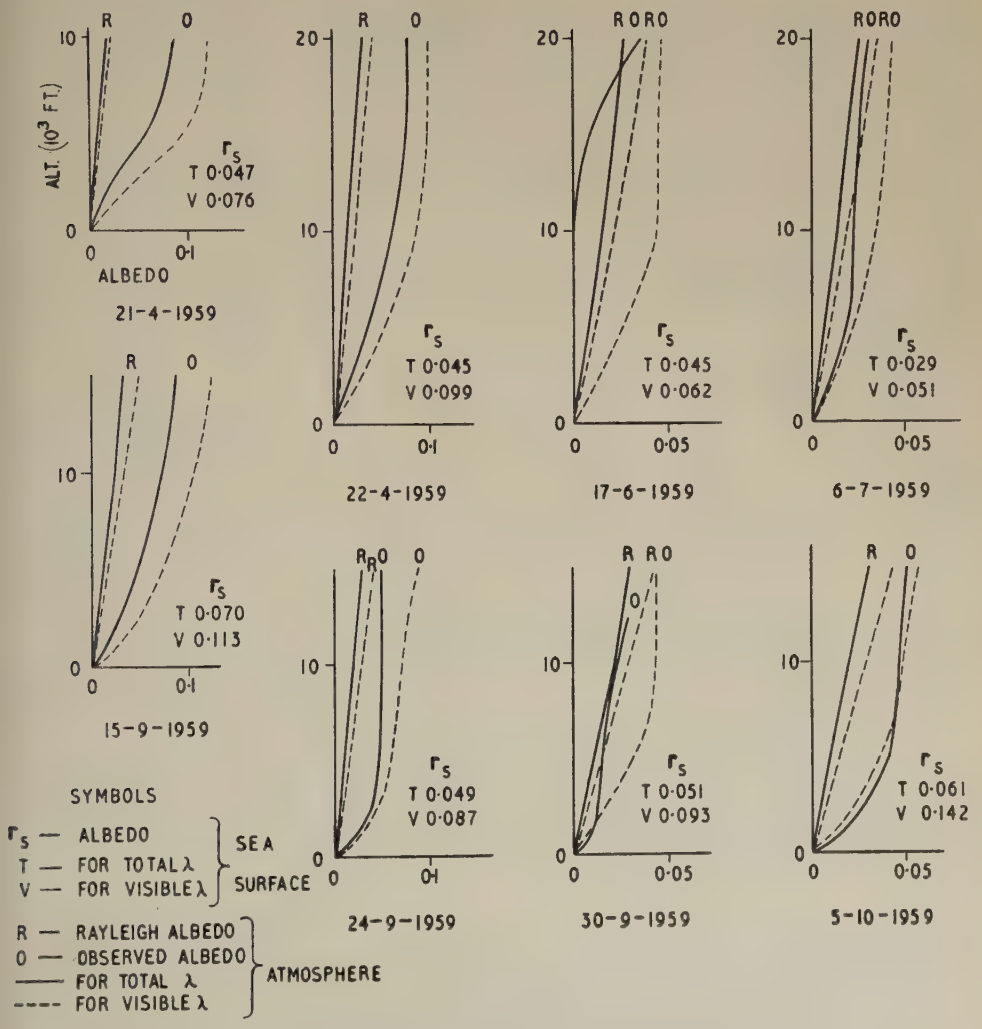

Figure 6. A comparison of observed albedos with Rayleigh albedos.

TABLE 2. FLIGHT REPORTS AND SYNOPTIC DATA

Date	V	Airmass	Flight report	Winds Surface	900 mb	700 mb	500 mb	P	Synoptic situation
21 April	5	L	Very hazy	230/05	000/10	020/25	020/40	1030	High over English Channel
22 April	3	M	Hazy	180/08	250/05	340/10	010/17	1026	High over North Sea
17 June	7	M	—	190/08	290/11	260/07	280/19	1018	Weak E-W ridge up Channel
19 June	6	M	Hazy	120/06	—/00	300/23	290/16	1023	High covering British Isles
6 July	18	M	Very clear	170/05	330/18	240/20	300/39	1027	High centred S.W. Approaches
15 September	12	C	Hazy	080/10	080/20	030/04	090/10	1016	High centred Faroes; old low 43°N 15°W
24 September	8	M	Slight haze	180/08	300/10	320/16	320/30	1020	High centred North Sea
30 September	7	C	Visibility ≃ 10 mi	100/11	120/08	140/15	110/13	1020	Large high covering N. Europe
5 October	2·5	C	Very hazy	100/11	130/28	140/24	130/19	1019	Large high N. Europe-S. Scandinavia

V – Reported mid-day visibility at Thorney Island in miles
M – Maritime
C – Continental
L – Indicates air recently passed over London area
P – Surface pressure in mb

The surface winds are taken from Thorney Island reports : the other winds are taken from the Crawley 1100 hr radiosonde ascent

22 April. Heating rates, although much less than on the day before, were still significant. H_T averages about $2H_C$ below the haze top at 8,000 ft; above 8,000 ft H_T does not depart significantly from H_C. N winds were reported between 6,000 and 14,000 ft, but there is no significant increase in H_T within this layer above values of H_T observed below 6,000 ft. H_V was negligible above 4,000 ft and small ($\simeq \frac{1}{2}$°C/day) below it.

17 June. H_T and H_C agree very well above 8,000 ft; below this level, H_T reaches a maximum of 4°C/day near the middle of the stable layer below 6,000 ft. H_V is almost negligible.

19 June. On this flight, the lower photometer failed, and the scatter of observations from the solarimeters was greater than usual owing to the presence of cirrus and contrails. Hence only the heating rate for the layer 0-10,000 ft is presented.

6 July. This was one of the clearest days of the series, although H_T was quite large in the lowest 3,000 ft. H_V was again very small. H_T is also large above 10,000 ft. This may be due entirely to the near infra-red bands of water-vapour and carbon dioxide. The value of H_C computed for this day (Fig. 4), although already large, may be under-estimated owing to a subsidence inversion above 20,000 ft not taken into account in the method of computation (Roach 1961).

15 September. The air on this flight was continental in origin and the ratio of H_V to H_T was observed to be much higher than on other flights. H_T was remarkably uniform throughout, while there was considerable variation in H_C due to the dry zones at 4,000 and 12,000 ft.

24 September. H_T was largest above 10,000 ft and least at 7,000 ft – in fact less than H_C just above the haze top. H_V was negligible throughout. The air was maritime in origin and reported as slightly hazy.

30 September. This is remarkable for the large values of H_T in the lowest 2,000 ft. H_V increases steadily from 10,000 ft to the ground, but has little apparent connexion with H_T. The increase in r_T is also abrupt in the lowest 2,000 ft whereas the increase in r_V is steady up to 7,000 ft where the rate of increase falls off. The air was continental in origin.

5 October. This shows a profile of H_T similar in character to that of 30 September. The correlation between H_T and H_V is more pronounced and there is a marked minimum of H_T just above the haze top which agrees well with H_C here.

(iv) *Downward solar fluxes and luminous efficiency*: A comparison of the observed and computed downward fluxes of solar radiation shows that these converge with height (e.g., Fig. 1) and also that the slopes of the observed and computed curves approach in most cases.

Since absolute values are of crude accuracy, this comparison serves mainly as a rough check on the calibration of the solarimeters since absorption above 20,000 ft is probably nearly all due to the near infra-red bands of water vapour and carbon dioxide which can be assessed with tolerable accuracy.

From observations of the luminous efficiency of the downward fluxes, we may also obtain a rough check on the absolute calibration of the photometers.

Blackwell (1953) quotes an extraterrestrial value of luminous efficiency of 104 lumen/watt (obtained by integrating Eq. (7) throughout the solar spectrum) based on data by Nicolet (1951) and finds this value increases to about 130 lumen/watt at the ground (Kew Observatory) owing mainly to absorption by the near infra-red bands of water vapour and carbon dioxide.

The luminous efficiency of the upward (reflected) fluxes of radiation are observed to be about 230 lumen/watt at the sea surface decreasing to about 180 lumen/watt at 15,000 ft (e.g. Fig. 1). This implies that very little infra-red radiation is reflected from the sea surface, but an appreciable back-scattering of infra-red radiation from the atmosphere causes the observed decrease of luminous efficiency with height.

5. Discussion

(a) *The nature of the additional absorption and albedo*

The main feature of the results requiring explanation is the large excess of observed absorption and albedo over that computed for known constituents of the atmosphere : the absorption expected being that due to the near infra-red bands of water vapour and carbon dioxide and the albedo expected being due to Rayleigh scattering by air molecules. It is natural to attribute the additional absorption and albedo to aerosol; this conclusion is supported by the following evidence.

After removal of the contributions to absorption and albedo due to known causes, the following quantities remain :

(i) additional heating ($H_T - H_C$; H_V)

(ii) additional absorption ($a_T - a_C$; a_V)

(iii) additional albedo ($r_T - R_T$; $r_V - R_V$).

Significant correlations are obtained between the following pairs of parameters taken from Table 1 :

(i) $a_T - a_C$ with a_V

(ii) $r_T - R_T$ with $r_V - R_V$

(iii) $a_T - a_C$ with $r_T - R_T$

(iv) a_V with $r_V - R_V$.

The first two correlations indicate that the additional absorptions and albedos in the visible and infra-red wavelengths occur together and probably have a common cause. The last two correlations indicate that absorption and backward scattering occur together suggesting that aerosol is the cause of the observed additional absorption and albedo through the wavelength band 0·3-3 μ. These conclusions are supported by comparison of the slopes of albedo curves (Fig. 6) with profiles of heating rates on individual flights – particularly the flight of 21 April.

The next features requiring explanation are the observed wavelength dependence of the mean additional absorption and albedo. The total albedo is less than the visible albedo implying a decrease of albedo with increasing wavelength, whereas the total absorption is greater than the visible absorption implying an increase of absorption with wavelength. Reference to Fig. 5 shows that most of the individual observations of absorption do not depart significantly from the grey case, but there remain a few observations of large absorption biased towards the near infra-red which are responsible for weighting the mean absorption (Table 1) towards this region.

If it is accepted that the additional absorption and albedo is due to aerosol, these features can be examined in terms of what is known about the attenuating properties of aerosol.

On both theoretical and observational grounds (e.g., Van de Hulst 1957; Middleton 1941) the monochromatic attenuation (or extinction) coefficient, β_λ, of a collection of aerosol of any size distribution is expected to decrease with increasing wavelength. Direct measurements in the cloud-free atmosphere yield an empirical relation of the form

$$\beta_\lambda \propto \lambda^{-\alpha} \quad . \quad . \quad . \quad . \quad . \quad (8)$$

where α varies between 1 and 2, tending towards 2 in very clear conditions. In fog or mist, $\alpha \simeq 0$.

Hence the absorbed and scattered components β_k and β_s, of the attenuation coefficient should also decrease with increasing wavelength, though a strong wavelength dependence of the optical properties of the aerosol will produce anomalies in the spectrum of β_k or β_s.

Thus, while the observed decrease of atmospheric albedo with increase in wavelength is not inconsistent with these comments, it is necessary to postulate a marked increase in the absorption index k (defined as the imaginary part of the refractive index, $n' = n(1 - ik)$) of an appreciable fraction of the total aerosol present in the near infra-red on the few flights in which the concentration of absorption in the near infra-red cannot be ignored.

The possibility of spurious results due to instrumental causes is considered by referring back to Section 3 (d).

(i) Error in absolute calibration: this would alter total heating rates slightly, but would not change observed fractional absorption.

(ii) Dependence of sensitivity on altitude: in order to account for the heating rates observed in the lowest 1,000 ft of the flights on 30 September and 5 October, a change of sensitivity of the order of 10 per cent would be required within this level. This is an order of magnitude greater than quoted (see Section 2 (d)) and if real, would not explain the rapid decrease in observed total heating rate above the surface layers.

(iii) Observational scatter: the much greater decrease in downward total flux compared with that of the visible flux near the sea surface is obvious from the flight record before any corrections or smoothing have been applied.

(iv) Changing conditions: the arrival of cloud would be expected to affect both visible and total fluxes roughly equally.

Thus instrumental causes of the required order of magnitude appear unlikely on the evidence presented, and no reason for doubting the validity of the results has been established.

(*b*) *Attenuation and forward scattering by aerosol*

The flight results only assess the absorbed and approximately back-scattered components of the total attenuation of the direct solar beam. However, an attempt has been made to assess the magnitude of these components relative to the total attenuation and forward scattered components by comparing their observed values in the lowest 1,000 ft with attenuation coefficients obtained from mid-day visibility reports from Thorney Island (on the Channel coast just north of the E-W flight track).

The attenuation coefficient for visible radiation, β_V, is related to the visibility, V, by Koschmieder's empirical expression

$$\exp(-\beta_V V) = \epsilon \quad . \quad . \quad . \quad . \quad (9)$$

where ϵ is usually taken as 0·02.

Since an attenuation in a horizontal direction (visibility) is being compared with one in a vertical direction, it has been assumed that the distribution of aerosol in the lowest 1,000 ft is uniform. In practice this is unlikely to be true but will suffice for this type of estimation.

The absorption coefficient for visible radiation in a horizontal direction, β_{KV}, is then given by

$$\beta_{KV}\,(\mathrm{km}^{-1}) = -3{\cdot}28 \ln a/\sec\psi \quad . \quad . \quad . \quad (10)$$

where a is the fractional absorption observed in the lowest 1,000 ft. In this way, we find $\beta_{KV}/\beta_V \sim 0{\cdot}05$.

The back-scattered component (from the albedo) is roughly equal to the absorbed component so it follows that about 90 per cent of visible radiation intercepted by aerosol is scattered in a forward direction (i.e., deflected through less than 90° from original direction).

The same estimate may be made for attenuation of total solar radiation if the total attenuation coefficient, β_T, can be estimated from β_V.

The value of attenuation coefficient β, obtained by measuring the transmission τ over a path x with a detector having a wavelength sensitivity K_λ is given by:

$$\exp[-\beta x] \equiv \tau = \int_0^\infty K_\lambda I_\lambda \exp\left[-\int_0^x \beta_\lambda \, dx\right] d\lambda \Big/ \int_0^\infty K_\lambda I_\lambda \, d\lambda \quad . \quad . \quad (11)$$

Using the extraterrestrial distribution of solar radiation for I_λ; substituting for β_λ from Eq. (8), and evaluating β_V and β_T by integrating Eq. (11) using the wavelength sensitivities of the photometer and solarimeter respectively, β_V/β_T changes from 1·28 for $\alpha = 1$ to 1·46 for $\alpha = 2$ for small optical paths. Increase in optical paths increases β_V/β_T only slightly.

Adopting a value of $\beta_V/\beta_T = 4/3$ and using Eq. (10) to obtain β_{KT} (horizontal absorption coefficient for total radiation), we obtain $\beta_{KT}/\beta_T \sim 0{\cdot}2$. The total back-scattered component is about $\frac{1}{4}$ of the absorption so that its contribution to total attenuation is again about 5 per cent.

Finally a rough estimate of these parameters for near infra-red wavelengths (0·7-3 μ) may be made by subtraction of the visible from the total components. The results are summarized in Table 3.

TABLE 3. COMPONENTS OF ATTENUATION IN LOWEST 1,000 FT OF THE ATMOSPHERE

	Visible λ per cent	Infra-red λ per cent	Total λ per cent
Absorption	5	35	20
Back-scattering	5	5	5
Forward-scattering	90	60	75
Total	100	100	100

(c) *Absorption above 10,000 ft*

On three flights – 6 July, 15 September, 24 September – heating rates of the order 3-4°C/day were observed above 10,000 ft. Observations were sparse above this level, and the heating rate in the top layer was tied heavily to a single flux observation made at the top flight level. For these reasons, errors in heating rates observed above 10,000 ft are probably twice those quoted in Section 3 (d), and the departures of H_T from H_C of some 2°C/day above 10,000 ft are therefore not considered significant.

(d) *Comparison with other work*

The only measurements of absorption in clear air from aircraft known to the author are those of Goysa (1955) who measured total solar flux divergence over a land surface in the Ukraine and found this to average 2·1 times H_C, which is in broad agreement with our results.

Blackwell, Eldridge and Robinson (1954) concluded from an examination of surface radiation records at Kew Observatory that in order to achieve internal consistency, it was necessary to postulate an approximately grey absorption of about 10 per cent, which is appreciably less than the mean value of 17 per cent in the lowest 10,000 ft obtained in the Channel flights.

6. Conclusions

The results suggest that a small fraction of the total attenuation of solar radiation by aerosol is due to absorption which, however, is capable on occasions of producing instantaneous heating rates in excess of 5°C/day. The absorption does not, in general, depart significantly from greyness except in a few cases of large absorption occurring in the lowest layers of the atmosphere, when it appears to be concentrated in near infra-red wavelengths. This is attributed to the dependence on wavelength of the optical properties of the aerosol.

The scattered radiation is concentrated strongly in a forward direction, particularly in visible wavelengths. This is consistent with the presence of an appreciable number of particles larger than about 0·5 μ in diameter.

These results suggest that heating rates in excess of 10°C/day (or 0·5°C/hr) may occur over heavily polluted areas and may become comparable to those associated with non-radiative processes. It is interesting to note that this heating in a haze layer cannot be counteracted by infra-red cooling (unless condensation sets in) owing to the comparative inability of aerosol to emit radiation of wavelengths large compared with the size of the constituent particles (see Roach and Goody 1958) so that the solar energy absorbed by the aerosol can only be dissipated by heating the ambient air.

In future flights, the intensity of the solar beam as a function of height will be measured, thus giving a direct observation of attenuation to be compared with observations of absorption and albedo.

Acknowledgments

The author is indebted to the Director-General of the Meteorological Office for permission to publish this paper; to the staff and R.A.F. aircrew of Meteorological Research Flight for their assistance in obtaining and reducing the flight data, and to Dr. R. J. Murgatroyd for his helpful and critical discussion of the paper.

References

Allen, C. W.	1958	*Quart. J. R. Met. Soc.*, **84**, p. 307.
Bener, P.	1951	*Arch. Met. Geophys. Biokl.*, B, **2**, p. 188.
Blackwell, M. J.	1953	*Air Ministry, Met. Res. Cttee., M.R.P.*, No. 831.
Blackwell, M. J., Eldridge, R. H. and Robinson, G. D.	1954	*Ibid.*, No. 894.
Goysa, N. I.	1955	Kiev. Ukrain Nauch-Issled. Godromet. Inst., T.Vyp. 3, p. 73. (Met. Office translation).
Howard, J. N., Burch, D. L. and Williams, D.	1955	'Near infra-red transmission through synthetic atmospheres.' GRP No. 40, GRD, AFCRC-TR-55-213 (Astia Ad-87679).
Kano, M.	1958	*Pap. Met. Geophys., Tokyo*, **9**, p. 113.
Middleton, W. E. K.	1941	*Visibility in meteorology*, Univ. Toronto Press, Canada.
Nicolet, M.	1951	*Arch. Met. Geophys. Biokl.*, B, **3**, p. 209.
Roach, W. T.	1961	*Quart. J. R. Met. Soc.*, **87**, p. 364.
Roach, W. T. and Goody, R. M.	1958	*Ibid.*, **84**, p. 319.
Robinson, G. D.	1958	*Arch. Met. Geophys. Biokl.*, Wien **9B**, p. 28.
Van de Hulst, H. C.	1957	*Light scattering by small particles*, Chapman and Hall, London.

551.521.31

The absorption of solar radiation by water vapour and carbon dioxide in a cloudless atmosphere

By W. T. ROACH
Meteorological Research Flight, Farnborough

(Manuscript received 3 November 1960; in revised form 16 February 1961)

SUMMARY

A method of computation of the direct absorption of solar radiation by the near infra-red bands of water vapour and carbon dioxide in a cloudless, non-scattering atmosphere using recent laboratory data compiled by Howard, Burch and Williams (1955) is described.

Three applications of this computation are discussed :

(i) Heating rates in an atmosphere whose water-vapour distribution is given by radiosonde or aircraft observations.

(ii) Instantaneous heating rates as a function of solar zenith angle, altitude and precipitable water vapour.

(iii) A climatological study of heating rates in a cloudless atmosphere integrated over a 24-hr period as a function of latitude, season, altitude and precipitable water vapour. The relative contributions to heating by water vapour and carbon dioxide are assessed between 10 and 1,000 mb.

The mixing ratio of carbon dioxide was assumed constant throughout the atmosphere, while idealized vertical distributions of water vapour mixing ratio were used in (ii) and (iii).

1. INTRODUCTION

Until recently, the only quantitative data on the absorption of near infra-red bands of water vapour known to the author were those due to Fowle (1915); they have provided the basis for later computations of direct solar heating of the atmosphere (e.g. Yamamoto and Onishi 1952). Fowle's experimental methods were sound but the reliability of his data is limited by the equipment and small theoretical knowledge then available : for instance, he did not study the effects of changing pressure and temperature on absorption, so that while his measurements of total absorption as a function of water vapour are approximately correct, they are inadequate for estimating the *rate of change* of absorption with optical path which is directly related to the heating rate. For a recent assessment of Fowle's work, see McDonald (1960).

Recently, however, a quantitative laboratory study of the molecular spectra of water vapour and carbon dioxide from the 0·94 μ water-vapour band to the 15 μ carbon-dioxide band has been published by Howard, Burch and Williams (1955, 1956). These consist of measurements of the absorptions of individual bands of water vapour and carbon dioxide as a function of pressure and optical path. Empirical relations were fitted by Howard *et al.* to these measurements, and they have been used in this paper to compute heating rates in the atmosphere.

The original reason for this computation was to compare its results with heating rates observed in a series of flights in a cloudless atmosphere over the English Channel (Roach 1961), and this application is discussed in § 2 (*d*). However, having access to the Ferranti Mercury Computer in the Royal Aircraft Establishment, it was not difficult to extend the calculations to the applications discussed in § 2 (*e*) and 2 (*f*). The results of the latter applications are presented in § 3.

2. COMPUTATION

All the computations to be described were programmed in Autocode for evaluation by the Ferranti Mercury Computer in the Royal Aircraft Establishment, Farnborough.

(a) *Data*

Howard *et al.* fitted two empirical relations to their results :

Weak absorption bands

$$A = \int A_\nu \, d\nu = cm^{\frac{1}{2}} (P + e)^k \text{ for } A < A_c \quad . \quad . \quad . \quad (1a)$$

Strong absorption bands

$$A = C + D \log m + K \log (P + e) \text{ for } A \geqslant A_c \quad . \quad . \quad (1b)$$

where ν wave-number (cm^{-1})

A band area in wave numbers (cm^{-1})

A_ν fractional absorption within band at ν

m absorbing path (g cm^{-2} for H_2O; cm atm for CO_2)

e partial pressure of absorbing gas (mm Hg)

P partial pressure of non-absorbing gas (mm Hg)

p total pressure $= P + e$

A_c critical band area above which the strong absorption band expression becomes applicable

c, k, C, D, K are empirically determined constants.

Eq. (1a) approximates to the square root law of absorption applicable when centres of individual lines are fully absorbed, but before they start overlapping appreciably. The constant k is 0·5 for a true square root absorption law, but is about 0·3-0·4 in practice, suggesting that some line overlap is present. Eq. (1b) represents the region where the effects of line overlap become severe. The linear law region (very weak lines) can be ignored for practical purposes.

For convenience, the constants for all relevant bands from Table XXIV of Howard *et al.* (1955) have been reproduced in Table 1.

TABLE 1. EMPIRICAL CONSTANTS USED IN COMPUTATIONS

Band λ (μ) Gas	c	k	C	D	K	A_c	I_0	Lower limit of validity pm	A
H_2O								gm cm^{-2} mb	cm^{-1}
0·94	38	0·27	(− 135)	(230)	(125)	(200)	72·5	28	54
1·1	(42)	0·26	(− 292)	(345)	(180)	(300)	72·0	0·66	12
1·38	163	0·30	(251)	460	198	350	64·3	0·17*	73
1·87	152	0·30	(143)	232	144	275	46·7	0·06*	34
2·7	316	0·32	(316)	246	150	200	27·8	0·011*	37
3·2	40·2	0·30	(− 144)	295	151	250	21·0	0·011*	1
6·3	356	0·30	302	218	157	160	7·0	0·04*	66
CO_2								cm atm mb	
1·4	0·058	0·41	-		-	80	63·7	$1·9 \times 10^5$	20
1·6	0·063	0·38	-		-	80	57·1	$1·9 \times 10^5$	12
2·0	0·492	0·39	(− 548)	138	114	80	43·2	$1·6 \times 10^4$	42
2·7	3·15	0·43	(− 137)	77	68	50	27·8	8·1*	23
4·3	-	-	27·5	34	31·5	50	13·2	13·5*	68
4·8	0·12	0·37		-	-	60	11·1	270	1
5·2	0·024	0·40		-	-	30	9·6	$2·5 \times 10^4$	2

I_0 is the mean extra-terrestrial solar intensity over the relevant band in erg cm^{-2} sec^{-1} (wave number)$^{-1}$ taken from Allen (1958).

Figures in brackets have been altered from the original for the following reasons :

(1) The 0·8 μ band of water vapour was not studied by Howard *et al.*, so we have estimated its intensity from Fowle's original paper and included it with the 1·1 μ band of water vapour, for convenience, since the value of I_0 at 0·8 μ is exactly the same as for the 1·1 μ band.

(2) No strong band fit was given for the 0·94 and 1·1 μ bands of water vapour, but examination of Howard's experimental points (also published) show a distinct departure from the weak-line fit for the largest values of m used, so we have constructed a strong-band fit.

(3) Owing to the varying values of P and m, discontinuities in A occur in changing from the weak-band to the strong-band expression. These discontinuities have been minimized by adjusting the quoted values of C; the adjustments are all quite small and do not affect rates of growth of A with m.

Range of validity

Since the absorption law at very small path lengths is expected to be proportional to $(pm)^{\frac{1}{2}}$, we have tabulated the smallest experimental values of pm used by Howard *et al.* and the corresponding observed band areas (A). The lower limit to pm appears to have been set by the experimental conditions in the case of the strong bands (marked by * in Table 1) and in the case of some of the weak bands by their becoming too weak to measure, although it is unfortunate that the 0·94 μ band of water vapour and the 1·4 μ and 2 μ bands of carbon dioxide were not observed at smaller values of pm than they were. The limits in the case of the strong bands correspond in the atmosphere to the absorption above about 100 mb.

Extrapolation to higher levels using Eq. (1a) is possible within reason. At 10 mb (§ 2 (f)) the error due to using an exponent of 0·3-0·4 instead of 0·5 for $\bar{p}$ is estimated to be not greater than 0·1°C/day, decreasing with increasing solar zenith angle and decreasing height.

(*b*) *Theory*

Let the total solar flux absorbed from the solar beam incident at zenith angle ψ above a pressure level p in a stratified atmosphere be E, then summing over all bands, we have

$$E = \sum_i I_{0_i} \cos\psi \,.\, A_i$$

whence

$$\frac{dE}{dp} = \cos\psi \sum_i I_{0_i} \cdot \frac{dA_i}{dp} \quad . \quad . \quad . \quad . \quad (2)$$

where Σ denotes summation over all bands

A_i denotes absorption in cm^{-1} of the ith band integrated from the top of the atmosphere to the pressure level p along a slant path parallel to the solar beam.

The rate of heating, H, is obtained via the hydrostatic equation :

$$H = \frac{dT}{dt} = \Gamma \frac{dE}{dp} \quad . \quad . \quad . \quad . \quad (3)$$

where Γ = dry adiabatic lapse rate ($= g/c_p$).

Hence, combination of Table 1 with Eqs. (1) to (3) will give the instantaneous heating rate if the vertical distribution of the absorbing gases is known.

It is assumed that scattering and absorption by other agents such as air molecules and aerosol are negligible. Note that scattering by air molecules is negligible in the near infra-red; scattering and absorption by aerosol is not often negligible in practice.

Overlapping of bands occurs in two cases :

(1) Overlapping of 1·4 μ bands of carbon dioxide with 1·38 μ band of water vapour. The former band is weak and the error incurred by assuming these bands are separate is negligible.

(2) The coincidence of water vapour and carbon dioxide bands at 2·7 μ is more serious, and Burch, Howard and Williams (1956) have shown how this may be allowed for :

They write

$$\int_{2\cdot7\,\mu} A_\nu\,(CO_2 + H_2O)\,d\nu = \int_{2\cdot7\,\mu} A_\nu\,(H_2O)\,d\nu + \epsilon \int_{2\cdot7\,\mu} A_\nu\,(CO_2)\,d\nu$$

where ϵ is an empirically determined function of $\int_{2\cdot7\,\mu} A_\nu\,(H_2O)\,d\nu$ which has been used in these computations.

(c) *Absorption along temperature and pressure gradients*

(i) *Temperature*

Individual absorption lines have a temperature dependence which increases roughly with the rotational number of the lower energy states of their transitions. Since there is also a rough negative correlation between line intensities and rotational number (i.e., the strongest lines with the least temperature dependence occur near the band centre) it follows that the total band intensity – determined mainly by its strong lines – will not be very temperature-dependent, so this has been neglected as a second-order effect.

For long atmospheric paths in which all energy has been absorbed from band centres, and solar heating is due mainly to weak bands and wings of strong bands, temperature dependence may become appreciable, but as this occurs, in general, in the lower troposphere where temperatures are comparable to laboratory temperatures, the error due to neglect of temperature dependence is also likely to be small.

(ii) *Pressure*

This effect cannot be neglected. In Eq. (1), we assume that $P \gg e$, i.e., that $p = P$ and assign a value, $\bar{p}$, to p given by

$$\bar{p} = \frac{\int p\,dm}{\int dm} \quad . \quad . \quad . \quad . \quad . \quad (4)$$

where the integrations are made from the top of the atmosphere to the level concerned. This expression was suggested by Curtis (1952); it places all the absorbing matter along a pressure gradient at one pressure, $\bar{p}$. Curtis estimated the errors introduced by this assumption to be negligible for the type of vertical distributions of water vapour and carbon dioxide observed in the atmosphere.

(d) *Heating rates in an arbitrary atmosphere*

The method described in this section was used to compute heating rates from frost points observed during flights in the Meteorological Research Flight Hastings aircraft, but can, in principle, be applied to compute the heating in any atmosphere in which the humidity has been determined at a number of levels, e.g., radiosonde ascents.

(i) *Theory*

For an atmosphere in which the mixing ratio of water vapour has been measured at a number of levels, the mean heating rate of a thin, but finite, slab of atmosphere (30-50 mb thick in practice) is estimated by assuming that the mixing ratio of water vapour within the slab is constant at a value given by the arithmetic mean of the mixing ratios* measured at its bounding surfaces and by recasting Eqs. (1) to (4) in finite-difference form.

* The water-vapour path, m, may be computed from the mixing ratio distribution via the hydrostatic equation : $g\,.\,dm = x\,.\,dp$, where x is the mixing ratio.

(ii) *Vertical distribution of absorbing gases*

Since observations of mixing ratio do not extend to the top of the atmosphere, a method of estimating the amount of solar radiation absorbed above the highest level of observation was developed. If the highest level is taken as level O, then the absorbing matter and its effective pressure (Eq. (4)) above this level is m_0 and $\bar{p}_0$.

Carbon dioxide

A constant volume mixing ratio of $2{\cdot}6 \times 10^{-4}$ (Goody 1954) is assumed. Hence using Eq. (4) we have

$$m_0 = \beta p_0 \quad \text{where} \quad \beta = 0{\cdot}208 \text{ cm atm mb}^{-1}$$

$$\bar{p}_0 = \tfrac{1}{2} p_0$$

Water vapour

Consideration of a summary of observations of frost point from aircraft up to 15 km over southern England (Tucker 1957) suggests that the mixing ratio, x, up to about 150 mb, may be quite well represented by an empirical expression of the form

$$x = \alpha p^4 \qquad (5)$$

where α is a constant.

Above 150 mb, the mixing ratio appears to become roughly constant at about 2 μg/g up to the aircraft ceiling (115 mb). Houghton and Seeley (1960) report about 0·5 mg cm^{-2} of water vapour above 150 mb which suggests a mixing ratio of about 3 μg/g to at least 25 km (30 mb). Hence it has been assumed that the mixing ratio above the top flight level falls off as p^4 until it reaches a value (x_c) of 2 μg/g at a level p_c given by

$$x_c = \alpha p_c^4 \qquad (6)$$

above which it remains constant at x_c to the top of the atmosphere.

α is defined from the measured water vapour path between the top and bottom flight levels using Eq. (5).

The values of m and $\bar{p}$ above any given level can then be computed using Eqs. (4) to (6), and then used in Eqs. (1) to (3) to obtain heating rates.

(iii) *Errors*

(1) Departure of true mixing ratio from that defined by this model above p_0. The largest errors are likely to be caused by subsidence inversions but are unlikely to exceed $\pm$ 0·3°C/day at p_0 and $\pm$ 0·1°C/day at (p_0 + 200) mb.

(2) Presence of a continuum extinction due to aerosol. Computed values of heating due to water vapour and carbon dioxide must be multiplied by a factor τ ($\leqslant 1$) given by $\tau = \sum_i H_i \tau_i / \sum_i H_i$ where H_i is the heating due to the ith band and τ_i is the mean transmissivity of the continuum in the ith band above the level concerned.

Aircraft observations suggest that τ approaches unity above 500 mb, but can decrease to 0·8 or less near the surface.

(e) *Instantantaneous heating rates in a model atmosphere*

Instantaneous values of heating rates are evaluated as a function of solar-zenith angle, altitude and total water-vapour path in a model atmosphere in which the mixing-ratio distribution is given by Eq. (5) from the surface to the level at which $x = x_c$ ($x_c = 2$ μg/g) above which x remains constant at x_c. The carbon-dioxide distribution is as described in § 2 (*d*).

Since the distribution of absorbing gases is completely determined by the model chosen, heating rates are obtained by direct differentiation of the relevant equations. We have

$$A_i \equiv A_i(m, \bar{p})$$

therefore

$$\frac{dA_i}{dp} = \frac{\partial A_i}{\partial m} \cdot \frac{dm}{dp} + \frac{\partial A_i}{\partial \bar{p}} \cdot \frac{d\bar{p}}{dp} \quad . \quad . \quad . \quad . \quad (7)$$

The value of dA_i/dp for each band is substituted in Eqs. (2) and (3) to obtain the instantaneous heating rate for given values of solar-zenith angle, pressure level and total water-vapour path (defined by α).

(*f*) *A climatological study of heating rates for a clear atmosphere*

In this section, instantaneous heating rates are integrated over a 24-hr period in 30 min steps from 10 to 1,000 mb as a function of north latitude and season. Cloud statistics have not been fed in at this stage although this will ultimately be necessary in a realistic model. However, the effect of cloud decreases with height and is probably negligible in the mean above 300 mb.

For each season and latitude, the zonal mean value of total precipitable water vapour above the surface has been obtained from Bannon and Steele (1960) and presented in Table 2. The vertical distribution of water vapour and carbon dioxide described in § 2 (*e*) has been used.

TABLE 2. PRECIPITABLE WATER-VAPOUR AMOUNT ($g\ cm^{-2}$) AS A FUNCTION OF LATITUDE AND SEASON (from Bannon and Steele 1960)

Lat. (°N)	0	15	30	45	60	75	90*	δ°
January	4·6	3·2	1·7	0·95	0·4	0·2	0·1	− 20·5
April	4·65	3·4	2·05	1·22	0·7	0·3	0·15	+ 9·8
July	4·4	4·5	3·6	2·7	2·2	1·3	0·65	+ 21·2
October	4·5	4·2	3·4	1·5	0·95	0·6	0·3	− 8·6

δ° – Mean solar declination for relevant month.

* Bannon and Steele's values do not extend north of 75°N so that it has been arbitrarily assumed that the precipitable water-vapour amount over the North Pole is half the average value at 75°N in all seasons. This is not expected to be far from the real value, and, in any case, the computed heating rates are not very sensitive to the total amount of precipitable water vapour, especially at low levels.

In extending this model of the vertical distribution of water vapour to all latitudes, some observational basis for its validity is obtained from frost-point measurements made on various occasions from the Meteorological Research Flight Canberra between 70°N and 10°S (Helliwell and Mackenzie 1957; Helliwell 1960; Kerley 1961) which shows that change of latitude has little effect on the form of Eq. (5) apart from altering the constant α. This is not surprising since the hydrolapse in the troposphere is closely tied to the temperature lapse and this does not change its shape much with latitude.

3. RESULTS

The results of the computation described in § 2 are discussed in this section.

(*a*) *Heating rates in an arbitrary atmosphere*

Heating rates were computed from frost-point observations on nine flights in the Meteorological Research Flight Hastings aircraft on which measurements of heating rates from direct observations of the upward and downward fluxes of solar radiation were made. Thus it was possible to compare observed with computed heating rates. These results appear in a separate paper (Roach 1961).

(*b*) *Instantaneous heating rates in a model atmosphere*

The results of this computation are displayed in Fig. 1, and the following features are of interest :

(1) The rapid increase in heating rate between 200 and 600 mb due to rapid increase of water-vapour path.

(2) The levelling out and slight decrease in heating rate below 600 mb as overlapping of individual lines within absorption bands slows the rate of increase of absorption with optical path.

(3) Increase in m and ψ both tend to shift the level of maximum heating upwards.

(4) Maximum values of heating rate ($\simeq 2{\cdot}5$°C/day) occur at about 500 mb under a zenith sun for values of $m > 5$ g cm^{-2}, i.e. representative of equatorial latitudes.

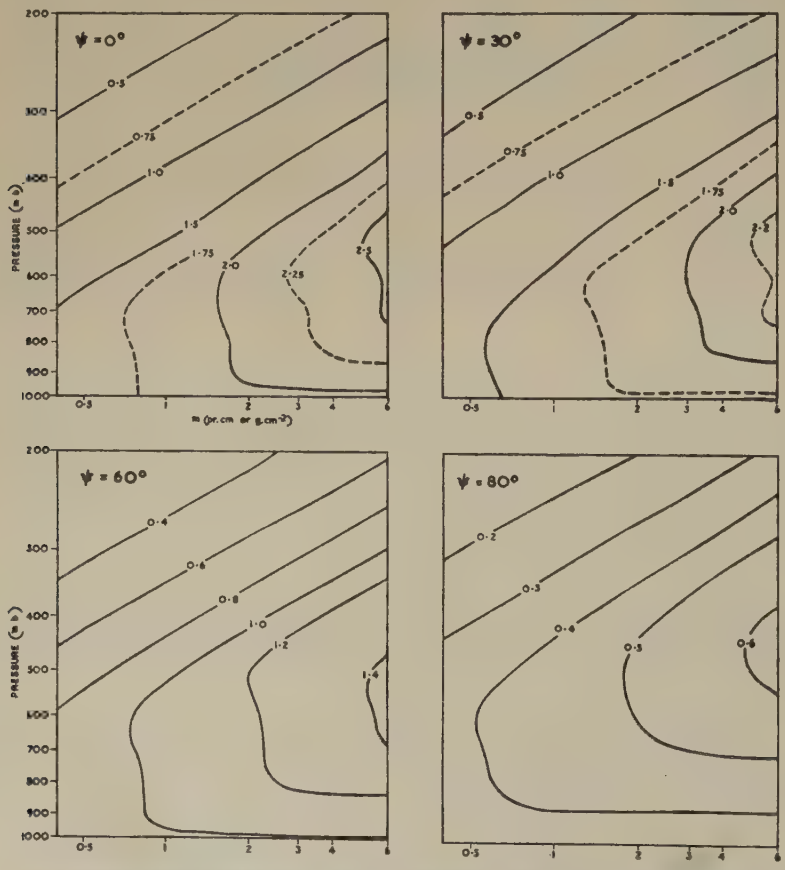

Figure 1. Instantaneous heating rates in °C/day as a function of total water-vapour path (pr cm or g cm^{-2}) above 1,000 mb pressure and solar-zenith angle (pr = precipitable).

(5) Increase in m has little or no effect below 800 mb for a given solar-zenith angle. This is because all the absorption bands of consequence have entered the strong band approximation region (Eq. (1b)).

(6) The heating rates for a solar zenith angle of 60° (air mass 2) are still over half those under a zenith sun, but decrease rapidly with further increase in zenith angle.

(7) An increase in the exponent in Eq. (5) of 0·3 for a given value of m (results not included in Fig. 1) was found to decrease heating rates by about 10 per cent near 200 mb, and increase them by about 5 per cent below 600 mb. This is to be expected since an increase in the exponent will concentrate water vapour and therefore the absorption nearer the ground at the expense of higher levels. A decrease of the exponent by 0·3 results in a reverse effect of about the same magnitude.

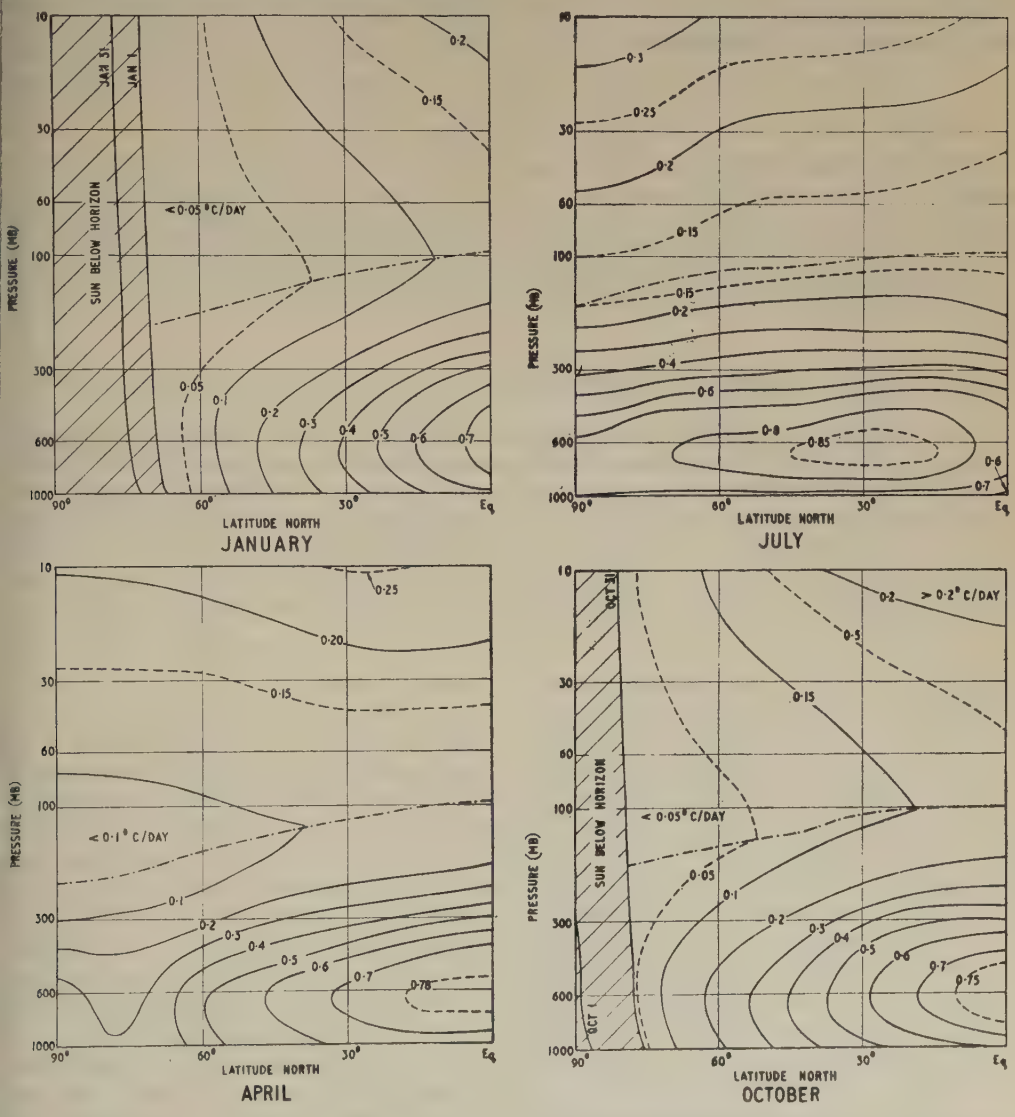

Figure 2. 24-hr heating rates (°C/day) as a function of latitude and season from 10 to 1,000 mb.

——— } isopleths of heating rate
- - - - -

· — · — locus of p_c (from Eq. (6); $x_c = 2\ \mu g/g$, α from Table 2).

(c) *A climatological study of heating rates for a clear atmosphere*

The results of this computation are displayed in Fig. 2, and the following features are of interest:

(1) Maximum values approach 1°C/day in the middle troposphere over the Equator in winter and in all latitudes in the summer hemisphere.

(2) A minimum ($\simeq$ 0·1°C/day) exists at all latitudes and in all seasons near p_c (Eq. (6)) which lies 1-2 km below the equatorial tropopause and 2-3 km above the polar tropopause.

(3) The development of a secondary maximum at the poles at high and low levels in April which spreads south to merge with the northward extension of the equatorial maximum by July as the effect of the rapidly increasing length of day offsets the larger solar zenith angles in polar regions.

(4) The seasonal variation in heating rate is small within 30° latitude of the Equator, but increases rapidly outside this zone.

(5) The heating rates between 10 and 100 mb do not exceed 0·35°C/day and are mainly in the range 0·1-0·25°C/day.

(6) The variation of solar constant due to variation of the distance of the earth from the sun (not included) will be to increase heating rates in January by about $3\frac{1}{2}$ per cent and reduce them by about the same amount in July.

(d) *The relative magnitudes of heating due to carbon dioxide and water-vapour bands*

The heating rates due to carbon-dioxide absorption in the troposphere are small compared to that due to water-vapour absorption and lie in the region 0·01-0·1°C/day. Between 400 and 100 mb, the water-vapour contribution decreases rapidly, equals the carbon-dioxide contribution at about 150 mb, and constitutes about one-quarter of the total heating between 10 and 100 mb on the assumption that the mixing ratio of water vapour is 2 μg/g in this region. An error in this assumption of a factor β will result in an error in computed heating rates (due to water vapour) of a factor of about $\beta^{\frac{1}{4}}$.

(e) *Comparison with other workers*

Yamamoto and Onishi (1952) describe a graphical method for deriving heating rates due to absorption by water-vapour bands using the Elsasser band absorption model and generalized absorption coefficients based on Fowle's data. Their correction for pressure dependence is similar to Curtis's, and they have also neglected temperature dependence of absorption. The use of the Elsasser model for water-vapour absorption has been criticized as being unsuitable (Goody 1952) due to the random appearance of the distribution of line position and intensities, but the errors incurred are not likely to be large. The heating rates derived from their graphical method appear to be about 80-85 per cent of those derived in this paper. Some of this difference may be attributed to their neglect of carbon-dioxide absorption, but we consider that the remainder is not significant mainly because of the different approach of this paper.

London (1952) computed solar heating in March as a function of latitude and height, and obtains a very similar picture to our April diagram in Fig. 2, with a maximum heating rate of 0·8-0·9°C/day at 550 mb and 11°N. He attempted to include cloudiness which reduces his values below 700 mb to about 0·5-0·7 of ours. He also assumed much higher humidities above 500 mb than in fact exist with the result that his decrease in heating rate with height above 500 mb is slower than ours.

4. Conclusions

Many papers on this subject have already been published, so that justification in producing another is sought in the fact that it is based on the most recent data on water-vapour and carbon-dioxide absorption and water-vapour distribution available. It has also been possible to extend its scope through access to modern computing facilities.

The results themselves are expected to be most realistic between about 50 and 300 mb. Below this level, the effect of cloud should be considered, while above it, little is known about the latitudinal and seasonal distribution of water vapour. Results by some workers (e.g., Murcray *et al.* 1960) suggest water-vapour mixing ratios as high as 300 μg/g above 30 mb over New Mexico, although these results have yet to be confirmed by independent workers. Finally, the effects of absorption of solar radiation by the Hartley and Huggins bands of ozone become appreciable (> 1°C/day) above about 30 mb. Between this level and the tropopause, this heating will probably vary between 0·01 and 1°C/day at any given time owing to the great variability of ozone concentration in this region.

Acknowledgments

The author is indebted to the Director-General of the Meteorological Office for permission to publish this paper; to the Staff of Mathematical Services, Royal Aircraft Establishment for their co-operation and use of their Ferranti Mercury Computer; and to Dr. R. J. Murgatroyd for his helpful and critical discussion of the paper.

References

Allen, C. W.	1958	*Quart. J. R. Met. Soc.*, **84**, p. 307.
Bannon, J. K. and Steele, L. P.	1960	*Geophys. Mem., Met. Office*, No. 102.
Burch, D. E., Howard, J. N. and Williams, D.	1956	*J. Opt. Soc. Am.*, **46**, p. 452.
Curtis, A. R.	1952	*Quart. J. R. Met. Soc.*, **78**, p. 638.
Fowle, F. E.	1915	*Astrophys. J.*, **35**, p. 149.
Goody, R. M.	1952	*Quart. J. R. Met. Soc.*, **78**, p. 165.
	1954	*The physics of the stratosphere*, p. 56, Cambridge University Press.
Helliwell, N. C. and Mackenzie, J. K.	1957	'Observations of humidity, temperature and wind at Idris 23 May-2 June 1956,' *Met. Res. Cttee., M.R.P.* No. 1024.
Helliwell, N. C.	1960	'Airborne measurements of the latitudinal variation of frost-point, temperature and wind.' *Met. Off. Sci. Pap.*, No. 1.
Houghton, J. T. and Seeley, J. S.	1960	*Quart. J. R. Met. Soc.*, **86**, p. 358.
Howard, J. N., Burch, D. L. and Williams, D.	1955	'Near infra-red transmission through synthetic atmospheres,' G.R.P. No. 40, G.R.D., A.F.C.R.C.-T.R.-55-213 (Astia A.D.-87679).
	1956	*J. Opt. Soc. Am.*, **46**, p. 186, p. 237, p. 242 and p. 334.
Kerley, M. J.	1961	*Met. Mag.*, London, **90**, p. 3.
London, J.	1952	'The distribution of radiational temperature change in the northern hemisphere during March,' G.R.P. No. 18, G.R.D., A.F.C.R.C.-T.R.-53-3.
McDonald, J. E.	1960	*J. Met.*, **17**, p. 319.
Murcray, D. G., Murcray, F. H., Williams, W. J. and Leslie, F. E.	1960	'Water vapour distribution above 90,000 ft,' *Sci. Rep.* No. 5, G.R.D., A.F.C.R.C.-T.N.-60-452.
Roach, W. T.	1961	*Quart. J. R. Met. Soc.*, **87**, p. 346.
Tucker, G. B.	1957	'An analysis of humidity measurements in the upper troposphere and lower stratosphere over southern England,' *Met. Res. Cttee., M.R.P.* No. 1052.
Yamamoto, G. and Onishi, G.	1952	*J. Met.*, **9**, p. 415.

551.509.313

A three-parameter model of the atmosphere suitable for numerical integration

By F. H. BUSHBY and CLARE J. WHITELAM
Meteorological Office, Dunstable

(Manuscript received 20 May 1960)

Summary

Subject to various approximations, a system of five simultaneous equations (three partial differential equations and two algebraic equations) is derived to predict the height of three contour surfaces corresponding to the bottom, middle and top of the troposphere and to evaluate the two fields of vertical motion corresponding to the upper and lower halves of the troposphere. The atmospheric model used is an extension of the two-parameter model proposed by Sawyer and Bushby (1953).

Numerical integrations have been carried out for 20 cases and the results are given in statistical form. Two forecasts are illustrated with diagrams. The accuracy is better than that obtained with the two-parameter model, and the forecasts are of the same standard as those produced by conventional methods.

1. Introduction

Several atmospheric models suitable for the production of forecasts by numerical methods of the movement and development of large-scale atmospheric disturbances have been formulated in recent years. A typical model using two variables to approximate to the structure of the atmosphere has been described by Sawyer and Bushby (1953). The results of computing 24-hr pressure changes based on this model have been described by Bushby and Hinds (1954; 1955) and by Knighting, Corby, Bushby and Wallington (1961). Statistically, the results of these numerical forecasts were of the same standard as those produced by conventional methods and it therefore seemed possible that if a more realistic model than that formulated by Sawyer and Bushby were to be used, there would be a significant increase in the accuracy of the numerical forecasts.

The present paper describes the introduction of a third parameter to enable the model to represent more accurately the equations of motion of the atmosphere. Charney and Phillips (1953) formulated a generalized model in which the atmosphere was divided into n layers, the motion being assumed barotropic in each layer. The three-parameter model formulated in this paper differs from the three-layer model of Charney and Phillips in that it consists of only two layers, the motion in each layer being baroclinic. This model is a logical extension of the Sawyer and Bushby two-parameter baroclinic model.

Numerical forecasts have been computed using the new model for 20 situations for which forecasts had previously been computed using the Sawyer-Bushby model. These 20 situations included 15 which were inadequately dealt with by the two-parameter model. Since the new results include forecasts of the 200 mb contours, similar forecasts have been calculated from the original computations by extrapolating from the results at 1,000 and 500 mb. The new results have been compared with those obtained from the two-parameter model and also with the forecasts prepared by conventional means.

2. The basic assumptions

The model of the atmosphere which is used consists of a baroclinic fluid bounded by two pressure surfaces, $p = p_0$ corresponding to a level near the ground and $p = p_1$ corresponding to the upper limit of the troposphere and we assume that the movement of air across these isobaric surfaces is negligible. We consider that this atmosphere is separated into two layers by the surface $p = p_m$ where $p_m = \frac{1}{2}(p_0 + p_1)$. In each layer we assume that the thermal wind is constant in direction in any vertical column and that the thermal wind speed is proportional to the pressure difference through any part of the column.

r and s are used as horizontal co-ordinates, these being orthogonal curvilinear distance co-ordinates on the earth's surface (treated as a sphere). u and v denote the components of the horizontal velocity $\mathbf{V}$ in the directions r and s respectively.

It is convenient to use α as a vertical co-ordinate, where

$$\alpha = (p_0 + p_1 - 2p)/(p_0 - p_1) \quad . \quad . \quad . \quad . \quad (1)$$

α then varies from -1 at p_0 to $+1$ at p_1. We can thus represent the horizontal wind velocity in our model by

$$\mathbf{V} = \mathbf{V}_m + \alpha \mathbf{V}_0^1 \quad \text{for} \quad -1 \leqslant \alpha \leqslant 0 \quad . \quad . \quad . \quad (2)$$

and

$$\mathbf{V} = \mathbf{V}_m + \alpha \mathbf{V}_1^1 \quad \text{for} \quad 0 \leqslant \alpha \leqslant 1 \quad . \quad . \quad . \quad (3)$$

where $\mathbf{V}_m$ is the horizontal wind at $p = p_m$, $\mathbf{V}_0^1$ is the wind shear through the layer from p_0 to p_m and $\mathbf{V}_1^1$ is the wind shear through the layer from p_m to p_1. Similarly, we can express the vertical component of vorticity as

$$\zeta = \zeta_m + \alpha \zeta_0^1 \quad \text{for} \quad -1 \leqslant \alpha \leqslant 0 \quad . \quad . \quad . \quad (4)$$

$$\zeta = \zeta \quad + \alpha \zeta_1^1 \quad \text{for} \quad 0 \leqslant \alpha \leqslant 1 \quad . \quad . \quad . \quad (5)$$

where ζ, ζ_m, ζ_0^1 and ζ_1^1 are the vertical components of the vorticity of the wind fields $\mathbf{V}$, $\mathbf{V}_m$, $\mathbf{V}_0^1$ and $\mathbf{V}_1^1$.

The equation of continuity can be written as

$$\mathrm{div}_s \mathbf{V} = -\frac{\partial \Pi}{\partial p} \quad . \quad . \quad . \quad . \quad (6)$$

where $\Pi = dp/dt$ and is a measure of the vertical motion. We shall assume $\Pi = 0$ at the top and bottom of our model atmosphere. The suffix s after a differential operator refers to differentiation with respect to r and s, all such differentiation being taken in an isobaric surface.

Finally we use the vorticity equation in the form

$$\frac{\partial}{\partial t}(\zeta + f) + \mathbf{V} \,.\, \mathrm{grad}_s (\zeta + f) + \Pi \frac{\partial}{\partial p}(\zeta + f) = -(\zeta + f)\,\mathrm{div}_s \mathbf{V} \quad . \quad (7)$$

where f is the Coriolis parameter.

3. The vertical motion profile

In order for the vertical motion profile to be consistent with Eqs. (2), (3) and (6) we have

$$2\frac{\partial \Pi}{\partial \alpha} = (p_0 - p_1)(\mathrm{div}_s \mathbf{V}_m + \alpha\, \mathrm{div}_s \mathbf{V}_0^1) \quad \text{for} \quad -1 \leqslant \alpha \leqslant 0 \quad . \quad . \quad (8)$$

and

$$2\frac{\partial \Pi}{\partial \alpha} = (p_0 - p_1)(\mathrm{div}_s \mathbf{V}_m + \alpha\, \mathrm{div}_s \mathbf{V}_1^1) \quad \text{for} \quad 0 \leqslant \alpha \leqslant 1 \quad . \quad . \quad (9)$$

Integrating Eqs. (8) and (9) with respect to α, since Π is continuous at $\alpha = 0$ and is zero at $\alpha = \pm 1$, we derive

$$\Pi = -a + b\alpha + (a + b)\alpha^2 \quad \text{for} \quad -1 \leqslant \alpha \leqslant 0 \quad . \quad . \quad (10)$$

and

$$\Pi = -a + b\alpha + (a - b)\alpha^2 \quad \text{for} \quad 0 \leqslant \alpha \leqslant 1 \quad . \quad . \quad (11)$$

where

$$a = 0{\cdot}125\,(p_0 - p_1)(\mathrm{div}_s \mathbf{V}_0^1 + \mathrm{div}_s \mathbf{V}_1^1)$$

and

$$b = 0{\cdot}125\,(p_0 - p_1)(\mathrm{div}_s \mathbf{V}_0^1 - \mathrm{div}_s \mathbf{V}_1^1)$$

4. Derivation of the prognostic equations

(a) *Equation for the mean motion of the atmosphere*

By eliminating $\mathrm{div}_s \mathbf{V}$ from Eqs. (6) and (7), we obtain Eq. (12) which does not contain the divergence explicitly

$$\frac{\partial}{\partial t}(\zeta + f) + \mathbf{V} \cdot \mathrm{grad}_s (\zeta + f) + \Pi \frac{\partial}{\partial p}(\zeta + f) = (\zeta + f) \frac{\partial \Pi}{\partial p} \quad . \quad . \quad (12)$$

This will enable us to approximate at a later stage by using the geostrophic wind relation.

Substituting for $\mathbf{V}$, ζ and Π in Eq. (12) from Eqs. (2), (3), (4), (5), (10) and (11) and integrating with respect to α from $\alpha = -1$ to $\alpha = +1$, we obtain

$$\frac{\partial}{\partial t}\{\zeta_m + \tfrac{1}{4}(\zeta_1{}^1 - \zeta_0{}^1)\} + \mathbf{V}_m \cdot \mathrm{grad}_s \{\zeta_m + \tfrac{1}{4}(\zeta_1{}^1 - \zeta_0{}^1) + f\} +$$

$$\tfrac{1}{4}(\mathbf{V}_1{}^1 - \mathbf{V}_0{}^1) \cdot \mathrm{grad}_s (\zeta_m + f) + \tfrac{1}{6}\{\mathbf{V}_0{}^1 \cdot \mathrm{grad}_s \zeta_0{}^1 + \mathbf{V}_1{}^1 \cdot \mathrm{grad}_s \zeta_1{}^1\} +$$

$$\frac{4a(\zeta_0{}^1 + \zeta_1{}^1) + b(\zeta_0{}^1 - \zeta_1{}^1)}{3(p_0 - p_1)} = 0 \quad . \quad . \quad . \quad (13)$$

It should be noted that one half of the last term in Eq. (13) corresponds to the vertical advection of vorticity term and the other half to the divergence term in Eq. (7). Although the corresponding term in the Sawyer-Bushby (1953) model is small initially compared with the horizontal advection of vorticity, it has been shown by Hollman (1956) and Arnason and Carstenson (1959) to be predominantly of one sign, and its inclusion in forecasts based on the two-parameter model occasionally produced a cumulative effect which destroyed the value of the forecast. It was also shown that this effect should to some extent be balanced by the terms involving the horizontal derivatives of Π which have been neglected in deriving Eq. (7). It was therefore decided to ignore the last term in Eq. (13) when carrying out the present series of numerical forecasts.

The geostrophic approximation can be written as

$$u = -\frac{g}{f}\frac{\partial h}{\partial s}, \qquad v = \frac{g}{f}\frac{\partial h}{\partial r} \quad . \quad . \quad . \quad . \quad (14)$$

where h is the height of the isobaric surface of pressure p, and g is the acceleration due to gravity. If we ignore small terms due to horizontal variations of the Coriolis parameter, the geostrophic approximation to the vorticity is given by

$$\zeta = \frac{g}{f} \nabla_s{}^2 h \quad . \quad . \quad . \quad . \quad . \quad (15)$$

By eliminating the wind and vorticity from Eq. (13) by means of the geostrophic approximation and ignoring the last term of Eq. (13) we obtain

$$\nabla_s{}^2 \left\{ \partial h_m / \partial t + \tfrac{1}{4}\left(\frac{\partial h_1{}^1}{\partial t} - \frac{\partial h_0{}^1}{\partial t} \right) \right\} + J_s \left[h_m, \frac{g}{f}\{\nabla_s{}^2 h_m + \tfrac{1}{4}(\nabla_s{}^2 h_1{}^1 - \nabla_s{}^2 h_0{}^1)\} + f \right]$$

$$+ J_s \left\{ \tfrac{1}{4}(h_1{}^1 - h_0{}^1), \frac{g}{f} \nabla_s{}^2 h_m + f \right\} + \tfrac{1}{6}\left\{ J_s \left(h_0{}^1, \frac{g}{f} \nabla_s{}^2 h_0{}^1 \right) + J_s \left(h_1{}^1, \frac{g}{f} \nabla_s{}^2 h_1{}^1 \right) \right\} = 0 \quad . \quad (16)$$

where ∇^2 and J are the two-dimensional Laplacian and Jacobian operators respectively, h_m is the height of the isobaric surface $p = p_m$ and $h_0{}^1$ and $h_1{}^1$ are the thicknesses of the layers from $p = p_0$ to $p = p_m$ and from $p = p_m$ to $p = p_1$ respectively.

In order to integrate Eq. (16) it is desirable to transform the earth's surface to a plane. A suitable transformation is a stereographic projection from the South Pole of the Northern Hemisphere on to a plane perpendicular to the earth's axis passing through the North Pole. If x and y are rectangular Cartesian co-ordinates on the plane and differential

operators without suffixes refer to differentiation in an isobaric surface with respect to x and y, Eq. (16) transforms to

$$\nabla^2\{\partial h_m/\partial t + \tfrac{1}{4}(\partial h_1^1/\partial t - \partial h_0^1/\partial t)\} + J\left[h_m, \frac{\beta^2 g}{f}\{\nabla^2 h_m + \tfrac{1}{4}\nabla^2(h_1^1 - h_0^1)\} + f\right]$$
$$+ J\left\{\tfrac{1}{4}(h_1^1 - h_0^1), \frac{\beta^2 g}{f}\nabla^2 h_m + f\right\} + \tfrac{1}{6}\left\{J\left(h_0^1, \frac{\beta^2 g}{f}\nabla^2 h_0^1\right) + J\left(h_1^1, \frac{\beta^2 g}{f}\nabla^2 h_1^1\right)\right\} = 0 \,. \quad (17)$$

where the magnification factor $\beta = \sec^2(\pi/4 - \theta/2)$, θ being the geographical latitude.

(b) *The equation for change of thickness*

An equation for the local rate of change of thickness of an isobaric layer has been given by Sutcliffe and Forsdyke (1950). Applying this equation to the two layers we are using in the current model we obtain

$$\partial h_0^1/\partial t = -\mathbf{V}_m \,.\, \mathrm{grad}_s\, h_0^1 - \frac{p_0 - p_1}{2g} R \int_{-1}^{0} \Gamma \frac{\Pi}{p}\, d\alpha + Q_0 \,. \quad (18)$$

and

$$\partial h_1^1/\partial t = -\mathbf{V}_m \,.\, \mathrm{grad}_s\, h_1^1 - \frac{p_0 - p_1}{2g} R \int_{0}^{1} \Gamma \frac{\Pi}{p}\, d\alpha + Q_1 \,. \quad (19)$$

where R is the gas constant, Γ is a measure of the departure of the lapse rate from the adiabatic given by $\Gamma = \partial T/\partial p - \gamma/g\rho$, γ being the appropriate wet or dry adiabatic lapse rate, ρ the density, T the absolute temperature, and Q_0 and Q_1 are measures of the non-adiabatic heating effects in the bottom and top layers of the model. The most important non-adiabatic heating effect in short-range forecasts is the heating of cold air-masses over the sea, and this is the only non-adiabatic term included in this analysis. The exchange of heat between the air and sea is carried out mainly by convective processes, and will usually be limited to the lower layer of our model. It was therefore decided to make $Q_1 = 0$. An empirical value for Q_0 similar to that used by Bushby and Hinds (1955) is given in Section 5.

If we assume Γ constant in each of the two layers and substitute from Eqs. (10) and (11) in Eqs. (18) and (19) we obtain

$$\partial h_0^1/\partial t = -\mathbf{V}_m \,.\, \mathrm{grad}_s\, h_0^1 + Q_0 + Aa + Bb \,. \quad (20)$$

$$\partial h_1^1/\partial t = -\mathbf{V}_m \,.\, \mathrm{grad}_s\, h_1^1 + Ca + Db \quad (21)$$

where

$$A \equiv \frac{R\,\Gamma_0}{2g\,(p_0 - p_1)^2}\left[8\,p_0\,p_1 \log_e \frac{p_0 + p_1}{2\,p_0} + (p_0 + 3\,p_1)(p_0 - p_1)\right]$$

$$B \equiv \frac{R\,\Gamma_0}{2g\,(p_0 - p_1)^2}\left[4\,p_0\,(p_0 + p_1) \log_e \frac{p_0 + p_1}{2\,p_0} + (p_1 + 3\,p_0)(p_0 - p_1)\right]$$

$$C \equiv \frac{R\,\Gamma_1}{2g\,(p_0 - p_1)^2}\left[8\,p_0\,p_1 \log_e \frac{2\,p_1}{p_0 + p_1} + (3\,p_0 + p_1)(p_0 - p_1)\right]$$

$$D \equiv \frac{R\,\Gamma_1}{2g\,(p_0 - p_1)^2}\left[-4\,p_1\,(p_0 + p_1) \log_e \frac{2\,p_1}{p_0 + p_1} - (p_0 + 3\,p_1)(p_0 - p_1)\right]$$

Γ_0 and Γ_1 being the values of Γ in the bottom and top layers respectively.

If we now make use of the geostrophic approximation in Eqs. (20) and (21), and transform to a stereographic projection we find

$$\partial h_0^1/\partial t = -\frac{\beta^2 g}{f} J(h_m, h_0^1) + Q_0 + Aa + Bb \quad (22)$$

$$\partial h_1^1/\partial t = -\frac{\beta^2 g}{f} J(h_m, h_1^1) + Ca + Db \quad (23)$$

Sutcliffe (1947) has shown another equation can be derived for the thickness change of a layer of the atmosphere by subtracting the vorticity equation (Eq. 12) referring to the bottom of the layer from the corresponding equation at the top of the layer. Applying this technique to our model we find

$$\partial\zeta_0^1/\partial t + \mathbf{V}_m \cdot \text{grad}_s\, \zeta_0^1 + \mathbf{V}_0^1 \cdot \text{grad}_s\, (\zeta_m - \zeta_0^1 + f)$$
$$= -\frac{2}{p_0 - p_1}\{2\,(a+b)\,(\zeta_m + f) - (a+b)\,\zeta_0^1\} \quad . \quad . \quad (24)$$

$$\partial\zeta_1^1/\partial t + \mathbf{V}_m \cdot \text{grad}_s\, \zeta_1^1 + \mathbf{V}_1^1 \cdot \text{grad}_s\, (\zeta_m + \zeta_1^1 + f)$$
$$= -\frac{2}{p_0 - p_1}\{2\,(a-b)\,(\zeta_m + f) + (a-b)\,\zeta_1^1\} \quad . \quad . \quad (25)$$

If we now use the geostrophic approximation and transform to a stereographic projection Eqs. (24) and (25) become

$$\nabla^2\,\partial h_0^1/\partial t + J\left(h_m, \frac{\beta^2 g}{f}\nabla^2 h_0^1\right) + J\left\{h_0^1, \frac{\beta^2 g}{f}\nabla^2 (h_m - h_0^1) + f\right\}$$
$$= -\frac{2}{p_0 - p_1}(a+b)\left\{2\left(\nabla^2 h_m + \frac{f^2}{\beta^2 g}\right) - \nabla^2 h_0^1\right\} \quad . \quad . \quad (26)$$

$$\nabla^2\,\partial h_1^1/\partial t + J\left(h_m, \frac{\beta^2 g}{f}\nabla^2 h_1^1\right) + J\left\{h_1^1, \frac{\beta^2 g}{f}\nabla^2 (h_m + h_1^1) + f\right\}$$
$$= -\frac{2}{p_0 - p_1}(a-b)\left\{2\left(\nabla^2 h_m + \frac{f^2}{\beta^2 g}\right) + \nabla^2 h_1^1\right\} \quad . \quad . \quad (27)$$

Eqs. (17), (22), (23), (26) and (27) are a set of five simultaneous linear equations (three of them being partial differential equations) which can be solved for $\partial h_m/\partial t$, $\partial h_0^1/\partial t$, $\partial h_1^1/\partial t$, a and b provided that $\partial h_m/\partial t$, $\partial h_0^1/\partial t$ and $\partial h_1^1/\partial t$ are specified on the boundary of the area for which a forecast is being computed.

5. Method of solution

The independent variables were represented by values at points of a rectangular 24 × 20 grid. The grid-length was approximately 200 naut. mi at the North Pole, and the network covered an area from the Hudson Bay eastwards to Russia and as far south as North Africa. h_m, h_0^1 and h_1^1 were assumed to remain fixed on the two outer rings of the grid, and a time step of $\frac{3}{4}$ hr was used. The computations were carried out at Dunstable on METEOR, a Ferranti mercury computer, and the calculations involved in each time-step took about one minute.

The computations were carried out for the layer of the atmosphere from 1,000 mb to 200 mb. Thus $p_0 = 1{,}000$ mb, $p_m = 600$ mb and $p_1 = 200$ mb. The heights of the 1,000 mb (h_0), 500 mb (h_{500}) and 200 mb (h_1) surfaces are fed into the computer. The heights of the 600 mb contours are not readily available, and they were therefore calculated from the formula

$$h_m = 0{\cdot}8\, h_{500} + 0{\cdot}2\, h_0 \quad . \quad . \quad . \quad . \quad (28)$$

This formula does not give good values for the absolute heights of the 600 mb surface, but it does give good approximations to the derivatives of the 600 mb height field which are consistent with the assumptions of the model. It is only derivatives of the height field which are used in the computations.

The empirical value used for Q_0 is given by

$$Q_0 \text{ (m hr}^{-1}) = 2{\cdot}068 \,.\, 10^{-2} (h_s^1 - h_0^1) \text{ for } h_s' > h_0' \text{ otherwise } Q_0 = 0 \quad . \quad (29)$$

$$\text{where } h_s \text{ (m)} = 129{\cdot}7 \,(T_s + 282{\cdot}5) \quad . \quad . \quad . \quad (30)$$

T_s being the monthly mean sea-surface temperature (°F). Γ_0 and Γ_1 were taken as -38°C per 900 mb and -46°C per 900 mb respectively. Thus the constants A, B, C and D can be evaluated. Eliminating a and b from Eqs. (20), (21), (26) and (27) leaves us with two simultaneous partial differential equations of the type

$$\nabla^2 \partial h_0^1/\partial t + E\,(x, y)\, \partial h_0^1/\partial t + F\,(x, y)\, \partial h_1^1/\partial t + G\,(x, y) = 0 \quad . \quad (31)$$

$$\nabla^2 \partial h_1^1/\partial t + L\,(x, y)\, \partial h_0^1/\partial t + M\,(x, y)\, \partial h_1^1/\partial t + N\,(x, y) = 0 \quad . \quad (32)$$

The finite-difference forms of these two equations were solved simultaneously at each grid point in turn, to give values of $\partial h_0^1/\partial t$ and $\partial h_1^1/\partial t$. The iterative process used requires an initial guess at the values of the tendencies; for the first time-step they were assumed to be zero everywhere, and 12-15 iterations were usually required to ensure that the solution had been obtained sufficiently accurately. For subsequent time-steps the last computed tendency values were found to be an excellent initial guess to commence the iterative process so that 3-6 iterations were sufficient.

Having calculated $\partial h_0^1/\partial t$ and $\partial h_1^1/\partial t$ we can obtain a and b from Eqs. (22) and (23). The mean vertical motions in the bottom and top layers of the model can then be calculated from the formulae

$$\overline{\Pi}_0 = -(\tfrac{2}{3} a + \tfrac{1}{3} b) \quad . \quad . \quad . \quad . \quad (33)$$

$$\overline{\Pi}_1 = -(\tfrac{2}{3} a - \tfrac{1}{3} b) \quad . \quad . \quad . \quad . \quad (34)$$

The finite-difference approximation to Eq. (17) can be solved by the Liebmann iterative process (Hartree 1952) for $\{\partial h_m/\partial t + \frac{1}{4}(\partial h_1^1/\partial t - \partial h_0^1/\partial t)\}$ from which $\partial h_m/\partial t$ can be evaluated. Having obtained values of $\partial h_m/\partial t$, $\partial h_0^1/\partial t$ and $\partial h_1^1/\partial t$, new values of h_m, h_0^1 and h_1^1 can be calculated as indicated by Sawyer and Bushby (1953). A sufficient boundary condition is that h_m, h_0^1 and h_1^1 should be known at all the grid points initially and at the two outer rings of points for the duration of the forecast period.

6. Results

(a) *Statistical results*

In order to assess the accuracy of the three-parameter forecasts they were compared with forecasts produced using the two-parameter model, and also with forecasts produced by conventional methods at the Central Forecasting Office (C.F.O.), Dunstable. Individual statistics for each case are given in the appendices, but the mean statistics for the 20 cases are shown in Table 1.

The statistics refer to 150 grid points covering the area for which forecast charts have been produced (see Fig. 1 (c)). The imposition of incorrect boundary values implies that the forecast must necessarily be wrong near those boundaries and therefore the area used for verification purposes does not contain a few rows of points near the edge of the original 24 × 20 grid. Winds have been evaluated geostrophically for this purpose by averaging over one grid length. It should be remembered that the twenty situations were not chosen at random but include 15 situations in which the two-parameter model forecasts contained large errors. The absolute r.m.s. errors in Table 1 are, therefore, almost certainly larger than would arise if 20 situations had been selected at random.

The 200 mb results obtained from the two-parameter model were calculated by computing 24-hr changes in the 200 mb field by extrapolation from the changes in the 1,000 mb and 500 mb fields and adding these changes to the original 200 mb field.

Statistically the three-parameter 1,000 mb forecasts for these 20 cases are much better than the two-parameter forecasts and are about the same as the C.F.O. forecasts. The 1,000-500 mb thicknesses and the 500 mb heights are much better forecast by the three-parameter model than by either C.F.O. or the two-parameter model. The thermal winds are also forecast better with the three-parameter model than with the two-parameter model. There is little to choose between the C.F.O. and three-parameter model forecasts of the 500-200 mb thicknesses and thermal winds, but the C.F.O. 200 mb forecast is rather better than that produced by the three parameter-model.

The forecasts of the 200 mb contours and 500-200 mb thickness produced by extrapolation from the two-parameter model were, not unexpectedly, worse than those produced by the other two methods. It should be noted that C.F.O. do not produce forecast charts of the 500-200 mb thickness, and that the values attributed to them have been obtained by subtracting their 500 mb forecasts from their 200 mb forecasts.

TABLE 1. MEAN STATISTICS FOR 20 CASES

		1	2	3	4	5
1,000 mb	(a)	0·71	72	0·89	25	0·66
	(b)	0·63	71	0·81	26	0·56
	(c)	0·62	94	0·85	37	0·59
1,000-500 mb	(a)	0·73	58	0·88	30	0·56
	(b)	0·67	67	0·86	27	0·57
	(c)	0·70	68	0·86	41	0·52
500 mb	(a)	0·75	77	0·94	28	0·76
	(b)	0·66	87	0·91	30	0·71
	(c)	0·66	98	0·93	31	0·74
500-200 mb	(a)	0·60	56	0·73	28	0·32
	(b)	0·58	59	0·72	25	0·28
	(c)	0·34	62	0·64	29	0·23
200 mb	(a)	0·69	96	0·93	34	0·74
	(b)	0·72	89	0·93	31	0·75
	(c)	0·66	114	0·91	44	0·66

1 = Correlation coefficient between actual and forecast 24-hr height changes.
2 = R.m.s. height error (m).
3 = Correlation coefficient between actual and forecast heights.
4 = R.m.s. vector wind error (kt).
5 = Stretch vector correlation coefficient between actual and forecast winds.

(a) = Three-parameter forecast.
(b) = C.F.O. forecast.
(c) = Two-parameter forecast.

(*b*) *Examples of forecasts*

The numerical forecasts using the three-parameter model based on data for 00 GMT 26 February 1959 and 5 May 1959 are shown in Figs. 1-8. These two situations were chosen because the former forecast produced a large r.m.s. error at 500 and 200 mb and was not one of the better forecasts, whereas the later was typical of one of the good forecasts.

A depression centred ESE of Newfoundland at 00 GMT 26 February 1959 (Fig. 1 (a)) moved rapidly NE and deepened 12 mb in the following 24 hr (Fig. 1 (b)). The axis of the

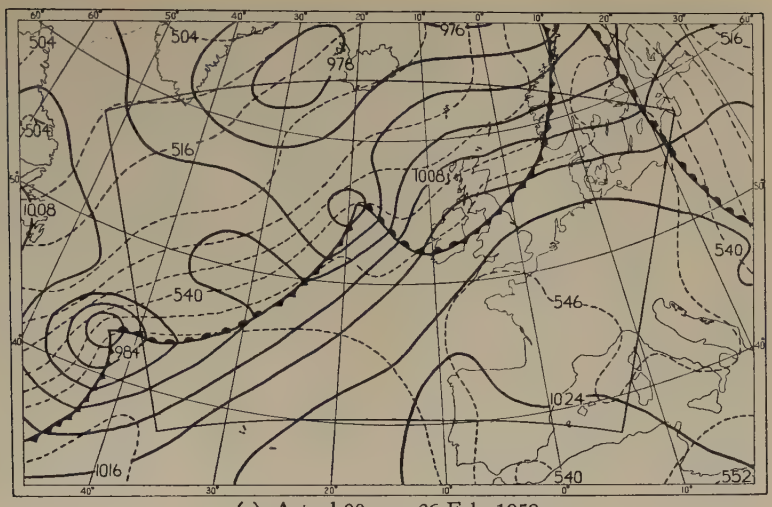

(a) Actual 00 GMT 26 Feb. 1959.

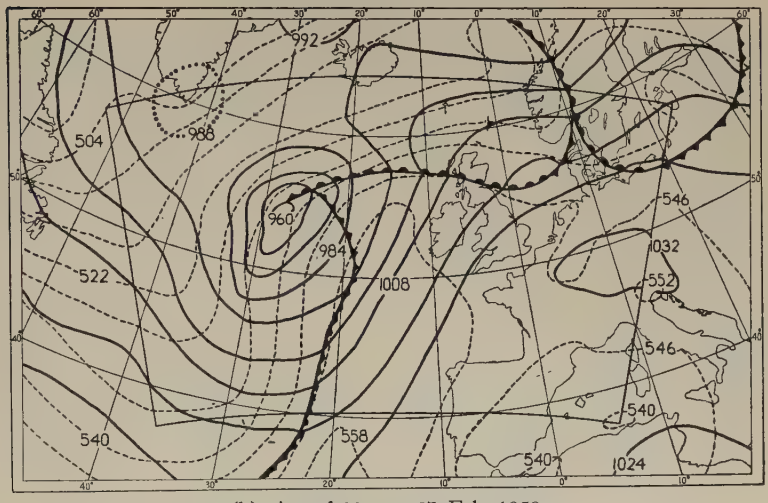

(b) Actual 00 GMT 27 Feb. 1959.

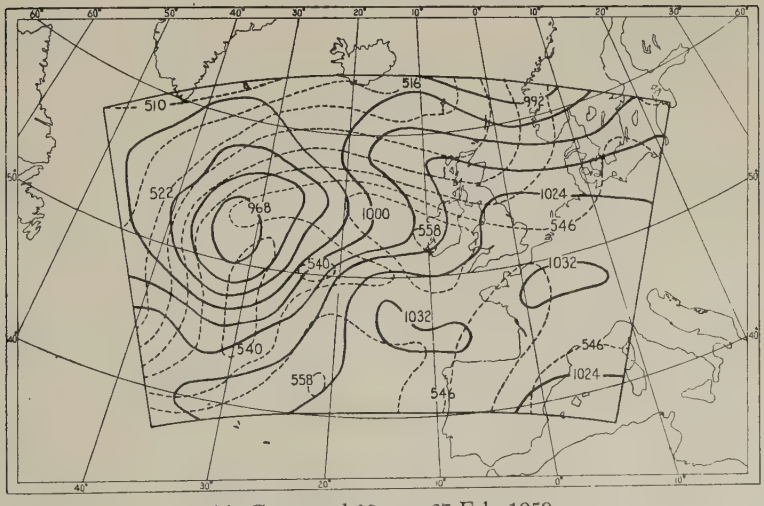

(c) Computed 00 GMT 27 Feb. 1959.

Figure 1. ——— m.s.l. isobars (mb), – – – – – 1,000-500 mb thickness (dm).

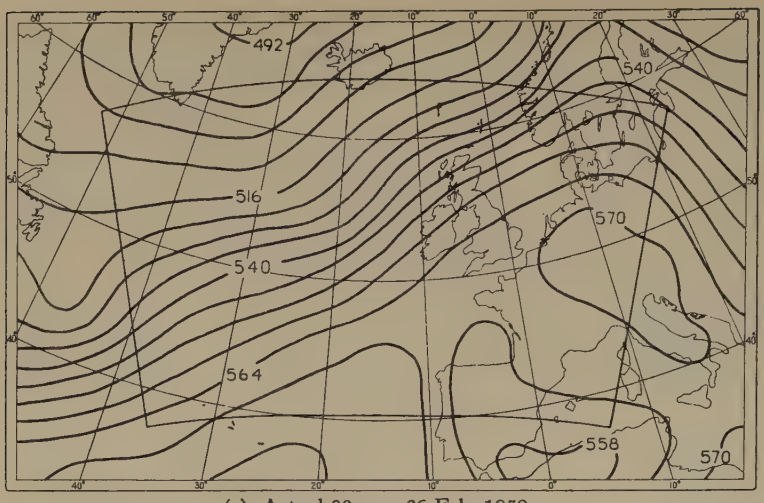

(a) Actual 00 GMT 26 Feb. 1959.

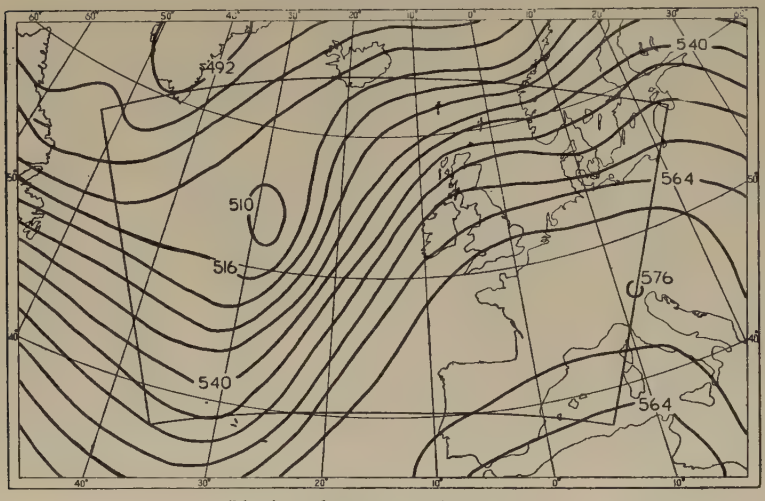

(b) Actual 00 GMT 27 Feb. 1959.

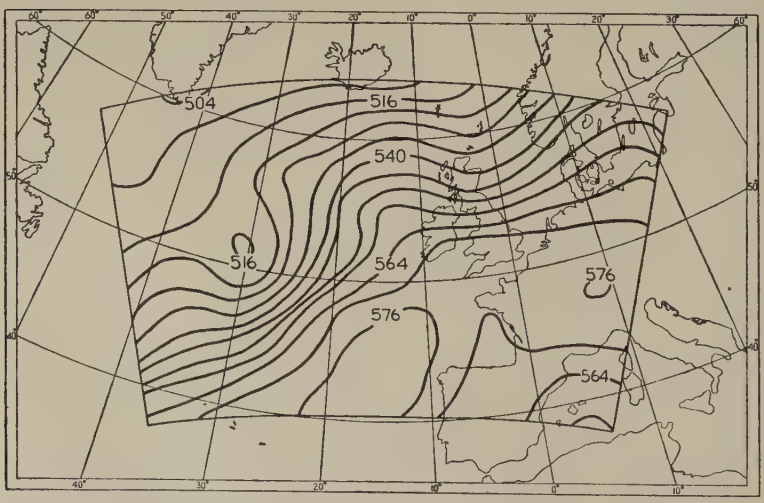

(c) Computed 00 GMT 27 Feb. 1959.

Figure 2. 500 mb contours (dm).

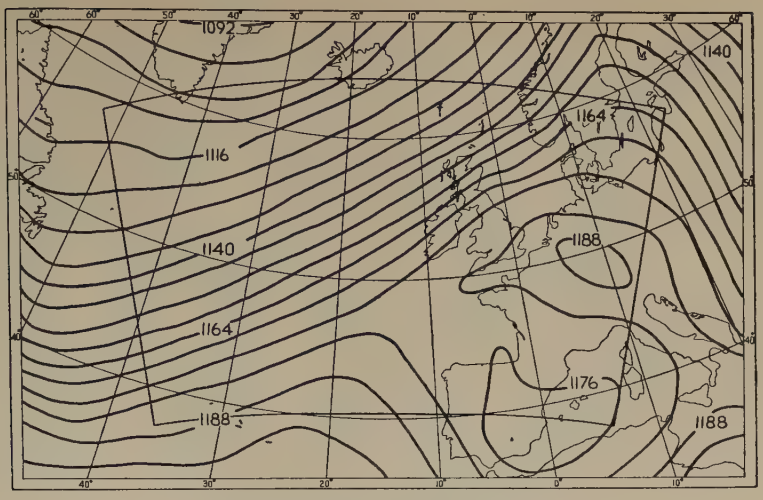

(a) Actual 00 GMT 26 Feb. 1959.

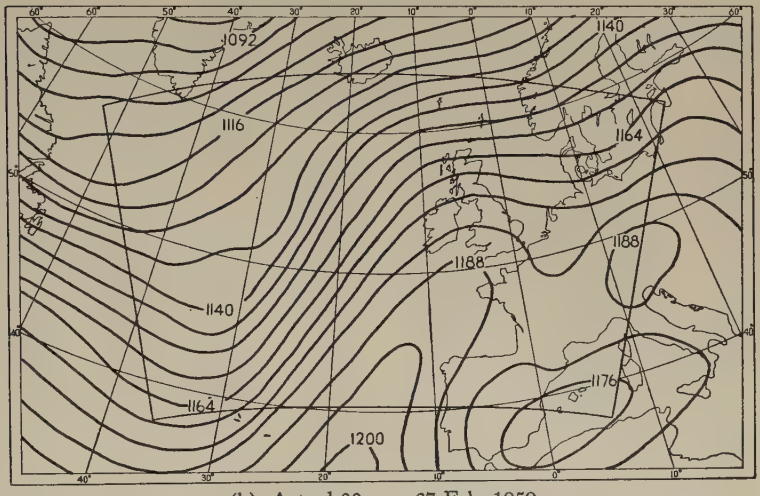

(b) Actual 00 GMT 27 Feb. 1959.

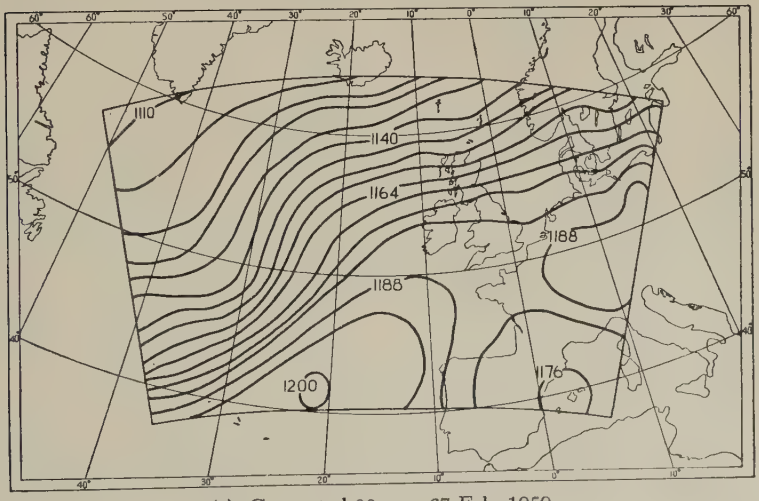

(c) Computed 00 GMT 27 Feb. 1959.

Figure 3. 200 mb contours (dm).

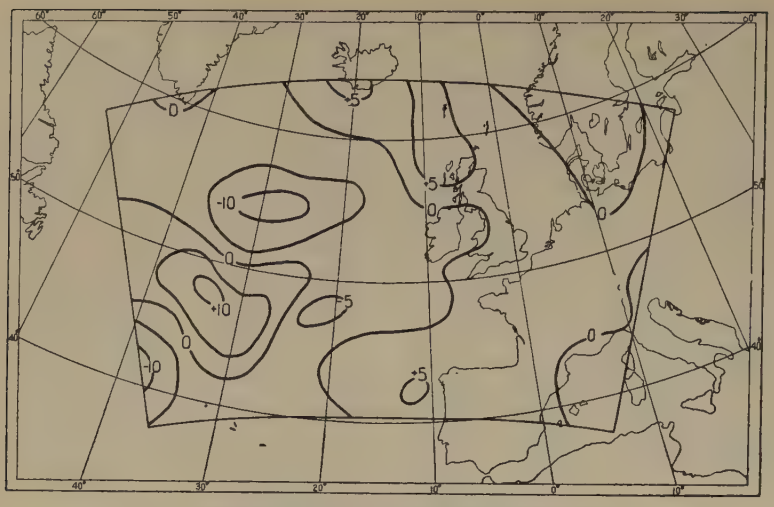

(a) Computed 00 GMT 27 Feb. 1959, 600-200 mb.

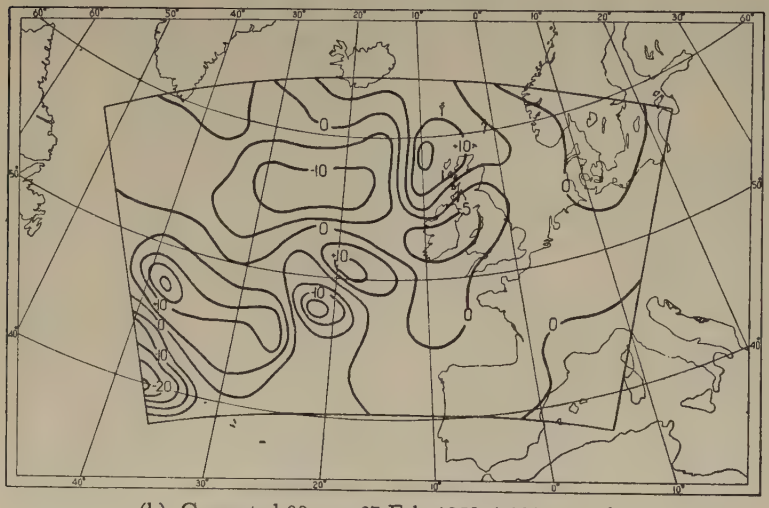

(b) Computed 00 GMT 27 Feb. 1959, 1,000-600 mb.

Figure 4. Vertical motion (mb hr^{-1}).

high-pressure ridge in mid-Atlantic also moved rapidly NE and was lying from Iceland to the northern North Sea at 00 GMT 26 February 1959. The smaller depression originally west of Ireland filled and its associated trough was orientated N-S over Eastern Norway. The numerical forecast dealt quite well with the main depression although the movement and deepening were not quite sufficient. The trough associated with the warm front and the preceding ridge were over-intensified and were not moved sufficiently north-eastwards. The weak trough over Norway was quite adequately forecast. Pressure was forecast to be about 8 mb too high in and to the west of the Bay of Biscay, the result of spurious anticyclogenesis.

An inspection of the 1,000-500 mb thickness charts indicates that the numerical forecast distorted the thermal pattern in the region of the depression much more than actually occurred, and this was one of the worse thickness forecasts of the series. This is a typical error of this model since the geostrophic wind used for advection of the thickness lines is much greater than the actual wind in regions of cyclonic curvature, and the advection is overdone.

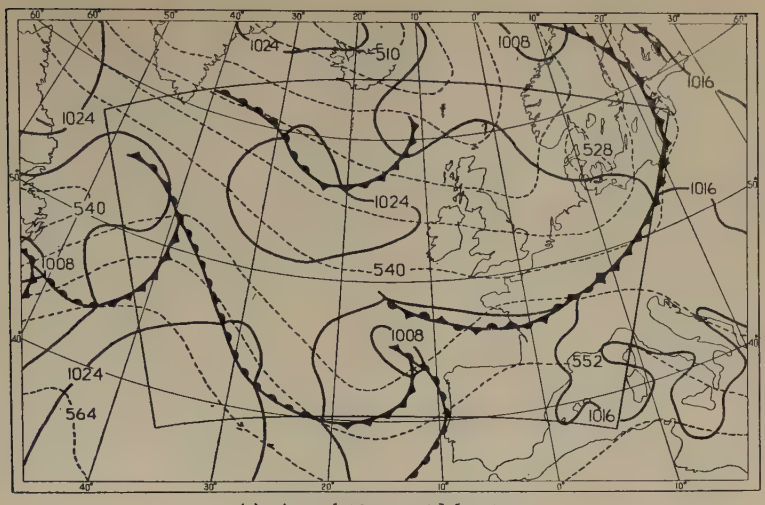

(a) Actual 00 GMT 5 May 1959.

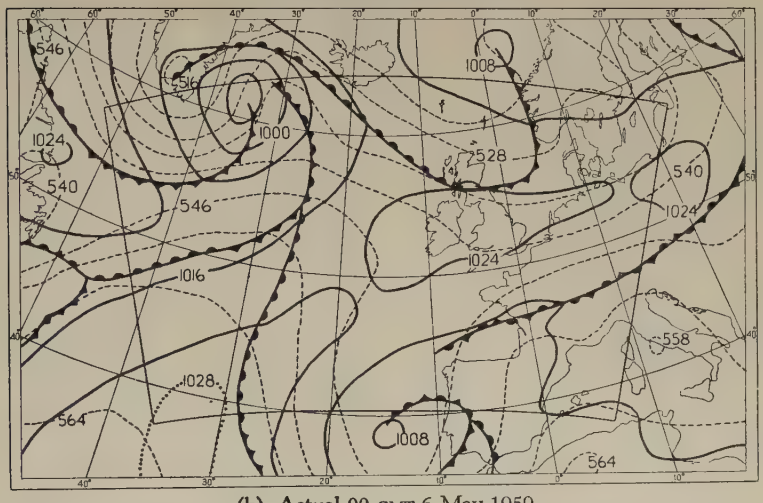

(b) Actual 00 GMT 6 May 1959.

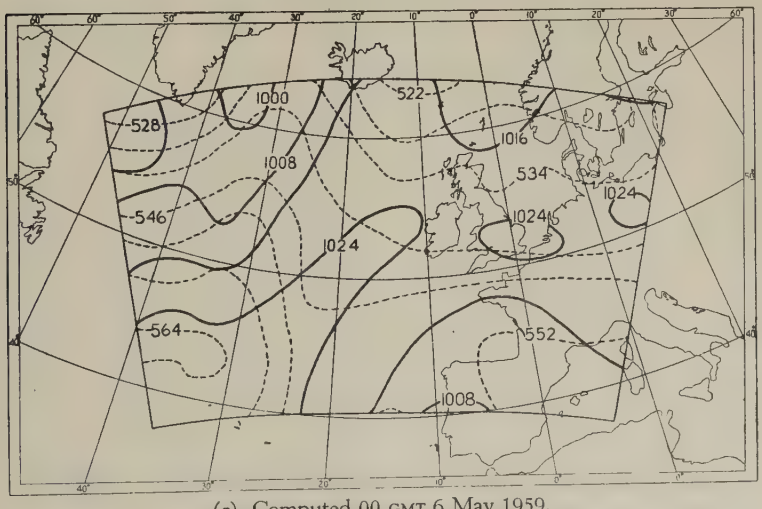

(c) Computed 00 GMT 6 May 1959.

Figure 5. ——— m.s.l. isobars (mb), – – – – – 1,000-500 mb thickness (dm).

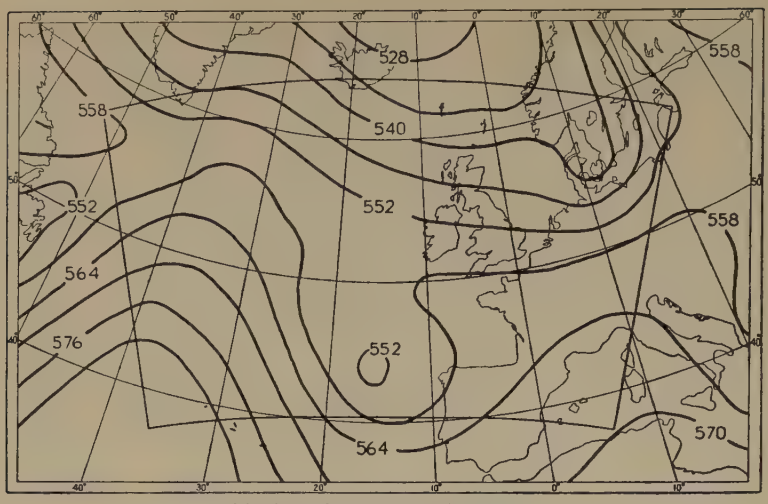

(a) Actual 00 GMT 5 May 1959.

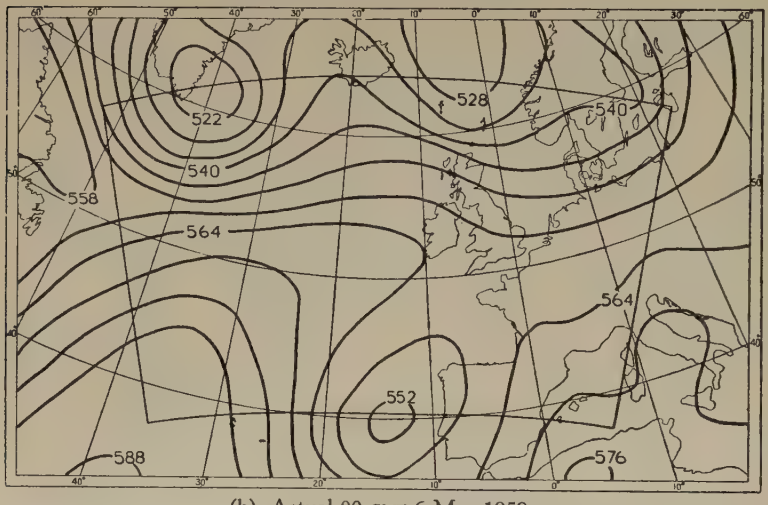

(b) Actual 00 GMT 6 May 1959.

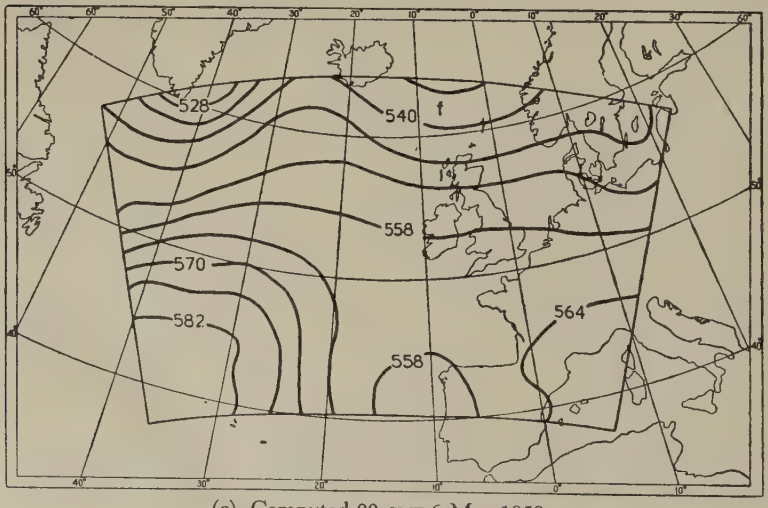

(c) Computed 00 GMT 6 May 1959.

Figure 6. 500 mb contours (dm).

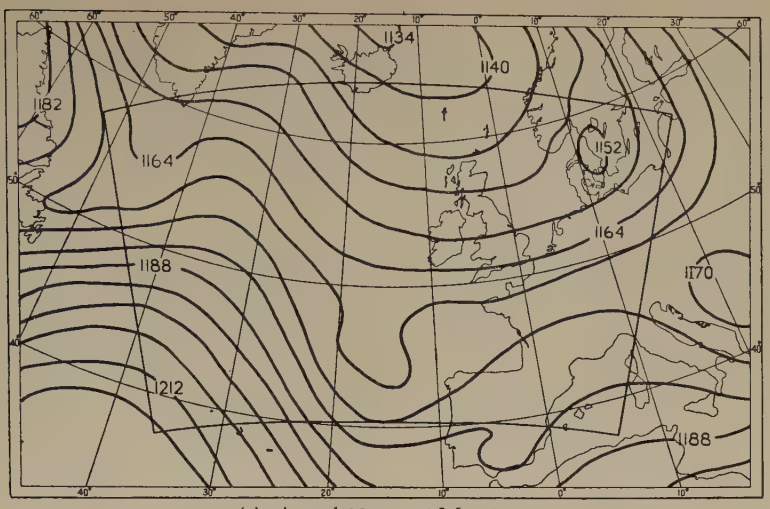

(a) Actual 00 GMT 5 May 1959.

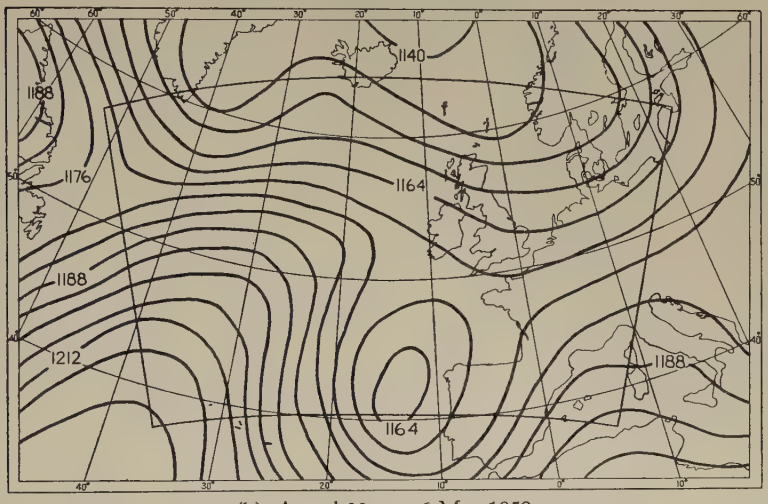

(b) Actual 00 GMT 6 May 1959.

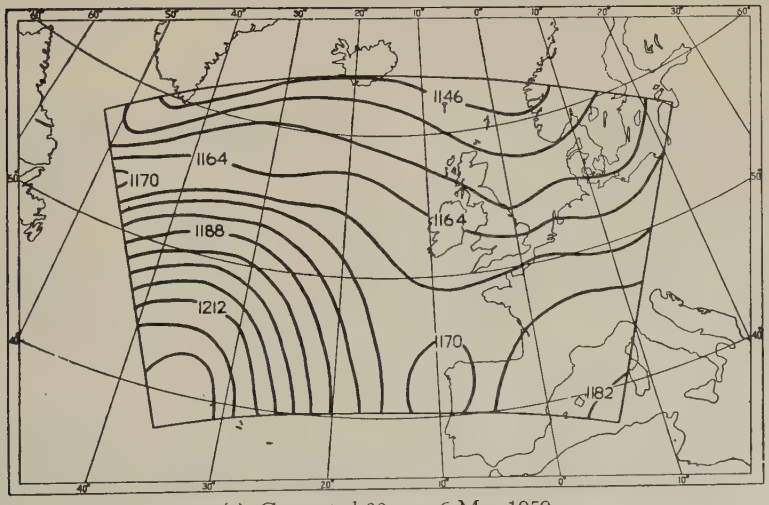

(c) Computed 00 GMT 6 May 1959.

Figure 7. 200 mb contours (dm).

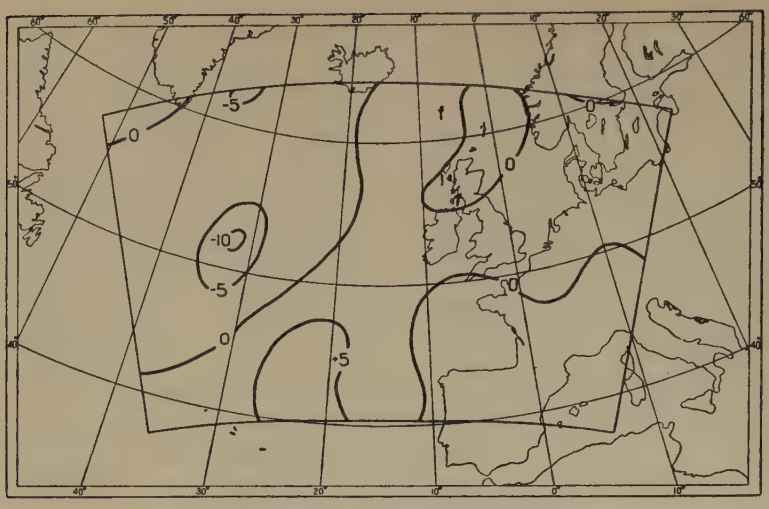

(a) Computed 00 GMT 6 May 1959, 600-200 mb.

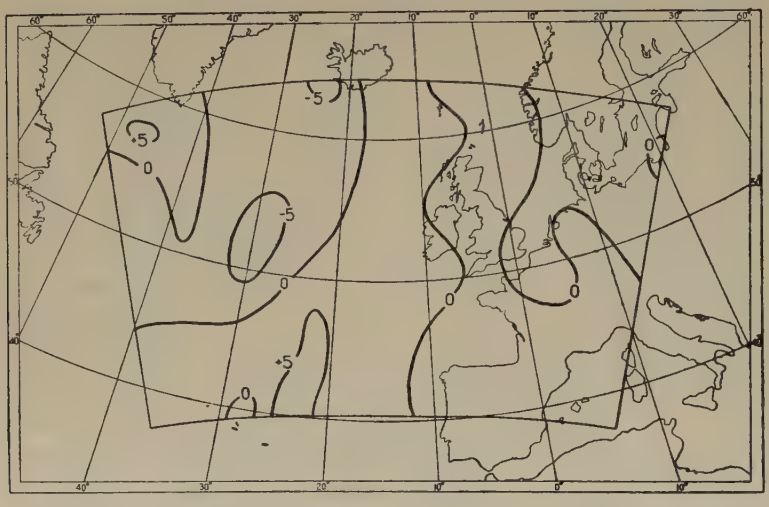

(b) Computed 00 GMT 6 May 1959, 1,000-600 mb.

Figure 8. Vertical motion (mb hr^{-1}).

Fig. 2 shows that the rapid movement of the 500 mb trough from east of Newfoundland to mid-Atlantic with the formation of a closed circulation was quite well forecast, although the trough was moved too rapidly in the south. Pressure was forecast to be too high between 10° and 20°W, a result of spurious anticyclogenesis.

Fig. 3 indicates that the 200 mb forecast gave much too high pressure in mid-Atlantic. The movement of the western Atlantic trough was quite reasonably forecast in middle latitudes but was moved too rapidly in the south. This rapid movement in the south was almost certainly associated with the strong gradients produced by the spurious anticyclogenesis.

The vertical motion charts are shown in Fig. 4 and are quite consistent with the forecast positions of the synoptic features. The pattern for the 600-200 mb layer is similar to that for the 1,000-600 mb layer, but the magnitudes of the vertical velocities measured in mb hr^{-1} are less in the 600-200 mb layer than in the bottom layer. If the vertical velocities had been computed in cm sec^{-1} the magnitudes in the two layers would have been more similar.

The numerical forecast based on the 00 GMT data for 5 May 1959 was one of the better numerical forecasts. An anticyclone moved eastwards from mid-Atlantic to the British Isles, and two shallow depressions in the vicinity of Newfoundland amalgamated and moved into the entrance to the Denmark Straits. These features were quite well forecast (see Fig. 5), although the central pressure of the depression was not quite right. The eastward movement of the Atlantic thermal ridge was forecast to be a little less than actually occurred, and a cold trough forecast about 50°N 20°W did not materialize.

Fig. 6 indicates that the movement and development of the troughs and ridges at 500 mb were forecast very well. The 200 mb forecast (Fig. 7) was also successful, especially near Portugal and in the vicinity of the British Isles. However, the forecast position of the 200 mb trough near Greenland was not correct. The vertical motion patterns in Fig. 8 are consistent with the synoptic features forecast in Figs. 5 to 7.

7. Conclusions

The forecasts based on the three-parameter model are significantly better than those based on the Sawyer-Bushby two-parameter model for the 20 situations investigated. The extra degree of freedom allowed in the new model does not give rise to such vigorous over-development as in the two-parameter model, and although spurious anticyclogenesis still occurs it is not usually so intense as previously. Knighting and Hinds (1960) showed that the incorporation of a stream function into the two-parameter model gave a significant improvement in the results, and it is quite likely that the introduction of a stream function into the present model would produce a further improvement.

The three-parameter forecasts of the 500 mb contours and the 1,000-500 mb thicknesses are statistically better than those produced by C.F.O., but there is little to choose between the corresponding forecasts for the 1,000 mb contours and the 500-200 mb thicknesses. At 200 mb the C.F.O. forecasts are slightly better than the three-parameter model, probably because no allowance is made in the numerical forecasts for the presence of a portion of the stratosphere below 200 mb. The accuracy of the 200 mb numerical forecasts seemed worse on days of a low tropopause over a significant part of the area than on days when the tropopause was nearer 200 mb.

Acknowledgments

The authors wish to thank the Director-General of the Meteorological Office for permission to publish this paper.

References

Arnason, G. and Carstenson, L. P.	1959	*Monthly Weather Review*, **87**, p. 119.
Bushby, F. H. and Hinds, M. K.	1954	*Quart. J. R. Met. Soc.*, **80**, p. 165.
	1955	*Ibid.*, **81**, p. 396.
Charney, J. G. and Phillips, N. A.	1953	*J. Met.*, **10**, p. 71.
Hartree, D. R.	1952	*Numerical analysis*, Clarendon Press, Oxford.
Hollman, G.	1956	*Met. Rund.*, **9**, p. 73.
Knighting, E. K. and Hinds, M. K.	1960	*Quart. J. R. Met. Soc.*, **86**, p. 504.
Knighting, E. K., Corby, G. A., Bushby, F. H. and Wallington, C. E.	1961	*Sci. Pap.*, No. 5, Met. Office, London.
Sawyer, J. S. and Bushby, F. H.	1953	*J. Met.*, **10**, p. 54.
Sutcliffe, R. C.	1947	*Quart. J. R. Met. Soc.* **73**, p. 370.
Sutcliffe, R. C. and Forsdyke, A. G.	1950	*Ibid.*, **76**, p. 189.

Appendix 1

1,000 mb contours

1959	Two-parameter forecast					Central Forecasting Office forecast					Three-parameter forecast				
	1	2	3	4	5	1	2	3	4	5	1	2	3	4	5
16 January	0·64	87	0·88	26	0·74	0·62	76	0·79	24	0·66	0·65	88	0·88	26	0·7
5 February	0·60	75	0·84	26	0·52	0·27	82	0·72	40	0·33	0·72	62	0·89	25	0·6
10 February	0·72	105	0·83	28	0·43	0·75	77	0·87	29	0·61	0·78	87	0·86	26	0·5
11 February	0·34	116	0·85	35	0·44	0·23	102	0·74	35	0·32	0·71	74	0·93	25	0·8
12 February	0·75	96	0·86	26	0·61	0·81	64	0·89	25	0·65	0·80	85	0·87	27	0·6
17 February	0·83	99	0·93	38	0·62	0·64	92	0·65	33	0·07	0·81	98	0·92	39	0·6
19 February	0·67	104	0·77	23	0·57	0·26	88	0·59	28	0·34	0·70	85	0·84	22	0·5
24 February	0·45	69	0·94	22	0·50	0·59	74	0·85	28	0·43	0·56	59	0·94	21	0·5
26 February	0·45	87	0·85	38	0·56	0·61	71	0·89	30	0·64	0·57	74	0·88	33	0·6
3 March	0·90	75	0·93	28	0·77	0·37	125	0·49	45	0·43	0·93	56	0·93	28	0·7
19 March	0·27	117	0·83	29	0·42	0·52	70	0·92	22	0·63	0·53	68	0·89	28	0·3
2 April	0·89	67	0·89	19	0·75	0·80	38	0·94	16	0·71	0·89	62	0·91	18	0·7
9 April	0·41	132	0·82	27	0·57	0·87	41	0·92	16	0·73	0·58	108	0·88	23	0·6
15 April	0·28	97	0·83	29	0·69	0·72	50	0·87	19	0·78	0·36	85	0·84	28	0·6
16 April	0·20	193	0·41	120	0·20	0·70	94	0·74	32	0·61	0·63	86	0·72	31	0·7
21 April	0·78	54	0·90	15	0·72	0.89	25	0·94	12	0·80	0·77	47	0·91	15	0·7
22 April	0·83	39	0·92	18	0·60	0·85	26	0·95	13	0·64	0·84	35	0·94	17	0·6
5 May	0·85	34	0·85	16	0·67	0·59	43	0·63	19	0·45	0·88	27	0·88	16	0·6
6 May	0·78	53	0·87	18	0·67	0·83	35	0·87	15	0·72	0·80	41	0·90	18	0·6
12 May	0·75	45	0·95	19	0·77	0·66	45	0·95	14	0·79	0·72	42	0·95	18	0·7

Appendix 2

1,000-500 mb thickness

1959	Two-parameter forecast					Central Forecasting Office forecast					Three-parameter forecast				
	1	2	3	4	5	1	2	3	4	5	1	2	3	4	5
16 January	0·88	40	0·93	27	0·59	0·70	59	0·85	25	0·44	0·84	46	0·91	30	0·55
5 February	0·76	63	0·69	31	0·55	0·81	70	0·68	41	0·45	0·85	47	0·83	33	0·39
10 February	0·45	85	0·87	39	0·46	0·83	63	0·88	31	0·53	0·57	74	0·90	37	0·51
11 February	0·80	78	0·88	41	0·51	0·58	91	0·77	43	0·21	0·89	55	0·92	31	0·77
12 February	0·86	61	0·95	30	0·74	0·83	51	0·95	22	0·76	0·88	60	0·95	35	0·67
17 February	0·80	67	0·86	36	0·35	0·42	100	0·71	31	0·32	0·70	80	0·78	43	0·25
19 February	0·77	60	0·95	22	0·71	0·19	84	0·76	26	0·47	0·73	63	0·94	25	0·67
24 February	0·63	70	0·88	27	0·60	0·45	85	0·89	32	0·47	0·62	68	0·88	27	0·57
26 February	0·59	82	0·84	38	0·38	0·76	70	0·91	26	0·69	0·60	81	0·84	39	0·38
3 March	0·80	66	0·91	30	0·67	0·39	132	0·82	41	0·48	0·76	63	0·91	28	0·64
19 March	0·43	66	0·87	36	0·46	0·77	45	0·91	24	0·65	0·64	48	0·91	33	0·47
2 April	0·91	46	0·93	23	0·73	0·92	44	0·93	21	0·74	0·89	51	0·92	26	0·69
9 April	0·69	48	0·88	28	0·50	0·71	38	0·90	19	0·68	0·74	40	0·90	25	0·58
15 April	0·68	54	0·86	28	0·68	0·78	44	0·94	23	0·79	0·63	58	0·82	29	0·64
16 April	0·49	163	0·57	131	0·13	0·80	64	0·79	26	0·65	0·82	85	0·84	32	0·62
21 April	0·71	46	0·83	23	0·44	0·67	43	0·88	18	0·55	0·67	48	0·82	24	0·44
22 April	0·76	41	0·90	22	0·58	0·85	30	0·93	16	0·62	0·81	36	0·92	21	0·64
5 May	0·75	37	0·95	23	0·60	0·82	33	0·97	16	0·69	0·73	36	0·95	21	0·60
6 May	0·70	47	0·92	26	0·56	0·85	51	0·96	15	0·82	0·71	45	0·93	23	0·61
12 May	0·62	39	0·80	23	0·19	0·21	45	0·72	17	0·40	0·58	41	0·78	24	0·22

1 = Correlation coefficient between actual and forecast 24-hr changes.
2 = R.m.s. height error.
3 = Correlation coefficient between actual and forecast heights.
4 = R.m.s. vector wind error.
5 = Stretch vector correlation coefficient between actual and forecast winds.

Appendix 3

500 mb contours

1959	Two-parameter forecast					Central Forecasting Office forecast					Three-parameter forecast				
	1	2	3	4	5	1	2	3	4	5	1	2	3	4	5
16 January	0·74	81	0·95	26	0·85	0·66	97	0·84	34	0·60	0·75	79	0·94	28	0·81
5 February	0·52	108	0·84	32	0·68	0·76	80	0·88	26	0·78	0·75	75	0·92	30	0·75
10 February	0·57	107	0·94	39	0·61	0·56	83	0·96	36	0·68	0·66	88	0·95	34	0·68
11 February	0·77	106	0·93	33	0·75	0·53	86	0·92	40	0·46	0·92	57	0·98	28	0·81
12 February	0·44	82	0·96	31	0·74	0·57	75	0·96	26	0·76	0·45	65	0·97	31	0·70
17 February	0·95	79	0·99	25	0·87	0·55	115	0·89	37	0·53	0·94	76	0·98	24	0·87
19 February	0·91	73	0·97	20	0·85	−0·07	127	0·76	33	0·60	0·92	54	0·98	19	0·86
24 February	0·53	101	0·96	30	0·77	0·64	91	0·95	23	0·76	0·56	90	0·96	30	0·73
26 February	0·38	112	0·91	42	0·57	0·55	99	0·93	34	0·70	0·53	100	0·93	38	0·60
3 March	0·81	76	0·95	29	0·83	0·43	99	0·89	38	0·66	0·82	64	0·96	28	0·84
19 March	0·26	150	0·83	41	0·55	0·77	72	0·94	30	0·74	0·66	84	0·91	41	0·49
2 April	0·93	59	0·95	24	0·82	0·91	58	0·97	23	0·81	0·93	52	0·96	23	0·81
9 April	0·56	144	0·91	32	0·74	0·86	54	0·95	20	0·86	0·76	109	0·95	24	0·85
15 April	0·29	112	0·91	32	0·81	0·62	78	0·93	24	0·87	0·46	95	0·91	28	0·83
16 April	0·44	172	0·81	54	0·61	0·75	123	0·80	36	0·74	0·66	135	0·81	41	0·74
21 April	0·82	57	0·93	23	0·67	0·89	48	0·91	21	0·65	0·84	51	0·93	22	0·68
22 April	0·86	57	0·94	20	0·78	0·88	38	0·96	17	0·77	0·91	47	0·97	17	0·83
5 May	0·86	43	0·96	24	0·73	0·72	58	0·94	24	0·68	0·85	39	0·96	22	0·75
6 May	0·77	75	0·94	26	0·73	0·92	44	0·98	16	0·87	0·80	63	0·95	23	0·78
12 May	0·85	45	0·96	21	0·81	0·75	123	0·80	36	0·74	0·82	45	0·96	21	0·80

Appendix 4

200-500 mb thickness

1959	Two-parameter forecast					Central Forecasting Office forecast					Three-parameter forecast				
	1	2	3	4	5	1	2	3	4	5	1	2	3	4	5
16 January	0·53	61	0·76	32	0·10	0·73	45	0·83	25	0·15	0·70	51	0·86	33	0·16
5 February	0·57	64	0·79	29	0·37	0·52	66	0·73	28	0·33	0·41	79	0·61	32	0·18
10 February	0·12	69	0·49	35	0·12	0·66	58	0·63	28	0·05	0·78	46	0·75	24	0·35
11 February	0·52	74	0·77	35	0·15	0·37	90	0·46	42	0·00	0·55	51	0·68	31	0·25
12 February	0·53	63	0·81	35	0·30	0·82	37	0·88	18	0·42	0·70	54	0·84	27	0·38
17 February	0·70	66	0·34	27	0·20	0·77	119	0·56	49	0·17	0·77	62	0·48	29	0·14
19 February	0·49	71	0·72	24	0·44	0·80	73	0·83	27	0·45	0·71	53	0·78	22	0·45
24 February	0·42	66	0·53	33	−0·08	0·66	49	0·66	24	0·13	0·75	46	0·67	29	0·15
26 February	0·18	66	0·33	33	0·14	0·20	68	0·42	29	0·07	0·24	67	0·45	34	0·10
3 March	0·73	49	0·88	28	0·30	0·89	40	0·92	20	0·57	0·84	89	0·79	39	0·41
19 March	0·40	46	0·75	24	0·39	0·55	44	0·82	22	0·24	0·36	47	0·74	28	0·19
2 April	0·19	74	0·19	36	0·02	0·72	43	0·65	25	0·31	0·64	56	0·67	30	0·34
9 April	−0·06	58	0·30	32	0·11	0·72	28	0·75	16	0·44	0·74	42	0·70	23	0·28
15 April	0·38	50	0·80	22	0·58	0·43	51	0·83	20	0·50	−0·48	84	0·38	28	0·22
16 April	0·47	74	0·84	29	0·40	0·51	63	0·72	28	0·09	0·58	59	0·84	29	0·31
21 April	0·43	51	0·56	24	0·23	0·69	44	0·72	19	0·29	0·82	36	0·80	22	0·42
22 April	0·40	42	0·79	25	0·08	0·58	37	0·83	17	0·33	0·83	44	0·92	21	0·40
5 May	0·13	61	0·69	25	0·28	−0·08	68	0·62	23	0·32	0·72	42	0·90	21	0·57
6 May	−0·13	71	0·73	33	0·13	0·50	53	0·84	23	0·35	0·79	41	0·91	24	0·54
12 May	−0·18	46	0·72	21	0·39	0·62	42	0·79	19	0·35	0·52	41	0·82	22	0·50

1 = Correlation coefficient between actual and forecast 24-hr changes.
2 = R.m.s. height error.
3 = Correlation coefficient between actual and forecast heights.
4 = R.m.s. vector wind error.
5 = Stretch vector correlation coefficient between actual and forecast winds.

Appendix 5

200 mb contours

1959	Two-parameter forecast					Central Forecasting Office forecast					Three-parameter forecast				
	1	2	3	4	5	1	2	3	4	5	1	2	3	4	5
16 January	0·70	103	0·93	42	0·71	0·78	96	0·92	37	0·61	0·76	96	0·96	33	0·81
5 February	0·67	106	0·79	44	0·60	0·76	99	0·83	36	0·70	0·68	94	0·83	33	0·68
10 February	0·43	112	0·95	49	0·62	0·26	105	0·94	40	0·66	0·47	90	0·96	37	0·69
11 February	0·78	126	0·91	54	0·65	0·86	61	0·98	28	0·80	0·87	70	0·97	30	0·78
12 February	0·56	107	0·94	55	0·65	0·72	75	0·97	27	0·83	0·77	61	0·98	34	0·77
17 February	0·91	105	0·97	34	0·81	0·86	84	0·96	34	0·76	0·89	102	0·97	31	0·82
19 February	0·92	64	0·97	29	0·83	0·88	77	0·95	23	0·90	0·93	58	0·97	23	0·89
24 February	0·59	127	0·95	41	0·71	0·61	104	0·93	35	0·66	0·57	110	0·95	38	0·73
26 February	0·50	103	0·94	52	0·56	0·55	110	0·94	39	0·69	0·53	105	0·94	42	0·59
3 March	0·81	86	0·96	48	0·76	0·40	119	0·92	46	0·66	0·65	125	0·92	48	0·73
19 March	0·34	155	0·81	47	0·49	0·83	67	0·93	29	0·74	0·59	92	0·87	41	0·51
2 April	0·86	103	0·87	46	0·61	0·90	69	0·96	24	0·82	0·92	53	0·96	28	0·77
9 April	0·59	171	0·87	47	0·59	0·83	53	0·95	21	0·83	0·56	106	0·95	30	0·77
15 April	0·28	150	0·86	42	0·79	0·60	109	0·91	28	0·87	−0·04	158	0·80	37	0·79
16 April	0·61	185	0·89	61	0·66	0·77	154	0·80	42	0·72	0·66	171	0·86	51	0·69
21 April	0·75	86	0·87	37	0·55	0·85	79	0·87	32	0·54	0·89	59	0·93	29	0·70
22 April	0·83	77	0·94	36	0·60	0·86	59	0·95	23	0·70	0·90	82	0·96	26	0·77
5 May	0·71	66	0·95	30	0·73	0·54	68	0·96	22	0·86	0·69	51	0·97	27	0·76
6 May	0·59	84	0·92	44	0·57	0·89	62	0·98	17	0·89	0·71	68	0·95	29	0·76
12 May	0·75	66	0·94	30	0·76	0·66	53	0·94	22	0·80	0·77	58	0·96	23	0·87

1 = Correlation coefficient between actual and forecast 24-hr changes.
2 = R.m.s. height error.
3 = Correlation coefficient between actual and forecast heights.
4 = R.m.s. vector wind error.
5 = Stretch vector correlation coefficient between actual and forecast winds.

551.509.314 : 551.509.325

A graphical method of objective forecasting derived by statistical techniques

By M. H. FREEMAN
Meteorological Office, Dunstable

(Manuscript received 18 January 1961)

SUMMARY

The objective forecasting technique described consists of a composite diagram from which the forecast value of the predictand can be read directly, given the values of the predictors. Each section of the diagram combines a new predictor with an estimate of the predictand obtained from the previous sections. The isopleths in the diagrams are obtained by fitting a curved surface (involving powers and cross-product terms of up to the fifth order) to the basic data by a ' least squares ' procedure. Only terms which are significant at the 5 per cent level are retained in the regression formulae so produced. At each stage the predictor to be selected is that which contributes most to the combination so far chosen.

The method was used to forecast visibility (as one of 32 code figures) at London Airport three and six hours ahead. When it was tested on two winters' independent data, correlation coefficients of 0·89 and 0·83 were obtained for the 3-hr and 6-hr forecasts, respectively. During the same period the figures for the normal subjective forecasts made at London Airport were 0·87 and 0·74.

1. INTRODUCTION

An objective method of forecasting may be described as one which calls for no judgment on the part of the forecaster. Given the same initial data any person using the method will produce the same forecast. Numerous objective techniques have been described by workers in the U.S.A., but objective forecasting has received much less attention in Great Britain. Swinbank (1949), Craddock and Pritchard (1951), and Saunders (1952) all produced methods of forecasting fog which were partly objective, but some of the predictors used had to be forecast subjectively.

Most objective techniques depend on the production of either formulae or diagrams, and both methods have been subject to various weaknesses which the system to be described attempts to overcome. Many of the earlier systems produced forecasts in terms of only a few categories, e.g., fog, fog in patches, or no fog; for aviation forecasting a forecast of visibility in yards or miles is required. Formulae may be deduced from physical principles, but more often they are devised by statistical processes to produce regression equations. These have almost always contained only linear terms whereas more complicated relations may be required. In the graphical methods the lines on the diagrams often had to be drawn subjectively and it was not easy to tell whether the best lines had been drawn or not. In many systems the choice of predictors to be used had to be made subjectively. Rigorous statistical methods were used in developing the present method, the computations being made on a Ferranti Mercury Computer at Meteorological Office, Dunstable.

The problem chosen for investigation during the development of the objective forecasting technique was the important one of forecasting visibility at London Airport. The system which was devised consists of a composite diagram such as that illustrated at Fig. 1. The pecked line on the diagram indicates its method of use. The top left-hand section is entered with the appropriate value of the first predictor and successive turns are made at the appropriate isopleths of each of the other predictors, the forecast being read from the scale on exit.

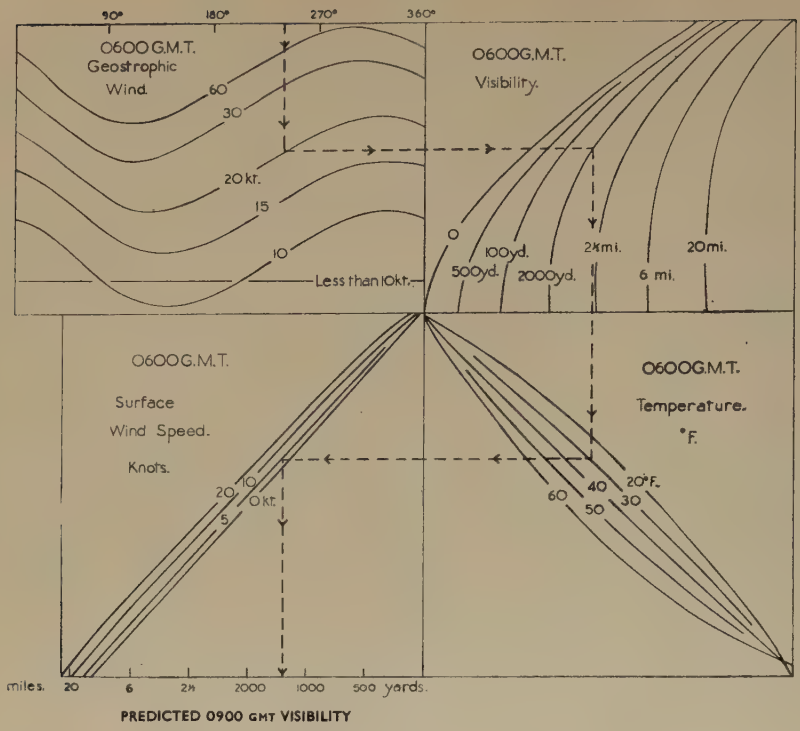

Figure 1. Winter visibility prediction diagram for 0900 GMT at London Airport.

2. Visibility prediction diagrams for London Airport

The particular problem specified was to forecast visibility at London Airport for 0900 and 1200 GMT using 0600 GMT data and for 1800 and 2100 GMT using 1500 GMT data (i.e., a 3-hr and a 6-hr forecast morning and evening). The winter period, November to January, was selected and forecasts were to be given to the nearest 100 yards up to 1,000 yd and at 200-yd intervals up to 2,000 yd. This requirement and the desirability of having an approximately logarithmic scale of visibility led to the use of the visibility code shown in Table 1.

TABLE 1. Visibility scale used in objective forecasting investigation

Visibility (yards)	Code	Visibility (yards)	Code	Visibility (miles)	Code
Less than 50	0	1,200	11	3½	22
100	1	1,400	12	4	23
200	2	1,600	13	5	24
300	3	1,800	14	6	25
400	4	2,000	15	8	26
500	5	2,500	16	10	27
600	6	3,000	17	12	28
700	7	3,500	18	16	29
800	8	4,000	19	20	30
900	9	2½ miles	20	Over 22	31
1,000	10	3 miles	21		

The selection of the parameters to be tried as predictors was one of the most important parts of the investigation. Anything which physical principles suggested might be relevant was included, and the advice of experienced forecasters at London Airport was sought. Most of the parameters tested are listed in Table 2. Many were extracted directly from the London Airport registers but some had to be specially computed. The geostrophic winds over London Airport were measured from surface charts at the Central Forecasting Office, Dunstable. The wind shear was defined as the ratio of the surface wind speed to the geostrophic wind speed. Computed pressure gradient was a complicated parameter obtained from pressures and pressure tendencies at four neighbouring stations. The lapse rates were obtained as the difference between the surface temperature at London and the temperature 50 mb (or 25 mb) above the surface at Crawley (or Larkhill for the early years). The hydrolapses were similarly defined using dewpoints instead of temperatures. Data for the eleven winters November 1946 to January 1957 (1,012 days in all), were recorded on specially printed Paramount edge-punched cards and were used in the development of the objective forecasting technique. Data for the three following winters were used to obtain an independent check on the efficacy of the system.

To assist in selecting the more promising predictors each parameter x was correlated in turn with the visibility to be forecast z. A polynomial of the form $z = a + bx + cx^2 + \ldots.$ was fitted to the data by the method of ' least squares,' successively higher order polynomials being tried until further terms gave no further reduction in the r.m.s. error (SE). The correlation coefficient r was calculated from the formula $r^2 = 1 - (SE/SD)^2$ where SD was the standard deviation of the visibility to be forecast. The predictors for 2100 GMT are shown in order in Table 2.

TABLE 2. CORRELATION OF INDIVIDUAL PARAMETERS WITH 2100 GMT VISIBILITY
(Standard deviation of 2100 visibility = 7·5)

1500 GMT Parameter	Correlation coefficient	Standard error
Surface wind speed	0·71	5·3
Geostrophic wind speed	0·69	5·4
Visibility	0·66	5·6
Computed pressure gradient	0·58	6·1
Geostrophic wind direction	0·57	6·2
Past weather	0·53	6·4
Surface wind direction	0·52	6·4
Lapse rate in lowest 50 mb	0·45	6·7
Amount of low cloud	0·44	6·7
Wind shear (ratio of surface to geostrophic wind speed)	0·44	6·8
Lapse rate in lowest 25 mb	0·43	6·8
Amount of low and medium cloud	0·41	6·8
Total amount of cloud	0·40	6·9
Temperature	0·37	7·0
Excess Kew 8 in. soil temperature over London air temperature	0·34	7·1
Relative humidity	0·33	7·1
Wet-bulb temperature	0·32	7·1
Depression of dewpoint	0·31	7·1
Depression of wet-bulb	0·28	7·2
Pressure tendency	0·24	7·3
Dewpoint	0·22	7·3
Hydrolapse in lowest 50 mb	0·20	7·4
State of ground	0·16	7·4
Change in visibility in past 3 hr	0·13	7·4
Hydrolapse in lowest 25 mb	0·09	7·5

The isopleths in the diagrams were obtained by fitting a curved surface to the data by the method of 'least squares.' A relation of the form $z = a + bx + cy + dx^2 + exy + fy^2 + \ldots$ was found, where z was the predictand and x and y two predictors. Equations involving powers of the predictors up to the fifth were evaluated. The quintic relation requires the formation of 86 sums of the type $\Sigma x^7 y^3$ (each sum comprising 1,012 terms) and the solution of 21 simultaneous equations to compute the values of the coefficients a, b, c, etc. The computer was programmed to do this arithmetic, calculate the r.m.s. error of the predicted visibility, print out a table of values from which the isopleths could be plotted and finally print out the graphs. For each of the original observations the value of the predicted visibility was computed according to the formula just found by 'least squares' and was stored in the machine. These values were then used as the x parameter for the next diagram, a new predictor being fed in for the y parameter. This process was repeated until the addition of further parameters produced no significant reduction in the standard error. With the London Airport visibility data this happened after four or five diagrams.

Even using an electronic computer it was not practicable to try all combinations of the possible predictors and some method of selection was required. The general procedure adopted was as follows. For stage 1, all combinations of two out of the first five or six predictors in Table 2 were used, and the best pair, i.e., that giving the lowest standard error, was selected. For stage 2, all the unused parameters in the first half of Table 2 were added in turn. By stage 3, all unused parameters were tried and placed in order; this order differed a good deal from that in the original table. For stages 4 and 5 it was worth trying only parameters in the top-half of the revised table.

The selection technique is one of successive approximation; it will pick out a good set of predictors but will not necessarily produce the very best set. In practice there is usually very little to choose between several of the better combinations, and the final choice may well be decided on other grounds, such as convenience in use. Even when the best predictors have been selected the method of successive approximation does not produce the theoretically best regression relations. For this the ideal would be a single formula involving all the powers (up to say the fifth) and all the cross-products of all the predictors. The evaluation of such a formula would be impracticable on a computer such as the Mercury. Even if it were worked out the formula would be very cumbersome to use, since the presence of the cross-product terms would preclude the use of diagrams or tables. In the course of the investigation, regression equations using only powers of the predictors and no cross-products, and which could therefore be used in the form of tables were evaluated, but none of the results was quite as good as the graphical successive-approximation method, indicating that for visibility forecasts the cross-product terms are important.

In forecasting visibility at London Airport it was soon found that three of the most useful predictors were wind speed, direction and visibility. If wind direction is not used as the first parameter the resulting isopleths will cross one another in a confusing way and the diagrams will be difficult to use. It was therefore decided always to use wind direction first if it qualified for inclusion at all, even although this did not produce the smallest standard error at stage 1. In general, the order in which parameters are used will affect the final answer, but in practice, it was usually found that differences were small.

Wind direction proved awkward to work with in other ways. Calm is normally coded as 00 but is not related to wind direction 010°, which is coded as 01, and when fitting a surface, calms had to be treated separately. The necessity for a smooth transition from 360° to 010° presented difficulties. Resolution of the wind into east and north components gave poorer forecasts than using wind speed and direction. A variety of wind direction codes was tried; the most satisfactory solution was to use values between 010° and 180° a second time with 360° added, thus giving a population ranging from 010° to 540°, which was fitted by least squares. The section between 090° and 440° was used to produce the operational diagrams, very little smoothing being necessary. Improved results were also obtained by modifying some of the other parameters, e.g., geostrophic

ind was coded as calm for speeds less than 10 kt, cloud amount for sky obscured was coded s — 1, and the order of the code figures for past weather was rearranged.

The parameters used in the final sets of diagrams, together with the resulting standard errors and correlation coefficients at each stage are shown in Table 3.

TABLE 3. PREDICTORS USED IN LONDON AIRPORT VISIBILITY PREDICTION DIAGRAMS

-hr Forecasts	Initial *SD* or residual *SE*	Correlation coefficient
0900 Visibility	8·2	
0600 geostrophic wind	5·2	0·77
0600 visibility	3·9	0·88
0600 temperature	3·7	0·89
0600 surface wind speed	3·7	0·89
1800 Visibility	6·8	
1500 geostrophic wind	4·3	0·77
1500 visibility	3·5	0·86
1500 amount of low cloud	3·3	0·87
1500 surface wind speed	3·3	0·88
5-hr Forecasts		
1200 Visibility	7·4	
0600 geostrophic wind	5·0	0·74
0600 visibility	4·4	0·81
0600 temperature	4·3	0·82
0600 amount of low cloud	4·2	0·83
2100 Visibility	7·5	
1500 geostrophic wind	4·9	0·76
1500 visibility	4·6	0·79
1500 amount of low cloud	4·4	0·81
1500 lapse rate in lowest 50 mb	4·3	0·82
1500 ratio surface/geostrophic wind speed	4·2	0·82

With the use of a quintic relation involving 21 terms there is a real danger of overfitting; the formula may represent the particular sample of data rather than the general population. A significance test was therefore written into the programme. The standard deviation, σ, of each regression coefficient, a_i, was computed, and the ratio a_i/σ was compared with Student's t, which for the 5 per cent level of significance and about 1,000 degrees of freedom was taken as 2. The coefficient a_i was considered to be significantly different from zero if the ratio a_i/σ was greater than 2. The standard deviation σ was calculated as follows: the terms which form the left-hand sides of the simultaneous equations which have to be solved to determine the regression coefficients a_i form a square matrix **A**. Let $|A|$ represent the determinant of **A** and $|Ai|$ the minor of $|A|$ obtained by deleting the ith row and column. Then

$$\sigma^2 = s^2 |Ai|/|A| (n - k - 1)$$

where s is the standard error of the observed residuals, n the number of observations and k the number of terms in the regression formula (see, for example, Kendall 1948, p. 154).

The selection of the terms to be used in the regression equation was completed automatically in the machine. A regression formula using all 21 terms of the quintic was first computed; then the term which was least significant (i.e., had the smallest ratio a_i/σ) was removed and the formula recomputed using 20 terms. This process was repeated until all remaining terms were significant. For the first diagrams using wind direction it was found that about 12 terms, including some of the fifth order, were retained. At subsequent stages three to five terms only were required, often with none higher than the third order.

3. Comparison of the objective technique with subjective methods

The graphical objective forecasting technique was tested on independent data for three winters, 1957-1960. It was possible to compare the results with normal subjective forecasts during the two last winters. In 1958-9 the forecasters at London Airport co-operated in the investigation by making subjective forecasts of visibility exactly corresponding to the objective forecasts. This winter provided a stringent test of any visibility forecasting procedure; the frequency of poor visibilities was greater than average, but there were no long periods of persistent fog; variations in visibility were frequent and often large. It was more difficult to obtain a reliable comparison of the subjective and objective methods during the winter 1959-60. During this period subjective forecasts were made and recorded in TAF code $1\frac{1}{2}$ hr before the objective forecast was made and were amended if necessary one and two hours later. For the purpose of the test the forecasts as amended $\frac{1}{2}$ hr after the time of the objective forecast was taken to be the London subjective forecast. When the TAF indicated temporary changes during the forecast period these were ignored, it being assumed that the most likely value of the visibility was that mentioned first. Standard errors of the two forecasts, together with those for persistence forecasts, and correlation coefficients between observed and forecast visibilities are shown in Table 4.

TABLE 4. Standard errors and correlation coefficients (test during two winters, 1958-60)

Period		3 hours			6 hours		
Time (GMT)		0900	1800	0900 and 1800	1200	2100	1200 and 2100
Standard deviation of visibility		8·4	7·5	8·0	8·0	8·6	8·3
Forecast							
Graphical objective	*SE*	3·7	3·7	3·7	4·6	4·8	4·7
	r	0·90	0·87	0·89	0·82	0·83	0·83
London subjective	*SE*	3·5	4·2	3·9	5·1	6·0	5·6
	r	0·91	0·83	0·87	0·77	0·71	0·74
Persistence	*SE*	5·2	4·9	5·0	6·4	7·1	6·8
	r	0·79	0·76	0·78	0·59	0·56	0·58

(*SE* = standard error. r = correlation coefficient)

The inclusion of the results for 1957-8 gives correlation coefficients for the objective forecast which are almost identical to those in Table 4. The correlations obtained when testing on independent data are almost the same as those found from the 11 years basic data. The system therefore appears to have extracted from this sample a significant element that is typical of the general population.

London Airport's subjective forecast for 0900 GMT was better than the objective forecast and was very good (only 17 per cent of the variance was not accounted for). For the other hours, and particularly 2100 GMT the objective forecasts were the better. Both were much better than persistence. The objective method accounted for all but 22 per cent of the variance on the 3-hr forecasts, and all but 32 per cent for the 6-hr forecasts. For the subjective forecasts the figures were 24 per cent and 45 per cent respectively.

The use of correlation coefficients and standard errors in assessing the success of forecast systems is open to criticism on the ground that large errors are very heavily penalised. A pilot using the forecast will want to know whether the visibility will be above or below certain operational limits and he may judge the forecast on the proportion of

mes the forecast correctly determines this. Table 5 shows the number of times various ethods rightly and wrongly forecast the visibility to be above or below certain operational mits.

TABLE 5. NUMBER OF OCCASIONS IN TWO WINTERS, 1958-60, WHEN VARIOUS FORECASTS RIGHTLY AND WRONGLY FORECAST THE VISIBILITY TO BE ABOVE OR BELOW CERTAIN LIMITS

(A = visibility above the limit; B = visibility below the limit)

Visibility limit (yards)		1320		880		660		550		440		330		220	
-hr Forecasts		Observed visibility													
0900 GMT		A	B	A	B	A	B	A	B	A	B	A	B	A	B
Graphical objective forecast	A	139	5	149	4	155	6	157	6	159	5	160	6	165	6
	B	12	28	9	22	5	18	4	17	4	16	5	13	6	7
London subjective forecast	A	145	2	153	3	154	3	159	2	160	2	161	4	164	3
	B	6	31	5	23	6	21	2	21	3	19	4	15	7	10
Persistence forecast	A	142	9	151	7	155	7	157	6	158	6	159	5	162	3
	B	9	24	7	19	5	17	4	17	5	15	6	14	9	10
1800 GMT															
Graphical objective forecast	A	139	13	157	7	165	7	167	6	170	5	171	5	174	5
	B	9	23	5	15	1	11	1	10	0	9	0	8	0	5
London subjective forecast	A	133	7	150	5	159	4	161	4	164	3	167	4	173	1
	B	15	29	12	17	7	14	7	12	6	11	4	9	1	9
Persistence forecast	A	144	18	158	8	164	6	167	4	168	4	170	5	173	3
	B	4	18	4	14	2	12	1	12	2	10	1	8	1	7
-hr Forecasts															
1200 GMT															
Graphical objective forecast	A	148	11	158	6	162	7	163	9	166	9	169	9	172	10
	B	6	19	5	15	4	11	5	7	5	4	2	4	1	1
London subjective forecast	A	149	15	160	13	164	11	165	11	168	11	168	11	171	11
	B	5	15	3	8	2	7	3	5	3	2	3	2	2	0
Persistence forecast	A	143	8	152	6	155	7	157	6	158	6	158	6	159	6
	B	11	22	11	15	11	11	11	10	13	7	13	7	14	5
2100 GMT															
Graphical objective forecast	A	131	16	148	16	155	18	157	16	163	11	165	10	169	13
	B	7	30	1	19	2	9	2	9	1	9	1	8	0	2
London subjective forecast	A	120	15	137	16	142	14	146	13	155	9	158	9	163	7
	B	18	31	12	19	15	13	13	12	9	11	8	9	6	8
Persistence forecast	A	131	31	144	22	151	19	154	17	160	12	163	12	167	9
	B	7	15	5	13	6	8	5	8	4	8	3	6	2	6

The method of analysis used for Table 5 confirms the superiority of London Airport subjective forecasts for 0900 GMT. At 1200 and 1800 GMT the graphical method was better than the subjective and at 2100 GMT it was much better. In fact, the afternoon subjective forecasts were not so good as persistence. The 6-hr objective forecasts were much better than persistence but the 3-hr forecasts only slightly improved on it. The forecasting of visibilities less than 220 yd is still a weakness of the objective systems. On the 3-hr forecasts London successfully forecast 19 out of 23 occassions when visibility was less than 220 yd, persistence was right 17 times and the graphical method 12. The standard was generally lower in the 6-hr forecasts; out of 26 occasions of visibility less than 220 yd the correct forecasts were : London 8, persistence 11, objective 3. A striking feature of

the objective forecasts was the small number of afternoon occasions when, if the objectiv method gave a forecast of anything less than 660 yd, the visibility was better than the fore cast. If the objective forecast is poor visibility, then it is very likely to be so.

4. Further applications of the technique

During the development of the graphical objective forecasting technique severa variations in its use were tried. One was to use as a predictor a subjectively forecas parameter. This destroyed the complete objectivity of the system but it produced som improvement in the forecast. The use of two subjectively forecast parameters, wind spee and cloud amount, gave no better results than wind speed only, the forecasting inaccuracie offsetting any possible gain from the extra predictor. An extra diagram, using a subjectivel forecast surface wind speed for the end of the forecast period, was added to each set fo optional use. On the two winters' test data the correlation coefficient between observe and forecast visibility was improved from 0·83 to 0·85 for the 6-hr forecasts, but wa unchanged for the 3-hr forecasts.

Another variation attempted to improve the accuracy for low visibilities by giving greater weight to these occasions. New sets of diagrams were produced using data weighte so that occasions of visibility of less than 2,000 yd were counted more than once. These diagrams were used at London Airport during the winter 1959-60. They certainly suc ceeded in correctly forecasting fog more often, yet the number of occasions when fo was forecast but did not occur was increased even more. This was considered undesirabl and the weighted scheme was discontinued.

A source of some of the larger errors was the passage of a front during the forecast period. A test was carried out with independent data from which occasions of frontal passages had been excluded. A small improvement in the correlation coefficients resulte but many good forecasts were excluded along with a few bad ones. Out of 1,104 forecast 82 errors of five points or less on the visibility scale of Table 1 and 16 errors of six point or more were removed. The chance expectation was 84 and 14 respectively. To achieve this small improvement the objective forecast had to be foregone on 9 per cent of occasions, which did not seem worth while.

Objective forecasting diagrams for a 12-hr forecast of the 1800 GMT visibility using 0600 GMT data were produced. On an independent 3-yr test a correlation coefficient of 0·73 was obtained. This was much better than persistence but it was not possible to compare it with a subjective forecast.

5. Conclusions

The graphical objective technique described provides a simple and quick method of obtaining a forecast, and is one which can be used by inexperienced forecasters. On balance it proved to be slightly superior to normal subjective methods when applied to 3-hr and 6-hr forecasts of visibility at London Airport.

The method can be applied to a wide range of problems and appears particularly suitable for short-range forecasts of elements required by aviators. It is being used to provide an objective method of forecasting the development of Atlantic depressions and could be applied to the forecasting of other large-scale processes.

Acknowledgment

This paper is published by permission of the Director-General of the Meteorological Office.

References

Craddock, J. M. and Pritchard, D. 1951 *Air Ministry Met. Res. Cttee., M.R.P.* No. 624.
Kendall, M. G. 1948 *Advanced theory of statistics*, Charles Griffin, London, Vol 2, p. 154.
Saunders, W. E. 1952 *Quart. J. R. Met. Soc.*, **78**, p. 603.
Swinbank, W. C. 1949 *Prof. Notes, Met. Off.*, London **6**, No. 100.

551.508.99 : 551.551.8

Measurements of evaporation and heat transfer in the lower atmosphere by an automatic eddy-correlation technique

By A. J. DYER

*C.S.I.R.O., Division of Meteorological Physics, Aspendale, Victoria, Australia**

(Manuscript received 18 October 1960)

SUMMARY

Following the development of an automatic instrument for the determination of evaporation and sensible-heat transfer by the eddy-correlation technique, a large number of measurements of these eddy fluxes have been made over level pasture-land. The observations, taken at a height of 4 m, are in excellent agreement with the energy balance. Individual measurements, of 5-min duration, are distributed about a strict energy balance with a standard deviation of 31 per cent, due mainly to horizontal gradients of wind, temperature, and humidity below 4 m height. Over a period of several hours these gradients average out to negligible values.

The short response time of the sensing equipment ($\simeq$ 0·3 sec) ensures that, for conditions of moderate and high instability, significant deficiencies in eddy-flux measurements occur only with winds exceeding 10 m sec^{-1}.

A quantity ϵ, the 'evaporation fraction,' i.e., the ratio of evaporation to evaporation plus sensible-heat transfer, is found to increase markedly after rain, and to gradually decrease during the succeeding dry period. This increase can be quantitatively related to the amount of rain. The average value of ϵ during February-March 1960 was 0·56, whilst a value of 0·54 can be computed from annual totals of precipitation and net day-time radiation income.

1. INTRODUCTION

The need for a method to measure the vertical transfer of water vapour and heat in the lowest layers of the atmosphere has long been recognized. A number of workers have attempted to relate the magnitudes of these fluxes to other meteorological parameters using varying degrees of empiricism, and have often employed formulae of doubtful validity.

In the case of water-vapour transfer, or evaporation, the lysimeter technique has provided useful results. This, however, is a somewhat cumbersome method, and is not readily made portable. The value of the aerodynamic method was established by Pasquill (1949), and more recent work has substantiated this in conditions of near neutrality (House, Rider and Tugwell 1960).

The eddy-correlation technique for measuring turbulent transfer, a method first applied by Swinbank (1951), merits extensive exploitation as it relies only on basic physical principles. This has not previously been practicable chiefly because of the laborious nature of the measurements, but this difficulty has now been overcome by the development of an automatic instrument, specially designed to employ this method.

A large number of measurements of evaporation and heat transfer were made at Edithvale, Victoria during 1959-1960. Profile measurements were made simultaneously with the above, and an analysis of these results will be published separately.

2. PRINCIPLE AND INSTRUMENTATION

It can readily be shown (e.g., Swinbank 1951; Priestley 1959), that the average vertical transfer of water vapour E (expressed in latent heat units) and sensible heat H, across unit area of a horizontal plane can be written in the form,

$$E = L\,\overline{(\rho w)'\,q'}, \qquad (1)$$

and

$$H = C_p\,\overline{(\rho w)'\,T'}, \qquad (2)$$

* Present affiliation, Dept. Agric. Engineering, University of California, U.S.A.

where L is the latent heat of vaporization of water, and C_p the specific heat of air at constant pressure; $(\rho w)'$, q' and T' represent the departure of the quantities ρw, q and T from their respective mean values; ρ is the air density, w the vertical wind component, q the specific humidity and T the air temperature. The bar denotes an average over the period of observation. In the derivation of Eqs. (1) and (2) it is assumed that $\overline{\rho w}$ is zero. This is true for a horizontally uniform surface if the period of observation is sufficiently long.

Swinbank (1955) has made use of this technique by recording the fluctuations of ρw, q and T, and subsequently obtaining the fluxes with the aid of a mechanical computer (Taylor and Webb 1955). This work established the practicability of the method, and has provided a most informative body of data. At that stage of instrumental development there remained, however, two main short-comings. Firstly, the limited speed of response of the recording equipment caused the fluxes to be underestimated; and secondly, the analysis and computation of the data was extremely laborious.

To eliminate these difficulties and to provide an instrument suitable for the measurement of evaporation by workers in allied fields, special equipment has been developed to give continuous electrical signals proportional to the relevant quantities, and to multiply and integrate automatically.

A general description of the complete instrument has previously been published (Taylor and Dyer 1958) and detailed information has been given for the anemometer by Taylor (1956), for the integrators by Dyer (1958), for the fine-wire resistance thermometers by McIlroy (1955) and for the electronic analogue of the saturated vapour-pressure curve by Taylor (1958). Pl. X, Fig. 1 (a), (b) and (c) shows the sensing heads and console.

In addition to the above, but not relevant to the present enquiry, the instrument also contained an anemometer (Dyer 1960) to measure the horizontal wind component u, so permitting measurements of momentum flux.

It is not possible to know the mean values of ρw, q and T in advance, so that signals proportional to $\rho w'$, q' and T' cannot be obtained. The use of adjustable working means, α, β and γ obviates this difficulty and the fluxes can then be calculated from the exact relationships,

$$E = L\,\overline{(\rho w)'\,q'} = L\,[\overline{(\rho w - \alpha)\,(q - \beta)} - \overline{(\rho w - \alpha)} \cdot \overline{(q - \beta)}]\,. \quad . \quad (3)$$

$$H = C_p \overline{(\rho w)'\,T'} = C_p [\overline{(\rho w - \alpha)\,(T - \gamma)} - \overline{(\rho w - \alpha)} \cdot \overline{(T - \gamma)}]\,. \quad . \quad (4)$$

Hence to determine E, or H, one analogue multiplier and three integrators are required.

The naturally occurring $\overline{\rho w}$ is very close to zero and thus no provision for α is necessary in practice.

The specific humidity term $q - \beta$, is obtained by mixing signals from two bridges containing fine-wire wet- and dry-bulb resistance thermometers. Adjustment of the working means β and γ is provided by the balancing control of the dry-bulb bridge. The above mixing is carried out according to a modified form of the psychrometric equation:

$$q - \beta = q_s\,(T_w) - \frac{C_p}{L}\,(T - T_w) - q_s\,(\delta) + \frac{C_p}{L}\,(\gamma - \delta) \quad . \quad . \quad (5)$$

where δ is a fixed working mean of the wet-bulb bridge and $q_s\,(T_w)$ and $q_s\,(\delta)$ represent the saturation specific humidities at temperatures T_w and δ respectively. A slight modification of the electronic analogue described by Taylor (1958) permits the simulation of the non-linear term $q_s\,(T_w) - q_s\,(\delta) + C_p/L\,(T_w - \delta)$. In the normal mode of operation, that of determining E, the output of the instrument is

$$E = L\,\overline{(\rho w)'\,q'}$$

$$= L\,\overline{(\rho w)'\left[q_s'\,(T_w) + \frac{C_p}{L}\,T_w'\right]} - C_p\,\overline{(\rho w)'\,T'} \quad . \quad . \quad (6)$$

The second term on the right-hand side of Eq. (6) is $-H$, hence the first term is $E + H$.

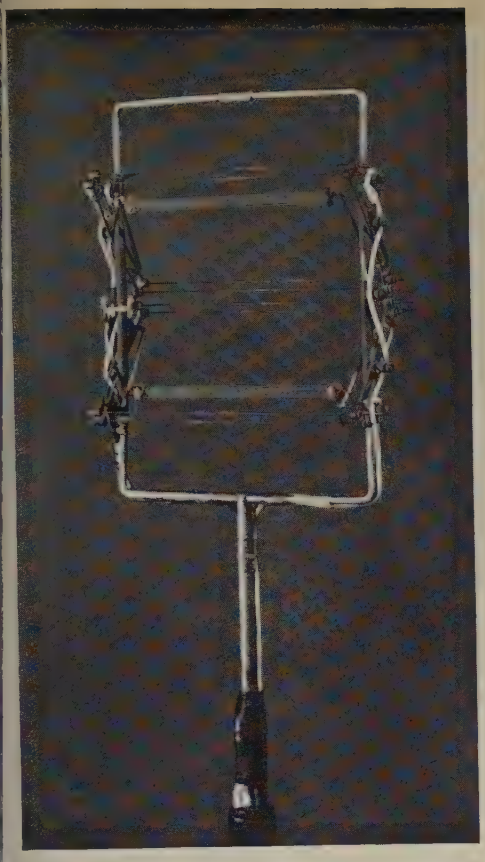

(a) Anemometer.

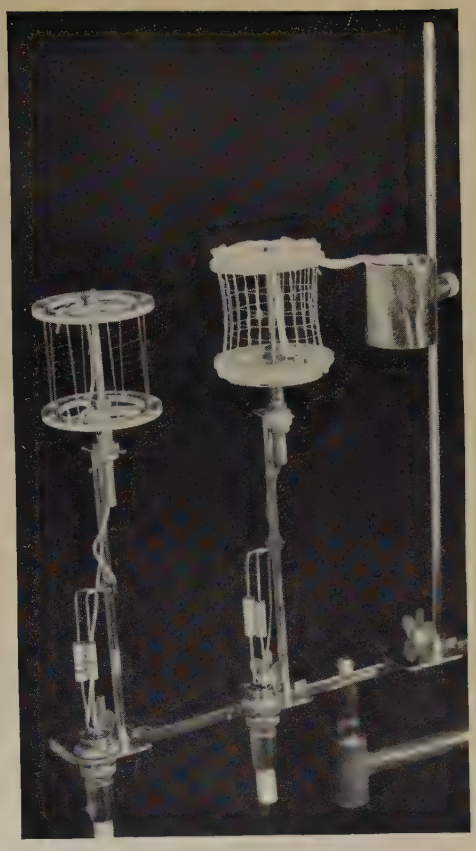

(b) Wet- and dry-bulb hygrometer.

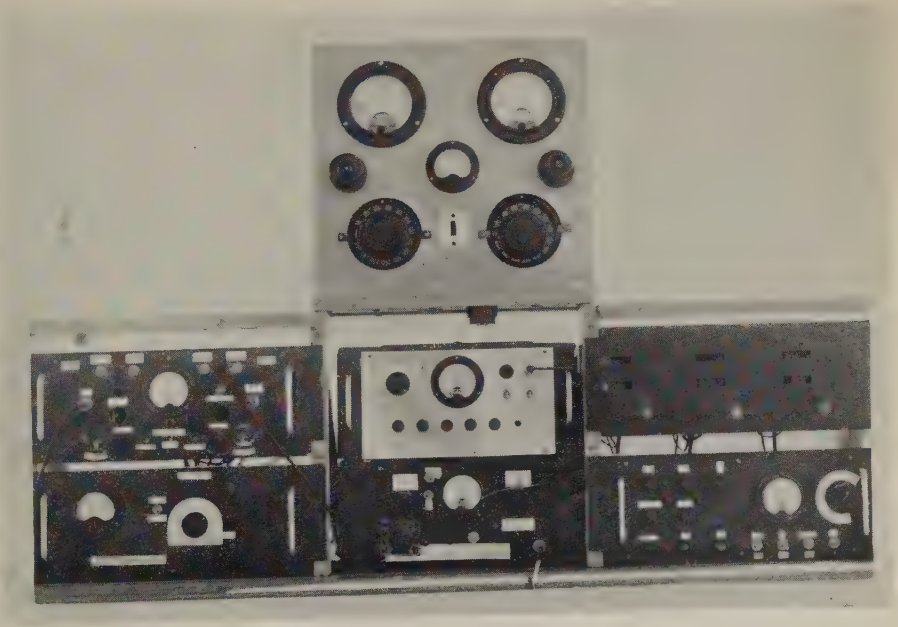

(c) Electric console.

Figure 1. Sensing elements and associated equipment.

To face page 402

The expression $q_s'(T_w) + C_p T_w'/L$ can be readily shown to represent fluctuations of quivalent temperature, and so the quantity $E + H$ may be conveniently referred to as *quivalent heat.*

By replacing the T element with a fixed resistor (i.e., making $T' = 0$), $E + H$ is etermined directly; and similarly, by suppressing the T_w circuit and so removing the rst term, the output of the instrument is made equal to $-H$.

With the present equipment only one of E, H, $E + H$, can be determined in a single neasurement, but the addition of a second multiplier and two integrators would permit he simultaneous measurement of two of them.

3. Verification of instrument performance

The basic test of the method is that over a reasonably uniform site it should satisfy he equation for energy balance at the ground surface,

$$E + H = R - G \quad . \quad . \quad . \quad . \quad (7)$$

where R is the net radiation income and G the heat flux into the ground. In the use of Eq. (9) all quantities will be expressed in mw cm^{-2}.

A large number of tests, each of 5-min duration, were carried out during 1959-1960 t the C.S.I.R.O. field station at Edithvale, Victoria, Australia. Previous experience ndicates that at the measuring heights used in this experiment a 5-min period is adequate (Swinbank 1955; Deacon 1955) and this was subsequently confirmed during the present programme. At the Edithvale site, level pasture-land bearing coarse grass in patchy clumps with occasional stalks up to 70 cm height extends in all directions for at least one mile.

R was measured with a ventilated net radiometer, which was periodically checked against standard silver-disc and Ångström pyrheliometers. Only trivial changes in calibration were found to occur. The output of the net radiometer was continuously recorded and a mean value obtained for each 5-min run.

G was determined by means of laboratory-calibrated flux-plates similar to those described by Deacon (1950). The outputs of seven such flux-plates installed 1 cm below the ground surface were combined to obtain a representative average which was also recorded.

No special attempt was made to allow for the change of heat storage in the shallow layer of soil above the flux plates. The tests were carried out more or less continuously over a period of several hours on each occasion, and the average rate-of-change of heat storage over such a period is easily shown to be negligible.

In the initial testing period the equivalent heat, $E + H$, was determined directly by the eddy correlation instrument, and compared with $R - G$. The ratio, $(E + H)/(R - G)$, called here the ' recovery factor,' and expressed as a percentage, is the fraction of the available energy which is ' recovered '; and so provides a measure of instrument performance. A perfect heat balance would obviously correspond to a recovery factor of 100 per cent.

For the later tests, E and H were measured alternately and then suitably combined to calculate the recovery factor. Except for periods of maintenance, a series of 5-min runs extending over several hours was made on each occasion, with an off-time between runs of either one or two minutes.

The measuring height was initially 1·5 m, and this was later increased to 3·5-4 m when it became evident that the fluxes were being underestimated because of the higher frequencies present in the eddy structure at the lower level. The main body of the results was obtained at either 3·5 m or 4 m, and results from lower levels are used only in connexion with response time considerations.

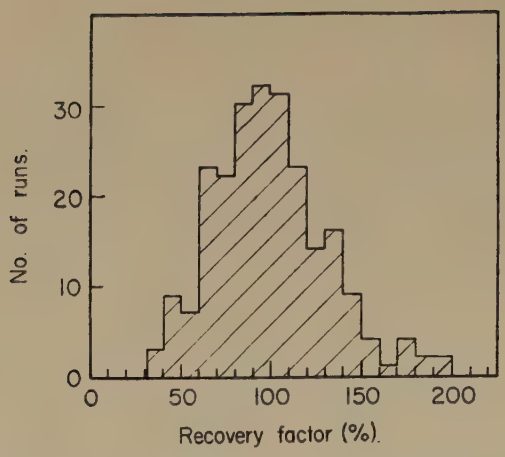

Figure 2. Distribution of recovery factor per cent for equivalent heat ($E + H$) measurements.

(a) $E + H$ *measured directly*

During April and October 1959, 311 runs of 5-min each were made at a measuring height of 3·5-4 m in which $E + H$, R and G were determined. The recovery factor for each run was calculated. Individual values of $R - G$ ranged from 10 mw cm^{-2} to 60 mw cm^{-2}.

The overall distribution of the recovery factor is shown in Fig. 2. The mean value is 99 $\pm$ 2 per cent, in excellent agreement with the energy balance. The standard deviation of the distribution is 31 $\pm$ 1 per cent.

A more detailed presentation of the data appears in Table 1. The variation of the mean daily recovery factor is in accord with the distribution of Fig. 2. A similar degree of scatter appears in the detailed daily records, a number of which are plotted in Fig. 3.

TABLE 1. MEAN DAILY RECOVERY FACTOR AT A NUMBER OF MEASURING HEIGHTS AND WIND SPEEDS ($E + H$ MEASURED DIRECTLY)

Date (1959)	Height (metres)	$\overline{R - G}$ (mw/cm^2)	No. of runs	Mean recovery factor (per cent)	$\bar{u}$ (m sec^{-1})
3 April	1·5	20·6	10	77 ± 10	–
23 April	1·5	27·0	17	86 ± 7	2·6
28 April	1·5	21·7	18	83 ± 7	2·3
24 April	2·5	28·0	19	86 ± 7	2·8
7 April	3·5	26·5	35	104 ± 5	5·0
8 April	3·5	21·6	9	94 ± 6	2·5
9 April	3·5	29·2	24	97 ± 6	4·5
10 April	3·5	21·4	17	102 ± 7	5·3
17 April	3·5	21·2	28	100 ± 6	3·5
20 April	3·5	21·0	9	92 ± 10	5·0
21 April	3·5	17·0	14	97 ± 7	4·0
5 October	4·0	21·8	11	95 ± 8	–
14 October	4·0	30·0	20	95 ± 6	4·7
15 October	4·0	34·8	19	108 ± 6	4·0
16 October	4·0	21·8	24	107 ± 6	4·2
19 October	4·0	36·0	12	87 ± 8	–
21 October	4·0	34·2	17	109 ± 7	7·6
22 October	4·0	16·9	25	102 ± 6	5·3
23 October	4·0	38·1	6	95 ± 12	–
27 October	4·0	15·3	14	93 ± 7	–
28 October	4·0	32·4	27	95 ± 5	–

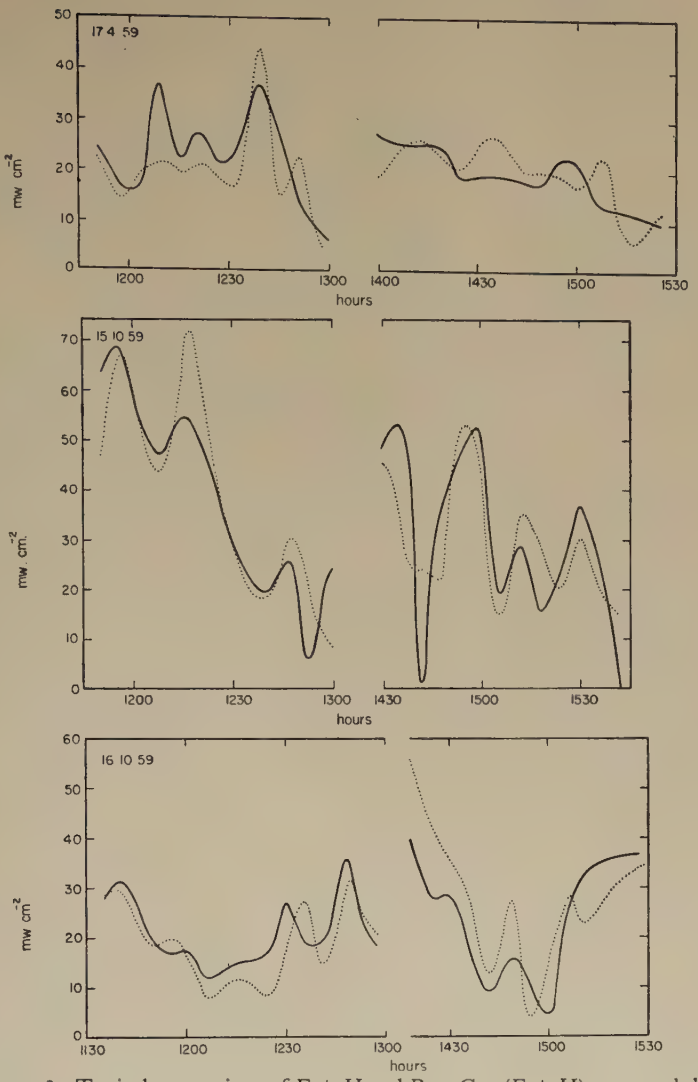

Figure 3. Typical comparison of $E + H$ and $R - G$. ($E + H$) measured directly.
——— $R - G$; · · · · · $E + H$.

(*b*) *E, H. Measured separately*

Commencing in January 1960, and extending through to April 1960, 417 5-min observations were made at 4 m height.

To compute the energy balance, these results were grouped into units. Each unit run contains two measurements each of E and H taken alternately, and is thus equivalent to two 5-min runs of $E + H$ measured directly. (A measurement of stress or momentum transfer was also included in each unit, but these results are not relevant to the present study).

The recovery factor was calculated for each unit run and the distribution plotted (Fig. 4). The mean value is 96 ± 2 per cent, again giving a satisfactory energy balance. The standard deviation, 22 ± 1 per cent, agrees well with the value of $31/\sqrt{2}$ per cent suggested by the results of the previous section.

The variation of the mean daily recovery factor (Table 2) is similar to that in Table 1. A few low values can be associated with greater wind speeds not generally encountered in the previous study. Omitting these, the overall mean recovery factor becomes 100 ± 2 per cent.

Some typical examples of continuous series of runs are shown in Fig. 5.

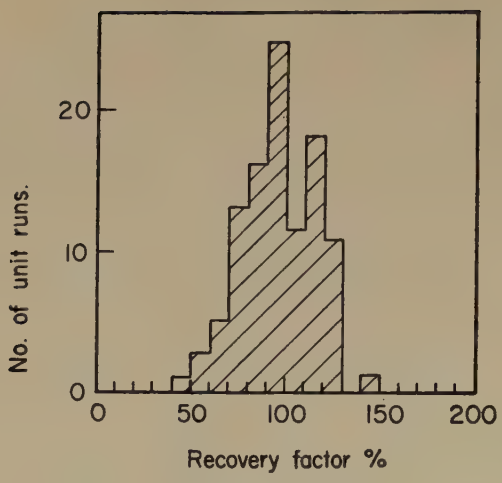

Figure 4. Distribution of recovery factor with E, H measured separately.

TABLE 2. MEAN DAILY RECOVERY FACTOR AT A MEASURING HEIGHT OF 4 m (E AND H MEASURED SEPARATELY)

Date (1960)	No. of 5-min runs	$\overline{E+H}$	$\overline{R+G}$	Recovery factor (per cent)	$\overline{u}$ (m sec^{-1})	$\epsilon = \frac{\overline{E}}{\overline{E}+\overline{H}}$
4 January	11	37·7	39·0	97 ± 13	4·99	0·28
5 January	20	45·0	50·2	90 ± 10	7·28	0·47
6 January	9	61·0	57·0	107 ± 14	4·27	0·53
25 January	8	24·0	23·8	101 ± 14	3·62	0·61
27 January	14	38·3	40·5	94 ± 12	3·24	0·59
29 January	22	43·2	44·7	97 ± 10	4·50	0·60
2 February	8	42·0	44·0	95 ± 14	5·02	0·46
3 February	20	36·7	42·7	85 ± 10	5·62	0·62
12 February	17	34·0	33·8	100 ± 10	5·03	0·52
19 February	7	33·6	32·5	103 ± 15	3·86	0·64
22 February	12	26·1	27·1	96 ± 14	6·28	0·60
26 February	32	33·8	41·8	82 ± 7	6·86	0·49
29 February	7	23·3	27·7	84 ± 15	4·04	0·67
1 March	20	35·8	37·6	96 ± 10	4·04	0·57
2 March	33	39·4	40·0	99 ± 7	4·32	0·64
4 March	22	26·7	23·6	108 ± 9	3·84	0·55
8 March	4	30·1	26·5	111 ± 20	1·96	0·48
9 March	16	27·0	29·2	92 ± 10	5·30	0·50
10 March	13	30·5	30·2	101 ± 14	5·00	0·72
15 March	12	30·2	33·2	91 ± 14	4·98	0·55
17 March	9	36·0	35·2	102 ± 15	4·53	0·49
18 March	23	29·5	29·5	100 ± 9	3·89	0·47
22 March	14	34·7	42·0	83 ± 12	5·51	0·47
23 March	23	14·3	14·1	102 ± 9	3·57	0·45
24 March	14	30·2	30·0	101 ± 12	4·29	0·64
28 March	7	23·2	22·0	105 ± 15	4·12	0·52
1 April	10	14·8	14·2	104 ± 15	4·49	0·32
11 April	17	13·5	13·2	102 ± 10	–	0·55

The ' evaporation fraction ' $\epsilon = \overline{E}/(\overline{E}+\overline{H})$, listed in Table 2, can be equated also to $\overline{E}/(\overline{R}-\overline{G})$. ϵ thus expresses the fraction of the available energy used for evaporation and emerges later as a most useful parameter.

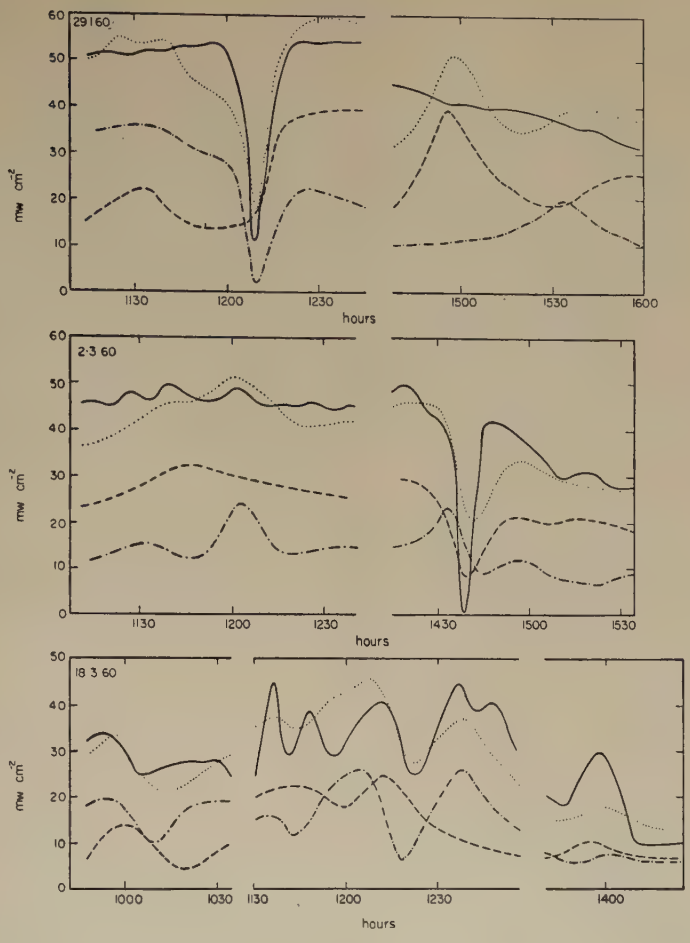

Figure 5. Typical comparisons of $E + H$, $R - G$, with E, H measured separately.

——— $R - G$; · · · · · $E + H$; · — · — · H; - - - - E.

(c) *The response-time effect*

It is essential to the eddy-flux technique that the sensing elements should have a sufficiently fast response to record the smallest eddies contributing to the correlation. Both the anemometer and the wet-bulb resistance thermometer have a response time* of approximately 0·3 sec (Taylor 1958; McIlroy 1955).

Deacon (1959) and McIlroy (1960) have presented analyses of response-time limitations, and the various effects of horizontal windspeed $\bar{u}$, response time τ, and measuring height z, have been incorporated by plotting the recovery factor as a function of the dimensionless parameter $\tau\,\bar{u}/z$. Their results have been summarized by the dotted lines of Fig. 6 for the limiting atmospheric conditions of neutrality and high instability.

A comparison with the present results can be made by plotting the data of Tables 1 and 2 in the above manner, and then grouping and averaging in convenient classes of $\tau\,\bar{u}/z$. Most of the data reported here were obtained in conditions of moderate instability, and it is seen from Fig. 6 that these lie within the limiting curves found by Deacon and McIlroy. The low value of $\tau\,\bar{u}/z = 0{\cdot}15$ is not statistically significant but may be due to sluggish operation of the wind-alignment vane at very low wind speeds.

* The term 'response time' is used here to denote the time required for the fraction $1 - e^{-1}$ of a step-function change to be recorded.

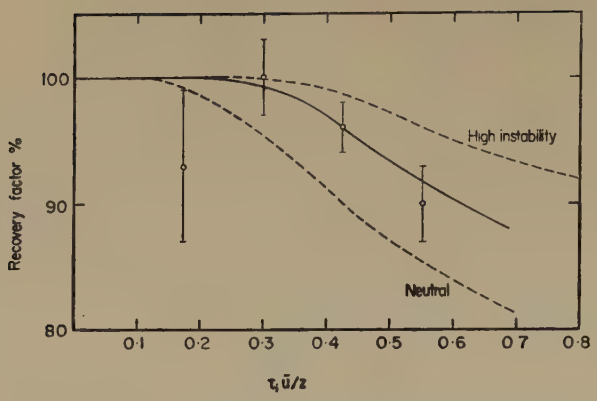

Figure 6. Recovery factor as a function of the parameter $\tau\,\bar{u}/z$.

From a curve of this type an assessment of the instrumental requirements for particular situation can be made. For example, with the present equipment operatin at a measuring height of 4 m, the recovery factor would fall to 90 per cent at a windspee of 8·4 m sec^{-1} under conditions of moderate instability.

4. Physical significance of recovery factor distribution

A careful examination of random errors in the radiation, ground-flux and eddy correlation equipment indicated that these, at the most, would account for about one-thir of the observed scatter of the recovery factor for 5-min runs. Of these, errors in the edd flux equipment were the most significant.

Fluctuating errors of a few per cent would arise in steady conditions from the neglec of heat-storage changes in the 1 cm of soil above the flux plates, and with extremely variabl insolation these could increase to as much as 40 per cent for a 5-min period.

The latter situation was, however, comparatively rare, and a significant contributio to the recovery factor distribution must therefore be sought in meteorological effect as well as instrumental.

To assess likely sources of error in determining the turbulent heat flux, Swinbank (1955) made a formal analysis of all terms entering into a detailed energy-balance equation and concluded that in conditions of steady radiation a maximum error of 20 per cen could occur for a 5-min run as a result of the non-vanishing of the horizontal gradient $\partial\overline{T}/\partial x$ and $\partial\overline{\rho u}/\partial x$. (From the equation of continuity $\overline{\rho w} = 0$ if $\partial\overline{\rho u}/\partial x = 0$). In the case of evaporation, the gradients $\partial\bar{q}/\partial x$ and $\partial\overline{\rho u}/\partial x$, could likewise cause a maximum erro of about 20 per cent.

On this basis a maximum discrepancy of 20 per cent might be expected in the simpl energy-balance equation. This value must be increased in the present instance for three reasons :

(1) The height of observation (4 m) was greater than that considered by Swinbank (1 m).

(2) Measurements were made under all conditions of radiation.

(3) The observed horizontal gradients leading to the above error estimates were both space and time averages. (The accurate measurement of a horizontal gradient at a point is, of course, extremely difficult, if not impossible).

This interpretation indicates that for a measuring height of 4 m, discrepancies in excess of 20 per cent might arise more readily than Swinbank's analysis would suggest, and with some contribution from the neglect of heat storage a standard deviation of about the observed magnitude (31 per cent) might therefore be anticipated.

The quantities $\partial\overline{\rho u}/\partial x$, $\partial\overline{T}/\partial x$, and $\partial\overline{q}/\partial x$ will, during the course of a day, be variable in sign, and with reasonably uniform surfaces may be expected to average out to negligible values.

Evidently the atmosphere achieves horizontal uniformity by a process of continual adjustment on a scale which becomes apparent if short running times are used. For longer periods, the naturally imposed averaging ensures that the simple energy balance of Eq. (7) is valid.

It is relevant to assess the standard error of a flux measurement by the eddy-correlation method for different periods of observation (Table 3), making use of the recovery-factor distributions reported earlier. In practice, the accuracy will be somewhat better than this because of the neglect of heat-storage changes in the experimental data.

TABLE 3. STANDARD ERROR OF MEASUREMENT OF AVERAGE EDDY-FLUX AT 4 m HEIGHT FOR DIFFERENT PERIODS OF OBSERVATION

Period of observation	Standard error (per cent)
5 min	31
10 min	22
30 min	13
1 hr	9
5 hr	4
10 hr	3

Over a period of one day, the average flux can be determined with a standard error of a few per cent. Where short-period results are required, these can be obtained at a somewhat reduced accuracy. In both cases the quality of the measurements would be better in steady-radiation conditions.

This assessment of the accuracy of the method by-passes any consideration of the response-time effect, which as discussed earlier, imposes a minor limitation at high wind speeds only.

5. THE RELATION BETWEEN G AND H

Priestley (1959, p. 97) has discussed the theoretical aspects of sharing between two media of the heat supplied by radiation at the interface, and favours a relation of the form

$$G = \frac{\rho' c' \sqrt{\kappa}}{\rho C_p \sqrt{K}} . H \quad . \quad . \quad . \quad . \quad (8)$$

where ρ, ρ' refers to density; C_p, c' to specific heat, and K, κ to diffusivity. The prime denotes the underlying medium. The values of K and κ appropriate here are the bulk values at some distance from the surface.

Analysing the measurements of G and H made by Swinbank (1955), Priestley suggests that a value of K of 10^5 cm^2 sec^{-1} by day provides a suitable agreement between experiment and theory. The value of $\rho' c' \sqrt{\kappa} = 0{\cdot}034$ used for Swinbank's results would not differ greatly from that appropriate to the present data.

Plotting average values of G in ranges of H (Fig. 7), the present results suggest a value of K of 10^5 cm^2 sec^{-1}, for the near-neutral atmosphere, increasing to 10^6 cm^2 sec^{-1} for the very unstable case. Priestley (1959, p. 100) quotes corresponding K values of 10^5 cm^2 sec^{-1} increasing to 10^7 cm^2 sec^{-1}.

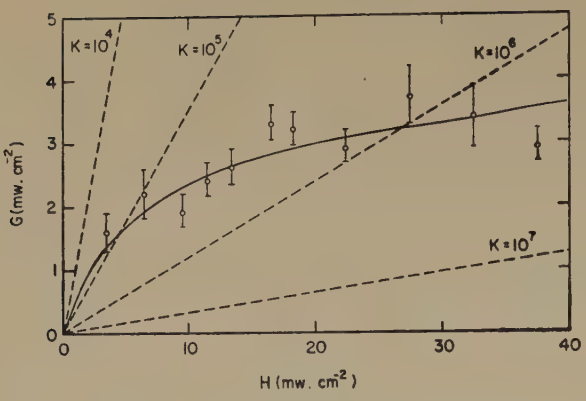

Figure 7. The relation between G and H.

The present results are obviously not universally applicable, and the detail of the $G - H$ relation would be dependent on such things as the type of soil and its moisture content, and the type of crop cover. The theoretical interpretation, nevertheless, would appear to provide a useful guide to the problem of heat sharing, particularly where variations in one parameter are under consideration.

6. Chronological association of precipitation and evaporation

It might be expected that the evaporation fraction ϵ will be chiefly determined by the availability of water for the evaporation process. For example, with rain following a dry period, ϵ would presumably increase and, in the absence of further rainfall, decline again gradually to its initial value. From day to day ϵ would obviously be a more conservative quantity than amount of evaporated water, since the latter would be more closely related to net radiation income, a highly variable quantity.

The data of Table 2 bear on this question, and in Fig. 8 ϵ is plotted in chronological sequence. For the period 20 February to 31 March there is good continuity of measurement, and some degree of correspondence with the expected behaviour of ϵ will be readily observed. The variation of ϵ outside this period cannot be so accurately delineated, but can be reasonably inferred.

Assuming that ϵ, as determined, can be applied to the whole day from sunrise to sunset, the daily totals of evaporation can be computed from known day-time totals of net radiation. G has been taken equal to $0{\cdot}08\,R$, the overall value found in the present experiment. Night-time evaporation (or condensation) is ignored.

The total evaporation thereby found for March is 2·46 in., whereas the total precipitation is only 0·33 in. Much of the water evaporated during this period must, therefore, have come from ground storage of earlier precipitation. Soil moisture profiles taken at the beginning and end of March showed little change down to a depth of 3 ft, suggesting that greater depths were involved. The grass roots are known to extend below this level.

With this method of computing daily evaporation, it is clear that areas under the curve of Fig. 8 can be expressed as amount of evaporated water, and the quantitative association of the peaks of the ϵ-time curve with the immediately preceding rainfall can be examined.

The precipitation data of Fig. 8 have been conveniently grouped (A, B, etc.) and associated areas accurately computed. The broken lines were then fitted to demarcate these areas under the appropriate peaks of the ϵ-time curve and, by trial, it was found possible to do this most readily with lines suggesting an approximately exponential decay of ϵ following a single rainfall. This interpretation of the ϵ-time curve is plausible in general physical terms, and is supported by the consistency of the pattern. The minor

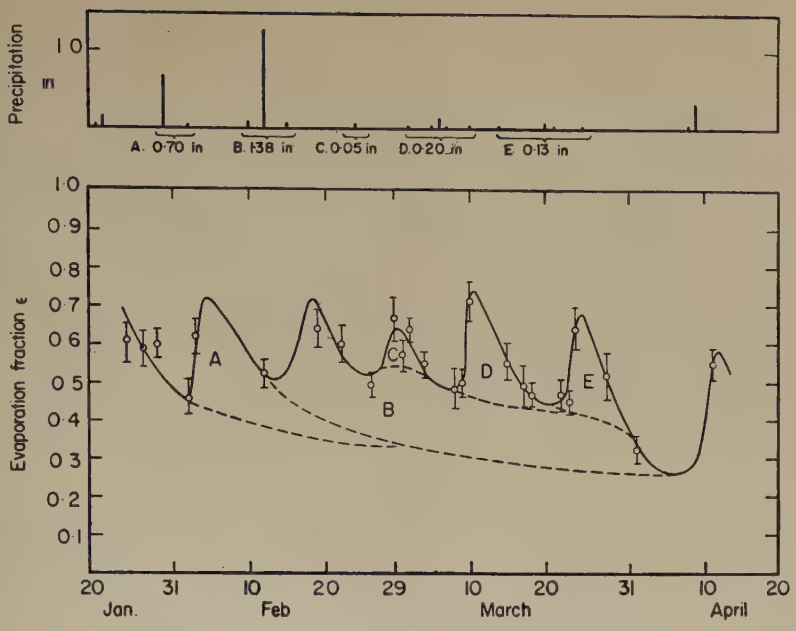

Figure 8. Evaporation fraction ϵ as a function of time.

discrepancy of group C is probably caused by an error in sampling, typical of such small amounts of rainfall. The detail of this analysis is clearly applicable to the present site alone, and an extension to other areas would require a knowledge of the effects of different types of soils and crops.

It is impracticable to attempt to correlate the fraction of the evaporation regarded as consequent on precipitation several months earlier. However, the long-period effects can be examined to a limited degree by noting that the average value of ϵ during February and March 1960 was 0·56.

Neglecting run-off, a long term (annual) value ϵ_A can be computed from the relationship : annual evaporation $= \epsilon_A \Sigma (R - G) =$ annual precipitation where, as before, R and G refer only to daylight hours.

The annual precipitation at Edithvale, Victoria is 26·1 in., and the annual value ΣR is 91 w hr cm^{-2}, i.e., equivalent to 52·2 in. Allowing for G as previously, we find $\epsilon_A = 0{\cdot}54$.

During the winter months ϵ would presumably increase because of the greater availability of water, but these higher values of ϵ would enter with very little weight into the determination of ϵ_A because of the much smaller radiation totals with which they are associated. Close agreement of ϵ_A with the experimental value found for late summer and early autumn might therefore be expected and is, in fact, obtained.

An interesting feature of Fig. 8, is that on three occasions (2 February, 8-9 March, 22-23 March) low values of ϵ persisted for up to three days following appreciable rainfall, and the maximum value of ϵ was not achieved until the fourth day. It has been suggested to the author that this can be ascribed to the accretion of suberin by the shallow roots during the dry period, and their delayed re-activation after rain. The slow diffusion of moisture down to the more active root systems is an alternative explanation.

7. Conclusions

The eddy-correlation technique has been demonstrated to be a practicable and accurate method for the measurement of evaporation and sensible-heat transfer over a reasonably uniform surface.

In conditions of near-neutrality, the accuracy of the technique is not limited by response-time effects over the range of wind speed normally encountered. With increasing atmospheric instability the useful wind-speed range is considerably extended and, unlike the aerodynamic method, optimum performance is obtained at maximum instability.

With a measuring height of 4 m as used in the present experiment, minor surface irregularities of up to several tens of centimetres are clearly of no consequence, and if sufficient fetch is available, greater irregularities could be readily accommodated by increasing the height and period of observation.

The usefulness of the eddy-correlation method to studies of the type described in the latter part of this paper is self-evident, and with this in mind, the development of portable equipment employing transistor circuitry has been undertaken. This latter instrument, called the 'Evapotron,' has performed satisfactorily in laboratory tests and field trials will commence shortly.

Acknowledgments

Many members of this Division have made significant contributions to the study of flux measurement by the eddy-correlation technique, and the author has derived much benefit from his association with them. A large part of the instrumentation was carried out by Mr. R. R. McGregor. Miss S-A. Yeo and Miss Y. Mullins assisted with the operation of the eddy-flux instrument, and Mr. J. Stevenson was responsible for many of the radiation and ground-flux measurements. The successful prosecution of the project depended very much on the expert construction of the sensing elements by Mr. G. Harris, and on their maintenance and calibration by Mr. G. Grauze.

References

Deacon, E. L.	1950	*Quart. J. R. Met. Soc.*, **76**, p. 479.
	1955	*C.S.I.R.O. Div. of Met. Phys.*, Tech. Pap. No. 2.
	1959	*Advances in Geophysics*, **6**, p. 211.
Dyer, A. J.	1958	*J. Sci. Instr.*, **35**, p. 240.
	1960	*Ibid.*, **37**, p. 166.
House, G. J., Rider, N. E. and Tugwell, C. P.	1960	*Quart. J. R. Met. Soc.*, **86**, p. 215.
McIlroy, I. C.	1955	*Austr. J. Agric. Res.*, **6**, p. 196.
	1960	*C.S.I.R.O., Div. of Met. Phys.*, Tech. Pap. No. 11.
Pasquill, F.	1949	*Proc. Roy. Soc.* A., **198**, p. 116.
Priestley, C. H. B.	1959	*Turbulent transfer in the lower atmosphere*, Chicago Univ. Press.
Swinbank, W. C.	1951	*J. Met.*, **8**, p. 135.
	1955	*C.S.I.R.O., Div. of Met. Phys.*, Tech. Pap. No. 2.
Taylor, R. J. and Webb, E. K.	1955	*Ibid.*, Tech. Pap. No. 6.
Taylor, R. J. and Dyer, A. J.	1958	*Nature*, **181**, p. 408.
Taylor, R. J.	1958	*J. Sci. Instr.*, **35**, p. 47.
	1956	*Ibid.*, **33**, p. 436.

551.574.12 : 551.574.13

Accretion in mixed clouds

By W. C. MACKLIN
*Imperial College, London**

(Manuscript received 21 July 1960; in revised form 31 January 1961)

Summary

An object on which ice is deposited when it moves through a supercooled cloud is warmer than its environment owing to the release of heat of fusion. If the rate of accretion is sufficiently great, the temperature of the object is raised to 0°C and its surface becomes wet. It has often been assumed that water in excess of that which can be frozen is shed into the wake of the object. The present experiments show that, at temperatures below − 2°C, the excess water is not shed but is incorporated into the ice structure, giving a ' spongy ' deposit. Even in the temperature range − 2 to 0°C, the excess water can be retained if a sufficient concentration of ice particles is introduced into the droplet cloud. It has also been found that over a wide range of conditions, considerable quantities of ice particles may be accreted in addition to the supercooled droplets, and the crystalline structure of the deposit is modified accordingly. It is considered that at temperatures near 0°C, and possibly at lower temperatures, the presence of ice particles in the supercooled cloud is necessary in order that none of the unfrozen water is shed.

The restriction formerly thought to be imposed on the growth rate of hailstones in the wet condition may now be removed.

1. Introduction

In his treatment of the growth of hailstones, Ludlam (1958) distinguishes between ' dry ' and ' wet ' growth regimes. If an ice particle is growing in a supercooled cloud by the accretion of water droplets, then the temperature of its surface is higher than that of its surroundings, owing to the release of the heat of fusion (Schumann 1938; Ludlam 1950). If the rate of accretion increases because of either an increase of the liquid-water concentration of the cloud or an increase in the size, and therefore fall-speed of the particle, then the temperature of the accreting surface is raised until the transfer of heat to the environment by conduction and evaporation again just balances the rate of liberation of heat by the freezing droplets. There is, however, an upper limit to the surface temperature, namely 0°C, the melting point of ice. For given values of the ambient temperature, fallspeed and diameter of the accreting particle, there is a critical liquid-water concentration, W_c, which will just maintain the surface temperature at 0°C. When the concentration of cloud water is less than W_c, the surface temperature is below 0°C, all the accreted water is frozen, and Ludlam speaks of growth in the ' dry ' regime. On the other hand, when the concentration exceeds W_c, more water is collected than can be frozen; the rate of growth of the ice mass is determined primarily by the rate of heat transfer into the environment and Ludlam refers to growth in the ' wet ' regime. (It should be pointed out that Ludlam has not considered the possibility that any unfrozen supercooled liquid could be warmed above the ambient temperature. In this event the concentration of water frozen is somewhat greater than W_c). Ludlam assumed that when the cloud-water concentration is greater than W_c, the excess collected by the ice particle accumulates as a liquid film, beneath which a layer of ice of density about 0·9 g cm^{-3} is deposited, or is shed into the wake of the particle. Since entry into the wet regime occurs with rather small cloud-water concentrations when the ice particle has the size of a hailstone, it has been regarded as greatly restricting the growth rate of natural hailstones; for example, the rate of increase of radius of a hailstone 1 cm in diameter growing wet at − 10°C in a supercooled cloud having a water concentration of 6 g m^{-3} (about the maximum to be anticipated inside large cumulonimbus) is about one-quarter of the value it would be if all the accreted water could be frozen. At higher cloud temperatures and for larger stones, this fraction is even smaller.

* Now at Physics Department, Nedlands, University of Western Australia.

In an experimental investigation of the factors affecting the density of ice formed by accretion (to be published) the writer found that when the cloud liquid-water concentration exceeded the critical value, the excess water which could not be frozen was not usually shed into the wake of the accreting object, as had been assumed, but was incorporated into the ice structure, producing a ' spongy ' or ' mushy ' deposit containing a substantial fraction of unfrozen liquid.

This phenomenon is well known to operators of icing tunnels. Fraser, Rush and Baxter (1952) describe experiments which resulted in deposits from which water could be squeezed ' as though from a wet sponge.' List (1959) has obtained deposits containing up to 72 per cent of liquid water. This type of ice has also been observed, under certain conditions, on aircraft flying through supercooled clouds (see, e.g., Brun 1957).

It was further noticed during the experiments that ice crystals occasionally present in the airstream became incorporated into rime structures and could be seen glinting in the surface. The number of ice crystals swept up in this way depended on the condition of the surface, and when the surface was wet, appreciable quantities of small ice particles deliberately introduced into the airstream, were collected. This has been observed by other investigators working on problems of ice accretion. Clark (1948) describes experiments carried out at the Mount Washington Observatory, U.S.A., in which objects were exposed in the supercooled cloud at the summit. Snow and fragments of rime were sometimes seen embedded in the accreted ice. Minervin (1956) states that when measurements of liquid-water concentration are made by accretion instruments in supercooled cloud the measured values of the liquid-water concentration may exceed the critical value for the instrument because ice crystals become frozen into the newly formed ice. Bigg, Day and McNaughton (1959) have found both in laboratory experiments and in flights through clouds, that mixtures of ice particles and supercooled water droplets may readily be accreted.

It is apparent that these two phenomena, the formation of mushy or spongy ice and the accretion of ice particles as well as supercooled droplets could well affect the growth of hail in the wet condition. Gaviola and Fuertes (1947) assert that ' the use of snow as a building material (of hailstones) in addition to sub-cooled water droplets, makes the growth to large sizes . . . . easier and explains the concentric layers.' Landis (1907) describes large oblate hailstones (about $2\frac{1}{4}$in. by $1\frac{3}{4}$ in.) having layers which were ' undoubtedly moist snow.' Pollard (1936) has also described hailstones with layers which appeared to be ' snow frozen hard.' These last two interpretations cannot be accepted without reserve, however, as there are varieties of rime ice which could give such impressions.

New interest has been aroused by the observation (Ludlam 1959) that only ' glaciated ' cloud towers, presumably containing a considerable proportion of frozen particles, have been found with rising speeds of the magnitude believed necessary for the production of large hailstones. Moreover, field data seemed also to indicate that the growth-times previously computed for large stones were excessive and, therefore, that the restriction by the entry into the wet-growth regime was not so severe as had been assumed. The writer therefore undertook the experiments on ice accretion in mixed clouds which are described below.

2. Experimental procedure

List of symbols

a – ventilation coefficient

d – cylinder diameter

E – efficiency of catch of a cylinder or hailstone for cloud droplets

k – coefficient of diffusion of water vapour in air

K – coefficient of thermal conductivity of air

L_f – latent heat of fusion of water

L_v – latent heat of vaporization of water

m_i – concentration of ice particles
R – radius of hailstone
Re – Reynolds number
T – ambient temperature
V – airspeed or fallspeed of hailstone
W – liquid-water concentration
W_d – water concentration effectively caught by a cylinder when supercooled droplets only were used
W_i – concentration in addition to W_d caught by a cylinder when ice particles were used in addition to the droplets
$\Delta\rho$ – difference between the value of the saturated vapour density at the surface of an accreting cylinder or hailstone and that in the environment.

A small wind tunnel with a working section 20 cm square, and capable of producing wind speeds of 13 to 14 m sec^{-1}, was installed in a cold room. This room was roughly a cube of side 8 m in which temperatures down to -15°C could readily be produced and maintained to within 1 or 2°C over a period of an hour or more. Temperature measurements were made with a standardised thermometer situated at the level of the wind tunnel, and are considered to represent the conditions in the tunnel to within 1°C. Only temperatures of -12°C and above were used in order that the wet condition could be readily attained.

The air speeds employed were measured by placing a small anemometer in the tunnel. As the interior of the tunnel became rimed during the course of an experiment the velocity decreased slightly; the speeds given are the mean of those measured at the beginning and end of each experiment and are considered to be correct to $\pm$ 5 per cent.

Water droplets were sprayed into the room from a bank of eight sprays housed in an insulated box. Ordinary tap-water was used and the sprays were directed towards the mouth of the tunnel from about three metres away, a distance sufficient for the droplets to cool practically to room temperature before being caught up in the airstream. The water concentrations were varied in steps according to the number of sprays in operation, and values up to 8 g m^{-3} could be produced at the velocities used.

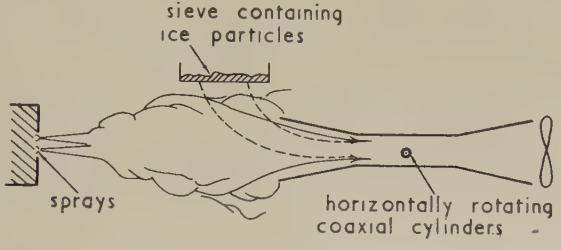

Figure 1. Schematic diagram of experimental arrangement.

Ice particles were introduced into the tunnel by sieving rime of low density (about 0·2 g cm^{-3}) through fine gauze near its mouth (see Fig. 1), and the mixture of ice and supercooled water was blown over a set of three coaxial cylinders, rotated horizontally to give uniform deposits. The rate of rotation was one revolution every two seconds, so that the peripheral speeds of the cylinders were negligible in comparison with the airspeeds. The cylinders were constructed of thin brass sleeves mounted on heat-insulating formers, with outside diameters of 0·10, 0·63 and 1·43 cm. It was possible to remove a section of each cylinder so that the mass of the deposit per unit length could be determined for each diameter. The radial dimensions were obtained photographically or by assuming

that the density of the deposit was 0·90 g cm^{-3}. The ice particles were dispensed manually at an approximately uniform rate, and the mass of ice used was determined by weighing the amount of ice in the sieve before and after each experiment, the fraction actually entering the tunnel being estimated visually. When the surface of the deposit remained just wet, even though ice particles were also being accreted, it was possible to obtain an independent measure of the ice concentration, since it could be assumed that virtually all the particles in the volume swept out by the cylinders were being collected. Ice concentrations up to 5 g m^{-3} were produced and estimated to about $\pm$ 30 per cent.

The size distributions of the droplets and ice particles were obtained by exposing in the tunnel narrow strips of perspex coated with oil and afterwards photographing them through a microscope. Each distribution was obtained separately. Two sets of sprays were used, giving drop-volume median diameters of 47 and 65 μ respectively. The drop size is not important for these experiments; the two sets of sprays were used to obtain smaller gradations in the liquid-water concentration. The number distribution of ice particles was roughly constant from 20 to 300 μ and the equivalent median volume diameter was estimated to be 260 μ. It was not possible to use larger ice particles as these could not be suspended in the airstream long enough to reach the cylinders.

For given conditions of ambient temperature, airspeed and liquid-water concentration droplets only were sprayed into the tunnel, and accretion permitted to occur on a set of cylinders for a chosen time; a period of two to ten minutes was sufficient to build up a coating a few millimetres thick at the liquid-water concentrations used. The experiment was repeated using another set of cylinders and adding ice particles to the airstream. Finally, a third control experiment was performed using droplets only. The three sets of cylinders were photographed and weighings made of sections from individual cylinders. The agreement between the mass measurements of the first and final experiments was better than 10 per cent.

3. Results and discussion

(a) *Experiments using droplets alone*

The critical liquid-water concentration W_c, which just maintains the surface temperature of an accreting cylinder at 0°C is given by the following equation (Ludlam 1951)

$$\frac{E\,W_c\,V\,(L_f + T)}{\pi} = \frac{0{\cdot}24\,(Re)^{0{\cdot}6}}{d}\,(L_v\,k\,\Delta\rho - KT) \qquad . \qquad . \qquad (1)$$

where L_f and L_v respectively are the latent heats of fusion and vapourization of water, T the ambient temperature (in °C), k the coefficient of diffusion of water vapour in air, V the airspeed, Re the Reynolds number, and $\Delta\rho$ the water-vapour density difference between the riming surface and the environment. E is the efficiency of catch of the cylinder of diameter d for the droplets in the airstream and its values for the present experimental conditions have been computed using the method given by Langmuir and Blodgett (1946). The expression in the left-hand side of the equation represents the rate of liberation of heat at the surface and that on the right-hand side the rate at which heat is removed by conduction and evaporation into the air flowing past the cylinder. The flow around the cylinders is assumed to be non-turbulent; if the flow is turbulent then the transfer of heat may be increased by perhaps 50 per cent (McAdams 1954, p. 261). The validity of this equation has been experimentally verified by Fraser, Rush and Baxter (1952) in icing-tunnel experiments.

The values of W_c have been computed from Eq. (1) for the present experimental conditions and these are plotted against the liquid-water concentrations (corrected for values of the collection efficiency less than unity) deduced from the mass accreted on the cylinders (Fig 2). The four conditions of the ice surface indicated in the diagram are: dry; just wet, as determined by a visible sheen on the surface; wet, when the surface is covered by a liquid film; and spongy. It can be seen that the liquid which may be retained by the cylinder exceeds the critical value deduced from Eq. (1) by as much as 7 times.

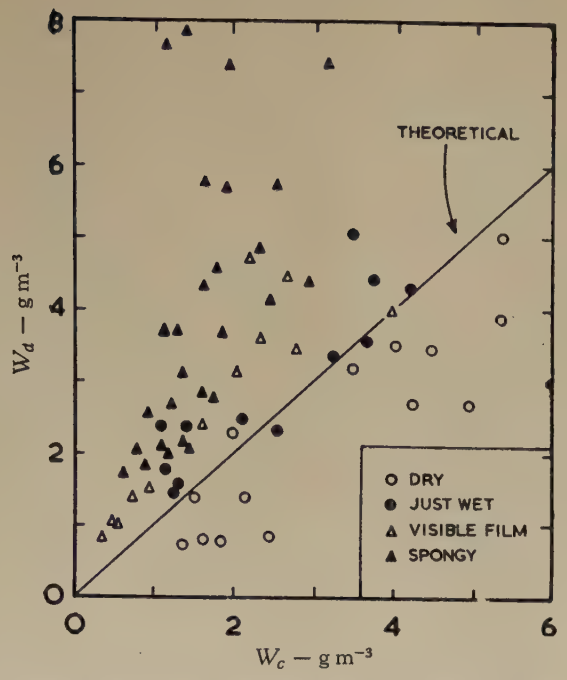

Figure 2. The liquid-water concentration effectively caught by the cylinders, W_d g m^{-3}, plotted against the critical liquid-water concentration, W_c g m^{-3}.

Eq. (1) defines the liquid-water concentration in which the surface temperature of the ice deposit on the cylinder is just 0°C. If the actual water concentration, W, is greater than the critical value, then it is possible that an additional amount of water $(W_c - W)\,T/80$ be frozen if the temperature of the excess water is raised to 0°C also. Further, when spongy, the deposit is readily moulded by the airstream, and becomes irregular and knobbly. This increases the surface area above that of a cylinder of comparable diameter, promotes turbulence and thus raises the rate of heat transfer.

The absorption of heat by the rotating cylinders should also be taken into account. The rate of heat conduction through the ice deposit into the cylinders may be comparable to the rate of transfer of heat to the environment so that the thermal capacities of the cylinders and of the insulating former cannot be ignored. These are such that, under the present conditions, the computed values of the critical liquid-water concentration are likely to be low by as much as 20 to 50 per cent in the case of the largest cylinder, depending on its initial temperature (normally ambient temperature). In the case of the smallest cylinder, the heat absorbed is only a few per cent of that released by the freezing droplets, while the 0.63 cm diameter cylinder absorbs about one-half as much as the largest one. The factor of 7 quoted above does not imply, therefore, that there is 7 times as much liquid as ice in the deposit; for this ratio a value of 2 or 3 is more likely, and was roughly confirmed by a visual examination when the deposits were broken up. Using a quantitative calorimetric method, List (1959) has determined values of up to 72 per cent for the proportion of unfrozen liquid within similar spongy ice deposits.

Spongy ice was produced at all temperatures down to — 12°C, the lowest employed in these experiments. There was, however, less tendency for significant spongy ice deposits to be produced at temperatures only just below freezing (— 1 to — 2°C). Although some of the liquid-water concentrations employed were considerably greater than the critical value, it was in fact only at these high temperatures that *any* of the unfrozen liquid was shed into the wake of the cylinders. At lower temperatures, as far as could be determined visually, all of the excess was retained.

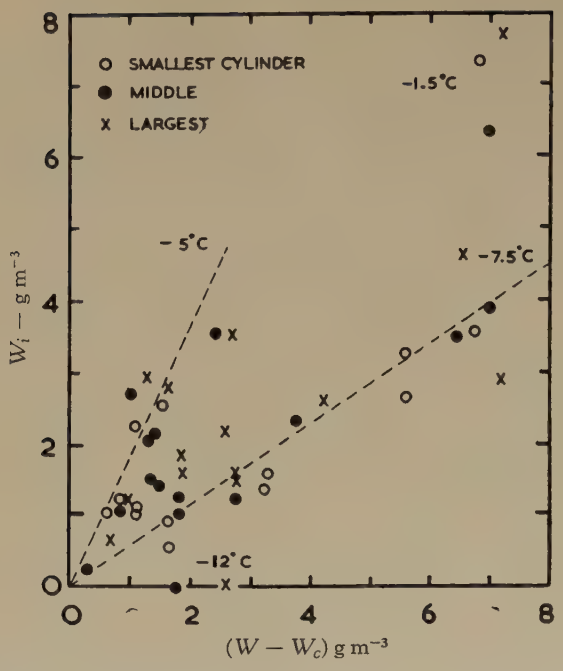

Figure 3. The concentration of ice particles, W_i g m^{-3}, accreted in addition to the supercooled droplets as a function of the excess liquid-water concentration $(W - W_c)$ g m^{-3}.

(*b*) *Experiments with mixed clouds*

If the accreting object has a wet or spongy surface layer, then it is obvious that an ice particle arriving with a speed of several metres per second can sink into it and be captured. This ice particle can remove the heat liberated by the freezing of a mass of water corresponding to the fraction $-T/160$ of its own mass (the specific heat of ice is about 0·5 cal g^{-1} °C^{-1} and the latent heat of fusion of water about 80 cal g^{-1}) and become frozen into the surface. Consequently, in mixed clouds, the rate of freezing of collected liquid is increased.

The experimental data for the smallest cylinder in mixed clouds are shown in Table 1; all relevant quantities are converted to corresponding spatial concentrations, being corrected for efficiencies of catch less than unity. Since in most cases no appreciable quantity of water was shed into the wake of the cylinder, the water concentration given by the sprays is assumed to be that determined from the mass of the deposit. It was only at temperatures near 0°C that these two quantities differed appreciably. The liquid-water concentrations given by the sprays under these latter conditions were estimated from the rate of accretion at lower temperatures. The values given are considered to be correct to $\pm$ 20 per cent.

If the surface was dry (i.e. $W < W_c$) then although individual ice crystals were incorporated into the ice structure, no appreciable quantities of ice were accreted. For values of $W > W_c$, the maximum quantity of ice accreted depended on the excess water concentration $W - W_c$, as indicated in Fig. 3 : here it is seen that it was possible to use for accretion approximately 1 g m^{-3} of ice for each g m^{-3} of excess water. There is a dependence on the temperature, the amount of ice which can be accreted increasing with temperature rise. A better parameter to use is the quantity $(W - W_c)/W_c$, since this is a measure of the ratio of unfrozen to frozen liquid or the ' degree of sponginess ' of the deposit formed from the water droplets above. The relationship between the concentration of ice particles accreted, W_i g m^{-3}, and this parameter is shown in Fig. 4. While there is still some scatter in the points, this does seem to be a better presentation of the data than Fig. 3. The value of the concentration of ice which was accreted was

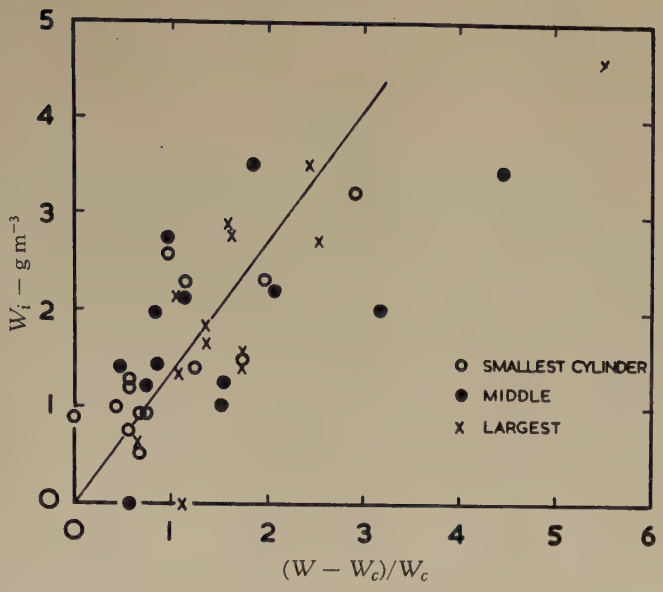

igure 4. The concentration of ice particles, W_i g m^{-3}, accreted in addition to the supercooled droplets, as a function of the quantity $(W - W_c)/W_c$.

pproximately 1·4 times the ratio of $(W - W_c)/W_c$. In both diagrams for the reasons iven above, W_c is an underestimate (by a factor of perhaps as much as 1·5 to 2 in the case f the largest cylinder) of the actual critical liquid-water concentrations of the cylinders nd this must be taken into account when applying these results.

Plate XI, Fig. 6, shows the iced cylinders after the experiments providing the data n the last entry of Table 1. The cylinders on the left were exposed to 7·5 g m^{-3} of droplets lone, the effective concentration being 1·4 g m^{-3}; the middle cylinders were exposed to ·1 g m^{-3} of ice particles, and those on the right to 2·5 g m^{-3} of ice, in addition to the roplets. The effective concentration in this last case was 7·8 g m^{-3}. The additional iquid collected was far in excess of the amount which could possibly be frozen by heat ransfer to the ice particles, which implies that the ice particles influence the manner n which the liquid water is held within the deposit. However, it was only at such high emperatures (— 1 to — 2°C) that the excess water needed substantial quantities of added ce in order to remain on the cylinders.

(*c*) *The nature of the accretion process during wet growth*

When all the liquid caught by an object in the supercooled cloud cannot be frozen film of water accumulates on the surface. This film has been observed during the experiments and it was estimated that, at the airspeeds used (about 13 m sec^{-1}), the thickness vas a fraction of a millimetre, $\frac{1}{4}$ mm or less. It was also noted that at the highest temperatures employed, the liquid water composing the film was blown rapidly to the downstream ide of the cylinders, where droplets 1 to 2 mm in diameter were being shed into the wake. The concentration of freezing nuclei (other than ice particles) which can cause nucleation t temperatures near 0°C is negligibly small, so that freezing progresses only outward rom the surface of the solid ice deposit underneath the liquid film. If the ice continues o grow as a compact mass of density about 0·9 g cm^{-3} as Ludlam (1958) suggests, there is o way in which liquid water can be held within the ice structure and excess must be lown away.

When ice particles are also accreted, the circumstances can be greatly changed Hallett (1960) considers that if an ice crystal alights with arbitrary orientation on a wate surface which is barely supercooled, crystal growth occurs both along the surface an into the liquid, the structure in the latter direction being a system of branching dendrites Provided there is effective nucleation, crystallization at the surface of the liquid film favoured, since it is cooler than the ice surface. When the number of accreted ice particles and therefore of surface nucleation centres is relatively large, an interwoven mesh dendritic ice structures can be supposed to form within the film. This traps excess liqui water so that a mushy or spongy-ice layer can develop and be retained if the mechanica strength of the dendritic system is sufficient.

An examination of the micro-crystalline structure of spongy ice deposits (see below suggests that ice-crystal concentrations of 1 to 10/litre are sufficient to ensure the trappin of liquid. Even if some of the droplets themselves did not freeze, incidental splinterin from rimed auxiliary equipment could readily produce free-ice particles in these con centrations. They are only fractions of a per cent of the droplet concentrations (orde 100 cm^{-3}) and would be undetectable in the droplet stream. Nevertheless, their presenc may be necessary for the formation of spongy-ice deposits.

On the other hand, very little is known about the way in which ice crystallizes fro the liquid under the conditions of the wet-growth regime. It is possible that the ice doe not continue to grow outward as a compact mass of high density, as Ludlam (1958 supposed, but that a crystalline structure similar to that envisaged in the last paragrap penetrates into the liquid film from the underlying ice surface. Even if this is the case ice particles present in the cloud will certainly aid the formation of spongy-ice deposits

In Table 1 it can be seen that at temperatures just below freezing, spongy growth was inhibited and it was not, in fact, until substantial quantities of ice particles wer deliberately introduced into the airstream that considerable deposits were produced. In this case the spongy growth is presumably formed in a different way, the ice particle being frozen together irregularly into an open structure, the interstices of which filled with water.

TABLE 1. EXPERIMENTAL DATA FOR THE SMALLEST CYLINDER

T – ambient temperature, V – airspeed, W_c – critical liquid-water concentration computed for the mea diameter of the iced cylinder, W – liquid-water concentration, W_d – water concentration effectively caugh by the cylinder when droplets were used, W_i – concentration in addition to W_d, caught when ice particle were used as well as the droplets, m_i – estimated concentration of the ice particles dispersed.

T °C	V m sec^{-1}	W_c g m^{-3}	W g m^{-3}	W_d g m^{-3}	W_i g m^{-3}	m_i g m^{-3}
− 12	13·2	4·0	4·0	4·0	0	2·1
	13·5	3·7	3·6	3·6	0	1·9
− 8	13·6	2·6	2·4	2·4	0	2·2
− 7·5	12·8	2·5	0·9	0·9	0	1·9
			5·8	5·8	1·4	1·4
					1·6	2·0
− 7	12·6	2·5	4·2	4·2	0·9	1·5
					0·6	5·3
	12·8	2·2	1·4	1·4	0	2·7
− 6	12·8	1·9	3·7	3·7	2·6	3·0
	13·0	1·9	7·5	7·5	2·6	2·8
					3·3	5·7
− 5	12·8	1·7	2·8	2·8	1·1	2·9
− 4·5	12·6	1·4	2·2	2·2	1·3	3·2
− 4	13·1	1·4	2·1	2·1	1·0	2·7
− 2	13·3	0·9	2·0	1·4	1·1	1·1
					2·3	2·9
− 1·5	13·3	0·8	7·5	1·4	3·6	1·1
					7·8	2·5

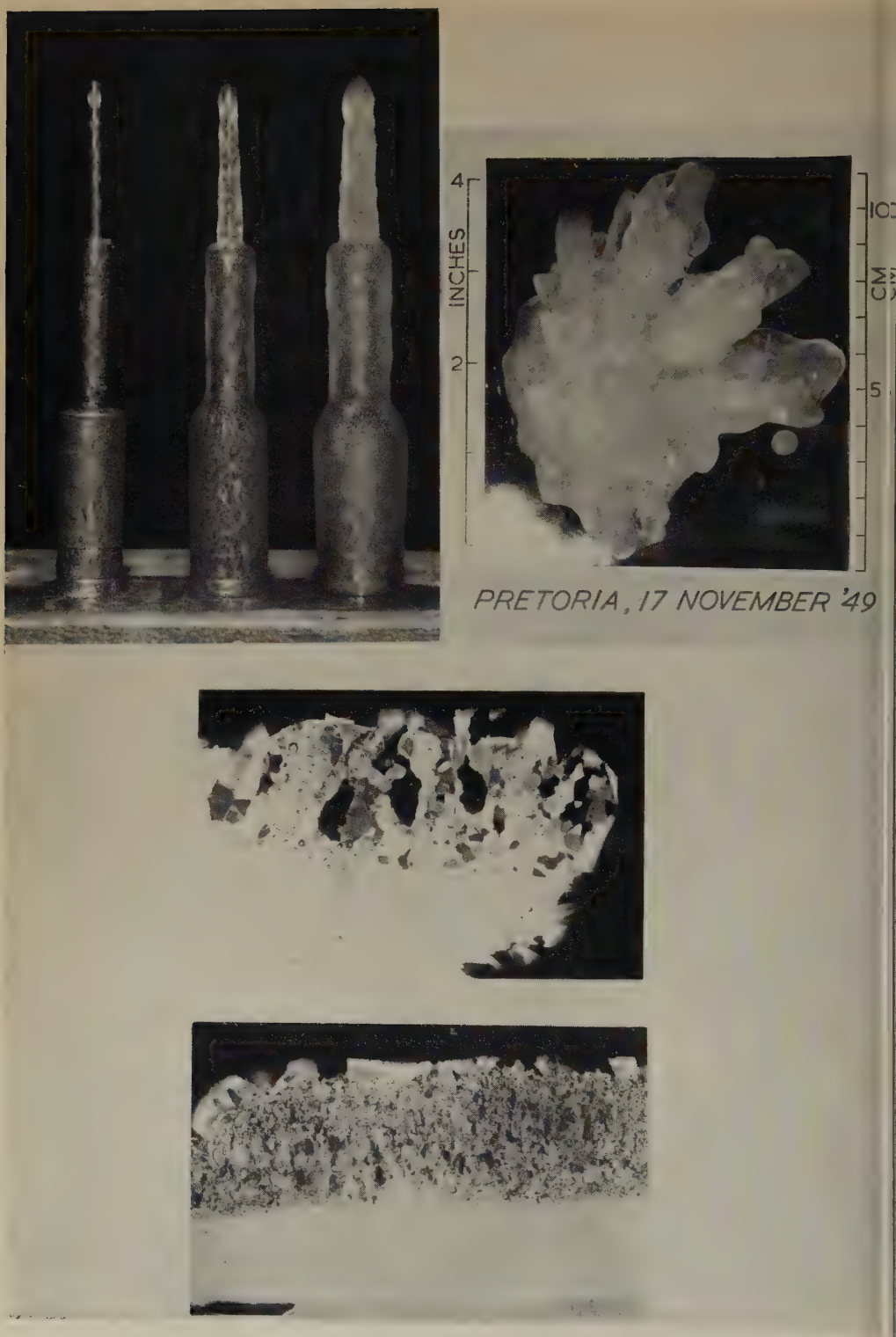

Figure 6. (a) The iced cylinders after the experiments providing the data in the last entry of Table 1
(b) Hailstone which fell at Pretoria, South Africa, November 1949 (Photo by courtesy of the South Africa
National Bureau of Standards); (c) and (d) Thin sections of spongy ice viewed between crossed polaroids

In the case of wet growth on non-rotating objects, spongy projections can grow in much the same manner as icicles. As liquid flows to the back of the object it tends to stream off any irregularities; since the heat transfer is favoured at the surface, the irregularities continue to grow outward as partially frozen cylindrical projections. Such structures have been observed by the writer in the laboratory. Plate XI, Fig. 6 shows a hailstone which, from its appearance, seems to have grown in this manner. Similar protuberances are found on many large hailstones.

There are, therefore, a number of possible ways in which the nature and structure of accreted ice may be affected during wet growth. Certainly water in excess of that which may be frozen is not always shed into the wake of the object, as formerly supposed; rather, at least a proportion can be incorporated into the ice structure and lead to growth rates much greater than previously envisaged. Ice particles, even when present in concentrations comparable with the droplet concentration, are readily incorporated into the deposit and, indeed, may be responsible for modifying the structure in such a way that none of the excess water is shed.

(*d*) *The micro-crystalline structure of ice deposits*

Since ice is anisotropic, its micro-crystalline structure is readily observed by placing a thin slice between crossed polaroids. When viewed with white light, neighbouring crystals, being differently orientated, give rise to different colours, and are thereby easily distinguished.

Samples of spongy ice were formed on an ice rod placed in a stream of supercooled droplets. The airspeed, liquid-water concentration and temperature in the droplet stream were about 10 m sec^{-1}, 8 g m^{-3} and $-12°C$ respectively. The spongy deposit was permitted to freeze completely and a section, about 0·3 mm thick, was made by melting it between two flat metal plates. Plate XI, Fig. 6 (a) shows the appearance of this section when placed between crossed polaroids. The single crystals are 1 to 2 mm long so that their volume is the order of 10^{-3} cm^3. If it is assumed that each crystal is grown upon one freezing nucleus – an ice particle in this case, since the nucleation temperature is virtually 0°C – then the free-air concentration implied is 1 to 10/litre. The ice-crystal concentration in the room was estimated visually to be 1/litre. After about 30 min the ice-crystal concentration had increased to 100/litre, and a second experiment was performed under the same conditions with the result shown in Plate XI, Fig. 6 (b). The dimension of the single crystals is smaller by a factor of about 4 to 5, implying an increase in the free-air ice crystal concentration of order 100, as observed.

This experiment shows that the internal structure of ice formed by accretion can be affected by the presence of ice crystals in the supercooled cloud, and the observations of hailstone structure (see Section 4) may be interpreted on this basis.

(*e*) *The effect produced on the crystalline structure of the deposit by the freezing of droplets in the airstream*

The supercooling of water has been investigated by a number of workers. Bigg (1953), for example, studied the supercooling of groups of water droplets of varying diameters (20 μ to 2 cm) suspended at the interface of two liquids of different densities. He showed that there was a linear relationship between the logarithm of the drop diameter and the median freezing temperature for each group. Langham and Mason (1958) have repeated these experiments using water of differing degrees of purity and they consider that Bigg's curves are typical of nucleation by foreign particles present in the liquid.

From a curve for rainwater given by Langham and Mason, the median freezing temperatures for groups of droplets of different sizes may be obtained, namely $-8°C$ for droplets of diameter 1 cm, $-19°C$ for a diameter of 1 mm, and $-31°C$ for a diameter of 100 μ. The nuclei present in the water would cause freezing of the droplets in the airstream in corresponding concentrations (about 10^{-2}, 10 and 10^4 per litre respectively for

a water concentration of 5 g m^{-3}) so that after they had nucleated the accreted water these three temperatures, individual crystals about 1 cm, 1 mm and 100 μ across wou be present in the deposit. For tap-water the temperatures appropriate to these thr sizes may be expected to be somewhat higher, for distilled water a few degrees lowe

It is apparent, therefore, that in normal icing experiments the crystalline structu of the deposits is dependent on the purity of the water used, as well as on other factor and there is never complete certainty that the droplet stream is free of ice particles.

4. Application to the growth of hailstones

The condition for the entry of hailstones into the wet-growth regime may be expresse in terms of an equation similar to that for cylinders, there being a critical liquid-wat concentration for which the surface temperature is just 0°C. For spherical stones th critical concentration is given by Ludlam (1958).

$$E\pi R^2 V W_c (L_f + T) = 4\pi R a (L_v k \Delta\rho - KT) \quad . \quad . \quad (1$$

where R is the radius of the stone and a the ventilation coefficient; the other symbo have the same meaning as before. The ventilation coefficient is a function of the Reynol number (Re) and Ludlam takes it to be approximately 0·3 $(Re)^{\frac{1}{2}}$. The condition for th entry of hailstones into the wet growth phase is illustrated in Fig. 5. This gives the radi of the hailstone as a function of the ambient temperature under which the surface is ju wet at various liquid-water concentrations, in an environment whose other properti are about those encountered in hailstorm weather (Ludlam 1958). If the position dete mined on the diagram by the temperature (or height) and size is to the left of the appropria water concentration isopleth, the stone is in the dry-growth regime; if the position is on th right-hand side, the surface of the stone is wet. In constructing this diagram, it has bee assumed that hailstones fall with the speeds of spheres of density 0·90 g cm^{-3}. The hig value for the density is justified by measurements made by Steyn (1950), Vittori ar

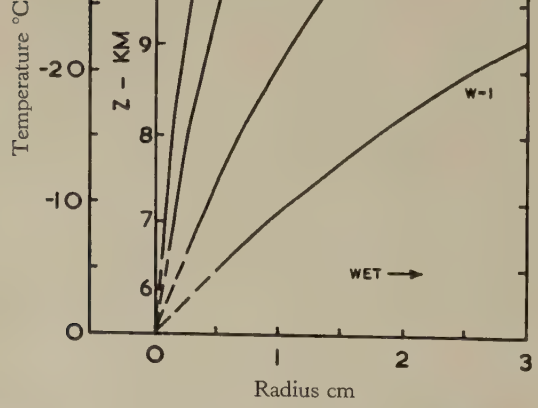

Figure 5. The condition for the entry of hailstones into the wet-growth phase. If the position of a hailsto on the diagram (determined by its size and the cloud temperature) is to the right of the appropriate liquid-wat concentration isopleth then its surface is wet; if to the left, its surface is dry.

Caporiacco (1959) and Macklin, Strauch and Ludlam (1960). It has been found that the drag coefficient of actual stones of markedly aspherical shape may be almost double those of spheres of the same mass, but they fall in a preferred attitude, in which the rate of accretion on the collecting surface is considerably increased, so that even in these cases it is thought that the critical liquid-water concentrations are unlikely to be underestimated by a factor of as much as 2. The curve shows that even in modest liquid-water concentrations, large hailstones are generally in the wet-growth regime. However, this need not imply a restriction on the growth rate as formerly supposed, since all of the liquid water and ice particles may be accreted and retained.

Examination of sections of hailstones a few centimetres in diameter indicates that the outer layers have been appreciably affected by the air flow (see, e.g., Ludlam and Macklin 1959). The 'front' surfaces are relatively smooth, while the 'back' surfaces are very irregular, with knobs several millimetres across, and quite often a depression is observed in a roughly central position. Such shapes cannot be due to melting, since the change in size in falling to the ground is very small (Ludlam 1958); it is considered that such a shape can arise only when the stone is very wet, and that the moulding by the airstream is enhanced when the ice is spongy.

As far as is known, large hailstones which arrive at the ground are hard; commonly they are reported to rebound from hard surfaces as much as several metres into the air. Thus, although a large part of the ice deposited during growth may be spongy, the outer layers of the large stones are probably frozen completely before their final fall. At levels where the temperature is below $-35°C$ a considerable fraction of the cloud water is likely to be frozen either by homogeneous or heterogeneous nucleation (see Langham and Mason 1958) and stones which are in the wet condition at these levels will accrete both the water droplets and ice particles. This produces an at least partially consolidated outer layer. Even at levels where the temperature is below $-40°C$ and virtually all of the cloud water is frozen, accretion of ice particles alone can continue until the outer surface is hardened. Further freezing of the water in the stones will occur either in the cloud tops at temperatures below $-40°C$ when no more liquid is accreted or in the clear air at temperatures below about $0°C$. The stones are then still likely to have liquid inclusions below the surface layer but it is unlikely that this would be noticed at the ground; stones preserved for examination have always been stored in a refrigerator, in which after a few hours, they would become completely frozen.

When freezing spreads inwards in this manner from the outer surface, the air which comes out of solution cannot escape but remains in bubbles which are trapped in the ice and cause it to have a milky or opaque appearance. The radial cracks which are often observed in large hailstones (see, e.g., Weickmann 1953) may be due to the strains which arise as freezing progresses under a hardened outer coat.

If hailstones grow by accreting significant concentrations of ice particles as well as supercooled droplets, then this must be reflected in their crystallographic structure. The writer has examined, between crossed polaroids, sections of some sixty stones which fell during a recent storm. The sections were made in the way previously mentioned, by melting down the stones between parallel metal plates. (This technique is useful only when the densities of the stones are high and the melting process does not affect the internal structure). In general, the centres of the stones were composed of a few single crystals, sometimes over a centimetre long, while the outer parts were commonly composed of crystals a few hundred microns across. This was not always the case, however; in some stones the central crystals extended to the outer edge even though the stones were 3 to 5 cm across (this investigation is being continued and details will be published later). The size of the stones examined was such that it is probable they were growing in the wet condition in the latter stages of their growth, so that the only nuclei which could have been effective are small ice particles. It has already been shown that the size of the single crystals in spongy ice is affected by the presence of ice particles. A possible interpretation of the micro-crystalline structure of hailstones is that it reflects the concentration of ice particles present in the cloud.

Acknowledgments

The writer is indebted to Dr. F. H. Ludlam for many helpful discussions during t course of this work, and to Mr. D. A. Rogers for his assistance with the experimen He is also indebted to the Royal Aircraft Establishment for providing the cold-roo facility and to the Commonwealth Scientific and Industrial Research Organisation Australia for the support of studies including the present investigation.

References

Bigg, E. K. 1953 'The supercooling of water,' *Proc. Phys. Soc. B.*, **66**, p. 6

Bigg, F. J., Day, D. J. and McNaughton, I. I. 1959 'Measurement of ice-crystal clouds,' *Aircraft Ice-Protect Conf.*, Napier & Son Ltd., Luton.

Brun, E. A. 1957 'Icing problems and recommended solutions,' *N.A.T. Advisory Group Aeronaut. Res. and De AGARDOGRAPH 16.*

Clark, V. 1948 'Icing nomenclature,' Mount Washington Icing Res. R 1946-47, *U.S.A.F. Tech. Rep.* No. 5676, p. 415.

Fraser, D., Rush, C. K. and Baxter, D. 1952 'Thermodynamic limitation of ice accretion instrument *Lab. Rep. LR-32*, N.A.E. Canada.

Gaviola, E. and Fuertes, F. A. 1947 'Hail formation, vertical currents and icing of aircra *J. Met.*, **4**, p. 116.

Hallett, J. 1960 'Crystal growth and the formation of spikes on the surf of supercooled water,' *J. Glaciol.*, **3**, No. 28, p. 698.

Landis, D. S. 1907 *Quart. J. R. Met. Soc.*, **33**, p. 63.

Langham, E. J. and Mason, B. J. 1958 'The heterogeneous and homogeneous nucleation supercooled water,' *Proc. Roy. Soc. A.*, **247**, p. 493.

Langmuir, I and Blodgett, K. B. 1946 'A mathematical investigation of water-droplet trajectori *U.S.A.A.F. Tech. Rep.* No. 5418.

List, R. 1959 'Wachstum von Eis – Wassergemischen in Hagelversuc skanal,' *Helvetica Physica Acta*, **32**, p. 293.

Ludlam, F. H. 1950 'The composition of coagulation-elements in cumulonimbu *Quart. J. R. Met. Soc.*, **76**, p. 52.

1951 'The heat economy of a rimed cylinder,' *Ibid.*, **77**, p. 66

1958 'The hail problem,' *Nubila*, **1**, p. 13.

1959 'Hailstorm studies 1958,' *Ibid.*, **2**, p. 7.

Ludlam, F. H. and Macklin, W. C. 1959 'Some aspects of a severe storm in S.E. England,' *Ibid.*, p. 38.

Macklin, W. C., Strauch, E. and Ludlam, F. H. 1960 'The density of hailstones collected from a summer storm *Ibid.*, **3**, p. 12.

Mason, B. J. and Maybank, J. 1960 'The fragmentation and electrification of freezing wat drops,' *Quart. J. R. Met. Soc.*, **86**, p. 176.

McAdams, W. H. 1954 *Heat transmission*, McGraw-Hill, New York.

Minervin, V. E. 1956 'On measurements of the liquid water content and of i accretion in supercooled clouds and on some err of these measurements,' *Tsent. Aerol. Obs.*, Mosco (T. Vyp. **17**, p. 15).

Pollard, A. E. 1936 'Large hailstones at Northampton,' *Met. Mag.*, Londo **71**, p. 15.

Schumann, T. E. W. 1938 'The theory of hailstone formation,' *Quart. J. R. Met. So* **64**, p. 3.

Steyn, K. 1950 *The Pretoria hailstorm*, Public Works of South Afric **10**, No. 75.

Vittori, O. and Caporiacco, G. 1959 'The density of hailstones,' *Nubila*, **2**, p. 52.

Weickmann, H. K. 1953 'Precipitation in cumulonimbus,' *Thunderstorm electricit* Univ. Chicago Press, p. 66.

551.521.14 : 551.584.42

Short-wave reflection coefficient for a field of maize

By W. G. GRAHAM and K. M. KING
Ontario Agricultural College, Guelph, Canada

(Manuscript received 16 June 1960; communicated by P. D. McTaggart-Cowan

Summary

Hourly and daily determinations of the reflection coefficient for a field of maize (*Zea mays*) were made on 17 days from July to September 1958. An Eppley pyrheliometer was used to measure incident solar radiation and a Kipp solarimeter was used to measure reflected radiation. The hourly determinations showed increased reflection at low solar altitudes. With a moist soil, the reflection coefficient based on the daily radiation was 0·12 to 0·15 when the plants were small and 0·17 to 0·19 when the crop was fully developed. When the soil surface was dry and the plants small, the coefficient was 0·21. Tassel formation and freezing of the plants had no effect on reflection.

1. Introduction

Monteith (1959) has reported the short-wave radiation reflection coefficient for several crops including grass, lucern, potatoes, sugar beet and wheat. For all these crops, the reflection coefficient was about 0·25 when the vegetation completely covered the ground, with lower values for potatoes and sugar beet when the plants did not completely cover the ground surface, for wheat on ripening, and for sugar beet near maturity. Kuhn (1961, unpublished) using an airborne beam reflector (Kuhn and Suomi 1958) obtained reflection coefficients of 0·08 to 0·12 for corn fields in Iowa and South Dakota. The diurnal variation was small and identical with that for a pasture as reported earlier by Kuhn and Suomi (1958).

2. Experimental site and methods

Measurements were made during 1958 over a corn plot near Guelph, Ontario (lat. 43° 30′ N). The plants were about 10 in. apart in 36 in. rows running in a north-east to south-west direction. The colour of the moist loam surface soil is very dark grey brown, 10YR 3/2 (Munsell 1954).

Data were obtained for 17 days from 15 July to 2 October. For all days, except 20 July, the soil had recently received rain or sprinkler irrigation so that the soil surface was moist. That is, the moisture content of the 0 to 2 cm soil layer was greater than 25 per cent on an oven-dry weight basis.

Incoming short-wave radiation was measured with an Eppley pyrheliometer mounted on the roof of a building about 900 m from the corn plot. Reflected short-wave radiation was measured by an inverted Kipp solarimeter mounted about 2 m above the corn plants. Both instruments were calibrated in an upright position at the beginning of the season by the Canada Department of Transport. Tests on an inverted Kipp solarimeter indicated that the calibration was within one per cent of the calibration in the upright position.

The outputs from both instruments were recorded on self-balancing potentiometers. The incoming radiation was sampled at two-minute intervals and the reflected radiation was sampled at three-minute intervals. From these instantaneous measurements the hourly and daily values of solar and reflected radiation were determined. Hourly values of reflection coefficient were obtained from the hourly radiation totals and daily reflection coefficients were obtained from the daily radiation totals.

3. Diurnal variation in reflection coefficient

Fig. 1 shows the diurnal variation in the reflection coefficient for four selected days. On 16 July, representative of days when the corn plants were small and the soil surface moist, the plants were approximately 50 cm high and covered 15 per cent of the soil surface. Plant height

was measured to leaf or tassel tip and percentage ground cover was determined by planimeterin photographs taken vertically from 7 m above the soil surface. The mid-day value of 0·10 — 0· for the reflection coefficient is similar to values reported for moist soil in the *Smithsonian Meteo ological Tables* (1951). The variations between 10 and 16 LMT may be due to variability in the clou conditions. Cumulus clouds started to form about 1100 and remained to 1700 hr. During thes hours the direct solar radiation was reduced by cloud approximately 50 per cent of the tim At low solar altitudes the reflection coefficient increased to 0·20-0·25. Fig. 2 shows the reflecti coefficient plotted against the solar altitude. The arrows indicate advancing time.

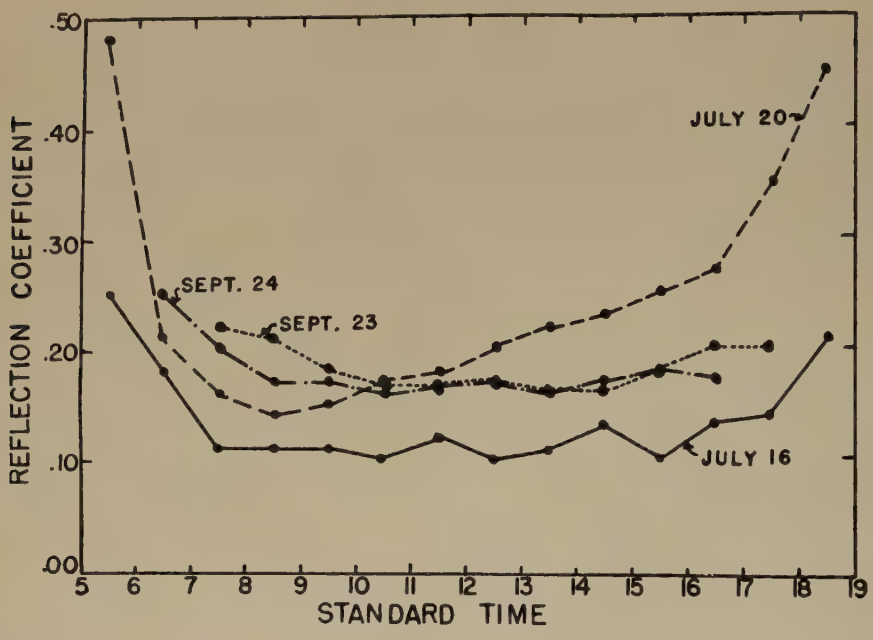

Figure 1. Diurnal variation in reflection coefficient of a field of *Zea mays* for four selected days, 1958.

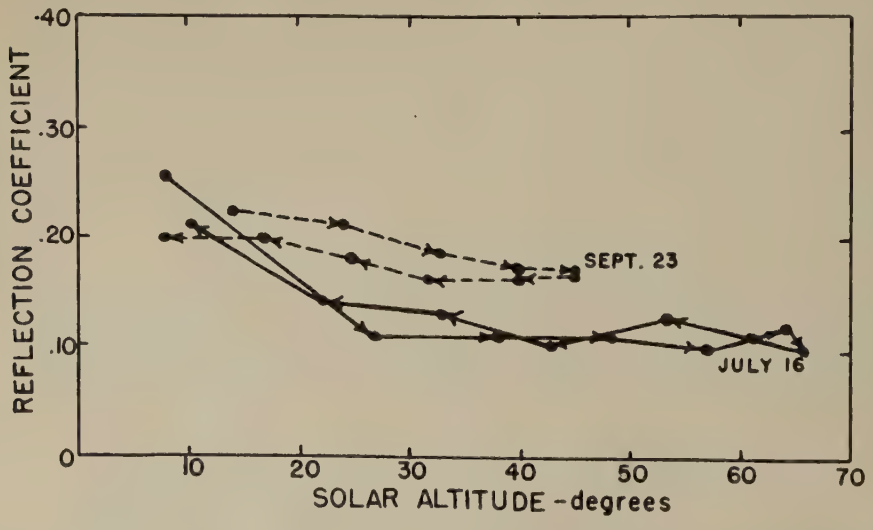

Figure 2. Variation of reflection coefficient with solar altitude for a field of *Zea mays* on two selected days 1958.

On 20 July the plants were small and the soil surface was drying. The soil surface was nearly air-dry by late afternoon, and at 1600 on the next day the 0-2 mm layer had a moisture content of only 3·9 per cent. Reflection coefficients of 0·20-0·25 for the dry soil are in agreement with previously reported values in the *Smithsonian Meteorological Tables* (1951). Low solar altitude had a greater effect on the reflection coefficient for the dry soil than for the moist soil.

The curves for 23 and 24 September illustrate the diurnal variation when the plants were fully developed. On these dates the corn was about 225 cm high and the ground cover was 80 per cent, the maximum attained. The corn was in the dent stage with the leaves turgid and green. A reflection coefficient of about 0·17 was found for the mid-day hours under these conditions. This value is similar to values reported for forests but much less than those given by Monteith for plants with a lower growth habit. Undoubtedly more of the radiant energy is trapped in the corn plants because of the greater depth of vegetation into which the radiation penetrates. In Fig. 2, it is shown that at low solar altitudes the reflection coefficient increased to 0·20-0·25. Less radiation is trapped at low solar altitudes presumably because the crop, as seen by the sun, becomes more like a flat surface.

The curves for 23 and 24 September may also be compared with respect to cloud conditions. September 23 was a relatively clear day with scattered cumulus clouds, whereas on 24 September the sky was heavily overcast for the entire day. The incoming solar radiation on 23 September was 446 langleys and on 24 September was 177 langleys. On these two days the reflection coefficients were equal for the mid-day hours, but at low solar altitudes, the reflection coefficient was slightly smaller on the overcast day than on the relatively clear day. This is in agreement with the observations of reflection coefficient over Lake Hefner (Anderson 1952).

4. Seasonal variation in reflection coefficient

Fig. 3 gives the daily reflection coefficients for the 17 days of observation. In July when the crop cover was 20 to 40 per cent, the reflection coefficient was in the range 0·12-0·15, for a moist soil surface. In August and September when the cover had attained its maximum value of 70 to 80 per cent, the reflection coefficient was between 0·17 and 0·19. Tassel formation (production of male flowers) first began on 5 August and was completely developed by 25 August, but this apparently had no effect on the reflectivity. Also, the freezing of the plants on the night of 1 October, resulting in desiccation and browning of the leaves, had no effect on the reflection coefficient measured on 2 October. As Monteith (1959) indicates, the colour of the plants may have little effect on the reflection coefficient since a large portion of the reflected solar radiation lies outside of the visible range.

The mean solar altitude was, of course, decreasing as the season advanced, from 67° at noon on 15 July to 42° on 1 October.

This may have a tendency to increase the reflection coefficient as the season advances as illustrated by Dirmhirn (1953). In the measurements here reported, this solar altitude effect may have been masked by vegetative changes, to produce under moist soil conditions an apparently constant reflection coefficient in *Zea mays* from the start of tassel formation to maturity.

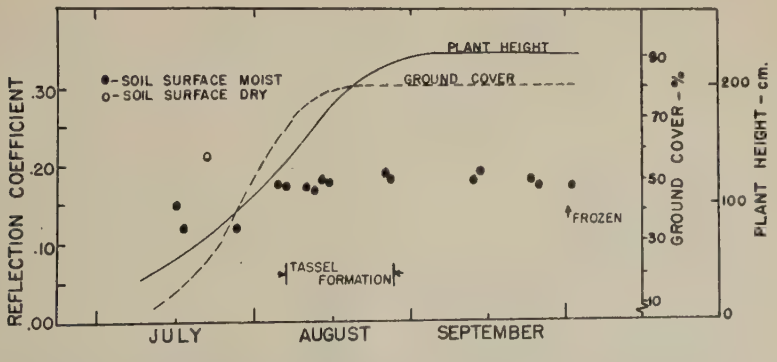

Figure 3. Daily reflection coefficient for seventeen days and crop growth for *Zea mays*, July to October 1958.

Acknowledgment

The authors are indebted to the Meteorological Branch, Canada Department of Transpo for the loan and calibration of the Kipp solarimeter.

References

Anderson, E. R.	1952	'Water-loss investigations,' **1** – Lake Hefner Studies Tech Rep. *Geological Survey Circular 229*, pp. 71-119.
Dirmhirn, I.	1953	*Wetter und Leben*, **5**, pp. 86-94.
Kuhn, P. M.	1961	Unpublished, personal communication.
Kuhn, P. M. and Suomi, V. E.	1958	*J. Met.*, **15**, pp. 172-174.
Monteith, J. L.	1959	*Quart. J. R. Met. Soc.*, **85**, pp. 386-392.
Munsell.	1954	*Munsell Soil-Colour Charts*, Munsell Colour Co. Inc. Baltimore 2, Maryland.
Smithsonian Institute	1951	*Smithsonian Meteorological Tables*, 6th Rev. Ed.

551.521.33

A note on the regular model of an absorption band

By R. M. GOODY
Harvard University, U.S.A.

(Manuscript received 18 January 1961)

1. Introduction

The regular model of an absorption band was the first realistic model to be proposed (Elsasser 1942), but there has never been a convincing experimental demonstration of its validity. This is partly because of overlapping by weak upper-state and isotope bands, and partly because of the difficulty of separating the variables in the complex transcendental function $\bar{A}_E(y, z)$ (the average absorption), where

$$y = \alpha/\delta, \quad (1)$$

$$z = Sm/2\pi\alpha, \quad (2)$$

and

$$\left.\begin{aligned} \alpha &= \text{line width} \\ \delta &= \text{line spacing} \\ S &= \text{line intensity} \end{aligned}\right\} \text{ assumed constant from line to line,}$$

$$m = \text{amount of absorbing gas.}$$

The publication of detailed measurements on the *P*- and *R*-branch maxima of the CO fundamental by Burch and Williams (1960) largely overcomes the first difficulty, for upper-state bands are negligible, and, near the *R*-branch maximum, isotopic lines do not appear in the solar spectrum (Migeotte, Neven and Swensson 1956; this is not true of the *P*-branch which would have to be treated as the product of two Elsasser bands, one for $C^{12}O$ and one for $C^{13}O$). The second difficulty can be overcome with the help of a suggestion by Dr. W. L. Godson which, to the writer's knowledge, has never been published. The only difficulty with this band is that the large rotational constant gives considerable intensity changes between adjacent lines, thus weakening the fundamental hypothesis of uniformity, upon which the regular model is based.

2. Godson's approximation

On the basis of the behaviour of $\bar{A}_E$ in the ' strong ' and ' weak line ' limits, Godson suggested that a relation of the type

$$\frac{1}{yz}\,\mathrm{Erf}^{-1}\,\bar{A}_E = F(z), \qquad (3)$$

should be approximately valid under all conditions. A numerical investigation shows that the condition for validity of (3) is $y \ll 1$; in fact $\bar{A}_E$ is given within 1 per cent if $y \ll 0{\cdot}1$. If we go to the limit of small y holding m constant $\bar{A}_E$ tends to the single-line asymptotic limit $\bar{A}_{S.L.}$. It follows that the function $F(z)$ must be determined by

$$yz\,F(z) = \frac{\sqrt{\pi}}{2}\,\bar{A}_{S.L.} \qquad (4)$$

$$= \pi^{3/2}\,yz\,e^{-z}\,(I_0(z) + I_1(z)), \qquad (5)$$

if the lines have the Lorentz profile, where I_0 and I_1 are hyperbolic Bessel functions. An alternative statement of Godson's approximation is therefore

$$\bar{A}_E = \mathrm{Erf}\,\frac{\sqrt{\pi}}{2}\,\bar{A}_{S.L.} \qquad (6)$$

It should be noted in passing that while Eq. (6) has a rather general form, somewhat analogous to that for the random model, it has only been proved for Lorentz lines of equal intensity and its extension to other cases cannot be presumed without proof.

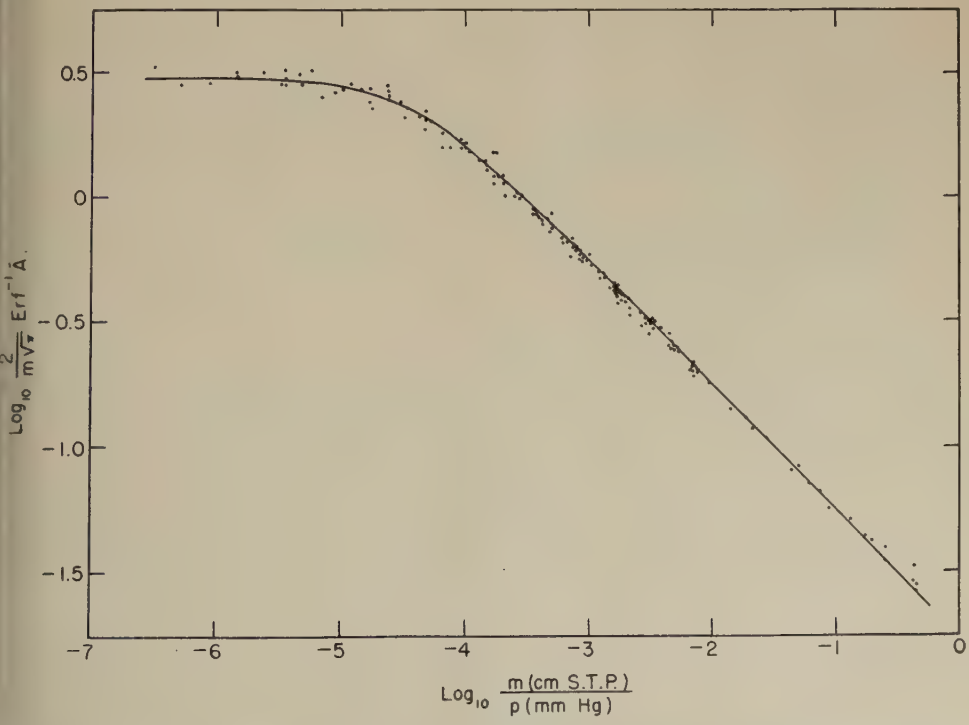

Figure 1. Absorption at the R-branch maximum of the fundamental band of CO. (Temperature is 303°K. Pressure range 5 to 3,000 mm Hg. Range of amount $9{\cdot}6 \times 10^{-4}$ to $4{\cdot}6 \times 10$ cm S.T.P. Path lengths 1·55, 6·35 and 400 cm. Data of Burch and Williams (1960)).

3. Results and discussion

In Fig. 1 are plotted results for the *R*-branch of the CO vibration band. The chosen axes a

$$\frac{m}{p} = \frac{2\pi\,\alpha/p}{S}\,z, \qquad ($$

where, according to the Lorentz theory, α/p is a constant, and

$$\frac{2}{m\sqrt{\pi}}\,\mathrm{Erf}^{-1}\,\bar{A} = \frac{2}{\sqrt{\pi}}\,\frac{2\pi\delta}{S}\,\frac{1}{yz}\,\mathrm{Erf}^{-1}\,\bar{A}. \qquad (3$$

Attempts to distinguish between runs at constant m or constant path length using differer symbols gave a chaotic muddle of points showing that Eq. (3) is correct to a high degree of accurac The line in the figure is given by Eq. (5), adjusted for best fit.

Not only is there good qualitative agreement between theory and observation, but the valu of S and α which can be derived, are in excellent agreement with high-resolution measurement Taking $\delta = 3{\cdot}60\ \mathrm{cm}^{-1}$ from published spectra we find from Fig. 1 that

$$S = 10{\cdot}77\ \mathrm{cm}^{-1}\,(\mathrm{cm\ S.T.P.})^{-1},$$

$$\alpha = 0{\cdot}069\ \mathrm{cm}^{-1}\ \text{at S.T.P.}$$

For the strong lines in the *R*-branch (ordinal value $\simeq 7$), at 303°K, the ratio between line an band intensity is 0·043, so we can obtain for the band intensity

$$S\,(\text{band}) = 245\ \mathrm{cm}^{-1}\,(\mathrm{cm\ S.T.P.})^{-1}.$$

Penner and Weber (1951) using a different technique, which is not necessarily more precise, fin

$$S\,(\text{band}) = 237\ \mathrm{cm}^{-1}\,(\mathrm{cm\ S.T.P.})^{-1}.$$

Shaw and France (1956) find that this value agrees well with their high-resolution measurement These authors also find, for similar ordinal values, line widths of 0·069, 0·063 and 0·068 cm at S.T.P. Unpublished results by Benedict give $0{\cdot}067\ \mathrm{cm}^{-1}$. The agreement between all thes results is excellent, confirming in a striking way the usefulness of the regular model under appro riate conditions.

We may note that at 3,000 mm Hg the value of y is 0·076 and therefore the applicablit of Godson's approximation is justified *a posteriori*.

Acknowledgments

I am indebted to Dr. Burch for details of his unpublished measurements, and to the Nationa Science Foundation for grants supporting atmospheric research at Harvard University.

References

Burch, D. E. and Williams, D. 1960 'Infra-red absorption by minor atmospheric constituents *Sci. Rep.* No. 1, Contract AF 19 (604)–2633; Ohi State University.

Elsasser, W. M. 1942 *Harvard Met. Studies*, No. 6.

Migeotte, M., Neven, L. and Swensson, J. 1956 'The solar spectrum from 2·8 to 23·7 microns,' Pt. 1 Photometric Atlas, *Mém. Soc. Roy. Sci.*, Liège Special Volume No. 1.

Penner, S. S. and Weber, D. 1951 *J. Chem. Phys.*, **19**, p. 807.

Shaw, J. H. and France, W. L. 1956 'Intensities and widths of single lines of the 4·7 micro CO fundamental band' *AFCRC–TN–56–466*; Ohi State University.

551.507.362.2 : 551.508.953 : 551.521.18

Design of interference filters for the observation of infra-red emission from atmospheric carbon dioxide by an earth satellite

By S. D. SMITH

J. J. Thomson Physical Laboratory, University of Reading

(Manuscript received 16 February 1961)

SUMMARY

Detailed proposals are made for the design of a high-order Fabry-Perot type interference filter in which the transmission bands of the filter are exactly matched to 15 lines of the *R*-branch of the CO_2 spectrum near 15 μ. The striking energy advantages of such an interferometer are discussed and it is shown that use of an optically worked high-index germanium spacer leads to a further considerable increase in light grasp. It is concluded that technical problems are not severe and a calculation of the energy that can be collected by the proposed system suggests that a detector of area 9 mm^2 with a noise-equivalent-power of 10^{-10} watts (i.e. comparable with a standard Golay cell) can provide adequate sensitivity.

1. INTRODUCTION

Kaplan (1959) has suggested that the temperature structure of the upper atmosphere can be explored by emission measurements from space, choosing varying absorption coefficients to give emission dominated by different levels. He suggests the use of a grating spectrometer and a band width of 5 cm^{-1}. This experiment has the disadvantage that such a band extends across several lines and interpretation is difficult. Houghton (1961) has recently proposed a more efficient method of using the collected energy by simultaneously passing 15 lines with a Fabry-Perot interferometer suitably matched. This system elegantly simplifies the interpretation by restricting the emission measured to that from individual lines (0·1 cm^{-1} in width), while reducing the total band-width (to 1·5 cm^{-1}) and hence the energy gathered, by a factor of four. However, the use of a Fabry-Perot interferometer implies very considerable advantages in addition to measuring 15 lines simultaneously. Several workers have shown (e.g., Jacquinot (1954)) that for a given resolving power, the flux through a Fabry-Perot etalon ($\psi_{F.P.}$) (with air as spacer) and that through a grating spectrometer ($\psi_{G.}$) is given by $\psi_{F.P.}/\psi_{G.} = 3{\cdot}4/\beta$, for equal areas, where β is the angular height of the slit. Kaplan takes as his model the spectrometer described by Goody (1957), for which $\beta = 1/50$. Thus the energy gain of the interferometer could be of the order of 170. The Interferometer derives its flux gain from its greater dispersion and its use of circular entrance and exit pupils instead of rectangular slits. For an emission observation from an extended source, in which the area of the entrance pupil determines the collected flux and which requires several bands to be passed simultaneously, the *interferometer* is an ideal instrument; it can be precisely designed for its particular task.

If germanium (refractive index 4·0) is used as the spacer material, instead of an air gap, the maximum permitted angle of incidence is increased by a factor of 4 and the light grasp by 16 times. Thus at its best, this sytem would show a gain of $\sim$4,000 over a grating looking at one line, or of 1,000 over Kaplan's proposal (i.e., 5 cm^{-1} band-width).

It is not realistic, however, to suppose that the area of the interferometer could be equal to that of the grating : a convenient size would lead to a loss of a factor of 10 (i.e., 6 in. $\times$ 6 in. $\rightarrow$ 2 in. diameter). However, the flux gain is still $\sim$ 100, the instrument is compact and the only really precise feature in its construction (i.e., the optical working of the spacer) is unlikely to be affected by launching stresses.

2. Design

The transmission maxima of the interferometer will occur at wave-numbers ν_P given by

$$\nu_P = N/2nd \cos\phi \quad . \quad . \quad . \quad . \quad . \quad (1$$

where N is the order, n the refractive index, d the thickness of the interferometer and ϕ the angl of incidence within the spacer layer. Thus the peaks are equally spaced in wave-number an separated, at normal incidence, by $\Delta\nu$ where $\Delta\nu = 1/2nd$. For a separation of 1·6 cm^{-1} nd = 3·12 mm and at 676 cm^{-1} (the centre of the CO_2 band), N = 415.

The shape of the pass bands is given by the well known Airy sum

$$T(\nu) = \frac{1}{\left(1 + \frac{A}{T}\right)^2} \cdot \frac{1}{1 + \frac{4R}{(1-R)^2}\sin^2\theta/2} \quad . \quad . \quad . \quad (2$$

where $T(\nu)$ is the transmittance of the interferometer, A, T, R are absorption, transmittance an reflectance of the bounding interfaces, and $\theta = 4\pi nd\,\nu\cos\phi$.

From this formula, a half-width of 0·1 cm^{-1} implies that R = 0·82 and this would be a con venient value to match the width of the CO_2 lines. The first term in Eq. (2) shows that the max imum of transmission (at $\sin^2\theta/2 = 0$) is limited by the value of A/T. A low value of A/T combined with a reflectivity of 0·82 can readily be obtained by the use of quarter-wave stacks o films of alternatively high (H) and low (L) index. With germanium (n_H = 4·0) and calcium fluorid (n_L = 1·35) only two layers are required, if combined with a germanium spacer – the theoretica reflectivity is 0·89 but may be a little lower in practice.

The interferometer will, therefore, be very simple – an optically worked, plane parallel fla of germanium 0·78 mm thick coated with two layers on each side (Fig. 1 (a)).

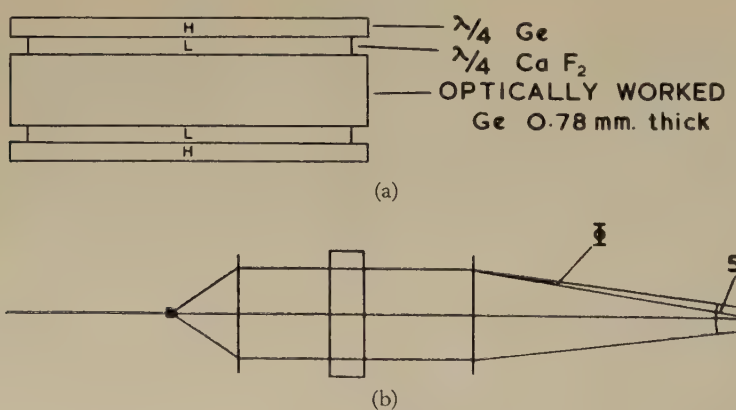

Figure 1. (a) Construction of the interferometer; (b) Optical system.

The suggested half-width (0·1 cm^{-1}) implies a finesse (ratio of spacing of peaks to half- width) of 16 : 1. The maximum finesse obtainable is limited by the flatness and parallelism of the etalon and is approximately the quotient of half the wavelength and the maximum departure from flatness. Thus a finesse of 16 : 1 at 15 μ implies that the plate must be flat and parallel to 0·5 μ, i.e., to one wavelength in the visible. This is not a severe requirement by normal optical standards where flats good to $\lambda/20$ are achieved. That the parallelism can also be obtained is evident from the results of Rank, Bennet and Cronemeyer (1954), who used a 3 mm thick plate of uncoated germanium, ground and polished flat and parallel to 1 sec. of arc over a diameter of 1·1 in. This implied a tolerance of 0·1 μ (i.e., five times as good as required for our interfero- meter) and indeed, good interference fringes at 2 μ were obtained, from which they deduced dispersion and temperature dependence of refractive index.

Germanium is a good optical material with excellent transparency and high index and is obtainable in large single crystals of high purity and uniform properties which should prove very suitable. Alternatively, if there is difficulty in the technique of grinding and polishing flat and parallel (no method was described in the paper of Rank *et al.*), silicon could be used. This material is transparent in the region in which image convertors can be used so that transmitted Fabry-Perot rings could be made visible, thus facilitating the optical working.

Thin self-supporting slices of both these materials have been made down to thicknesses of 1 μ, so that their mechanical properties should be satisfactory.

3. Flux transmitted by the interferometer

This is determined by the area of the interferometer and the maximum angle of incidence (Φ) which is permitted inside the spacer layer. The shape of the transmission band of the interferometer is given by summing all rays from normal incidence to Φ. If $T'(\nu)$ is the transmittance as a function of wave-number under these circumstances, then

$$T'(\nu) = \frac{1}{\epsilon}\int_{\theta_0}^{\theta_0+\epsilon} \frac{d\theta}{1 + F\sin^2\theta/2}$$

where $F = 4R/(1-R)^2$, ϵ is the maximum change of θ with angle of incidence and $\theta_0 = 4\pi nd\,\nu$.

This integral has been given by Polster (1954) and numerical calculation (Smith and Heavens 1957) shows that a value of $\epsilon/2\pi$ equivalent to $1/32^{th}$ of an order does not unduly distort a pass-band with a finesse of 16. ϵ represents the maximum change in phase difference between successive beams introduced by the angle of incidence Φ and hence

$$\epsilon = 4\pi nd\,\nu - 4\pi nd\,\nu\cos\Phi \simeq 2\pi nd\,\nu\,\Phi^2.$$

Since $N = 2nd\,\nu$

$$\Phi^1 = \frac{G}{2\pi}\cdot\frac{2}{N}$$

whence $\Phi = 1/84$ radian or 0·7 degrees.

Suppose we assume an interferometer of 2·5 cm diameter and that radiation is collected from a 5° cone to give good spatial resolution; this implies a focal length of 25 cm (Fig. 1 (b)). With a germanium etalon, the radius of the entrance pupil is $4 \times 25/84 = 1{\cdot}2$ cm and the area is 4·2 cm^2. A reduction of about 7 : 1 would then be required to make all the energy fall on a detector of 3 mm × 3 mm, i.e., a mirror of aperture ratio 1·2, which is quite usual.

The power falling on an area of 4·24 cm^2 in a 5° cone from a black body at 200°K is $1{\cdot}5 \times 10^{-6}$ watts in a bandwidth of 1·5 cm^{-1}. If we assume a transmission coefficient of 0·1 for the interferometer and its auxiliary filtering and require an accuracy of 1 per cent, the detector must have a noise equivalent power of $1{\cdot}5 \times 10^{-9}$ watts and an area of 3 × 3 mm^2. This is some 10 times greater than the minimum detectable energy of a standard Golay-cell detector.

4. Scanning and temperature stability

It is proposed to scan from the peaks to the troughs of the CO_2 lines by varying the angle of incidence. A tilt of about 11° would be required.

The temperature dependence of refractive index can cause a drift in the positions of the transmission bands which at a maximum may be 0·1 cm^{-1}/°C. This need not be serious if the interferometer is continually scanning from peak to trough at a rate fast compared with the thermal drifts.

5. Auxiliary filtering

A suitable band-pass filter with a width of 25 cm^{-1} at 667 cm^{-1} has previously been designed by the author (1958). It is a seven-layer system HLLHLHLLH of germanium and calcium fluoride and has been successfully constructed at 2 μ. The filter can be modified for deposition on a germanium substrate, which is likely to be the most convenient, by insertion of a quarter-wave of index 2·0 (M) becoming GeMHLLHLHLLH. A calculated curve of the transmittance of this filter and the interferometer is shown in Fig. 2. Since the auxiliary filter will also have a pass band at about 1,000 cm^{-1} further auxiliary filters of InSb (transmission) and MgO (reststrahlen) may be required, but both these are of very high efficiency.

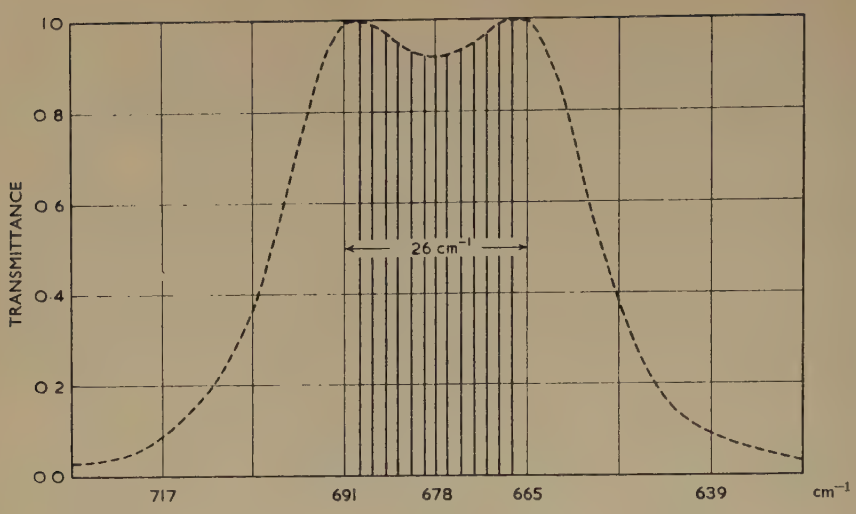

Figure 2. Transmittance of interferometer and auxiliary filters.

Conclusions

Detailed examination of the requirements of a Fabry-Perot interference filter constructed to fit the CO_2 spectrum shows that the instrument is feasible and can collect sufficient energy to bring the proposed CO_2 emission experiment within the range of attainable detector sensitivity. A fast photo-conductive detector such as Zn-doped germanium would probably be the most convenient but if the interferometer achieves its predicted performance detectors of lower sensitivity such as uncooled bolometers could be considered. Such detectors are sufficiently rugged to withstand rocket launching.

Acknowledgments

The author wishes to acknowledge discussion with Messrs. J. T. Houghton, S. C. Warren of Standard Telephones and Cables, and Professor P. A. Sheppard, Chairman of the Meteorology Working Group of the British National Committee for Space Research. A development programme on interference filters is being initiated with the financial support of the Space Research Committee.

References

Goody, R. M.	1957	*Quart. J. R. Met. Soc.*, **83**, p. 517.
Houghton, J. T.	1961	*Ibid.*, **87**, p. 102.
Jacquinot, P.	1954	*J. Opt. Soc. Amer.*, **44**, p. 761.
Kaplan, L. D.	1959	*Ibid.*, **49**, p. 1004.
Polster, H. D.	1954	*Ibid.*, **44**, p. 503.
Rank, D. H., Bennet, H. E. and Cronemeyer, D. C.	1954	*Ibid.*, **44**, p. 13.
Smith, S. D. and Heavens, O. S.	1957	*J. Sci. Instr.*, **34**, p. 392.
Smith, S. D.	1958	*J. Opt. Soc. Amer.*, **48**, p. 43.

Correspondence

551.524.34 : 551.583.1

Temperature fluctuations and trends over the earth

By H. E. Landsberg and J. M. Mitchell, Jr.

One of us (Mitchell 1961) recently completed a study similar to that of Callendar. Inasmuch as this study was based on a rather different selection of data and method of analysis, due originally to Willett (1950), it is of some interest to compare Callendar's 30-yr changes of annual mean temperature in various latitude bands, shown in his Table 1, with the comparable changes derived from Willett and Mitchell's data.

Such a comparison is shown in the accompanying Table, and reveals good agreement in all latitude zones except the south temperate zone. There, Callendar's value is about twice as large as that of Willett and Mitchell. Without further information on Callendar's choice of stations in that zone, the reason for this discrepancy is obscure. At any rate, the differing trends found by Callendar for north temperate and south temperate regions is seen from Willett and Mitchell's data *not* to have followed solely from the fact that dissimilar increments of latitude were compared : a point that seemed to us to deserve verification.

The generally favourable outcome of the accompanying comparisons tends to justify Willett and Mitchell's earlier belief that little is gained by the use of more than the 120 to 180 stations they chose for their studies. This follows because additional stations are concentrated in relatively small geographical regions, whence the information they contribute to trend analysis is highly redundant.

Callendar's estimate of the magnitude of the ' urban effect ' in his data agrees rather well with an estimate Mitchell has made for his and Willett's data. We can therefore agree with Callendar that urban growth has probably had a relatively small effect on the computed global trends, although we share a hope that this matter can be investigated more thoroughly in the future.

We also agree with Callendar that the short-term fluctuations and the long-term trends of global climate should be attributed to different causes. On the other hand, Callendar's reasons for dismissing the solar and dust hypotheses of long-term global trends do not appear compelling. It seems to us that the *direct* influence on the global temperature field of factors that change the heating field of the atmosphere may become overwhelmed by the *indirect* influence on temperature governed by induced changes of the general circulation. Incidentally, the dust hypothesis may require further attention because of the remarkable variations of dust in interplanetary space detected by means of satellite observations (Dubin 1960).

Further, several facts conspire to challenge Callendar's conclusion that the lesser secular warming of the south temperate zone, as compared with the north temperate zone, may be attributable to greater industrial CO_2 production in the Northern Hemisphere. Firstly, a comparison of trends for larger but equal ranges of latitude in the two hemispheres reveals that the excess of warming in the Northern Hemisphere is relatively small (see comparison for 0-60°N and 0-60°S at the bottom of the accompanying table), and secondly, Vogel (1961) has recently determined from C^{14} measurements that the mean exchange time of air between the northern and southern tropospheres is of the order of one or two years. This represents a rate of mixing that is much too rapid to enable a substantially greater secular increase of industrial CO_2 in the Northern Hemisphere than in the Southern. Vogel has also assembled new data on the secularly increasing dilution of C^{14} in both hemispheres, due to fossil fuel combustion, that indicate approximately equal secular increases of CO_2 in both hemispheres. It thus appears that the solitary tree in the Southern Hemisphere analysed from this viewpoint by Arnold and Anderson (1957) was for some reason anomalous. Thirdly, the observations over the Atlantic from 60°N to 60°S published by Takahashi (1961) show no significant differences in atmospheric CO_2 concentration between the hemispheres.

A number of other questions come to mind when reading Callendar's paper. For example, how many stations contributed data for the various curves in his Figs. 1 and 2 ? What governed the unique choice of areas for comparison in Fig. 2 ? And why were available early records (before the 1890's) for Japan not used to extend the curve in Fig. 2 for that nation ?

30-YR CHANGE OF ANNUAL MEAN TEMPERATURE FOR VARIOUS LATITUDE ZONES*

Zone	Callendar		Willett-Mitchell	
	Latitude limits	T (C°)	Latitude limits	T (C
North temperate†	60-25°N	0·39	60-20°N	0·3
Tropical†	25°N-25°S	0·17	30°N-30°S	0·1
South temperate†	25-50°S	0·14	20-50°S	0·0
			20-60°S	0·1
N-T-S†	60°N-50°S	0·23	60°N-60°S	0·2
			80°N-60°S	0·2
Northern Hemisphere			80-0°N	0·3
			60-0°N	0·2
Southern Hemisphere			0-60°S	0·1

* 1921-1950 minus 1891-1920 (Callendar); 1920-1949 minus 1890-1919 (Willett and Mitchell). Willett-Mitchell data based
records for between 120 and 180 stations, not more than one station from each 10°-latitude-longitude square.

† Terminology after Callendar.

References

Arnold, J. R. and Anderson, E. C. 1957 'The distribution of carbon-14 in nature,' *Tellus*, **9**, 1, p.

Dubin, M. 1960 'Meteoritic dust measured from Explorer I,' *Planet. Sp Sci.*, **2**, p. 121.

Mitchell, J. M., Jr. 1961 'Recent secular changes of global temperature,' Proceedin Conf. on Solar Variations, Climatic Change and Relat Geophysical Problems, N.Y. Acad. Sci., (in prepar tion).

Takahashi, T. 1961 'Carbon dioxide in the atmosphere and in the Atlant Ocean water,' *J. Geophys. Res.*, **66**, 2, p. 477.

Vogel, J. C. 1961 'Information of atmospheric mixing obtained from C^{14} an tritium analyses,' Proc., Conf. on Solar Variation Climatic Change and Related Geophysical Problem N.Y. Acad. Sci. (in preparation).

Willett, H. C. 1950 'Temperature trends of the past century,' *Cent. Proc Roy. Met. Soc.*, p. 195.

U.S. Weather Bureau,
Washington, 25, D.C.

20 March 1961.

Reply

By G. S. Callendar

I was glad to see such good agreement between my zonal temperature changes and thos computed from Willett's and Mitchell's data, apart from the south temperate zone, where, a I mentioned in my paper, the nineteenth century values are few and partially unreliable. Hence for this zone, a more reliable change period is 1921-50 minus 1901-30, which is covered by abou 40 stations in *World Weather Records*. This period gives a rise of 0·10°C, quite close to Mitchell' value for the longer period.

I fully agree with their conclusion that the indirect influence on temperature of induce changes in the general circulation may overwhelm primary effects. The recent big rise in the sub Arctic zone is an outstanding example of this kind. On the other hand, if increased solar heatin is assumed to be the cause of rising trends in world temperature, it is difficult to account for stabl temperatures over the past 70 years in the arid basin of west central Asia, or sunny Australia One would expect a primary response of temperature to solar heating changes in these areas

As regards the distribution of excess CO_2, I think it best to compare the temperature trends in the westerly wind zones of north and south rather than the whole hemispheres, because almost all the industrial CO_2 has been released in 30°-60°N latitude, and would take longer to reach similar southern latitudes.

The new data quoted certainly indicate a more even distribution of CO_2 over the earth than I had assumed in my paper, and the mixing time for the whole atmosphere of 1 to 2 years seems remarkably rapid. No doubt the thermal inertia of the southern oceans and ice could account, in part at least, for the much smaller temperature rise there.

14 Parsonage Road,
Horsham, Surrey.
24 March 1961.

551.511.6 : 532.517.4 : 536.2

An alternative derivation of the diabatic wind profile

By C. H. B. Priestley

For bridging the transition in the wind profile between free and forced convection there is now Ellison's interpolation formula (*J. Fluid Mech.*, 1957, p, 456) and my own smoothing hypothesis (*Q.J.*, 1960, p. 232), both of which fit existing data as well as could be hoped; the derivations of Businger (*J. Met.*, 1959, p. 516) and Swinbank (*Nature*, 1960, p. 463), more fundamental in intent; and Panofsky's recent elegant analysis (*Q.J.*, 1961, p. 109) which at first glance appears to combine both virtues. This, however, contains one vital assumption which is made but not stated, and some explanation is due before the contribution can be properly judged.

In the usual notation the open assumptions are that

$$K = f(z, \epsilon_1, \epsilon_2) \qquad . \quad . \quad . \quad . \quad . \quad (1)$$

where the suffixes 1 and 2 distinguish the rates of creation of mechanical and convective turbulent energy respectively. Actually the vertical velocity is used as intermediary but this is unnecessary. From dimensional reasoning then, so Panofsky states,

$$K = C\, z^{4/3} (\epsilon_1 + \gamma\, \epsilon_2)^{1/3} \qquad . \quad . \quad . \quad . \quad (2)$$

where C and γ are constants. There would be little room for quarrel with this thesis if it were held that it was the *total* energy creation which was physically relevant, i.e. $\gamma = 1$. But this is clearly not the case, and it is found empirically elsewhere that (2) is most successful with γ about 15 : ϵ_1 and ϵ_2 therefore operate in quite different ways, as indeed is now well known from fine-structure studies.

All that dimensional reasoning from the stated premises really tells us is that

$$K = C\, z^{4/3}\, \epsilon_1^{1/3}\, f\left(\frac{\epsilon_1}{\epsilon_2}\right) \qquad . \quad . \quad . \quad . \quad (3)$$

where f is a function to be discovered by experiment or by further physical reasoning. What, one must therefore ask, is the underlying physical thinking which selects (2) from among the infinity of forms contained in (3) : or has Panofsky merely shifted the old empiricism, without changing its character, by writing down an interpolation formula for K instead of for $\partial V/\partial z$?

C.S.I.R.O.,
Division of Meteorological Physics,
Station Street,
Aspendale, S.13, Victoria, Australia.
9 March 1961.

Reply

By Hans A. Panofsky

Dr. Priestley's comments are well taken. Of course, the infinity of possible interpolatio formulae is a considerably smaller infinity than Dr. Priestley suggests. For, when ϵ_2 is larg the eddy viscosity K must vary as $\epsilon_2^{1/3}$.

However, the main purpose of the note was not so much to derive this particular interpolatio formula (although it fits the observations better than other similar formulae), but to show tha in such formulae the height z is a measure of the ' vertical eddy size,' both in neutral and unstabl air.

In addition, the derivation shows clearly the relative role of mechanical turbulence and hea convection in producing momentum transport.

University of Minnesota,
School of Physics,
Institute of Technology,
Minneapolis, 14.
26 April 1961.

551.509.311 : 551.511.3 : 551.515.8

A theory of fronts in relation to surface stress

By F. K. BALL

(Read 19 October 1960; see *Q.J.*, **86**, p. 51)

Dr. R. S. Scorer : After Eq. (11) Q is called the ' mass flow beneath the inversion.' Actually it is the volume flow, and could be very different from zero if there were a wind towards the front at high levels in the cold air and away from the front at low levels. (These winds are, of course, relative to the front). This would require a downslope wind close to the front – not an uncommon occurrence. The air approaching the front would then be of smaller density than the air moving away so that a considerable mass flow away from the front would occur if there were no volume flow ($Q = 0$). The inertia force corresponding to this acceleration of air away from the front might easily equal the force due to surface friction. The point is that there is a correlation between ρ and u' which has been assumed to disappear from the mean equations but which would not vanish in this case, and would still not vanish if the equations were expressed in terms of potential temperature instead of density. If there is no mass flux then in the case of vertical motion near the front $Q \neq 0$.

Mr. C. E. Wallington : I wonder whether the terms ' katabatic ' and ' anabatic ' have been applied too easily and perhaps prematurely to the fronts mentioned in this paper. It is a matter for conjecture whether the phenomena dealt with are likely to include the deeper variety of ' airmass ' fronts and a kata-cold front of the type described in Dr. Sansom's paper in 1947 is not necessarily of the katabatic classification in Mr. Ball's paper. There was, in fact, considerable discussion at cross-purposes due to nomenclature when Dr. Sansom's paper was presented.

However, this is a very minor criticism. We must not be too critical of the assumptions made in this paper. Mr. Ball has clearly specified the class of motion he has studied.

Mr. J. S. Sawyer : I am sure that Mr. Ball's paper is valuable in formulating the effects which surface friction may have on the form of fronts and his theory gives a plausible explanation for the shapes of the isobars which synoptic analysts have drawn for a long time adjacent to fronts, often on slender evidence. However, in order to treat the problem, Mr. Ball has so simplified it that it is difficult to assess to what extent we should expect real fronts to conform to the theory. In particular, the large-scale convergence in the lower troposphere usually necessary to create and maintain the front, is not adequately represented in Mr. Ball's model, and the consequent vertical motion ignored as a factor which would distort the frontal surface. Consequently I do not think that Mr. Ball's theory can apply to frontal slope in mid-troposphere but may apply near the ground, where large-scale vertical motions are smaller. Can Mr. Ball say to what height he regards his theory as applicable ?

Mr. F. K. Ball (*in reply*) : Dr. Scorer states that I have called Q the mass flow beneath the inversion when strictly it should have been called the volume flow. In fact, the statement after Eq. (11) is : ' Q is a constant representing the mass flow beneath the inversion relative to the motion of the system.' In an incompressible model, which is all that I discussed, the ratio between mass flow and volume flow is constant and constancy of one implies constancy of the other. If a compressible atmosphere is considered under the same assumption, i.e., that there is no *mass* flow across the inversion, then clearly the *mass* flow under the inversion will be constant. This constant will play a part closely analogous to the part that Q plays in the compressible case. For example in a compressible atmosphere, Eq. (11) becomes :

$$\delta p\,(\overline{\rho u}/\overline{\rho} - c) = gQ$$

where Q now really is the mass flux and $\delta\rho$ is the difference between the surface pressure and the inversion pressure.

As Dr. Scorer points out, in the compressible case, the primed terms will also contain density fluctuations. It can be shown for instance that corresponding to $\overline{u'^2}$ in Eq. (6) the terms $\overline{u'^2}(1 + s) - s\,\overline{u'^2}$ appear, where $s = \rho'/\overline{\rho}$. The last term is usually small and in any case tends to reduce the contribution from $\overline{u'^2}$. The term $\overline{u'^2 s}$ may be comparable with $\overline{u'^2}$ when $\delta\rho > 500$ mb.

I agree with Mr. Wallington that the ana- kata- classification of real fronts on the basis of the observed characteristics will not usually correspond exactly with the classification in my theoretical model. The precise definition that I have given should be borne in mind if such a comparison is made.

In answer to Mr. Sawyer I would guess that the theory is most likely to be applicable up to about 700 mb or maybe 600 mb. I would like to add, however, that there are few problems in dynamic meteorology which have been treated theoretically without so much simplification that it is difficult to assess to what extent we should expect the real phenomenon to confirm to the theory. In the present state of knowledge we cannot expect very good detailed agreement between theory and observation in this type of problem. I think we must be satisfied with finding theoretical models which describe a phenomenon *better* than previous models, particularly if they also indicate the physical processes that are important and so increase our understanding of the physics of the phenomenon.

Dr. J. M. Stagg (*President*) thanked Mr. Ball for his stimulating paper and hoped he would find opportunity for continuing to work on those lines.

551.521.32 : 551.524.35 : 551.524.4 : 551.551.8 : 551.575

Measured radiative flux divergence near the ground at night

By J. P. FUNK

(Read 16 November 1960; Presented by Dr. G. D. Robinson; See *Q.J.*, **86**, p. 382)

Dr. J. M. Stagg (*President*) : Like Professor Sheppard I am puzzled by the rôle attributed to haze in accounting for discrepancies in flux measurements of this kind. With observations made at different times at two sites was it not possible to segregate the observations into two groups, one of greater and one of less haze, according to recency of rain, or kind of air mass air track ? More drastically, could not some of the stuff be introduced artificially by kindling a fire to windward ? If the haze acts primarily as nuclei for aggregating water as Dr. Funk suggests it is odd that no relationship with humidity was found.

Dr. J. L. Monteith : The table in which Dr. Funk heads a column of observations with the unit μW cm^{-3} is surely unique. Most people would be glad to get the sign right but Dr. Funk gives us two significant figures – a measure of the technical skill and ingenuity which lie behind this paper. It would have been surprising if calculated and measured values of flux divergence had been in close agreement, but I am unhappy about the author's claim that there is systematic *underestimation* of div R by the chart method; has he examined every possibility of systematic error within his instrument ?

For example, there is no discussion of how vertical temperature gradients might affect performance. By setting up the heat balance of the instrument one can show that a temperature difference ΔT between the air in contact with the upper and lower surfaces of the thermopile corresponds to an *apparent* radiative flux $h\Delta T - h$ being the appropriate heat-transfer coefficient, about 1·7 mW cm^{-2} °C^{-1} in similar instruments. Sweeping assumptions are necessary to get a quantitative estimate of $h\Delta T$: for example, we may assume that ΔT is given by the difference between the temperature of the ambient air 2 cm above and 2 cm below the thermopile; and that on a calm clear night ΔT is 0·04°C at 0·5 m and 0·01°C at 1·5 m. Then the flux error is $-$ 68 μW cm^{-2} at 0·5 m but only $-$ 17 μW cm^{-2} at 1·5 m. Div R would then be overestimated by 0·5 μW cm^{-3}. Very small temperature gradients within the instrument, maintained by gradients of ambient temperature rather than by radiative flux, would be sufficient to account for the discrepancy between observed and calculated values of div R.

There may well be errors in the chart method, but before we start to theorise about the effects of haze, I think we should have some assurance from Dr. Funk (a) that the instrument is insensitive to ambient temperature gradients, and (b) that heat transfer coefficients are identical for both thermopile surfaces. If they are not, output will not be strictly proportional to radiative flux.

Dr. K. H. Stewart : I wonder if another possible source of systematic error was considered; instruments of this type usually have an appreciable temperature coefficient, and in these measurements the lower instrument would have been systematically cooler than the upper one.

It would be interesting to know if any calculations have been made on the amount of haze required to explain the observed cooling. On the basis of estimates I made some years ago (for considerably deeper layers) (*M.R.P.* No. 912, quoted by Funk) it would be sufficient to cause an obvious reduction in visibility.

Dr. R. C. Sutcliffe : There is a great need for reliable observations in this subject : without them theory is arid. I therefore greatly welcome this paper and I hope the instrument will prove acceptable. Could Dr. Robinson say if the observations could account for the occurrence on 'radiation nights' of a temperature minimum in the atmosphere raised above the actual surface. This has several times been reported – I do not know if it is accepted as established.

Mr. L. C. W. Bonacina (*communicated*) : If I have followed correctly the technical argument a layer of haze will radiate heat outward to space but it should also radiate it inward towards the ground thereby raising the night minimum air temperature.

If this inference is sound then I think the presence of London smoke haze may help to explain why neither Kew nor Hampstead are at all conspicuous for low night minima in comparison with some other stations in southern England – even allowing for the fact that neither of these two London observatories occupy hollows favourable to severe radiation frosts.

Dr. J. P. Funk (*in reply, communicated*) : Firstly I want to thank Dr. Robinson for reading the paper on my behalf.

I am thankful to Dr. Stagg for his suggestion of correlating the observations with recency of rain. There seems to be an indication that rain tends to lower the ratio observed/calculated. Nevertheless I am of the opinion, and recent results here confirm this, that the vertical distribution, rather than quantity of haze, is the important factor.

Dr. Stagg's suggestion of introducing artificial haze has some attraction, but there are doubts as to the realism of such a procedure.

Dr. Monteith's doubts seem to be unfounded : regarding (a), in the course of an investigation into the errors introduced when, during certain long-wave calibration procedures, net radiometers are additionally exposed to different air temperatures on their two sides (Funk, 1961) the effective heat transfer coefficient h of our net radiometer was also determined. In the unstable case, and with an air temperature difference of 16°C, h was found to be about 0·2 mW cm^{-2} °C^{-1} (Monteith's h seems to refer only to the thermopile itself). Incidentally, this also takes into account additional radiative heat transfer due to radiation coming from the two not completely transparent polythene hemispheres, being at different temperatures. Even applying this h in the same way as Dr. Monteith did, in which case an unrealistic temperature discontinuity across the plane of the instrument is being assumed, the error would only be about 0·06 μW cm^{-3}. In practice, however, not only is there no temperature discontinuity, but it seems rather doubtful whether any worthwhile temperature difference exists between any two points on the upper and lower hemispheres, since the streamlines around the instrument originate essentially at the same level. The effect of ambient temperature gradients would therefore be very small indeed, if present at all.

As to (b), the instruments are checked in the laboratory for identical sensitivity of the two thermopile surfaces. This identity would be practically maintained in the field since heat transfer through the air spaces under the hemispheres is only a fraction of the total. Moreover, differential convection effects, if present at all, would be small; since the Rayleigh number for these airspaces is near critical for the temperature differences likely to occur.

Mr. Bonacina is perfectly correct that haze in a deep enough layer would, by reducing the outgoing radiation, raise the night minimum air temperature. On the other hand, haze in shallow layers may not appreciably affect the outgoing radiation whilst still causing a strong increase of div R in those same layers.

The temperature coefficient, mentioned by Dr. Stewart, in spite of being only + 0·001 (Norris and Funk 1961), could, under certain circumstances, be a source of small systematic error. However, in our case, the time the instrument body takes to reach temperature equilibrium with the surroundings under light wind conditions is very much greater than the radiation time constant of the instrument, During balancing the instrument would, therefore, practically maintain the same temperature as at its previous height and the difference in sensitivity due to different instrument temperatures is thus automatically taken into account.

As to whether haze need be sufficient to reduce the visibility in order to explain the observed cooling – this would only have to be the case if haze were uniformly distributed with height. If not, and I think this is the case, then a comparatively small additional emissivity in the window regions would explain the increased cooling.

In answer to Dr. Sutcliffe, it seems that the observations could, in so far as they have show that radiation phenomena need not qualitatively be in agreement with previous theoretical co siderations, point to an explanation of the temperature minimum above the actual surface. Th temperature minimum (Ramdas's effect) seems to be well established and has also been observe here.

References

Funk, J. P. 1961 'A note on the long-wave calibration of convectively shielde net radiometers,' *Arch. Met. Geohpys. Biokl.*, (in pres

Norris, D. J. and Funk, J. P. 1961 'Radiation observations at Mawson, Antarctica,' Aus *J. Appl. Sci.*, **12**, No. 2.

551.501.7 : 551.511.3 : 551.558.

Some computations of the variation of vertical velocity with pressure on a synoptic scale

By E. KNIGHTING

(Read 18 January 1961; See *Q.J.*, **86**, p. 318)

Mr. A. G. Matthewman : Mr. Knighting has just pointed out that later computations c other data have sometimes given mean distributions of ω differing from his Figs. 3-6. Neverthele in three out of four of the cases here cited (Figs. 3, 4 and 5) the calculated maximum ω occu at a higher level than the conventional $\frac{1}{2}(1{,}000 + 200) = 600$ mb, employed in the Sawye Bushby model. I wonder if an improvement would be obtained in the average situation with almo the same model by simply replacing isobaric co-ordinates by log-isobaric co-ordinates, measurin say, L vertically upwards, where $L = -(R\,T_0/g)\ln(p/p_0)$ and T_0, p_0 are suitable constant The middle of the troposphere on the L-scale could then be chosen as vertex of the assume parabolic distribution of dL/dt. It happens that when density is eliminated from the usual meteo ological equations in favour of pressure and temperature, pressure always occurs in logarithm form, as in Mr. Knighting's Eq. (4), which seems to invite log-isobaric coordinates.

Dr. R. S. Scorer : Mr. Knighting has produced some very interesting figures which a likely to be quoted as typical. Will he be happy if the following typical values are given publicity

(1) Velocity of ascent or subsidence in moving pressure systems away from fronts – 3 mb hr

(2) Subsidence ahead of approaching and developing anticyclone or ascent ahead of surfa warm front of a vigorous depression – 10 mb hr^{-1}.

(3) Subsidence behind marked cold front of moving depression, or ascent ahead of centr of vigorous depression with open warm sector – 20 mb hr^{-1}.

These rates can be converted into rates-of-change of temperature at a point if the lapse ra is known. Each of these extends over a horizontal distance of the order of 500 miles and appli to a particle of air for a time of the order of $\frac{1}{2}$ to 1 day.

Dr. F. H. Ludlam : Mr. Knighting's results are most interesting and stimulating, not lea to those interested in weather-producing processes rather than in testing a simple model of th profile of verticle velocity. In so far as the basic data were derived from radiosonde observation mostly separated by distances of at least two grid lengths, is it not true that substantial difference between profiles at neighbouring grid-points cannot be real ?

Dr. J. M. Stagg (*President*) : Mr. Knighting's diagrams certainly show many areas of loc consistency, relative to the 1,000 mb synoptic features, in the dominant direction of vertic velocities. But more particularly there seems to be a local consistency in the level of non-dive gence – 400 mb in some areas, e.g., ahead of the secondary low on 27 April 1959, and 600 mb i other areas. If this difference in level were real and not just an accident of the computation what would be the physical significance in terms of the weather ?

Mr. E. KNIGHTING (*in reply*) : I would not mind if the computed values of vertical velocity given in the paper and the corresponding temperature changes quoted by Dr. Scorer were taken as typical, with the exception of regions where the air is nearly saturated. There can be little doubt that the constant value of the static stability used in the computations is inapplicable in the regions where rain is falling, for example, and that the computed vertical velocities are a considerable underestimate.

Dr. Ludlam is, of course, right in saying that the computations depend upon the analysis of charts which rests upon a few upper-air observations, which in the Atlantic are far apart. However, I am quite sure that the differences in the profiles on the two sides of a frontal trough are real and meaningful. The computations depend upon the gradients of the wind fields at different levels and we have always believed that the wind fields over the Atlantic are deducible from a few observations. The introduction of more observations would certainly vary the detail of the profiles, but would not change the general shape; this view is supported by examination of the profiles over land where data are more plentiful.

In reply to the President, Dr. Palmén told me that he too, had found that the level of non-divergence ahead of frontal lows was rather above the mid-tropospheric level; his computations were not similar to mine. I take it that the effect in terms of weather is a thickening of the cloud layer and an increase in precipitation.

Mr. Matthewman's suggestion of using $\log p$ as a vertical co-ordinate was tried some years ago in U.S. If equal intervals are taken then the quarter points refer to about 1,000, 700, 400, 300 and 200 mb, so that more weight is attached to the upper-level observations. This seems inappropriate when forecasting for the lower troposphere. The adoption of $\log p$ instead of p as a vertical co-ordinate would scarcely be practical in the computations that I carried out, since it would involve analysis at pressure levels at which there are no reports. Thus it would demand interpolation and a different finite-difference scheme in the vertical. In principle, since I made no assumption with regard to the profile of vertical velocity, we should get the same results except for interpolation and truncation errors; it would, of course, be easy in the two-level models to raise the level of non-divergence by changing the analytic form of the profile.

Translations of Russian meteorological literature

To assist in making Russian meteorological literature more readily available the Society, in 1958, proposed to certain other meteorological institutions that each should undertake the translation in whole or in part of Russian meteorological journals, the translations to be distributed by exchange between participants. To avoid duplication the Society undertook to act as coordinator.

For its own part in this scheme the Society proposed to translate the journal *Works of the Central Aerological Observatory of the U.S.S.R.* Translations of the first two papers are now ready. They are :

Works of the Central Aerological Observatory, Pt. 21, 1958.

' Investigation of the variability and diurnal change of wind in the atmosphere,' by V. D. Reshetvo, pp. 3-51.

' Investigation of the pulses of the horizontal component of wind up to a height of 5 km,' by V. A. Devyatova, R. V. Pyatyshev, R. O. Tydelskaya and I. A. Cherenkova, pp. 52-175.

The translations are complete with tables and diagrams.

Some 50 subscribers to the *Quarterly Journal* have expressed a wish to buy these translations, and, accordingly, copies have been duplicated. A number of copies are still available, at the price of 3 guineas, and may be had on application to the Assistant Secretary.

Report of the Council

for the year 1960

Submitted to the Annual General Meeting, 19 April 1961

General

The Council is pleased to report the continued progress of the Society in its many activities ; ventures launched in recent years have become firmly established and new activities have bee initiated.

The series of Evening Discourses begun three years ago is now a regular and importan feature of the Society's calendar, and appreciation of the lectures for senior physics pupils fro London and neighbouring areas given for the first time in 1959 was reflected in the increase audiences in 1960.

A successful Two-day Summer Meeting, the seventh of the series, was held at Queen' College, Dundee, University of St. Andrews.

In 1960 your Council instituted a new L. F. Richardson Prize for the special encouragemen of the younger members of the Society.

An additional course and extended programmes of Field Studies were initiated with generou financial support from the Carnegie United Kingdom Trust.

In making grants from the Scientific Activities Fund your Council introduced a change o emphasis. Special consideration is now given to applications from the younger members o the Society for assistance in presenting their work at meteorological conferences.

Sir O. Graham Sutton, F.R.S., represented the Society at the tercentenary celebrations of the Royal Society and Dr. R. M. Goody represented it at the celebrations of the fortieth anniversary of the American Meteorological Society. Congratulatory messages from the Society were conveyed on both occasions.

As a result of the free-of-interest loan obtained from the Nuffield Trust for reprinting back numbers of the *Quarterly Journal*, the Society's stock of post-war numbers has now bee replenished. Further valuable additions to the stock of *Quarterly Journals* have been made as a result of generous action by a number of Fellows donating their private collections.

The entrance hall and stairs of the Society's house were refurbished and improved facilitie were provided in the main cloakroom.

Council

From 1 January to 30 September the constitution of the Council was as recorded in the 1959 Annual Report.

From 1 October 1960 the following Council held office :

President

James Martin Stagg, C.B., O.B.E., M.A., D.Sc.

Vice-Presidents

Arthur George Forsdyke, A.R.C.S., Ph.D.
Richard Mead Goody, M.A., Ph.D.
George David Robinson, Ph.D., F.Inst.P.
Percival Albert Sheppard, Hon.A.R.C.S., B.Sc., F.Inst.P.

Vice-President for Canada

Warren Lehman Godson, Ph.D.

Vice-President for Scotland

Robert Cranna, M.A., B.Sc.

Treasurer

Brian Cecil Vernon Oddie, B.Sc.

Secretaries

Patrick John Meade, O.B.E., B.Sc., A.R.C.S.
Richard Segar Scorer, M.A., Ph.D.
John Stanley Sawyer, M.A. (Editor)
George Arthur Bull, B.Sc., M.I. Inf. Sc. (Librarian)

Councillors

John Alan Chalmers, M.A., Ph.D., F.Inst.P.
George Arthur Corby, B.Sc.
John Robert Dark Francis, B.Sc. (Eng.), A.I.C.E.
Arthur Leonard Maidens, B.Sc.
John Lennox Monteith, Ph.D.
Paul Robert Owen, B.Sc., A.F.R.Ae.S.
Reginald Charles Rainey, Ph.D.
John Brodrick Rigg, M.A.
John Russell Thorp, R.N., O.B.E., M.A.
Gilbert Brian Tucker, Ph.D.
Charles Desmond Walshaw, M.A., Ph.D.
Henry Lionel Wright, M.A.

The Council met six times during the year and there were thirty-one Committee Meetings.

Membership

The following tables show the main features of the Society's Membership in 1960, and the trend of membership during this century.

Class of membership	31 Dec. 1959	31 Dec. 1960	During 1960					
			Elected	Readmitted	Transferred	Deceased	Resigned	Struck-off
Fellow	15	18			3			
Honorary								
Fellow	1,422*	1,175	84	2	− 1	(− 4)†	− 32	− 43
Foreign Fellow		223						
Life Fellow	167	164			− 2	(− 1)†		
Corporate	9	9	9					
Nominee Fellow		13						
Student	93	106	26		− 2	− 1	− 3	− 7
Total	1,706*	1,708	119	2	− 2	− 1	− 35	− 50
Canadian Branch								
Fellow	329	328					− 1	
Life	5	5						
Student		1	1					
Total	334	334	1				− 1	
Grand Total	2,040*	2,042	120	2	− 2	− 1	− 36	− 50

* Includes 22 members elected in 1959, who paid their subscriptions for 1960 in 1959; also 9 Corporate Members.
† Subscriptions for 1960 paid.

Total Membership Since 1900

1900	1910	1920	1930	1940	1945	1950	1955	1956	1957	1958	1959	196
620	758	795	762	881	1,443	1,733	2,069	2,076	2,099	2,066	2,040	2,04

Deaths

Council records with sorrow the deaths of C. F. Aitken, Fellow (1950); Professor W. L. Bal F.R.S., Fellow (1935); A. A. King, Fellow (1940); D. Miles, Student (1958); W. J. Nicholso Fellow (1957); T. L. F. Rutledge, Life Fellow (1950); E. Sandeman, Fellow (1935).

Awards and Honorary Fellowships

The following awards were made at the Annual General Meeting on 20 April :

Buchan Prize in respect of the period 1955-59 :

Robert James Murgatroyd, Ph.D., for his outstanding contributions to the study of th physical processes of the atmosphere.

Hugh Robert Mill Medal and Prize for 1959 :

Basil John Mason, M.Sc., D.Sc., for his notable contribution to the understanding of th physical processes of rainfall.

Darton Prizes for 1959 :

Home Awards :

First Prize : Dr. C. J. Adkins.
Second Prize : Dr. J. P. Funk.

Canadian Awards :

First Prize : Dr. R. H. Douglas and Dr. W. Hitschfeld.
Second Prize : Mr. D. K. A. Gillies.

The Council elected into Honorary Fellowship in 1960 :

Professor S. Chapman, F.R.S., M.A., D.Sc.
Mr. C. K. M. Douglas, O.B.E., M.A.
Dr. K. R. K. Ramanathan, M.A., D.Sc.

Meetings

Eight ordinary meetings, one special meeting, three meetings for the Evening Discourse and three for the lecture to sixth-form physics pupils were held in the Society's rooms durin the year. The Evening Discourses were given by :

Mr. C. E. Wallington on ' Mountain waves ';
Dr. H. L. Penman on ' Weather, soil and plant factors in hydrology ';
Dr. A. W. Brewer on ' The stratosphere.'

The lecture to physics pupils on three successive evenings to a total audience of about 30 was given by :

Dr. T. W. Wormell on ' Electrical phenomena in the atmosphere.'

In addition to those meetings the Symons Memorial Lecture was given by :

Dr. Ragnar Fjørtoft, Director of the Norwegian Meteorological Office, who spoke on ' The general circulation of the atmosphere.'

A joint meeting with the Royal Astronomical Society was held in the rooms of the Royal Society of Arts on, ' The British rocket programme.'

In the County Hall, Westminster, Dr. R. C. Rainey gave the eleventh in the series of Popular Lectures on two successive evenings; his subject was ' Meteorology, locusts and Africa.' Each lecture was attended by about 400 pupils from grammar and public schools in London and adjacent areas.

At the Annual General Meeting in the Society's rooms on 20 April, the Report of Council and Annual Accounts for 1959 were adopted and the awards referred to earlier in this report, were presented. Dr. J. M. Stagg gave his Presidential Address on the theme ' Has meteorology become too professionalized ? '

Summer Visit and Summer Meeting

The Summer Visit on 20 July 1960 was to the Lasham Gliding Centre near Alton, Hampshire, by the kind invitation of the Lasham Gliding Society. Owing to indifferent weather only about two dozen members attended, but they were able to spend an informal and most interesting afternoon visiting the various hangars, workshops and the launching site where several visitors were able to take short flights around the airfield. Col. H. V. S. Muller, the General Manager, assisted by Dr. James, directed the party on its tour of inspection of the airfield and the Society's thanks are due to them for an enjoyable afternoon.

The seventh *Two-day Summer Meeting* of the Society was held at Queen's College, Dundee, University of St. Andrews, by kind permission of the Master, Professor A. M. Matheson, Q.C., M.A., LL.B., and the College Council. Professor Matheson and Mrs. Matheson, with Miss Rhona Morrison, the warden of the West Park Hall, held a reception on 29 June at the Hall, when the meeting was officially opened.

Two symposia were held during the meeting; on the first day the subject was ' Convection ' and on the second, ' Agricultural meteorology.'

Visits during the Meeting were made to the Freshwater Fisheries Laboratory of the Scottish Home Department and to the Central Control Hydro-electric Station of the North of Scotland's Hydro-electric Board at Pitlochry.

The Lord Provost and the Corporation of Dundee gave a luncheon in honour of the Society in the City Chambers when Dr. J. M. Stagg replied to a speech of welcome by the Lord Provost and expressed the thanks of the Society for the hospitality extended to them by the City. The meeting terminated with visits to the Tidal Model of the Dundee Harbour Trust and the Scottish Horticultural Research Institution, Mylnefield.

Council wishes to record its thanks to Mr. G. A. Corby, who acted for the Society as co-ordinator for the meeting; to Mr. R. Cranna (Vice-President for Scotland) and to Dr. R. P. Pearce and their colleagues on the Scottish Centre Committee, whose efforts contributed so much to the success of the meeting.

Field Studies

During the year five vacation courses were held in conjunction with the Field Studies Council, one at Malham Tarn, two at Preston Montford and two at Dale Fort, Pembrokeshire, of which last, one, on ' Weather and bird movement,' was new. The total number of students who attended these courses in 1960 was about 80. In association with the British Gliding Association, week-end courses were held at Lasham, Long Mynd and Dunstable and a new programme was started at the Scottish Gliding Union at Kinross.

Council is grateful for the continued generous financial support from the Carnegie Unit Kingdom Trust which has enabled the Society to increase the number and enlarge the sco of these various courses : Council is also appreciative of the work of Dr. R. S. Scorer and H chief instructors, Dr. D. H. McIntosh, Mr. J. B. Rigg, Dr. R. P. Pearce, Mr. D. E. Pedgle Dr. G. B. Tucker and Mr. C. E. Wallington in organizing and operating these courses.

Publications

Quarterly Journal. The number of papers submitted for publication in the *Quarterly Journ* again showed a slight increase. Papers submitted during the year totalled 74 against 67 in 195 62 in 1958 and 64 in 1957. The average time between receipt of approved copy for publicati and appearance in the *Quarterly Journal* was about 4 months.

Council expresses its thanks to the Editor, Mr. J. S. Sawyer, his Editing Committee an Mr. E. L. Hawke, the proof reader, for their valuable work in the production of the *Quarter Journal.*

Weather. To bring *Weather* into closer relationship with the other activities of the Societ while leaving its Committee's corporate initiative and responsibility unimpaired, Council decide at the end of 1959 to make some changes, which were introduced in 1960 as opportunity offere The committee became an Editorial Board of five members including the Editor, together with Business Manager, all nominated by Council; the Editor is either a member of Council or close associated with its work. Capt. J. R. Thorp, R.N., became the first Editor and he was succeede by Mr. H. L. Wright.

During the year the high standard of production and technical content of the magazin were maintained, and for this, Council is greatly indebted to the Editors and their colleagu on the Editorial Board and to the Business Manager, Mr. N. Bradbury.

Scientific Activities Fund

During the year grants were made from the Scientific Activities Fund to Fellows attendi conferences abroad, towards the cost of research programmes and field expeditions, and in maki instruments available to Fellows. Grants were also made to enable foreign visitors to prese papers at Society meetings and to students attending the courses of field study.

The policy for allocating grants has been modified, emphasis being given to helping young Fellows to establish themselves in new fields by presenting work at conferences or by researc and to enabling more senior Fellows to make more extended visits than would otherwise b possible. Visits by meteorologists from overseas are also encouraged.

Library

Loans of books, journals, films and filmstrips were at an appreciably higher level than i earlier years and the demand for the use of lantern slides continues.

Ten additional series of journals and memoirs have been received : for one of these th *Quarterly Journal* is supplied in exchange and *Weather* is supplied for another. A considerabl number of text-books and memoirs have also been presented by the U.S.S.R.

Three lists of accessions to the library and two addenda to the catalogue of journals an memoirs were issued during the year.

Further progress has been made in the rebinding of older journals and books, and anothe section of the open shelves has been glazed to provide better protection for the books.

A selection of 24 cloud photographs from the Clarke and Cave collections was made for new set of postcard reproductions. These were printed and were on sale before the end of th year.

Duplicate copies and older editions of books which were surplus to the requirements of the library were collected for disposal. Members were notified that a list of these was available on request.

Branch and Centres

Canadian Branch

At the Annual Meeting held 19 April 1960 the following Executive was installed to office : President, Mr. J. M. Leaver; Vice-President, Prof. J. S. Marshall; Recording Secretary, Mr. B. W. Boville; Corresponding Secretary, Mr. R. Anderson; Treasurer, Mr. H. M. Hutchon; Vice-President for Canada, Dr. W. L. Godson; Councillors-at-large, Chairman of Montreal Centre, Chairman of Winnipeg Centre, Chairman of Toronto Centre, Mr. E. A. Barks, Mr. L. B. MacHattie, Prof. B. W. Currie and Mr. A. F. McQuarrie.

The highlight of the year's activities was a meeting at Queen's University, Kingston, Ontario, on 7 and 8 June as a component of the Conference of Learned Societies. Twenty-one papers were presented at this meeting on a wide variety of subjects.

Montreal Centre

The five meetings held in 1960 covered a wide range of topics. Local meteorologists reported on their work on stratospheric circulation, snow measurement, cloud physics and operational weather radar, and Capt. George Lothian, Superintendent of Flying, T.C.A., commented from a pilot's viewpoint. The Annual General Meeting, which was held in May, was followed by a talk on 'Numerical weather prediction' by Dr. George P. Cressman, Director of the National Meteorological Centre, Washington, D.C.

The following officers were elected for the current year : Chairman, Mr. R. Strachan; Secretary, Miss C. Wilson and Treasurer, Mr. P. Summers.

Winnipeg Centre

Five meetings were held during the year. Average attendance at the meetings was fifteen to twenty with the exception of the 14 March meeting when some forty people were present including the Commanding Officer of the R.C.A.F. Station Winnipeg and various military personnel who had been invited. A highlight of the 4 April meeting, at which the President of the Canadian Branch was the guest speaker, was the presentation of the President's Prize to Messrs. A. B. Lowe and G. A. McKay for their paper 'The tornado in Western Canada.' The Executive Committee of the Winnipeg Centre for 1960 was as follows : Honorary Chairman, Mr. D. M. Robertson; Chairman, Mr. A. H. Lamont; Vice-Chairman, Mr. J. J. Labelle; Secretary-Treasurer, Mr. L. C. Oddy. In March Mr. Lamont was posted overseas and Mr. Oddy to Toronto. The Executive Committee changes were then : Chairman, Mr. J. J. Labelle; Vice-Chairman, Mr. D. G. Black and Secretary-Treasurer, Mr. F. J. Sebastian.

Toronto Centre

Seven meetings were held by the Toronto Centre during 1960. Besides gatherings which were addressed by Branch personnel, two excursions were arranged, one to the Malton Forecast Office and one to the Scarborough Physical Research Unit. Speakers from outside the immediate circle included Dr. Mariano Estoque of the U.S.A.F. Cambridge, Research Center, Mr. M. Kwizak from the Central Analysis Office, Dr. W. M. Cameron, Director of Oceanographic Research, and Dr. Stewart Marshall, MacDonald Professor of Physics at McGill University. Attendance at these meetings ranged from 60 to 80 members and guests.

Officers from 1 June 1960 were : Chairman, Mr. K. T. McLeod; Secretary, Mr. S. J. Buckler; Programme Secretary, Mr. J. P. Bruce; Treasurer, Mr. T. D. Wiacek.

When Mr. McLeod accepted his position with the W.M.O. Secretariat in September, his place as Chairman was filled by Mr. H. Bindon.

Scottish Centre

The Committee consisted of : Chairman and Vice-President for Scotland, Mr. R. Crann Secretary and Treasurer, Dr. D. H. McIntosh; and eleven other Fellows.

Four meetings were held during the year at Edinburgh University. The Society Two-d Summer Meeting held in Dundee took the place of the Centre's normal summer excursion.

The Popular Lecture entitled ' Meteorology in Antarctica ' was given by Mr. J. MacDow in Glasgow and Edinburgh on 28 and 29 March, respectively. A lecture entitled ' Light ar colour in the sky ' was given by Mr. J. Paton to senior pupils in Dundee on 13 June.

Manchester Centre

Seven meetings of the Centre were held during the year – six of these took the form addresses by various speakers and in early July several members visited the University Colleg of North Staffordshire at Keele. On the latter occasion the members were the guests of Profess S. H. Beaver and of the College Authorities. After lunch, visits were made to the Meteorologic Station and to the Department of Geography. Professor Beaver had arranged an exhibitio of meteorological records obtained at Keele during the previous nine years.

Attendances remain generally at about fifteen members and guests at each meeting. Ther was no Popular Lecture given to sixth-form pupils in Manchester during 1960 but Dr. Raine will repeat the 1960 London lecture in late February of 1961.

Representatives

The Society's representatives on other scientific bodies were :

Gassiot Committee, President, Dr. J. M. Stagg;

British National Committee for Geodesy and Geophysics, Dr. R. C. Sutcliffe, Dr. T. W. Wormell

British National Committee for Physics, Dr. F. Pasquill;

British National Committee for Oceanic Research, Dr. T. H. Ellison;

National Committee for Antarctic Research, Mr. H. H. Lamb;

National Committee for Space Research, Professor P. A. Sheppard;

Cambridge University Meteorological Committee, Professor P. A. Sheppard;

Royal Astronomical Society, Geophysical Committee, Mr. J. S. Sawyer;

Advisory Committee on Meteorology for Scotland, Professor P. A. Sheppard;

British Glaciological Society, Professor Gordon Manley.

Staff

Council records with regret the death, after a long illness, of Mr. J. H. Rogers, B.Comm (London), the Accounting Assistant. In September, Miss D. E. Hall resigned her appointmen as Secretarial Assistant after 2½ years' service. To fill these vacancies Council, on the recommenda tion of the Officers appointed Mr. H. H. Hoyle in August to be Accounting Assistant on a part time basis and Miss B. A. Aked as Secretarial Assistant from October.

Other members of the staff comprised Mr. R. H. Levinson, M.A., F.C.A., Assistant Secretary; Mr. R. S. Read, I.S.O., M.A., B.Sc., A.R.C.S., F.Inst.P., Assistant Librarian; Mrs. W. A. Steward, Editorial Assistant and Publications Clerk; Miss E. Crafts, *Weather* Clerk; Miss E. Hooper, General Clerk.

In conjunction with a well-known Life Assurance Company, a staff pension scheme was introduced for the benefit of permanent full-time members of staff.

Council records its high appreciation of the excellent work carried out by all members of the staff during the past year.

Finance

The Accounts show a deficit of £696 for the year, compared with a surplus of £1,755 for 959. This apparent decline in the Society's financial position was due to unusually heavy capital pending.

The main items were the reprinting of back numbers of the *Quarterly Journal* (£944) and f a new Members List (£326 including the cost of distribution) and a bill for structural work n the Society's premises (£972). This last item includes the cost of modernising the gentlemen's loakroom. The cost of printing the *Quarterly Journal* was also higher than in 1959 by nearly £500. In a sense, this is a matter for congratulation, since it results from a substantial increase n the amount of material published. No other items under Expenditure call for special comment.

On the Income side, it is gratifying to note that sales of both our publications have again isen, but there is a drop in advertising revenue. Steps are being taken to remedy this. The ociety has once more to acknowledge, with thanks, a Royal Society grant of £300 towards the ehabilitation of the library. This grant is however unlikely to be renewed in 1961.

The Society's new Pensions Scheme, mentioned under 'Staff,' is not only more atisfactory to the staff but considerably cheaper to the Society. The old 'Staff Pension Fund' as now been wound up, and securities worth about £2,000 have been transferred to the General Fund: but another block of securities, worth about £2,900, has been placed in a Staff Benevolent Fund for administration at the discretion of Council. These operations are shown in the Balance heet.

The value of the Society's investments declined by about £1,700 during the year, which was ne of mild but general recession. No new investments were made beyond taking up 'rights' ssues, the cost of which was £297.

A new appeal was made to Fellows to enter into Covenants for the payment of their subscrip-ions, and Council records its thanks to the 51 Fellows who have responded. The Society will enefit to the extent of £135 11s. 6d. annually.

RECEIPTS AND PAYMENTS OF SPECIAL FUNDS FOR 1960

	Balance at 1 Jan. 1960	Receipts for year	Outgoings for year	Balances at 31 Dec. 1960 Investments	Balances at 31 Dec. 1960 Balance at Bank	Totals as per Balance Sheet 31 Dec. 1960
	£	£	£	£	£	£
Awards Fund	6	—	—	—	6	6
British Rainfall Organization Fund	4,422	214	138 (a)	4,336	162	4,498
Life Composition Fund	2,372	130	150 (b)	2,322	30	2,352
Napier Shaw Memorial Fund	679	38	—	472	245	717
Scientific Activities Fund	1,089	170 (c)	340	784	135	919
Symons Memorial Fund	554	36	16	519	55	574
Hampton Brown Fund	907	63	26	915	29	944
Staff Pension Fund	3,699	229	3,928 (d)	—	—	—
Staff Benevolent Fund	—	2,400 (e)	100 (f)	2,113	187	2,300
	£13,728	£3,280	£4,698	£11,461 (g)	£849	£12,310

a) Includes £15 transferred to "A" Account. (b) Transferred to "A" Account. (c) Includes £100 ransferred from "A" Account. (d) Value of Fund at 31 December 1960 transferred to Accumulated Fund. (e) Transfer from Accumulated Fund. (f) Ex-gratia payment to member of staff. (g) Market Value f Investments at 31 December 1960 was £13,296.

Examined and found correct.
March 1961

BALL, BAKER, DEED & CO.,
Chartered Accountants.

GENERA

BALANCE SHEET A

31.12.59						
£	£	£		£	£	£
			ACCUMULATED FUND—			
12,691			Excess of Assets over Liabilities at 1 January 1960			14,44
—			*Add* Staff Pension Fund Transferred			3,99
12,691						18,33
	683		*Deduct* Library Equipment Fund		825	
	—		Transfer to Staff Benevolent Fund		2,400	
683						3,22
12,008						15,14
	—		*Deduct* Loss on Revaluation of Investments ..		849	
	1,755		Excess of Expenditure over Income		696	
1,755 (Cr.)						1,55
13,763						13,66
683			LIBRARY EQUIPMENT FUND			82
550			REPAIRS RESERVE FUND			55
1,960			NUFFIELD FOUNDATION – LOAN UNSECURED ..			1,96
			CURRENT LIABILITIES—			
	960		Creditors and Accrued Charges		939	
			Amounts Received in Advance :			
		1,767	Publications	1,553		
		469	Subscriptions	315		
	2,236				1,868	
3,196						2,80
			SPECIAL FUNDS—			
13,728			Per Schedule on page 451			12,31
£33,880						£32,05

J. M. STAGG—*President*
B. C. V. ODDIE—*Treasurer*

We have examined the above Balance Sheet and annexed Income and Expenditure Account which in our opinion respectively give a true and fair view of the state of the Society's affairs as at 31 December 1960, and of its Income and Expenditure for the year ended on that date.

Lloyds Bank Buildings,
55/61 Moorgate,
London, E.C.2.
March 1961

BALL, BAKER, DEED & CO.,
Chartered Accountants

FUND

31 DECEMBER 1960

31.12.59						
£	£				£	£
		FIXED ASSETS—				
5,375		Freehold Property – Estimated value (in 1925) of the Society's House, 49 Cromwell Road				5,375
		Furniture and Equipment—				
			At 1.1.60	Additions during year	Accumulated Depreciation	Net
			£	£	£	£
1,134		General	1,826	173	842	1,157
683		Library	950	231	356	825
1,817			£2,776	£404	£1,198	£1,982	1,982
		(No amount has been included for the value of the Library and the stock of publications)				
		INVESTMENTS—				
6,623		Valued at lower of Cost or Market Value 31.12.60 ..				7,790
		(Market Value 31.12.60 – £10,877)				
		(Market Value 31.12.59 – £9,198)				
		CURRENT ASSETS—				
295		*Weather* Paper Stock				297
		Debtors—				
	1,415	Subscriptions			550	
	1,202	Publications			769	
	2,617				1,319	
	425	*Less* Provision for Bad and Doubtful Debts			425	
	2,192				894	
	242	Tax Reclaims – Dividends and Covenants			608	
	52	Payments in Advance			136	
	—	Amount due from Carnegie Fund			463	
	3,556	Balance at Bankers and Cash in Hand			2,201	
6,042						4,302
		SPECIAL FUNDS—				
		Investments – Per Schedule on page 451				
	13,204	Valued at lower of Cost or Market Value 31.12.60 ..			11,461	
		(Market Value at 31.12.60 – £13,296)				
		(Market Value at 31.12.59 – £16,708)				
	524	Balances at Bankers			849	
13,728						12,310
£33,880						£32,056

GENERAL

INCOME AND EXPENDITURE ACCOUNT

EXPENDITURE

1959 £	£		£	£
		ESTABLISHMENT—		
	28	Water Rates	26	
	308	Cleaning Wages and Materials	315	
	30	Insurance	38	
	214	Lighting and Heating	230	
	262	Repairs and Maintenance	820	
	200	Transfer to Repairs Reserve Fund	—	
	136	Depreciation of Furniture and Equipment	150	
1,178				1,577
		ADMINISTRATION—		
	3,420	Salaries	3,546	
	390	Contribution to Staff Pension Fund	—	
	—	Staff Pension Premiums	125	
	146	Printing	104	
	369	Stationery	482	
	977	Postage, Carriage and Packing	1,137	
	93	Telephone	94	
		Audit and Accountancy Fees—		
	136	Royal Meteorological Society and *Weather* Magazine	136	
	74	Sundries	110	
5,605				5,733
		PUBLICATIONS—		
	3,637	Current *Quarterly Journal*	4,139	
	—	Back numbers *Quarterly Journal*	944	
	2,526	*Weather*	2,612	
	381	Illustrations	322	
	26	*Cloud Study*	58	
	126	Reprints of *Weather*	151	
	256	Reprints of Papers (*Q.J.*)	320	
	35	*Monthly Weather Report*	28	
	51	Translation Russian Journal	71	
	30	Secondhand Journals	15	
	—	Membership List	326	
7,068				8,989
		LIBRARY—		
	491	Salary	491	
	226	Books, Bindings, etc.	78	
	62	Depreciation of Equipment	89	
779				658
		MEETINGS' EXPENSES—		
	82	Travelling Expenses	81	
	92	London	210	
	40	Scotland	40	
	30	Manchester	30	
	32	*Weather* Meetings	33	
276				394
175		PROVISION FOR BAD AND DOUBTFUL DEBTS—		—
		GRANTS AND PRIZES—		
	100	Scientific Activities Fund	100	
	40	Grant to Society for Promotion of Field Studies	—	
140				100
1,755		BALANCE, BEING EXCESS OF INCOME OVER EXPENDITURE		—
£16,976				£17,451

FUND

FOR THE YEAR ENDING 31 DECEMBER 1960

INCOME

1959 £	£	£		£	£	£
			SUBSCRIPTIONS, ETC.—			
	7,004		Subscriptions		6,907	
	81		Entrance Fees		74	
	6		Donations		12	
	7,091				6,993	
	236		Less Adjustments for Lapsed Membership (By-Law 40)		199	
6,855						6,794
898			Tax Recovered under Deed of Covenant 1957/58, 1958/59 and 1959/60			359
			PUBLICATIONS—			
	4,005		Sale of Publications – current *Q.J.*		4,173	
	347		Sale of Publications – back numbers *Q.J.*		145	
	1,691		Sale of *Weather* – excluding members' copies		1,770	
	79		Sale of *Cloud Study*		112	
	336		Reprints, *Q.J.*		384	
	139		Reprints, *Weather*		181	
	555		Advertisements, *Q.J.*		501	
	1,051		Advertisements, *Weather*		934	
	6		Sundry Sales		5	
8,209						8,205
			INVESTMENT INCOME—			
	—		Interest on Deposit		125	
	124		Interest on Government Stocks (Gross)		84	
	191		Interest on Industrial Securities (Gross)		244	
		495	Rent of Maisonettes	527		
		—	*Less* : Repairs	152		
	495	—		—	375	
810						828
			PHOTOGRAPHS—			
	5		Sale of Cloud Postcards		4	
	84		Clarke and Cave Copyright Fees		100	
89						104
			LIBRARY—			
—			Grant from Royal Society			300
			AMOUNTS RECEIVED FROM OTHER FUNDS—			
	100		Life Composition Fund		150	
	15		British Rainfall Organization Fund (for Administration)		15	
115						165
—			BALANCE, BEING EXCESS OF EXPENDITURE OVER INCOME			696
£16,976						£17,451

VALUATION OF INVESTMENTS AT 31 DECEMBER 1960

Market Value 31.12.59			*Market Value 31.12.60*	
£	£		£	£
		*General Fund**		
1,569		£2,150 4% Consolidated Stock 1957 or after x.d.	1,419	
187		£200 4% Funding Stock 1960/90	175	
163		£250 3½% War Stock 1952 or after	149	
584		£649.1.7 Government of Commonwealth of Australia 4% Registered Stock 1955/70	548	
547		£500 5¾% Hawker Siddeley Conv. Deb. Stock 1979/84	515	
550		£200 Burmah Oil Co. Ltd. Ordinary Stock	388	
1,309		£287 Guest Keen & Nettlefold Ltd. Ordinary Stock	1,112	
—		£47 Guest Keen & Nettlefold Ltd. New Ordinary Stock. Issued at 70/–; 30/– paid up†	93	
667		£266 Courtaulds Ltd. Ordinary Stock	575	
912		240 Marks & Spencer Ltd. "A" Ordinary 5/– Shares	1,134	
390		£160 Babcock & Wilcox Ltd. Ordinary Stock	262	
494		£250 Vickers Ltd. Ordinary Stock	359	
925		£131 Unilever Ltd. Ordinary Stock	950	
699		£130 John Dickinson & Company Ltd. Ordinary Stock	690	
1,022		£300 Tube Investments Ltd. Ordinary Stock	1,106	
866		£330 English Electric Co. Ltd. Ordinary Stock	577	
829		£300 Turner & Newall Ltd. Ordinary Stock	825	
11,713				10,877
		Staff Benevolent Fund		
474		£600 3½% Treasury Stock 1979/81	432	
400		£500 4% Trinidad Government Stock 1973/76	362	
158		£150 British Petroleum Co. Ltd. 6% Conv. Deb. Stock 1976/80	140	
715		£240 Bowater Paper Corporation Ordinary Stock	642	
731		375 Distillers Company Ltd. Ordinary 10/– shares	740	
723		300 Beecham Group Ltd. Ordinary 5/– shares	623	
3,201				2,93[illegible]
		Scientific Activities Fund		
65		£100 3½% Conversion Loan 1961 or after	59	
800		£1,000 4% Trinidad Government Stock 1973/76	725	
865				78[illegible]
		Life Composition Fund		
255		£350 4% Consolidated Stock 1957 or after x.d.	231	
790		£1,000 3½% Treasury Stock 1979/81	720	
715		£240 Bowater Paper Corporation Ordinary Stock	642	
915		£300 Imperial Chemical Industries Ltd. Ordinary Stock	960	
200		£25 Shell Transport & Trading Co. Ltd. Ordinary Stock (Reg.)	164	
333		21 Royal Dutch Petroleum Co. Fl.20 Shares (Bearer)	235	
3,208				2,95[illegible]
		British Rainfall Organization Fund		
491		£750 3½% War Stock 1952 or after	446	
2,091		£3,097.10.0 British Transport 3% Guaranteed Stock 1978/88	1,858	
73		£100 4% Consolidated Stock 1957 or after x.d.	66	
237		£300 3½% Treasury Stock 1979/81	216	
1,850		£2,000 4% Government of Commonwealth of Australia Registered Stock 1966/68 x.d.	1,750	
4,742				4,336
		Napier Shaw Memorial Fund		
229		£350 3½% Conversion Loan 1961 or after	208	
292		£400 4% Consolidated Stock 1957 or after x.d.	264	
521				47[illegible]
		Symons Memorial Fund		
425		£650 3½% Conversion Loan 1961 or after	387	
146		£200 4% Consolidated Stock 1957 or after x.d.	132	
571				51[illegible]
		Hampton Brown Fund		
734		£500 Hawker Siddeley Group Ltd. Ordinary £1 Shares	725	
351		500 Marley Tile (Holding) Co. Ltd. 5/– Ordinary Shares	437	
—		150 Marley Tile 5/– New Ordinary Shares	132	
1,085				1,29[illegible]
£25,906				£24,17[illegible]

* General Fund also includes the Freehold of 49 Cromwell Road, S.W.7.

† There is a contingent liability of £94 in respect of call of 40/– on these shares.

The Society also holds £750 National Savings Certificates and £400 Building Society Shares which have been set aside for a former Assistant Secretary's Pension.

Examined and securities seen.
March 1961

BALL, BAKER, DEED & CO.,
Chartered Accountants

Proceedings at meetings of the Society

Symons Memorial Lecture, 1 March 1961

Dr. D. G. King-Hele, Royal Aircraft Establishment, Farnborough, delivered the Symons Memorial Lecture, his subject being 'Satellites and the earth's outer atmosphere.'

Ordinary Meeting, 15 March 1961

The following candidates were declared to have been elected that day by the Council :

Fellows

Henderson, James Porteus, M.Sc., East African Meteorological Department, Private Post Bag, Nairobi, Kenya.
Hughes, Nicholas David Peter, B.A., Colehill, Newborough, Burton-on-Trent, Staffs.
Smith, Brian, B.Sc., 11 Pinfold Road, Streatham, London, S.W.16.
Thomas, Derek Malcolm Charles, B.A., A.R.I.C., 95 Western Avenue, Woodley, Berks.
Warren, Francis William George, B.Sc., Department of Applied Mathematics, University of Sheffield, Sheffield 10, Yorks.
Philpott, Instr. Lt. Cdr. David R. M., R.N., B.A., H.M.S. Collingwood, Fareham, Hants. (*reinstatement*; elected 1953; resigned December 1955).

Foreign Member

Jiusto, James E., B.A., M.A., 4248 Roxbury Drive, Buffalo 21, New York, U.S.A.

Corporate Members

Decca Radar Limited, Decca House, 9 Albert Embankment, London, S.E.1. (*Nominee* : Gp. Capt. E. Fennessy, C.B.E., B.Sc., M.I.E.E.).
Silver City Airways Limited, 62 Brompton Road, London, S.W.3. (*Nominee* : A. E. Barnes).

Canadian Members

Fellows

Gunn, Kenrick Lewis Stuart, B.A., M.Sc., Ph.D., Department of Physics, McGill University, Montreal 2, Quebec.
Layton, Donald Walker, B.Sc., Aviation Forecast Office, R.C.A.F. Station, Greenwood, Nova Scotia.
Page, Fred Albert, B.A., 46 Dorlen Avenue, Islington, Ontario.
Shannon, Robert Stewart, B.A., 315 Bloor Street West, Toronto, Ontario.
McGlening, Leslie Keith, B.A., 17 Lascelles Boulevard, Toronto 7, Ontario.

The following papers were read and discussed :

1. 'Total ozone and the middle stratosphere over arctic and sub-arctic areas in winter and spring' by W. L. Godson (*Q.J.*, **86**, p. 301), presented by Dr. A. W. Brewer.
2. 'Control of inversion height by surface heating' by F. K. Ball (*Q.J.*, **86**, p. 483), presented by Mr. J. S. Sawyer.

Evening Discourse, 5 April 1961

The third and last of the series of Evening Discourses, planned for the 1960/1961 session, was delivered by Professor T. Bergeron, University of Uppsala, Sweden, who spoke on 'The history of meteorology.'

Annual General Meeting, 19 April 1961

Dr. J. M. Stagg, C.B., O.B.E., M.A., D.Sc., President, in the Chair. The Minutes of the Annual General Meeting held on 20 April 1960 were confirmed and signed.

The President in presenting the Report of the Council for 1960 referred to the main items of interest.

In 1960, a new prize, known as the L. F. Richardson Prize, was instituted for the special encouragement of the younger members of the Society.

Special reference was made to the change in policy for allocating grants from the Scientific Activities Fund, emphasis now being given to helping younger Fellows of the Society in presenting their work at meteorological conferences.

The series of Evening Discourses, begun in 1958, was continued and appreciation of the lectures was reflected in the increased audiences.

Assistance given by the Nuffield Trust had made possible the reprinting of several post-war numbers of the *Quarterly Journal*. The generous action of a number of Fellows in donating their private collections of Journals had provided further valuable additions to the Society's stock.

Special mention was made of the additional course and extended programmes of Field Studies which had been successfully introduced with generous support from the Carnegie United Kingdom Trust.

The Summer Visit was to the Lasham Gliding Centre near Alton, Hampshire.

The seventh Two-day Summer Meeting, was successfully held at Queen's College, Dundee, University of St. Andrews.

The policy of refurbishing and improving facilities at the Society's house was being continued.

The *Quarterly Journal* had maintained its traditionally high standards and the number of papers submitted again showed an increase.

The high standard of technical content in *Weather* had been maintained and to bring the magazine into closer relationship with the activities of the Society, Council had decided that the committee should become an Editorial Board of five members with a Business Manager and be nominated by Council.

The President referred to the increased use of the services offered by the Library and expressed the hope that this would continue. Progress has been made in the glazing of open shelves and in rebinding journals and books.

In reviewing the membership of the Society, the President drew attention to the steadiness of its numbers and to the fact that the grade of Corporate Membership, instituted on 1 January 1960, had acquired nine members during the year, while 13 Fellows were nominees of Corporate Bodies.

Before calling on the Treasurer to present his Report, the President expressed thanks to all those who had devoted a great deal of their time to furthering the interest of the Society and referred with satisfaction to the services of the Staff during the year.

The Treasurer, Mr. B. C. V. Oddie, drew attention to items of unusually heavy capital expenditure, i.e., the reprinting of back numbers of *Quarterly Journal*; the new Members' List; and the structural repair and redecoration of the Society's premises which accounted for the deficit of £696. The cost of printing the *Quarterly Journal* was higher than in the previous year by some £500, owing to the substantial increase in the amount of material published.

It was gratifying to note that sales of *Quarterly Journal* and *Weather* had again risen. Revenue from advertising had fallen and steps were being taken to remedy this.

The Society once again had received a grant of £300 from the Royal Society, but this was unlikely to be renewed in 1961.

The value of the Society's investments had declined by about £1,700 during the year, which was one of mild but general recession. Beyond taking up ' rights ' issues costing £297, no new investments had been made.

A new appeal had been made to Fellows to enter into Covenants for the payment of their subscriptions. Fifty-one Fellows had responded and the Society would benefit to the extent of some £135 annually.

A Pensions Scheme had been introduced for the benefit of permanent full-time members of the Staff. The old ' Staff Pension Fund ' had been wound up and securities transferred to the General Fund. Another block of securities had been placed in a Staff Benevolent Fund for administration at the discretion of Council.

The Treasurer referred to By-law 88 and proposed that a sum of not more than £1,000 should be approved for investment during the coming twelve months. This motion was unanimously approved.

The President moved that the Report be received and adopted and that it be printed in the *Quarterly Journal*. The motion was carried unanimously.

Professor L. Jacobs proposed a vote of thanks to the President and Council for their work during 1960 and this was seconded by Mr. H. H. Lamb.

The President then announced the following awards :

(*a*) *Symons Memorial Gold Medal for 1961* :

To Professor Jule G. Charney of the Massachusetts Institute of Technology, for his distinguished work in dynamical meteorology, as given in the following citation :

The Symons Gold Medal is awarded to Professor Jule G. Charney of the Massachusetts Institute of Technology for his distinguished work in dynamical meteorology.

Important papers by Dr. Charney began to appear soon after the end of World War II and quickly established the author as a leading worker in the application of fluid dynamics to realistic problems of large-scale atmospheric motion. This work developed into a major advance in meteorological science, perhaps the most outstanding achievement of a generation. It gave for the first time acceptable theoretical explanations of the behaviour of the atmosphere on the large synoptic scale, and led to practical weather prediction by dynamical calculation using modern electronic computers. Dr. Charney has continued to make major contributions to this work and, with a powerful combination of physical insight and mathematical skill, has done as much as any man to enhance the status of dynamical meteorology in physical science.

The medal was then presented to Dr. Thomas H. Osgood, Science Attaché at the United States Embassy in London, who received it on behalf of Professor Charney and read the following message of thanks from him :

I wish to express my deep gratitude to the Royal Meteorological Society for the great honour it has conferred upon me by the award of the Symons Memorial Gold Medal.

In accepting this award I am profoundly conscious of my debt to earlier scientific workers in the field of meteorology and to my present and former collaborators from many countries. It is a particular source of pride and satisfaction to me that many of my intellectual godfathers are included among those who have been similarly honoured by the Society. One man, however, I should like to mention by name : to the extent that my work in numerical weather prediction has been of value, it has been a vindication of the vision of my distinguished predecessor, Lewis F. Richardson, a former Secretary of this Society.

Nowhere is the continuity and tradition of our science better represented than by this oldest and most respected of all meteorological societies. To have been selected by it for recognition is to become identified with a truly international fellowship of science. This is especially gratifying to me at a time when fellowship in all spheres of peaceful human endeavour is becoming a pre-requisite to human existence.

(*b*) *L. F. Richardson Prize for 1961* :

To Gilbert Brian Tucker, Ph.D., for his paper ' Mean meridional circulations in the atmosphere ' (*Q.J.*, **85**, 365, p. 209).

(*c*) *Darton Prizes for 1960* :

Home Award : Mr. Allan A. Jackson of Wye College, Ashford, Kent, for his articles on ' The ecoclimatology of Dutch lights,' (*Weather*, April, May 1959).

Canadian award : Dr. W. L. Godson, M.A., Meteorological Office, Toronto, for his paper ' Total ozone and the middle stratosphere over arctic and sub-arctic areas in winter and spring ' (*Q.J.*, **86**, 369, p. 301). The award was presented to Mr. H. A. C. Patterson, C.B.E., Attaché for Civil Aviation and Commerce at Canada House, who accepted it on behalf of Dr. Godson.

Dr. J. M. Stagg, C.B., O.B.E., M.A., D.Sc., then delivered the Presidential Address, his subject being ' Meteorology and the community.'

Dr. R. C. Rainey proposed a vote of thanks to the President for his address and asked that he would allow it to be printed in the *Quarterly Journal*. Mr. N. Bradbury seconded the vote of thanks.

The meeting was declared closed at 7.15 p.m.

Monsoons of the world. New Delhi (India Meteorological Department), 1960. Pp. x, 270, Figures; Tables. 12.00 Rupees.

This is the report on the symposium on ' Monsoons of the world ' held at New Delhi in February 1953 following the second session of the Commission for Synoptic Meteorology of the World Meteorological Organization. The majority of the 34 contributions were from the staff of the India Meteorological Department; the rest from Australia, Ghana, W. Germany, Japan, Madagascar and the U.S.S.R. Most of the papers are printed in full, but a few are in summary only. The report is divided into seven sections, each dealing with a particular aspect of the subject. It concludes with a brief summary of the discussions.

The first section is descriptive climatology. It includes charts showing the mean temperatures and winds for several upper levels for selected months over India and S.E. Asia, together with summary tables showing the mean variation with height of the thermodynamical parameters. A paper by H. O. Walker describes the monsoons of West Africa on the basis of atmospheric structure as indicated by temperature, humidity and air flow, and the distribution of weather.

Section II, consisting of 12 papers, discusses monsoons in relation to the general circulation. Of outstanding interest are two papers by Prof. H. Flohn. The first ascribes the monsoonal changes to the seasonal shifts of the planetary wind systems, enhanced particularly over Africa and Southern Asia by Continental heating and cooling. The second suggests relationships between the onset of the monsoon and other features of the general circulation such as the blocking anticyclones of late Spring over N.W. Europe, and, more particularly, the formation of a warm anticyclone in the mid-troposphere over Tibet in early Summer. While suggesting some highly plausible relationships these papers go on to propose some yet more interesting problems whose solutions require more upper-air data than are at present available.

The promise of the title in the next section, ' The dynamics of the monsoons,' is not fulfilled. This section contains a descriptive list of work on the monsoons carried out in the U.S.S.R., and an appraisal of Jeffreys's simplified theory of monsoons put forward in 1926, but it gives no modern dynamical treatment.

Section IV – ' Depressions and perturbations in the monsoon,' Section V – ' Rain and Clouds ' and Section VI – ' Variability of the monsoons ' are mainly descriptive, with some statistics. Research workers will find many useful facts and references here. The final section describes some of the methods, mainly statistical, used now and formerly, for extended-range forecasting of the monsoon in India.

Like some other reports of symposia, this is a heterogeneous collection of papers of which only a few, the most interesting to the reviewer, can be mentioned in this notice. Some of the papers pose penetrating questions, few of which, however, are answered. In a few places, the approach is too facile; for example, rainfall is freely attributed to convergence, but it is not shown how to diagnose the convergence, apart from through its association with rainfall. The descriptive parts of the report, however, provide much information which makes it a useful work of reference.

A.G.F.

The earth's problem climates. By G. T. Trewartha. (University of Wisconsin), Madison, 1961. Pp. vi, 334; 168 Figures; Tables. $7.50.

Intending this book for a ' professional audience,' the author states that his aim is ' to make an inventory of the more important of the earth's problem climates and to offer a brief and precise description of their characteristics.' Problem climates are considered to be those which differ from what Thornthwaite and others (no reference given) consider to be the general pattern that might develop on a hypothetical continent. The book is divided into six parts, one part dealing with each of the climates of Latin America, Australia-New Zealand-Equatorial Pacific, Africa, Southern and Eastern Asia, Europe and the Mediterranean Borderlands, and Anglo-America (by which is meant the United States of America, excluding Alaska and Hawaii, and southern Canada.'

Although the title is somewhat unfortunate, in some respects the approach is refreshing, and constitutes a much needed change from the more usual type of climatological text which regards climate merely as the average of various meteorological parameters rather than the net result of all scales of atmospheric processes which are far from static. A genuine attempt has been made in this book to introduce an appreciation of the dynamical character of climate. This treatment can only be commended and welcomed; however, there are several aspects of the presentation which must be criticized.

The author appears to regard ' normal ' climates as those which conform in distribution to the pattern on Thornthwaite's hypothetical continent. He implies that the way in which ' the great planetary controls of solar energy distribution and the general circulation of the atmosphere and ocean water, modified by the differential effects of continents and oceans ' can explain them is well known. The reviewer would venture to suggest that climatology is, as yet, capable of adequately explaining very few climates. Because a climate is found in several roughly similar geographic positions it must not be supposed that it is adequately accounted for merely by saying that because it is found in similar circumstances it is therefore normal and is the result of normal atmospheric processes. This may be true, but it does not follow that it is consequently well understood.

Although breaking new ground for climatological text books, unfortunately there are still several examples f circumlocution of the kind that often passes for explanation in traditional climatology, and goes unchallenged. 'or example on p. 95 we are told that part of the explanation of the ' unusual ' southward penetration of the ahara dry climate ' lies in the vertical structure of the I.T.C., in that area. There follows a good account f the structure of the Intertropical Convergence Zone in these areas derived from authoritative sources, ut this merely describes the weather associated with the I.T.C., the ' explanation ' for which we wait is y-passed. It is unfortunate that although the author has declared his aim to be to catalogue and describe, specious vein of implied explanation runs throughout the book.

Another disappointing feature is that while it is pointed out that pressure is the result of atmospheric irculation, nevertheless much space is spent on describing surface-pressure systems as though they were he *cause* of what is going on throughout the atmosphere. For example, on p. 92 we are told that eastern Africa acks the effects of maritime air *because* there is no permanent anticyclone over the Arabian Sea; and on p. 12 hat a break in the sub-tropical high pressure belt *permits* a meridional exchange of air.

A glaring inaccuracy occurs on p. 17 where we read that in ' low latitudes the rainfall, characteristically ollows the sun . . . . . in its diurnal course.' This in itself is somewhat ambiguous, but the following remarks larify it by saying that 80 per cent of rain falling at night is a major departure from this rule. This is com- letely incorrect because there are many locations in the tropics where a very large proportion of rain falls t night. It is interesting to note in passing that a satisfactory explanation of this fairly common phenomenon s not yet to be found in the meteorological literature.

There are also some minor points which should be mentioned. However valuable as descriptive tools he Koppen and Thornthwaite classifications might be, phrases like ' the *Aw* merges into *Caf* (*w*) ' (p. 13) re irritating, particularly when the folding map showing the distribution of these alphabetic complications aces the wrong way to be of best use as a reference map. The dichotomous arrangement of print which ecessitates the eye performing a carriage-return line-feed every seven words or so, and the rather awkward ystem of references are not conducive to easy reading. The maps and diagrams are excellently drawn and, ogether with the tables, are clear and well-devised; these features and the standard of paper and binding nake for a well-produced publication.

There is much in *The earth's problem climates* to be applauded, but also, much that could have been mproved. It represents a significant and praiseworthy departure from the more conventional climatological extbooks but should be read very critically lest misconceptions be obtained.

G.B.T.

A history of the United States Weather Bureau. By D. R. Whitnah. Urbana (University of Illinois Press), 1961. Pp. ix, 267 : 8 pp. Photographs. $6.

The greater part of the book is based on the author's thesis for a Ph.D degree in history. The author's nterest in meteorology arose from his five- or six-year association with the Illinois State Water Survey Division.

Various attempts dating from the early nineteenth century to maintain observational networks and to upply weather information in the U.S.A. led to the demand for a national weather service, which was instituted n 1870 under military operation by the Signal Service (later Corps). In 1891, after prolonged controversy, he service was transferred as a civilian organization – the Weather Bureau – to the control of the Department f Agriculture. It was further transferred in 1940 to the Department of Commerce.

With primary emphasis on the provision of public services in the broadest sense, though with due attention o research and international co-operation, the development of the service since 1870 is traced in chapters 2-10. We learn of the state and progress of the main activities in convenient successive epochs, and of the rustrations and other vicissitudes, sometimes partly attributable to fluctuations in politic-administrative olicy. Information on many aspects is given or indicated in considerable detail : there are some 950 footnote eferences to published and unpublished source material. We read not only of the basic general forecasting nd climatological activities but also of the several diverse specialized services developed throughout the years, .g., of the continued efforts to build up effective warning systems for hurricanes and river floods. Services or aviation are the subject of a separate chapter of 34 pages. The final chapter (10) deals with the commitments f the Bureau in World War II and thereafter. It includes discussion of projects undertaken outside the J.S.A., extensions of services within the country, the application of modern improved operating techniques, esearch conducted or assisted by the Bureau and, in the last page or two, the significance of space weather tations (Tiros I and successors).

The author does not disguise the fact that the national service has been subjected at times to heavy riticism, on technical or management grounds, not always justifiably. Nor does he gloss over the unfortunate ircumstances of the removal of two Chiefs of Bureau from office many years ago.

An experienced career meteorologist might possibly have adopted a rather different treatment of the ubject of Professor Whitnah's study, but readers of this book will certainly gain a good insight into the orking, problems and achievements, and their background, of a great national meteorological service in s different phases; and also learn something of the characteristics and contributions of many of the leading ersonalities associated with the service.

H.W.L.A.

Space research. Ed. by H. K. Bijl. (Proceedings of the first international space-science symposium. Nice 1960). (North Holland Publishing Co., Amsterdam), 1960. Pp. xvi, 1195; Figures; Tables; Plates. 170

Space research, which is a unity of disciplines relying on a common means of accomplishment – the rocket or artificial satellite, is still not quite a respectable subject in the eyes of some scientists, and for a variety of reasons. The name itself is grandiose or in some way ill-chosen, though in the absence of an alternative with any appeal it is probably here to stay; the subject is too closely associated through its ordnance with political rivalries and military back-up; and there is the feeling that its great expense is not justifiable against the demands of other science and for the more widespread application of the world's finite technological effort to under-developed countries in particular. Such objections are, I imagine, appreciated and to some extent shared by nearly all. But few eschew the motor-car because it has become the bane of modern urban life and a highly lethal weapon, or because it is an archsymbol of a materialist society which people may right to fear. Fortunately, one does not have to become an active space researcher to remain an active scientist in the fields concerned, but there is no doubt that space research has already become a major field of scientific endeavour and that, in the fields concerned, scientific health demands attention to its possibilities and its findings. The evidence is before us in the volume under review : 2,000 pages and nearly 100 original papers presented at the first international symposium ever to be held specifically for space research, when the subject is still quite an infant but growing mightily fast.

The discipline of basic technique – the high-speed instrumental platform and telemetric data reception – does not in itself provide the unity for a coherent science symposium, and so we find this volume divided into the following parts : ' The earth's atmosphere,' ' The ionosphere,' ' Tracking and telemetering (as science geodesy and the paths of bodies in complex gravitational fields),' ' Solar radiation,' ' Cosmic radiation,' ' Interplanetary dust,' ' The moon and the planets.' Nearly every branch of observational science is thus represented and some biology appears, too, at the very end. No one scientist today can have a vital interest in all these fields but the common bond of technique, for some part at least of the research in each field, is salutary in this age of increasing diversification, specialization and isolation – salutary both for realising the possible relations of one field with another, solar radiation with meteorology for example, and for discerning the growing points of observational science and the techniques by which they are achieved. Just to turn over the pages, halting occasionally for a while, was for me a most enjoyable experience and one I would particularly recommend to meteorologists. So many of the major meteorological problems are of such long standing and the observational data so many, that it can be invigorating to see neighbouring fields, in very different case, coming by exciting new data and new problems, as on the Van Allen radiation belts in the fields of cosmic rays and geomagnetism.

About 220 pages and 17 papers are to be found in Pt. I on the earth's atmosphere above 30 km or so. They deal with the temperature, wind, density and composition (including dissociation and diffusive separation) in the high atmosphere, satellites having been particularly productive of data on air density from satellite drag at levels necessarily above about 200 km. The climatology begins to appear in more detail and at greater heights than Dr. Murgatroyd was able to achieve in his invaluable review in this Journal in 1957 and the ' weather ' also is being disclosed. The satellite is, of course, potentially supreme in exploring weather but it is notable that rockets are already used sufficiently often to provide day-to-day or even more frequent changes. Thus rockets have shown that the winter westerlies of the polar mesosphere have broken down concurrently with their breakdown in the polar stratosphere. The reader will also find a discussion of the energy absorption in high levels and the mechanisms by which a quasi-balance of the thermal field may be achieved, while the potentialities of Tiros are presented and can now be compared with the actual results of Tiros I which was launched soon after the conference. It is also of interest to note that the southern and northern hemispheres continue to show markedly different behaviours of the diurnal and semi-diurnal tidal winds above 80 km.

There is no space here to continue with the description of results in other parts of the volume, even of those results which have a meteorological flavour. The book is primarily a large repository of new results in atmospheric physics, not yet much co-ordinated, but offering interest of different kinds to different experience brought to it. Considering the speed with which the volume was edited and published the standard of presentation is high and, for a subject which changes so rapidly, the publication is timely. It will enable those with a growing interest in the field, but who are not yet committed, to see what is involved and to form their judgements on firmer grounds than would otherwise be possible. A quotation from one author in the volume may or may not be discouraging in this respect. He says : ' One is reminded of the great difficulty of designing a first-generation experiment which accomplishes more than establishing the design parameters for further experiments to follow.' Roughly half the papers come from the United States and a third of the remainder from the United Kingdom.

P.A.S.

Klima-atlas von Nordrhein-Westfalen. (Ed.) Offenbach a. M. (Deutscher Wetterdienst) 1960. Pp. 38, 77 maps, 10 Figures. DM.44.

This publication is the fifth of a series of climatic atlases for the ten German Länder. It covers an area of great industrial and agricultural importance to Germany and its appearance is an event of some significance. As would be expected, all the standard meteorological elements are dealt with, but there is a great difference

in the methods adopted for the various elements. For example, the treatment of precipitation is largely conventional, with maps of monthly and annual isohyets. On the other hand, maps of mean temperature are given only for January, April, July, October, the year and the vegetation period May-July. Other temperature maps give information on the average dates of the beginning and end of the period with mean temperature $\geqslant 5°C$ and 10°C; on the number of ice-days, frost-days and summer-days; and on the mean dates of last and first air frosts. It is perhaps arguable whether the exclusion of maps for eight months is justified and whether monthly values of mean daily maximum and minimum should be completely ignored, but granted that a selection of maps is necessary, a large volume of useful information on temperature is contained in the atlas.

For some of the remaining elements only the months of highest or lowest values have been selected. This is carried to the extreme for humidity, for which the only map is one of mean relative humidity at 1400 hr in May. The German interest in agricultural meteorology is evident from the eight phenological maps, maps of drought index and diagrammatic representation of soil and earth temperature for selected periods.

The explanatory notes cover 38 pages and give definitions and details of the observations on which the atlas is based. In addition, they contain descriptions of the weather and phenological occurrences to be expected in an ' average ' year, as well as tables adding to the information on rainfall and temperature, mainly in respect of extreme values.

The scale of the maps is 1 : 1,000,000, their quality is excellent, the colours are pleasing, the isopleths are thin but distinct and the background is a model of clarity. The maps are loose in a folder and care is necessary to avoid damage to the edges. The atlas costs about £4 but for those interested in the climate of this region it would be money well spent.

W.H.H.

Das Klima der Bodennahen Luftschicht. By R. Geiger. Braunschweig (Friedr. Vieweg & Sohn). 4th revised edition, 1961. Pp. xii, 646; 281 Figures; Tables. DM.54.

With the ever-increasing applications of meteorology to industry, agriculture, planning and other economic and social activities it is evident that our knowledge, even of the macroclimate of inhabited regions, leaves much to be desired. But for many of these applications the macroclimate is only the first step from which some estimates of the microclimate must be made. A great deal of microclimatic work has been carried out by scientists in a number of fields but inevitably the results are scattered in publications not readily accessible to meterologists. Rudolf Geiger has spent over 30 years as a microclimatologist and nobody is better qualified to present a survey of the subject. The publication of the 4th edition of his book in the series *Die Wissenschaft* is therefore most welcome, particularly as it has been enlarged and to some extent rewritten, incorporating a good deal of new material.

The book is divided into eight main sections, starting with a consideration of the heat exchange near the earth's surface which, the author feels, is all too little understood by workers in microclimatology. The subsequent sections deal with the effects of soil, plants, forests, land-forms, and animals (including humans) on the climate of the lowest layers of the atmosphere. A short, general section on the methods of making measurements in microclimatic and micrometeorological investigations follows, written by Gustav Hofman.

The range of information contained in this book is difficult to convey. Perhaps it is best attempted by the selection of a few items at random – the mulching of soils; the microclimates of gardens and potato fields; variations of light intensity in a forest; the flow of rain down tree-trunks; the date of blossom in different parts of an isolated pine-tree; slope- and valley-winds; irrigation; climates in animal houses; town climates; shelter belts; protection against frost. On all of these topics, and very many more, there is some basic information, usually with many references.

Professor Geiger has set out with two main objects in view, to produce a textbook for those approaching the study of microclimatology for the first time and also to provide a reference book. There is perhaps some difficulty in achieving both these aims in one publication, particularly when the variety of interests of the potential readers is remembered. Undoubtedly the book succeeds and two of the factors contributing to its success are the large number of diagrams and a most extensive bibliography. The quality of the diagrams is very high; the photographs are not quite so good. The bibliography contains over 1,200 entries and there can be only very few microclimatic topics without a reference. The book is clearly printed on good paper and is a pleasure to handle. The price of about £5 is not unreasonable and all workers in this field should have access to this publication.

W.H.H.

Obituary Notices

Mr. J. H. Hall

We have to record the death on 13 March 1961, in his 80th year, of James Harry Hall. Mr. Hall, who resided at Ashton-under-Lyne, Lancashire, had held Fellowship in the Society since 1936.

E.L.H.

Mr. R. Y. Sanders, F.S.S., F.R.Econ.S.

Mr Reginald Yorath Sanders, Deputy Commercial and Development Adviser to the Electricity Council in 1958-59, died suddenly on 3 February 1961 at the age of 65. Mr. Sanders was one of the first officers appointed to the headquarters staff of the Central Electricity Board on its establishment in 1927. During his long term of service he held a number of important positions on the Board, including secretaryship of the National Consultative Committee from 1944 to 1948. In the latter year he became Deputy Commercial Manager to the British Electricity Authority; later he was Deputy Chief Commercial Officer. In 1956 he went to Russia as a member of the delegation to that country representing the British electricity supply industry. For many years he served on committees of the U.N. Economic Commission for Europe and the O.E.E.C. Mr. Sanders was elected to Fellowship of this Society in 1948.

E.L.H.

WEATHER RADAR

Capable of providing accurate and continuous observation of the position, movement and extent of precipitation areas, Decca weather radars are designed to meet the general requirements of meteorological services for local and aviation forecasting and the more specialised tasks of research, agriculture, flood control, etc.

64 WORLD METEOROLOGICAL SERVICES use DECCA RADAR

WINDFINDING RADAR

Decca windfinding radars provide the highest performance consistent with low operating cost. The speed and direction of upper winds are accurately measured to the 100,000-foot level. The equipment can be operated by one man and additional equipment can be supplied to meet the specialised data processing requirements of meteorological service. The outstanding performance of these windfinding systems permits the use of a small and inexpensive balloon-borne passive target.

Decca Radar, the world's leading suppliers of meteorological radars, offer simple, reliable equipment proved by prolonged operational use and backed by a comprehensive operational and technical training organisation and by the Company's world-wide service organisation.

DECCA RADAR

DECCA RADAR LIMITED, LONDON, ENGLAND

DR162

F. DARTON & CO. LTD.

Makers of :

THERMOGRAPHS
BAROGRAPHS
HYGROGRAPHS
PRECISION HAIR HYGROMETERS
ALTIMETER CALIBRATORS
KEW PATTERN BAROMETERS
FORTIN'S PRINCIPLE BAROMETERS
GRASS & SOLAR THERMOMETERS
RAIN GAUGES, etc.

All enquiries to : Established 1834

WATFORD FIELDS, WATFORD, HERTS

Tel. : WATFORD 26019 & 26010

TRADE HEZZANITH MARK

Meteorological and Scientific Instruments

There is a century of richi experience behind the manufacture of every "HEZZANITH" Instrument

CATALOGUES ARE AVAILABLE UPON REQUEST (RMS.A1)

Heath, Hicks & Perken *(THERMOMETERS)* ***Ltd.***
New Eltham, London, S.E.9
Phone : ELTHAM 3836. Grams : "OPTIMUS," Souphone, London

THE FINEST SOUNDING AND PILOT BALLOONS AVAILABLE

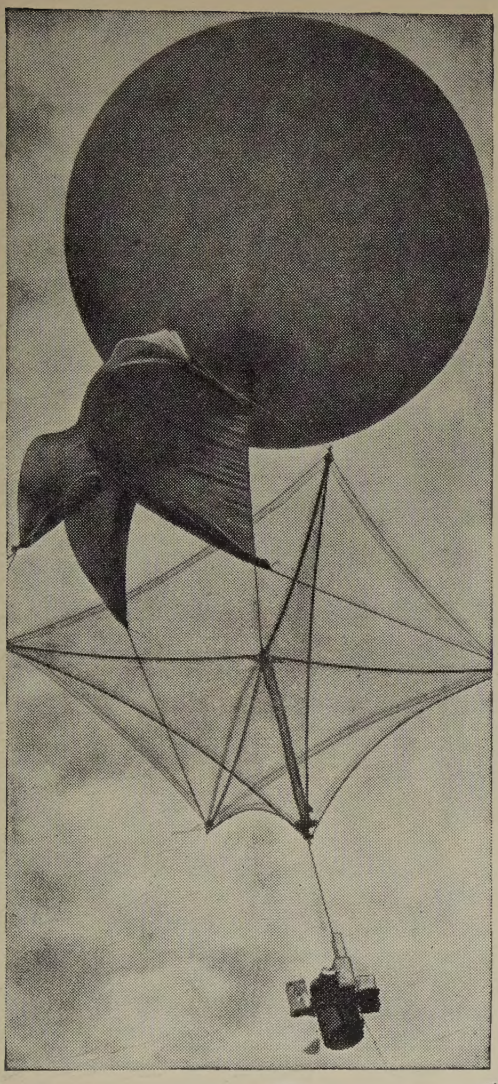

Manufactured by the Guide Bridge Rubber Company of Vulcan Mill, Bury, these balloons are in use throughout the world.

OVERSEAS SALES

Phillips Patents Limited
250 Western Avenue, Acton, London, W.3

HOME SALES

Guide Bridge Rubber Co. Ltd, Vulcan Mill, Butcher Lane, Bury, Lancs

Beritex SEAMLESS

REGD.

Mufax

THROUGHOUT THE WORLD

12

USA

IDLEWILD AIRPORT

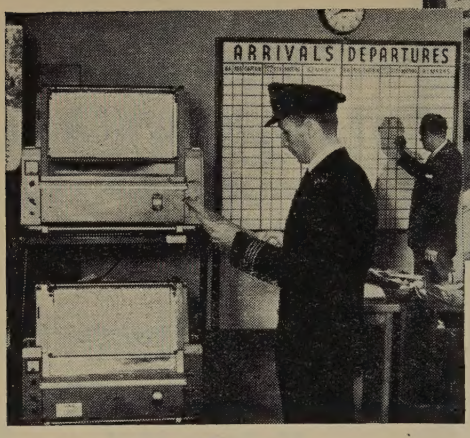

Photographs by the courtesy of the Port of New York Authority

Every hour of every day BOAC liners are flying the Atlantic. Every minute of every hour it is essential to have vital weather information available for the pilots. This information is provided at Idlewild from the BOAC Offices visible to the left of the Observation Tower in the upper picture. In the lower picture Mr. A. Murray, Senior Flight Operations Officer, is seen studying the latest information received on the D-649-G/AX Mufax Chart Recorders.

MUIRHEAD

MUIRHEAD & CO. LIMITED, Beckenham, Kent, England.
Tel: Beckenham 4888

MUIRHEAD INSTRUMENTS LTD., Stratford, Ontario, Canada.
Tel: 271-3880

MUIRHEAD INSTRUMENTS INC., 441 Lexington Av., New York 17, N.Y., U.S.A.
Tel: Murray Hill 2-8131

PYRHELIOMETER

For the Measurement of SOLAR RADIATION

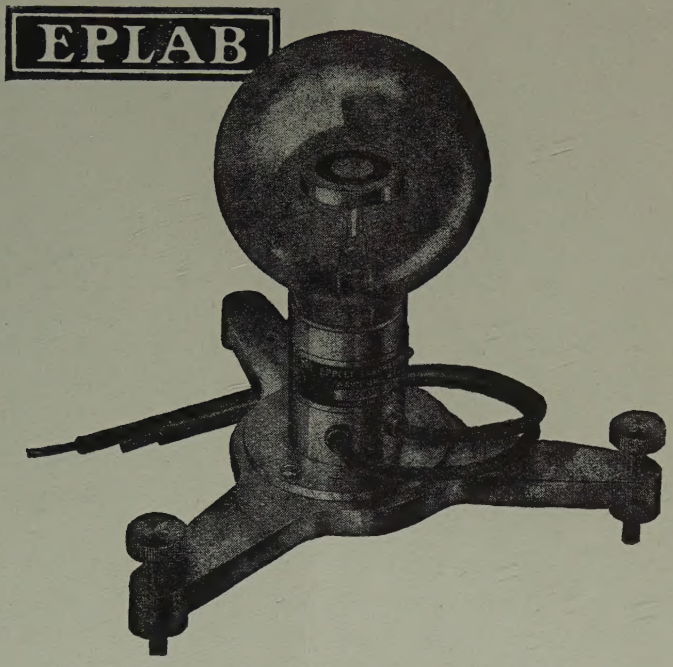

Eppley Pyrheliometers are used for solar radiation measurements at ninety-eight weather stations in the continental United States, Canada, Alaska, Greenland, Iceland, Caribbean Sea, and the Pacific Ocean. Sixty-two of these stations are under the direction of the United States Weather Bureau.

The Eppley Pyrheliometer was adopted as standard equipment by the Weather Bureau after considerable experimentation. It was found to be the best instrument so far tested by the Bureau.

Used in conjunction with a suitable recorder, the Eppley Pyrheliometer will provide an accurate and reliable record of total solar and sky radiation on a horizontal surface.

Bulletin No. 2 on Request

THE EPPLEY LABORATORY INC.

Scientific Instruments

20 Sheffield Avenue Newport, Rhode Island, U.S.A.

THE NAPIER SHAW MEMORIAL PRIZE

Announcement of third competition

The Royal Meteorological Society announces the third competition for the Napier Shaw Prize. The competition will be open to anyone without restriction of nationality. The prize of £100 is offered on this occasion for an original essay on **'The Upper Atmosphere.'**

> For the purpose of this competition the upper atmosphere is regarded as the atmosphere above the tropopause and below the exosphere. Essays on the dynamics, constitution or physics of the atmosphere in this region, or in any part of it, will be accepted, but an essay on purely electrical properties of the ionosphere is not sought. Preference will be given to essays relating two or more aspects of the state of the upper atmosphere. Essays on the inter-relations between the upper atmosphere and the troposphere will also be welcome.

The essay, which must be in English, may include material which the candidate has already published. Essays may be submitted jointly in the names of more than one author.

Candidates are required to submit three copies of their essay, which must be printed or typewritten. In the latter case, only one side of the paper should be used, double spacing should be employed and two of the copies may be good carbon copies. Unless the essay is printed, any mathematics should be written in carefully by hand. Although the scale of the essay will be considerably greater than that of an ordinary paper, candidates are recommended to consult, for general advice, the pamphlet, 'Preparation of papers for the Quarterly Journal.' This may be obtained, free of charge, on application to the Assistant Secretary.

It is required that any essay for which a prize is awarded shall be offered to the Society for publication.

All entries for the competition should be addressed to the Assistant Secretary, Royal Meteorological Society, 49 Cromwell Road, London, S.W.7 and marked clearly 'Napier Shaw Prize.'

Essays for the competition must be received at the Society's Offices *not later* than 1 January 1962.

Printed in Great Britain in Horley Series by The Salisbury Press Ltd., Publicity House, Wilton Road, Salisbury, Wilts. (28731)